

THEME SECTION

Integrated Multi-Trophic Aquaculture (IMTA) in Sanggou Bay, China

Idea: J. Fang

Editors: T. Dempster, M. Holmer, P. Cranford, S. Dworjanyn, S. Lefebvre, S. Mirto

Fang J, Zhang J, Xiao T, Huang D, Liu S <i>INTRODUCTION: Integrated multi-trophic aquaculture (IMTA) in Sanggou Bay, China</i> 201–205	Chang Y, Zhang J, Qu J, Jiang Z, Zhang R Influence of mariculture on the distribution of dissolved inorganic selenium in Sanggou Bay, northern China 247–260
Mahmood T, Fang J, Jiang Z, Zhang J Carbon and nitrogen flow, and trophic relationships, among the cultured species in an integrated multi-trophic aquaculture (IMTA) bay 207–219	Zhao L, Zhao Y, Xu J, Zhang W, Huang L, Jiang Z, Fang J, Xiao T Distribution and seasonal variation of pico-plankton in Sanggou Bay, China 261–271
Ning Z, Liu S, Zhang G, Ning X, Li R, Jiang Z, Fang J, Zhang J Impacts of an integrated multi-trophic aquaculture system on benthic nutrient fluxes: a case study in Sanggou Bay, China 221–232	Zhang J, Wu W, Ren JS, Lin F A model for the growth of mariculture kelp <i>Saccharina japonica</i> in Sanggou Bay, China 273–283
Kang X, Liu S, Ning X Reduced inorganic sulfur in sediments of the mariculture region of Sanggou Bay, China 233–246	Li R, Liu S, Zhang J, Jiang Z, Fang J Sources and export of nutrients associated with integrated multi-trophic aquaculture in Sanggou Bay, China 285–309



INTRODUCTION

Integrated multi-trophic aquaculture (IMTA) in Sanggou Bay, China

Jianguang Fang^{1,2,*}, Jing Zhang³, Tian Xiao^{4,5}, Daji Huang⁶, Sumei Liu^{7,8}

¹Key Laboratory for Sustainable Utilization of Marine Fisheries Resources, Ministry of Agriculture, Yellow Sea Fisheries Research Institute, 266071 Qingdao, PR China

²Function Laboratory for Marine Fisheries Science and Food Production Processes, Qingdao National Laboratory for Marine Science and Technology, 266237 Qingdao, PR China

³State Key Laboratory of Estuarine and Coastal Research, East China Normal University, 200062 Shanghai, PR China

⁴Key Laboratory of Marine Ecology & Environmental Sciences, Institute of Oceanology, Chinese Academy of Sciences, 266071 Qingdao, PR China

⁵Laboratory for Marine Ecology and Environmental Science, Qingdao National Laboratory for Marine Science and Technology, 266237 Qingdao, PR China

⁶State Key Laboratory of Satellite Ocean Environment Dynamics, Second Institute of Oceanography, State Oceanic Administration, 310012 Hangzhou, PR China

⁷Key Laboratory of Marine Chemistry Theory and Technology, Ocean University of China/Qingdao Collaborative Innovation Center of Marine Science and Technology, 266100 Qingdao, PR China

⁸Qingdao National Laboratory for Marine Science and Technology, 266237 Qingdao, PR China

ABSTRACT: Integrated multi-trophic aquaculture (IMTA) involves the farming of species from different trophic positions or nutritional levels in the same system. In China, IMTA has been practiced for many decades, with dozens of species farmed in close proximity to each other at the scale of whole coastal bays. Articles in this Theme Section present results from the MoST-China Project on 'Sustainability of Marine Ecosystem Production under Multi-stressors and Adaptive Management' (2011–2015). This project sought to understand the interactions between biogeochemical cycles and ecosystem function in the IMTA system of Sanggou Bay, China, which produces a total of >240 000 t of seafood each year from >30 species in approximately 100 km² of production space. Results include measurements of carbon, nitrogen flow and trophic relationships among cultured species; impacts of IMTA on benthic nutrient fluxes, reduced inorganic sulfur in sediments, distribution of dissolved inorganic selenium, and nutrient cycling; distribution and seasonal variation of picoplankton; and a model for kelp growth. Combined, the articles enable a complex understanding of the dynamics between IMTA and the environment in one of the most important coastal aquaculture production systems in the world.

KEY WORDS: Integrated multi-trophic aquaculture · Sanggou Bay · Biogenic elements · Ecological aquaculture

Introduction

In the 'Millennium Ecosystem Assessments' of the United Nations, climate, water, food, and health were identified as critical issues that need to be considered in adaptive ecosystem-based management plans to sustain human well-being (www.millenniumassess-

ment.org). Marine aquaculture is increasingly seen as an alternative to fishing to provide a growing human population with high-quality protein. Aquaculture of high value species (e.g. fish in cages) relies on external food supplies and has a negative impact on water quality. Culture of seaweeds, which can reduce nutrient loadings to the environment from fish aquaculture, has

*Corresponding author: fangjg@ysfri.ac.cn

not been attractive in many countries as algal products typically have a low value. However, combining different species in aquaculture systems could provide more profit and have concomitant ecological benefits.

In 2011, the Ministry of Science and Technology (MoST) of China launched a 5 yr research project on 'Sustainability of marine ecosystem production under multi-stressors and adaptive management' (MEcoPAM; MoST Grant No. 2011CB409800). The project addressed the following questions: (1) What are the impacts of multi-stressors on biogeochemical cycles in coastal ecosystems? (2) How do ecosystem functions in the hypoxic zone of the East China Sea respond to multi-stressors? (3) What adaptive strategies are possible for coastal aquaculture systems with multi-stressors?

Implementation of MEcoPAM's research strategy involved investigations off the Shandong Peninsula of North China, particularly in aquaculture areas of Sanggou Bay (Fig. 1). Field observations, microcosm experiments and modeling studies analyzed the combined effects of fish-catch, aquaculture, and enhancement activities on the structure and function of the coastal ecosystem, as well as responses of the ecosystem to multiple stressors. The goal was to develop adaptive management strategies for sustainable aquaculture systems.

Aquaculture in Sanggou Bay

Sanggou Bay is located on the eastern tip of Shandong Peninsula, China and is well known in the field of marine aquaculture, especially in integrated multi-trophic aquaculture (IMTA). Overall, >100 km² of the

163 km² bay area are used for aquaculture, producing >240 000 t of seafood per year (China Bay Records Compiling Committee 1991, Liu et al. 2014). More than 30 important aquaculture species, including kelp, scallops, oysters, abalone and sea cucumbers, are grown using various culturing methods such as long-lines, cages, bottom sowing and enhancement, pools in the intertidal zone, and tidal flat culture (Zhang et al. 2007).

The concept of IMTA was coined in 2004 and refers to the incorporation of species from different trophic positions or nutritional levels in the same system (Chopin & Robinson 2004). However, IMTA has been successfully practiced in Sanggou Bay since the late 1980s (Fang et al. 1996). There are several IMTA modes in Sanggou Bay (Fig. 2), with benefits at the ecosystem level. For instance, co-culture of abalone and kelp provides combined benefits of a food source and waste reduction: abalone feed on kelp, and the kelp takes up nutrients released from the abalone (Tang et al. 2013). Co-culture of finfish, bivalves and kelp links organisms from different trophic levels so that the algae absorb nutrients released from finfish and bivalves, and bivalves feed on suspended fecal particles from the fish. Since kelp and *Gracilaria lemaneiformis* are cultured from December to May and from June to November, respectively, nutrients are absorbed by the algae throughout the year. These examples of multi-trophic culture maximize the utilization of space by aquaculture as they combine culture techniques in the pelagic and benthic zones. Implementation of IMTA in Sanggou Bay has improved economic benefits, maintained environmental quality, created new jobs, and led to culture technique innovations (Fang & Zhang 2015).

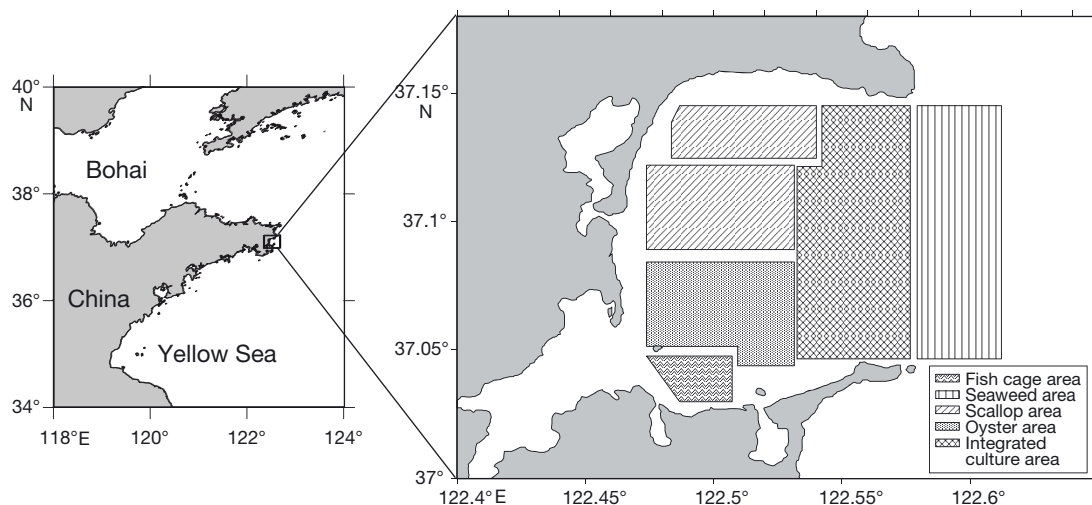


Fig. 1. Aquaculture areas in Sanggou Bay, Shandong Province, China

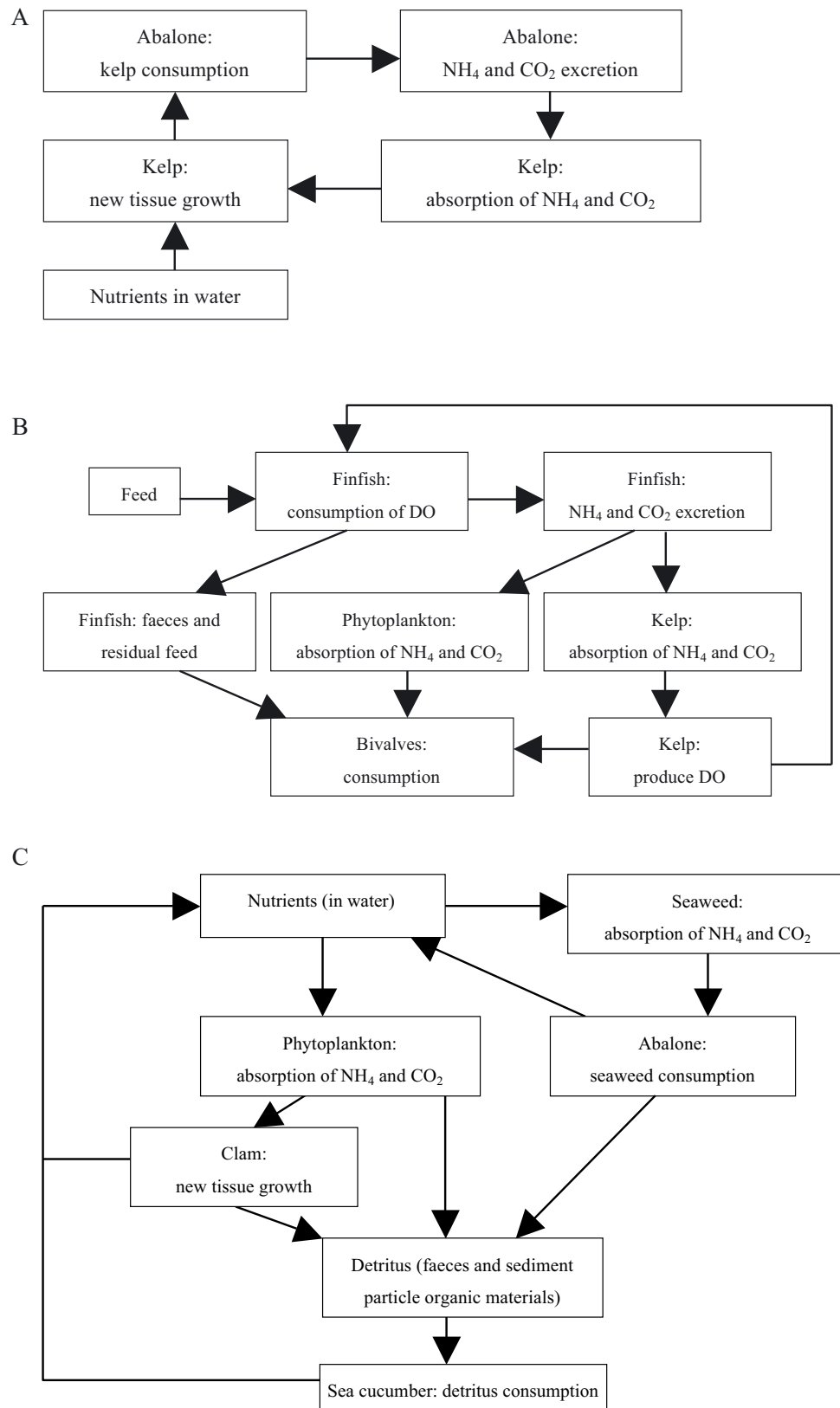


Fig. 2. Integrated multi-trophic aquaculture (IMTA) modes in Sanggou Bay, China, modified from Tang et al. (2013). (A) Long-line culture of abalone and kelp, (B) long-line culture of finfish, bivalve and kelp, and (C) benthic culture of abalone, sea cucumber, clam and seaweed. DO: dissolved oxygen

Moreover, the implementation of IMTA can increase the beneficial functions of an ecosystem. For instance, cage-culture of fish produces wastes in the form of uneaten feed, which induces the release of greenhouse gases into the atmosphere (i.e. a CO₂ source). Fish farming in combination with seaweed culture can turn the system into a CO₂ sink through photosynthesis and uptake of nutrients (Tang et al. 2011).

Studies included in this Theme Section

During the implementation of MEcoPAM in 2011–2015, Sanggou Bay has been a focal area to examine IMTA practices through interdisciplinary studies, combining physics, chemistry, biology and fisheries research. The papers included in this Theme Section reveal important connections between growth and production of cultured organisms and environmental quality, using approaches to understand cycling of biogenic elements and the function of the microbial loop.

Mahmood et al. (2016) measured stable isotopic signatures of organic carbon ($\delta^{13}\text{C}$) and total nitrogen ($\delta^{15}\text{N}$) in suspended particulates and sediments to understand the sources of organic matter (OM), water quality and flow of organic carbon and nitrogen among IMTA species, as well as to evaluate the role of IMTA practices in accumulation and assimilation of OM during both wet and dry seasons.

Ning et al. (2016) measured benthic nutrient fluxes in Sanggou Bay in June and September 2012. In June, the early growth phase of cultured finfish and bivalves contributed little to biodeposition, and benthic nutrient fluxes tended to come from the sediment to the seawater and contributed to algal growth. In September, culture of finfish and bivalves resulted in high concentrations of nutrients in seawater and TOC in the sediment; 64 % of the nitrogen and 25 % of the phosphorus metabolized by bivalves were transferred from the seawater to the sediment.

Kang et al. (2016) compared reduced inorganic sulfur (including sediment acid-volatile sulfide, pyrite sulfur, elemental sulfur) and organic matter (OM) between a mariculture region of Sanggou Bay and a reference station to assess the influence of mariculture on sulfide accumulation and the benthic environment. They found that given the mariculture activities in Sanggou Bay, there was no potential threat of toxic sulfide to the benthic biomass.

Chang et al. (2016) investigated dissolved inorganic selenium concentrations in the water column,

selenium content in biological species and sources of dissolved inorganic selenium entering Sanggou Bay. They discovered that the main source of dissolved inorganic selenium was water exchange with the Yellow Sea, whereas the most important sink was the intensive and widespread seaweed and bivalve aquaculture, which removed 53 % of incoming selenium from bay waters.

Brown tide, caused by picoplankton, is a serious environmental problem in the world (Gastrich & Wazniak 2002, Nuzzi & Waters 2004, Zhang et al. 2012). Zhao et al. (2016) observed different patterns of picoplankton abundance and biomass, and analyzed the factors that affect the distribution and variation in abundance and biomass of picoplankton in aquaculture areas of Sanggou Bay.

Kelp *Saccharina japonica* is one of the most important mariculture species in China (Ministry of Agriculture 2015). Zhang et al. (2016) developed a dynamic growth model to evaluate environmental effects on kelp growth in Sanggou Bay. The model output provided useful information for improving the production and quality of kelp.

Aquaculture activities play an important role in nutrient cycling in Sanggou Bay (Li et al. 2016). Seasonal variations in nutrient concentrations were detected in the rivers entering the bay, particularly enrichment of dissolved inorganic nitrogen and silicate. The composition and distribution of nutrients were also affected by the species being cultured. The bivalve aquaculture was the major source of PO₄³⁻, contributing 64 % of total influx, and led to increased riverine fluxes of PO₄³⁻. The substantial quantities of nitrogen and dissolved silicate accumulated in sediments or were transformed into other forms. Large quantities of DIN and PO₄³⁻ were removed from the bay through harvesting of seaweeds and bivalves.

Future directions

Sustainable development in coastal ecosystems should be an important focus of modern aquaculture. Where aquaculture is to be embedded in coastal ecosystems, the inter-connections between production systems and the environment must be thoroughly understood. As a result, interest in exploring the potential for integrated aquaculture in brackish and marine ecosystems is growing (Soto 2009). The interactions among species in IMTA systems are complicated. Observational data and previous experience have shown the many positive aspects, both economic and environmental, of IMTA systems. Cur-

rently, management of large-scale IMTA areas remains difficult, principally due to limited knowledge of how the separate components interact and function as a whole. The papers in this Theme Section provide detailed knowledge of how different IMTA species interact and affect the environment in regions that practice IMTA. Constructing and applying diagnostic models based on an understanding of the connections among species in IMTA systems and the surrounding environment can provide guidance to adaptively manage IMTA systems to ensure ongoing sustainability.

Acknowledgements. The guest editors thank all the contributors to this Theme Section and the reviewers for their valuable comments, and especially Dr. Tim Dempster for managing the Theme Section. Funding of Sanggou Bay studies came from the National Basic Research Program of China for the project 'Sustainability of Marine Ecosystem Production under Multi-stressors and Adaptive Management' (MoST Grant No. 2011CB409800). We also thank Prof. Qisheng Tang for advice and help in the implementation of IMTA, and Drs. Zeng Jie Jiang and Jing Hui Fang for preparing this Theme Section. We acknowledge the government and companies from Rongcheng for their help in facilitating our experiments in Sanggou Bay.

LITERATURE CITED

- Chang Y, Zhang J, Qu J, Jiang Z, Zhang R (2016) Influence of mariculture on the distribution of dissolved inorganic selenium in Sanggou Bay, northern China. *Aquacult Environ Interact* 8:247–260
- China Bay Records Compiling Committee (1991) Chinese bay records: the third section. Ocean Press, Beijing, p 377
- Chopin T, Robinson S (2004) Defining the appropriate regulatory and policy framework for the development of integrated multi-trophic aquaculture practices: introduction to the workshop and positioning of the issues. *Bull Aquacult Assoc Can* 104:4–10
- Fang J, Zhang J (2015) Types of integrated multi-trophic aquaculture practiced in China. *World Aquacult* 46: 26–30
- Fang J, Kuang S, Sun H, Li F, Zhang A, Wang X, Tang T (1996) Mariculture status and optimizing measurements for the culture of scallop *Chlamys farreri* and kelp *Laminaria japonica* in Sanggou Bay. *Mar Fish Res* 17:95–102
- Gastrich MD, Wazniak CE (2002) A brown tide bloom index based on the potential harmful effects of the brown tide alga, *Aureococcus anophagefferens*. *Aquat Ecosyst Health Manage* 5:435–441
- Kang X, Liu S, Ning X (2016) Reduced inorganic sulfur in sediments of the mariculture region of Sanggou Bay, China. *Aquacult Environ Interact* 8:233–246
- Li R, Liu S, Zhang J, Jiang Z, Fang J (2016) Sources and export of nutrients associated with integrated multi-trophic aquaculture in Sanggou Bay, China. *Aquacult Environ Interact* 8:285–309
- Liu S, Yang Q, Yang S, Sun Y, Yang G (2014) The long-term records of carbon burial fluxes in sediment cores of culture zones from Sanggou Bay. *Acta Oceanol Sin* 36: 30–38
- Mahmood T, Fang J, Jiang Z, Zhang J (2016) Carbon and nitrogen flow, and trophic relationships, among the cultured species in an integrated multi-trophic aquaculture (IMTA) bay. *Aquacult Environ Interact* 8:207–219
- Ministry of Agriculture (2015) China fishery statistic year book 2014. Chinese Agriculture Publishing House, Beijing
- Ning Z, Liu S, Zhang G, Ning X and others (2016) Impacts of an integrated multi-trophic aquaculture system on benthic nutrient fluxes: a case study in Sanggou Bay, China. *Aquacult Environ Interact* 8:221–232
- Nuzzi R, Waters RM (2004) Long-term perspective on the dynamics of brown tide blooms in Long Island coastal bays. *Harmful Algae* 3:279–293
- Soto D (ed) (2009) Integrated mariculture: a global review. FAO Fisheries and Aquaculture Technical Paper No. 529. FAO, Rome
- Tang Q, Zhang J, Fang J (2011) Shellfish and seaweed mariculture increase atmospheric CO₂ absorption by coastal ecosystems. *Mar Ecol Prog Ser* 424:97–104
- Tang Q, Fang J, Zhang J, Jiang Z, Liu H (2013) Impacts of multiple stressors on coastal ocean ecosystems and integrated multi-trophic aquaculture. *Prog Fish Sci* 34:1–11
- Zhang J, Wu W, Ren JS, Lin F (2016) A model for the growth of mariculture kelp *Saccharina japonica* in Sanggou Bay, China. *Aquacult Environ Interact* 8:273–283
- Zhang Y, Zhang Y, Zhang W, Zhang J, Duan J, Li L, Lu S (2012) Size fraction of chlorophyll a during and after brown tide in Qinhuangdao coastal waters. *Ecol Sci* 31: 357–363
- Zhang ZH, Lü JB, Ye SF, Zhu MY (2007) Values of marine ecosystem services in Sanggou Bay. *Chin J Appl Ecol* 18: 2540–2547
- Zhao L, Zhao Y, Xu J, Zhang W and others (2016) Distribution and seasonal variation of picoplankton in Sanggou Bay, China. *Aquacult Environ Interact* 8:261–271



Carbon and nitrogen flow, and trophic relationships, among the cultured species in an integrated multi-trophic aquaculture (IMTA) bay

Tariq Mahmood^{1,4,*}, Jianguang Fang², Zengjie Jiang², Jing Zhang³

¹School of Resources and Environmental Science, East China Normal University, 3663 North Zhongshan Road, Shanghai 200062, PR China

²Key Laboratory of Sustainable Utilization of Marine Fisheries Resources, Ministry of Agriculture, Yellow Sea Fisheries Research Institute, Chinese Academy of Fishery Sciences, Qingdao 266071, PR China

³State Key Laboratory of Estuarine and Coastal Research, East China Normal University, 3663 North Zhongshan Road, Shanghai 200062, PR China

⁴Present address: National Institute of Oceanography, St 47, Block 1, Clifton, Karachi 75600, Pakistan

ABSTRACT: Stable isotopic signatures of organic carbon ($\delta^{13}\text{C}$) and total nitrogen ($\delta^{15}\text{N}$) were measured on suspended particulates and sediments in order to understand the sources of organic matter (OM), water quality and flow of organic carbon and nitrogen among integrated multi-trophic aquaculture (IMTA) species, as well as to evaluate the role of IMTA practice in accumulation and assimilation of OM during wet and dry seasons. OM distribution and composition were studied during 2011 in Sanggou Bay (SGB) of northern China, a system that receives terrestrial and oceanic inputs, and which is used for IMTA ventures. Results showed that higher terrestrial input of OM occurs during the wet compared to the dry season in the SGB. OM in suspended particulates (POM) showed marine- and terrestrial-derived signatures during the wet season, as revealed from their ranges in $\delta^{13}\text{C}$ (-27.4 to -20.7‰) and $\delta^{15}\text{N}$ (4.7 to 9.4‰). Sedimentary organic matter (SOM) showed signatures of marine-derived OM during both seasons, with ranges in $\delta^{13}\text{C}$ and $\delta^{15}\text{N}$ of -22.4 to -21.4‰ and 1.7 to 6.4‰ , respectively. Shellfish and combined (shellfish, seaweed) cultures in SGB have the potential to reduce OM received from the fish cages as well as from the seasonal inputs from rivers. Mixing with Yellow Sea water, combined with prevailing circulation, favours the dispersal, dilution and transformation of OM and maintains and improves water quality. Based on our results, and compared with previous studies, the water quality of the SGB is likely to be sustained by IMTA activities.

KEY WORDS: IMTA · POM · SOM · Carbon isotope · Nitrogen isotope · Trophic levels · Sanggou Bay

INTRODUCTION

Excess amounts of carbon and nitrogen produced either from land-based or offshore aquaculture activities are considered to be one of the main sources of pollution in coastal environments. Increasing coastal area development as well as aquaculture activities have been of particular concern to the health of coastal ecosystems. Land-based aquaculture waste is

often discharged directly into shallow coastal areas, causing excessive organic and nutrient loads (Alabaster 1982). Offshore cage culture is considered to be a direct source of organic matter (OM) to the surrounding waters in the form of suspended detritus (Karakassis et al. 2000, Mazzola & Sarà 2001), which mainly consists of uneaten feed and excretion products from the cultured fish (Holby & Hall 1991, Hall et al. 1992). Furthermore, anthropogenic input provides

*Corresponding author: tariqnio@gmail.com

additional nutrient and OM enrichment in the coastal marine system (Evgenidou & Valiela 2002). This waste affects not only the area in close proximity to the sources but can alter a wider coastal zone at various ecosystem levels; reducing the biomass, density and diversity of the benthos, plankton and nekton, and modifying natural food webs and stimulating eutrophication (Gowen et al. 1991, Pillay 1991, Vollenweider 1992, Duarte 1995). However, the offshore cultivation of shellfish together with seaweed could reduce the impact of OM waste and nutrients on the environment, as substantiated by land-based integrated aquaculture practice (Shpigel et al. 1991, Shpigel & Neori 1996). The aquaculture-derived nutrients can be removed by seaweed biofilters (Buschmann et al. 2008). Such a combined species cultivation method, so-called integrated multi-trophic aquaculture (IMTA), is practiced in Chinese coastal zones. Besides the feasible ventures in mariculture schemes, the combination of trophic levels among cultured species in IMTA systems is also important in improving water quality. The IMTA of shellfish, seaweed and fish is common on the coast of northern China and has been in practice over 3 decades (Fang et al. 1996a,b, 2009).

Sanggou Bay (SGB) receives OM from both natural and anthropogenic sources, which subsequently impact the water quality of the bay. SGB is surrounded by a population of ca. 0.6 million in Rongcheng City of Shandong Peninsula. River runoff from Rongcheng City is considered the main source of nutrients into SGB and is composed on average of 65% crop land waste and 35% urban waste (Project SPEAR; Ferreira et al. 2007). Stable isotope analysis has been used successfully in determining sources of nutrition for consumers, evaluation of trophic relationship among organisms, understanding different sources of OM (terrestrial and marine) and environmental impact assessment (Wada et al. 1987, Risk & Erdmann 2000, Costanzo et al. 2001). Stable isotope ratios of organic carbon ($\delta^{13}\text{C}$) and total nitrogen ($\delta^{15}\text{N}$) have also been used to determine the impact of aquaculture waste on the environment (Ye et al. 1991, Vizzini & Mazzola 2004, Yokoyama et al. 2006, Jiang et al. 2012). Aquaculture waste enters the food web and alters the natural isotopic composition of OM sources at both the base and upper trophic levels. Nitrogen-rich fish waste mainly affects $\delta^{15}\text{N}$ values without or little alteration of $\delta^{13}\text{C}$ (Vizzini & Mazzola 2004). Aquaculture and human waste can affect at different levels of the ecosystem—reducing the biomass, density and diversity of the benthos, plankton and

nekton—and modify natural food webs in coastal areas (Gowen et al. 1991, Pillay 1991).

In the present study, our first goal was to investigate the carbon and nitrogen flow from (1) phytoplankton, particulate OM (POM), sediment OM (SOM) or seaweed to filter feeders and (2) trash fish (feed provided to fish in fish cages) or plankton to omnivorous fish in an IMTA system in SGB using dual isotopic technique. A second objective was to study the isotopic profile ($\delta^{13}\text{C}$ and $\delta^{15}\text{N}$) of SOM and POM to understand the sources of carbon and nitrogen in SGB. Our study focused on understanding the role of lower trophic levels in the reduction of OM and clarifying whether aquaculture- and land-derived OM impact the water quality of the bay.

MATERIALS AND METHODS

Study area

The SGB (37° 01' to 37° 09' N and 122° 24' to 122° 35' E) is located in Rongcheng Town, in Weihai City, on the Shandong Peninsula in northeastern China (Fig. 1). The bay is semi-enclosed and opens into the Yellow Sea (YS) in the east, covering an area of 144 km². Freshwater inputs to the bay are mainly from one large river (the Gu River) and some small rivers (Ba, Sanggan, Yetao and Xiaolou Rivers). The bay experiences seasonal terrigenous inputs, with freshwater inflow being maximum in summer and with an average discharge of $1.7 \times 10^8 \text{ m}^3$ to $2.3 \times 10^8 \text{ m}^3$ (Rongcheng River Report 2012, www.rcsl.gov.cn). Water in the bay is well mixed and depth varies between 7.5 and 21 m (Zhao et al. 1996). IMTA is an important commercial activity in SGB. On the basis of culturing activities, the bay is divided into 4 culture areas. The southwest is used for shellfish and fish culture (hereafter, SF+F), the central part is dominated by polyculture of shellfish and seaweed (SF+SW), and the outer bay is cultivated with seaweed (SW) monoculture along the eastern boundary that opens into the YS (Fig. 1). Fish is cultured between May and October, while bivalve culture lasts between 1 and 2 yr. Red seaweed and kelp are cultivated from June–October and November–April, respectively (Zhao et al. 1996, SPEAR 2007). Shellfish and seaweed are cultivated in long lines around fish cages. Bivalve production includes the Chinese scallop *Chlamys farreri* ($\sim 60 \times 10^3 \text{ t yr}^{-1}$) and the Pacific oyster *Crassostrea gigas* ($\sim 15 \times 10^3 \text{ t yr}^{-1}$). Seaweed production includes kelp *Saccharina japonica* ($\sim 84 \times 10^3 \text{ t yr}^{-1}$) and red alga *Gracilaria lemaneiformis*

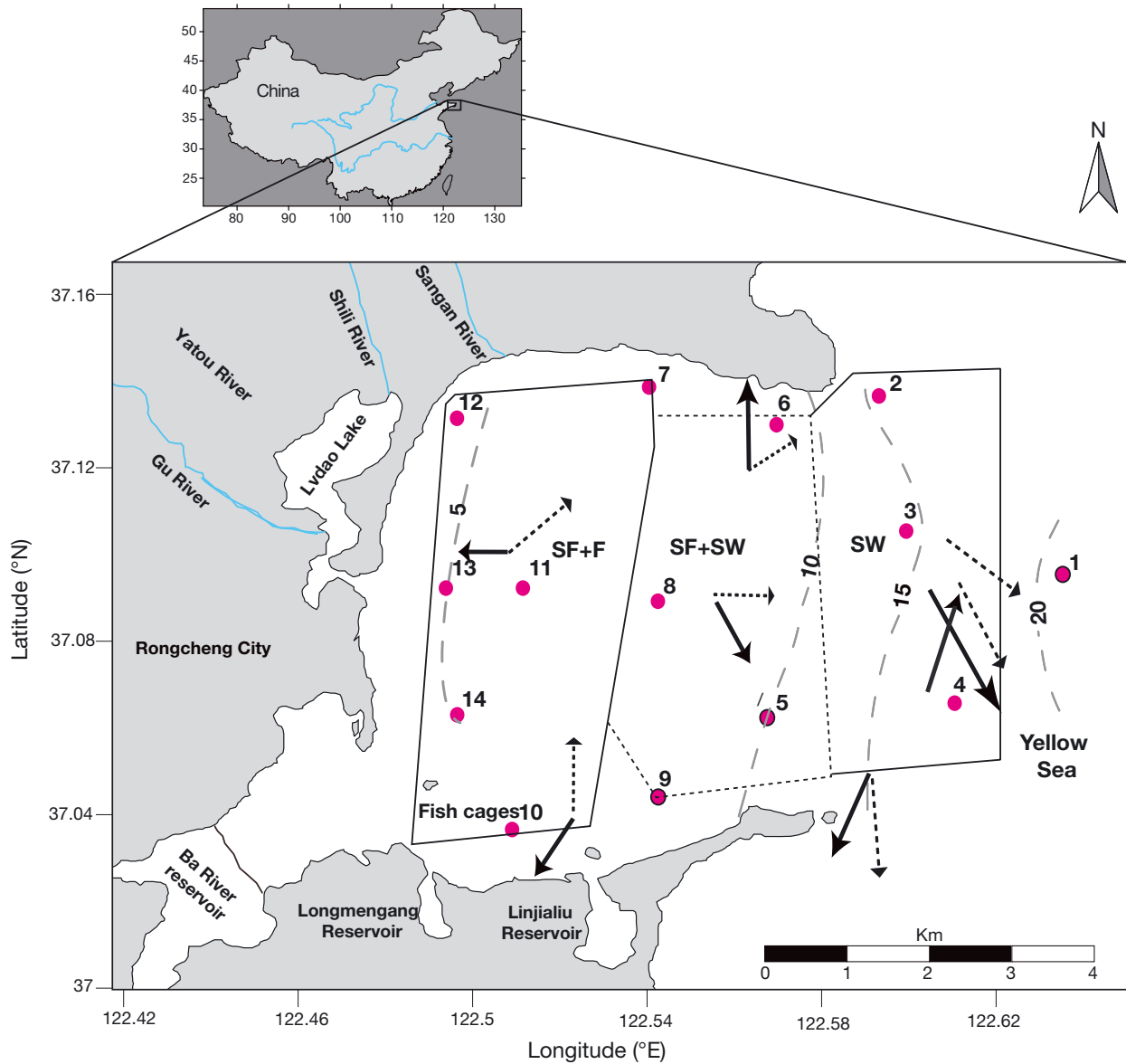


Fig. 1. Map of Sanggou Bay, showing culture areas (polygons with solid and dotted lines) and 14 stations (red dots) of cruises in August 2011 (wet season, summer) and January 2012 (dry season, winter). Culture areas include combined culture of shellfish and fish (SF+F), shellfish and seaweed (SF+SW) and monoculture of seaweed (SW). Solid arrows denote surface water current and dashed arrows bottom flow (source: Ferreira et al. 2007). Grey dashed lines denote isobaths (m)

($\sim 25 \times 10^3 \text{ t yr}^{-1}$). The production of Japanese flounder *Paralichthys olivaceus* is $\sim 24 \times 10^3 \text{ t yr}^{-1}$ (Rongcheng Fisheries Technology Extension Station 2012 statistics [www.rchy.gov.cn], summarized in Table 1).

Sampling and analysis

Samples for hydrographic parameters, POM, SOM, phytoplankton, zooplankton, shellfish (oyster and scallop), seaweed, cultured fish and trash fish were

collected in August 2011 (wet season, i.e. summer) and January 2012 (dry season, i.e. winter). Surface water samples were collected using a Niskin water sampler at 14 stations covering all 3 culture areas in SGB (Fig. 1). The water samples were immediately screened through a 200 μm mesh net to remove larger zooplankton and debris. They were filtered under vacuum onto prewashed, pre-combusted (450°C , 4h) and pre-weighed Whatman GF/F filter papers (0.7 μm pore size). The samples were subsequently stored at -40°C in a freezer until laboratory analysis.

Table 1. Summary of aquaculture in Sanggou Bay, where species are cultured in combination (SF+F, SF+SW) and monoculture (SW) in integrated multi-trophic aquaculture (IMTA). Additional details on the cultured area, annual production, and stocking, harvesting and culture periods for the different groups are also given (data from Zhao et al. 1996, Ferreira et al. 2007, Rongcheng Fisheries Technology Extension Station 2012 statistics [www.rchy.gov.cn])

Cultured species	Cultured area (km ²), total per group	Stocking period	Harvesting period	Culture period	Production (t yr ⁻¹)
Shellfish (SF)					
<i>Chlamys farreri</i> (Chinese scallop)	32	May	March	1–2 yr	~60 × 10 ³
<i>Crassostrea gigas</i> (Pacific oyster)		May	March	1–2 yr	~15 × 10 ³
Seaweed (SW)					
<i>Saccharina japonica</i> (kelp)	40	November	April	6 mo	~84 × 10 ³
<i>Gracilaria lemaneiformis</i> (Gracilaria)		June	October	5 mo	~25 × 10 ³
Fish (F)					
<i>Paralichthys olivaceus</i> (Japanese flounder)	0.36	May	October	6 mo	~24 × 10 ³

Bottom sediment samples were collected with a Van Veen grab (Hydro-bios) from a few stations and then frozen at –20°C until analysis. Salinity and chlorophyll *a* (chl *a*) were measured *in situ* with a multi-parameter instrument (Model: YSI Professional plus USA) and an ACLW-RS chlorophyll sensor, respectively. Cultured fish, shellfish, seaweed and trash fish samples were collected by local fishermen at some sampling sites. Phytoplankton (60 µm) and zooplankton (200 µm) nets were used to collect plankton samples. Plankton samples were filtered through Whatman GF/F filter papers, then frozen at –40 °C until analysis. All samples of fish, shellfish and trash fish were rinsed carefully with filtered seawater and guts were removed to reduce bias. Muscle of cultured fish, trash fish and shellfish, as well as sediments and particulate samples, were dried at 60°C for at least 24 h prior to stable isotope analysis. Cultured fish, trash fish and bivalve samples were soaked in 1.2 N HCl for 30 min, rinsed with distilled water, dried at 60°C and ground to a powder. The bottom sediment samples were ground and sieved through a 0.2 µm mesh, and then both the sediments and particulate samples were digested with 1 M HCl to remove carbonates and dried at 60°C for 12 h. Samples for total nitrogen concentration and isotopes were directly measured without the acid treatment (Cui et al. 2012).

Organic carbon, total nitrogen content and isotopes of carbon and nitrogen were measured using a Finnigan EA-1112 elemental analyzer interfaced with a Finnigan Delta plus XP continuous flow isotope ratio mass spectrometer. Carbon and nitrogen isotope ratios are expressed in the delta notation $\delta^{13}\text{C}$ and $\delta^{15}\text{N}$ relative to Vienna Pee Dee Belemnite and atmospheric nitrogen, respectively, and expressed as (Hayes 2004):

$$\delta X = [(R_{\text{sample}}/R_{\text{standard}}) - 1] \times 1000 (\text{‰}) \quad (1)$$

where, $X = ^{13}\text{C}$ or ^{15}N , and $R = ^{13}\text{C}:^{12}\text{C}$ for $\delta^{13}\text{C}$ or $^{15}\text{N}:^{14}\text{N}$ for $\delta^{15}\text{N}$.

Internal standards of caffeine and cellulose were used for calibration during the measurements. The average precision for organic carbon and total nitrogen measurements during this study was $\pm 0.1\%$.

Trophic levels among the cultured species were calculated using the following formula (Wan et al. 2010):

$$\text{Trophic level} = \frac{[(\text{consumer } \delta^{15}\text{N} - \text{phyto } \delta^{15}\text{N})/3.2] + 1}{1} \quad (2)$$

where 3.2 represents the average enrichment of $\delta^{15}\text{N}$ among trophic levels in the present study, obtained by calculating the average value of $\delta^{15}\text{N}$ of each trophic level. This value is close to the enrichment factor of 3.1 reported by Wan et al. (2010) in a YS trophic level study.

Statistical analysis

SPSS 17.0 and Golden Software Grapher 9 were used to perform data analysis. Seasonal variation in $\delta^{13}\text{C}$ and $\delta^{15}\text{N}$ of POM and SOM were examined using 1-way ANOVA. Difference of $\delta^{13}\text{C}$ and $\delta^{15}\text{N}$ values of POM and SOM were analyzed by a paired *t*-test (Cui et al. 2012).

RESULTS

Hydrographic parameters

A negative correlation between salinity and chl *a* was observed in the wet season ($r^2 = -0.82$; $p < 0.05$). The coastal region was dominated by low salinity

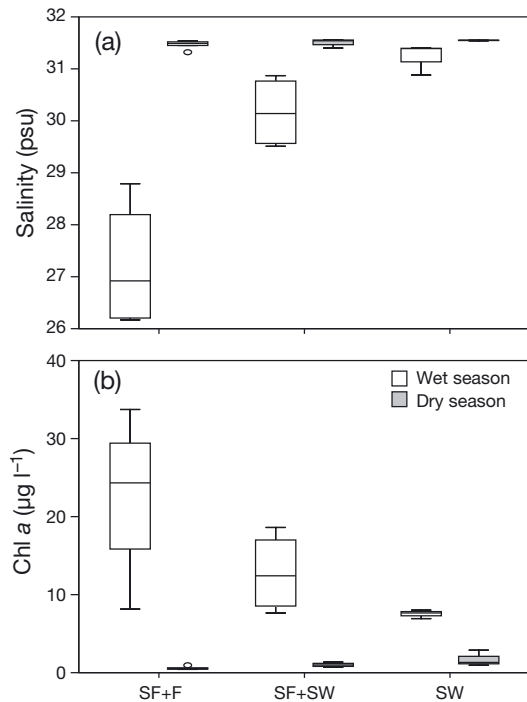


Fig. 2. Surface distribution of (a) salinity and (b) chlorophyll *a* in the 3 culture areas (see Fig. 1) in Sanggou Bay during the wet and dry seasons. Box plots show the median value (line), 25 and 75% quantiles (box), 5 and 95% quantiles (whiskers), and outliers (circles)

and high chl *a* concentration. Slightly lower salinity and higher chl *a* concentrations were found in the SF+F culture area of the bay compared to SF+SW and SW culture areas. The other 2 culture areas showed high salinity and low chl *a* concentrations. The maximum salinity and minimum chl *a* values were observed in the SW culture region (Fig. 2). The average values of salinity and chl *a* during the wet season in SGB were 29.4 ± 2.0 psu and 15.5 ± 10.9 $\mu\text{g l}^{-1}$ (Fig. 2), respectively. There was no significant variation in salinity among the aquaculture areas during the dry season (Fig. 2), due to low freshwater input into the bay. Considering all culture areas of SGB in the dry season, salinity ranged between 31 and 32 psu, with an average (\pm SD) of 31.5 ± 0.07 psu. During the dry season, the average (\pm SD) chl *a* concentration was 1.0 ± 0.63 $\mu\text{g l}^{-1}$. Chl *a* was significantly higher in the SW culture area in the offshore region than in the SF+F area in the coastal region of the bay (Fig. 2).

Stable isotope analysis of biological samples

The weight percentages of organic carbon in cultured fish and shellfish were higher than in plankton

and seaweed. The maximum values of nitrogen (% dry wt) were found in cultured fish and minimum values in plankton (Fig. 3). The C/N ratios of cultured fish, oysters, scallops and trash fish were in the range of 2.7–2.8, 3.6–4.0, 5.2–5.4 and 4.4–4.5, respectively, which were lower than the C/N ratios of phytoplankton (9.9), zooplankton (11.6) and *Gracilaria* spp. (hereafter simply *Gracilaria*) (10.0). $\delta^{13}\text{C}$ versus $\delta^{15}\text{N}$ values of SOM, POM, biological samples and the trophic level of the cultured species are shown in Fig. 4. The respective average values (\pm SD) of $\delta^{13}\text{C}$ and $\delta^{15}\text{N}$ were $-21.1 \pm 0.1\text{‰}$ and $9.2 \pm 0.4\text{‰}$ for scallops, $-21.1 \pm 0.2\text{‰}$ and $11.2 \pm 0.3\text{‰}$ for oysters, $-20.9 \pm 0.1\text{‰}$ and 6.7‰ for *Gracilaria*, $-19.0 \pm 0.2\text{‰}$ and $-21.0 \pm 0.6\text{‰}$ for cultured fish, and $11.1 \pm 0.3\text{‰}$ and $9.6 \pm 1.2\text{‰}$ for trash fish.

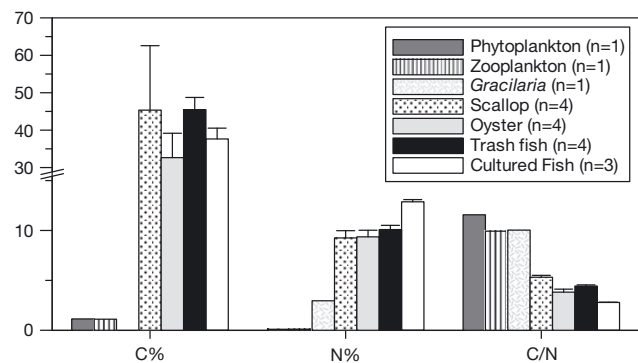


Fig. 3. Carbon and nitrogen contents (% dry wt) and C/N ratios of cultured species (seaweed, shellfish and fish; see Table 1) and of phyto- and zooplankton and input feed (i.e. trash fish) in Sanggou Bay during the wet season. Means \pm SD

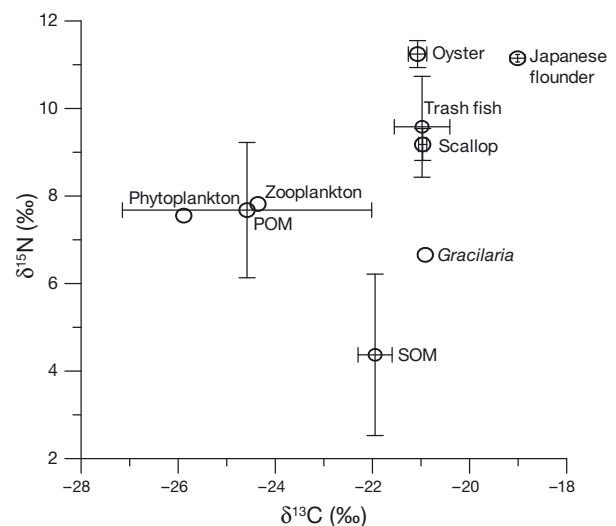


Fig. 4. $\delta^{15}\text{N}$ versus $\delta^{13}\text{C}$ isotopic signatures of plankton, cultured species, trash fish, and particulate and sediment organic matter from Sanggou Bay during the wet season. Means given \pm SD, if $n > 1$

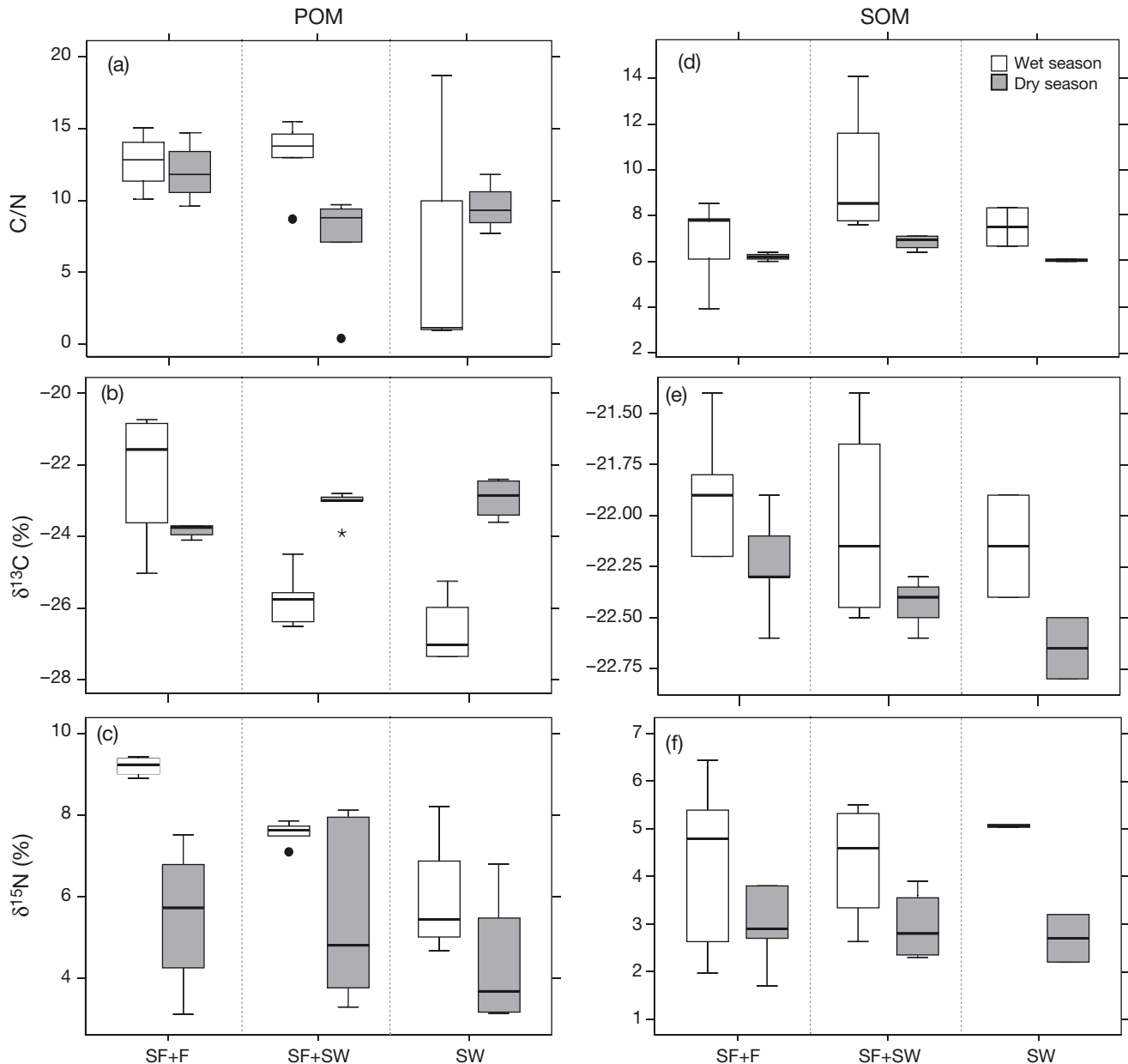


Fig. 5. Distribution of C/N, $\delta^{13}\text{C}$ (‰) and $\delta^{15}\text{N}$ (‰) of (a–c) particulate (POM) and (d–f) sediment organic matter (SOM) in the 3 culture areas (see Fig. 1) of Sanggou Bay during the wet and dry seasons. Box plots show the median value (line), 25 and 75 % quantiles (box), 5 and 95 % quantiles (whiskers), outliers (black dots) and extremes (stars)

Stable isotope analysis of SOM and POM in culture areas

The distribution of C/N, $\delta^{13}\text{C}$ and $\delta^{15}\text{N}$ of SOM ($n = 26$) and POM ($n = 28$) in the 3 culture areas of SGB during the wet and dry seasons is shown in Fig. 5. The fish cage culture and long-line culture of *Gracilaria* in SGB are performed during the wet season. Mixing of the bay water with the YS is higher in the SW culture area compared to the central (SF+SW)

area. In the wet season, the lowest (1.16) and highest (18.68) C/N values of POM were observed in the SW culture area (Fig. 5a). For SOM, the lowest C/N value (3.93) was found in the SF+F culture area and the highest (14.09) in the SF+SW area (Fig. 5d). Highest values of $\delta^{13}\text{C}$ and $\delta^{15}\text{N}$ of POM were found in the SF+F culture area (-20.74‰ and 9.43‰ , respectively) and the lowest in the SW culture area (-27.35‰ and 4.68‰ , respectively) (Fig. 5b,c). The $\delta^{15}\text{N}$ values of POM showed a decreasing trend from SF+F to sea-

ward (Fig. 5c). In contrast, no significant difference was found in the distribution of $\delta^{13}\text{C}$ of SOM among the 3 culture areas in the wet season (Fig. 5e). $\delta^{15}\text{N}$ values of SOM also showed no significant difference among the 3 culture areas in the wet season (Fig. 5f).

In the dry season, POM maximum and minimum C/N ratios were observed in SF+F (14.77) and SF+SW (0.39) culture areas, respectively, whereas for SOM no significance difference was found in C/N ratios among the 3 culture areas (Fig. 5a,d). The $\delta^{13}\text{C}$ values of POM and SOM were in the range of -24.06‰ to -21.88‰ , with only minor variations being observed between POM and SOM (Fig. 5b,e). The lowest value (3.12‰) of $\delta^{15}\text{N}$ of POM was found in the SF+F culture area and the highest (8.12‰) in SF+SW (Fig. 5c). A slight, though non-significant, decrease in SOM $\delta^{15}\text{N}$ was observed from SF+F to SW culture areas (Fig. 5f).

Within SGB overall, significant differences in $\delta^{13}\text{C}$, $\delta^{15}\text{N}$ and C/N values of SOM and POM between wet and dry seasons ($p < 0.05$) were found. In both seasons, SOM had slightly higher values of $\delta^{13}\text{C}$ than POM. In contrast, SOM had lower values of $\delta^{15}\text{N}$ and C/N compared to POM in both seasons.

DISCUSSION

Trophic relationships among the cultured species

In the present study, the C/N ratio (>11) of phytoplankton (being a major fraction of POM) indicates that terrestrial material from the rivers is a major source of carbon, since these values are higher than those previously reported for marine phytoplankton (range: 6.7–10) and closer to vascular plants (>12) (Redfield et al. 1963, Holligan et al. 1984, Meyers 1994, Hedges & Oades 1997, Bale & Morris 1998, Bates et al. 2005, Lamb et al. 2006). The $\delta^{13}\text{C}$ values of plankton (range: -25.4‰ to -25.9‰) in this study were lower than those reported for Narragansett Bay, USA (mean \pm SD: $-22 \pm 0.6\text{‰}$) and Osaka Bay in Japan (range: -18.0‰ to -24.0‰) (Gearing et al. 1984, Mishima et al. 1996). The $\delta^{15}\text{N}$ values of phyto- and zooplankton (range: 7.6–7.8‰) were within the range reported for marine phytoplankton (3.0–10‰) (Wada et al. 1991). For oysters, we determined relatively lower values of $\delta^{13}\text{C}$ (mean \pm SD: $-20.03 \pm 0.18\text{‰}$) and higher values of $\delta^{15}\text{N}$ ($8.27 \pm 0.13\text{‰}$) compared to values reported from oysters around a fish cage area in Ailian Bay, China (mean \pm SD: $-20.03 \pm 0.18\text{‰}$; Jiang et al. 2012), indicating that river runoff has been a source of carbon and nitrogen

in oysters of the present study. The $\delta^{13}\text{C}$ and $\delta^{15}\text{N}$ values (-19.0‰ and 11.1‰) we determined in cultured fish were lower than the average values (-17‰ and 13‰ , respectively) observed for marine fishes (Mays 2000).

The wet season in SGB is characterized by peak IMTA activities, when fish cage culture occurs in conjunction with shellfish and seaweed. In addition, maximum freshwater inputs influence the sources and flow of OM (carbon and nitrogen) among cultured species and other organisms at various trophic levels. In the wet season, along with integrated aquaculture, primary production is a large carbon source for higher trophic levels. In the summer months, SGB usually experiences comparatively high light intensity and water temperature, which promote phytoplankton growth. This is reflected by the high chl *a* concentrations we observed in this season and the positive correlation between chl *a* and the $\delta^{13}\text{C}$ of POM that is dominated by phytoplankton (Fig. 6). Similar findings were reported by Lehmann et al. (2004), who showed that an increase in $\delta^{13}\text{C}$ values of POC is associated with increasing primary productivity due to the seasonal environmental conditions, including water temperature and light intensity. The enhanced primary production is connected to the high input of nutrients by freshwater inflow, as indicated by depleted $\delta^{13}\text{C}$ values of POM in the present study. It is possible that zooplankton in this bay feed on terrestrial detritus, which has $\delta^{13}\text{C}$ and $\delta^{15}\text{N}$ values similar to POM. Shellfish are usually considered to derive a large proportion of organic carbon from phytoplankton (Xu & Yang 2007). By identifying the relative con-

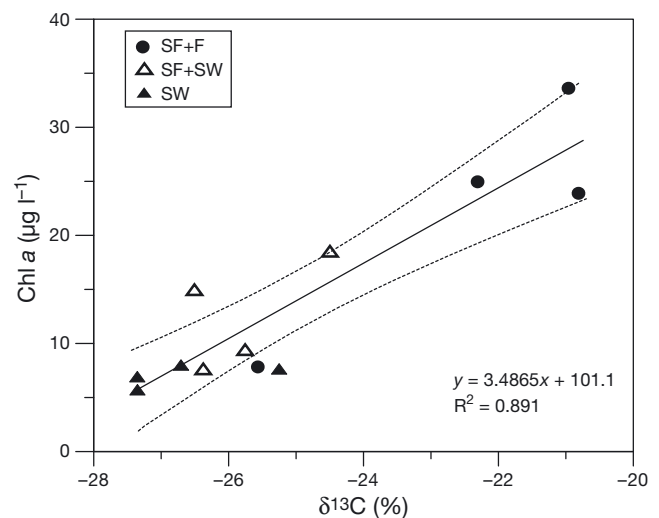


Fig. 6. Relationship between $\delta^{13}\text{C}$ (‰) of particulate organic matter and chlorophyll *a* concentration in 3 different aquaculture areas (see Fig. 1) of Sanggou Bay during the wet season

tribution of aquaculture-derived OM and its impact on water quality, the present study shows that shellfish can be considered to function as biological filters in coastal integrated aquaculture, as was reported previously for land-based integrated aquaculture (Shpigel et al. 1991, Shpigel & Neori 1996). In the coastal area different kinds of POM are present that may serve as a food source for shellfish (oyster and scallop) (Dame 1996). The observed increase in $\delta^{15}\text{N}$ from phytoplankton and POM to omnivorous fish was indicative of the trophic position of the cultured species in SGB: $\delta^{15}\text{N}$ ranged from 6.7‰ for autotrophs to up to 11.2‰ for heterotrophs, reflecting the enrichment in $\delta^{15}\text{N}$ with increasing trophic level. The $\delta^{15}\text{N}$ signatures of primary producers (phytoplankton and seaweed) clearly separated the filter feeders (shellfish) from omnivorous fish (Japanese flounder) (Fig. 4). Some species shared the same trophic level, such as cultured fish and oyster (2.16), but differed in $\delta^{13}\text{C}$ values (fish: $-19.0 \pm 0.2\text{‰}$, oyster: $-21.1 \pm 0.2\text{‰}$; mean \pm SD), indicating that these species are up-taking carbon from different sources. In spite of this, cultured fish showed 2‰ enrichment in $\delta^{13}\text{C}$ from its primary input source of feeding, i.e. trash fish, while oysters also showed a $\delta^{13}\text{C}$ signature similar to trash fish with 0‰ enrichment. In contrast, some species, such as scallop and oyster, showed similar $\delta^{13}\text{C}$ values ($-21.0 \pm 0.1\text{‰}$ and $-21.1 \pm 0.2\text{‰}$ [mean \pm SD], respectively) indicating the same carbon source, but the difference in their $\delta^{15}\text{N}$ values revealed that they belong to different trophic levels (1.52 and 2.16, respectively). Similar findings of the same trophic relationship (i.e. different carbon sources with same trophic level and similar carbon sources with different trophic levels) were reported in Jinghai Bay, China (Feng et al. 2014).

In the present study, scallop showed low $\delta^{15}\text{N}$ isotopic fractionation compared to the average fractionation factor reported elsewhere (3.4; Minagawa & Wada 1984). Several studies have reported low nitrogen fractionation values for shellfish (Raikow & Hamilton 2001, Post 2002, Marin-Leal et al. 2008), suggesting that low $\delta^{15}\text{N}$ enrichment may be due to the specific physiological characteristics of scallops. Moreover, the $\delta^{13}\text{C}$ values of trash fish, seaweed and shellfish were close to each other. We did not collect faeces samples but used an average ($\delta^{13}\text{C} = -21.8\text{‰}$) of respective values from the literature (Table 2). This average value was close to the $\delta^{13}\text{C}$ value of shellfish, suggesting that shellfish in SGB may also use carbon

Table 2. Carbon and nitrogen isotopes signatures of fish faecal material reported in previous literature and resulting average value that was adopted as reference value for this study

Study area	$\delta^{13}\text{C}$ (‰)	$\delta^{15}\text{N}$ (‰)	References
Gokasho Bay, Japan	-24.3	6.3	Yokoyama et al. (2006)
Gokasho Bay, Japan	-24.7	5.6	Yokoyama et al. (2010)
Gokasho Bay, Japan	-20.6	6.2	Yokoyama (2013)
Kat O Bay, Hong Kong	-21.6	4.4	Wai et al. (2011)
Nansha Bay, China	-17.5	7.5	Jiang et al. (2012)
Average	-21.8	6.0	

sources from faecal material released from fish cages, uneaten particles of trash fish and rotten seaweed. Therefore, shellfish cultured in SGB possibly not only help in reducing OM but may also be able to increase the economic benefit and production and survival rate of other species in the IMTA system by maintaining water quality. Based upon stable isotope analysis, a conceptual model of OM flow among the integrated aquaculture species in SGB was established (Fig. 7). The trophic level efficiency was calculated by dividing the $\delta^{13}\text{C}$ and $\delta^{15}\text{N}$ values of one trophic level to the next. POM integrated both phytoplankton and zooplankton and acted as a large source of OM that could be transferred to all the upper trophic levels in the integrated food web structure of SGB. Stable isotope results indicate that scallop and oyster are taking up >80% of the OM from these sources in SGB. Bivalves accumulated approx. 90% of their carbon and 60% of the nitrogen from fish faeces and uneaten particles of trash fish, but during the wet season only; as opposed to the dry season, when shellfish mostly relied on POM, phytoplankton and zooplankton. Feeding on faeces and trash fish remains during the warm wet season probably helped to meet the high metabolic demand of the shellfish in warmer water temperatures. Alternative sources of OM in the dry season at low temperature may be provided through large-scale cultivation of kelp. Kelp culture produces a considerable amount of rotten kelp particles that can serve as a source of OM to shellfish, whereas shellfish would only be provided a minute amount (1%) of OM from *Gracilaria* culture. Omnivorous cultured fish obtained most of their carbon (90%) and nitrogen (60%) from trash fish, while other sources were OM from producers and herbivores. In the food web structure of the cultured species of the present study, shellfish played a crucial role in OM accumulation from various sources. In summary, the water quality of SGB is not impacted by OM generated by caged fish and shellfish culture activities; on the contrary, shellfish

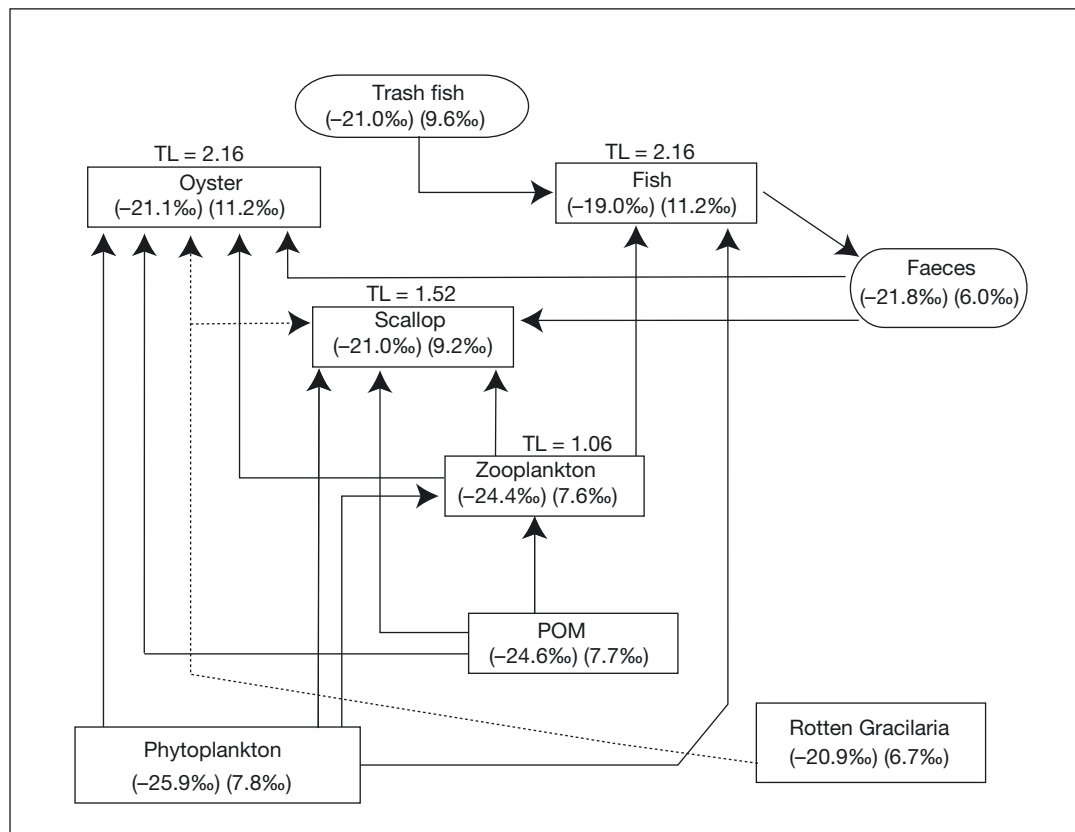


Fig. 7. Conceptual model of carbon flow among the aquaculture species in Sanggou Bay on the basis of stable isotope analysis. Values in parentheses are δ¹³C (first) and δ¹⁵N (second) isotopic signatures (‰) of various species and represent the flow (arrows; dotted arrows originate from rotten *Gracilaria*) from one trophic level (TL) to the next, showing the trophic efficiency. The TL is given for each cultured species

co-culture combined with proximity to the YS to allow for water mixing may be helpful in maintaining the water quality of the bay.

Sources of suspended and sedimentary OM across the bay

In the wet season, higher C/N values (>10) of POM in the SF+F (near coast) and SF+SW (central bay) culture areas indicate the influence of terrestrial OM. The lower C/N ratio in the *Gracilaria* monoculture area (near YS) may indicate the high consumption of nitrogen in this area or mixing with YS water. In the wet season, POM in the SF+F culture area showed higher values of δ¹³C with a decreasing trend towards offshore, indicating OM load in the SF+F near-coast area compared to the other 2 areas. The lower values of δ¹³C towards offshore may have resulted from the presence of degraded OM (Khodse et al. 2007). Another reason could be that high freshwater discharge during the wet season may have resulted

in the rapid distribution of OM to offshore waters, preventing utilization and deposition of OM in the bay. By contrast, the higher values of δ¹⁵N of POM in the SF+F culture area (near-shore area) compared to the central SF+SW and outer SW culture areas may be attributed to nitrate derived from human activities coupled with increased denitrification (Michener & Schell 1994, McClelland et al. 1997, Chanton and Lewis 1999, Miller et al. 2010). The decreasing trend of δ¹⁵N in POM towards the sea suggests an offshore source of nitrogen (Miller et al. 2011). In the wet season, higher values of δ¹³C (-22.4 ‰ to -21.4 ‰) in SOM of 3 culture areas displayed the isotopic signature of marine-derived OM (Wada et al. 1987, Tan et al. 1991, Mishima et al. 1996, Barros et al. 2010). Similar results for SOM δ¹³C were found by Meksumpun et al. (2005) (avg. δ¹³C = -21.0‰) in the Gulf of Thailand, as well as in an earlier study by Gearing et al. (1984), who reported δ¹³C values indicative of a plankton source in SOM, ranging from -22.2 ± 0.6‰ to -20.3 ± 0.6‰ in Narragansett Bay, USA and an average value of -21.0‰ in Malaysian waters. Rela-

tively low values of $\delta^{15}\text{N}$ in SOM of all culture areas in the present study indicate a marine source of the deposited OM. This is supported by an increasing trend of $\delta^{15}\text{N}$ in SOM of the 3 aquaculture areas from shellfish to polyculture to seaweed, suggesting the import of OM from the sea.

In the present study, $\delta^{13}\text{C}$, $\delta^{15}\text{N}$ and C/N of POM are applied to describe OM sources. The $\delta^{13}\text{C}$ of POM in the wet season has either lower or higher values than SOM in the 3 culture areas. Therefore, in the wet season, due to maximum freshwater discharge into the bay, as indicated by a decreasing inshore salinity trend, fluctuations in $\delta^{13}\text{C}$ and $\delta^{15}\text{N}$ values of POM among the stations imply different sources of OM. The results of the present study suggest that during the wet season, OM in SGB originates from 2 sources; marine and terrestrial. Hence to quantify the relative contribution of each source, a 2 end-member mixing model has been applied to the wet season data, using terrestrial and marine end-members values based on the model by Calder & Parker (1968).

The equation used in this model is given as:

$$\text{TC (\%)} = \frac{\delta^{13}\text{C}_{\text{mar}} - \delta^{13}\text{C}_{\text{sam}}}{\delta^{13}\text{C}_{\text{mar}} - \delta^{13}\text{C}_{\text{ters}}} \times 100 \quad (3)$$

where TC is the terrestrial carbon, $\delta^{13}\text{C}_{\text{mar}}$ is the marine end-member, $\delta^{13}\text{C}_{\text{ters}}$ is the terrestrial end-member, and $\delta^{13}\text{C}_{\text{sam}}$ is the measured value of the samples at each station. Generally, terrestrial OM has relatively low values of $\delta^{13}\text{C}$ and $\delta^{15}\text{N}$. Therefore, in our study, $\delta^{13}\text{C}$ (-27.4‰) and $\delta^{15}\text{N}$ (4.7‰) values of POM were selected as terrestrial end-members, which are closer to terrestrial end-member values of $\delta^{13}\text{C}$ and $\delta^{15}\text{N}$ identified in a number of previous studies (Peters et al. 1978, Wada et al. 1987, Middleburg & Nieuwenhuize 1998, Barros et al. 2010). In the present study, mean $\delta^{13}\text{C}$ (-19.0‰) and $\delta^{15}\text{N}$ (9.4‰) values of cultured fish and oyster, respectively, have been selected as marine end-members and are close to the values of Middleburg & Nieuwenhuize (1998). Model results indicated that during the wet season in

SGB, an average of $\sim 72\%$ of OM in POM is derived from the land.

In contrast to the wet season, during the dry season the range and average values of $\delta^{13}\text{C}$ and $\delta^{15}\text{N}$ of POM in all culture areas were within the range of marine-derived OM reported in previous studies (Gearing et al. 1984, Wada & Hattori 1991, Meyers 1997, Lamb et al. 2006). The high C/N values observed among SF+F culture stations might have resulted from the presence of degraded OM (Khodse et al. 2007) due to limited river inflow during the dry season, while in the other 2 culture areas, C/N values were in the range of marine-derived OM (Meyers 1994). SOM of all culture areas was assumed to be derived from suspended matter during the dry season, as indicated by their mean values of $\delta^{13}\text{C}$ (SOM = $-22.4 \pm 0.3\text{‰}$ and POM = $-23.2 \pm 0.6\text{‰}$; ANOVA, $p < 0.05$), revealing material exchange between the 2 different OM pools (Meksumpun et al. 2005).

Comparing both seasons, significant differences were found between $\delta^{13}\text{C}$ and $\delta^{15}\text{N}$ values of SOM and POM (ANOVA, $p < 0.05$). The relatively high values of $\delta^{13}\text{C}$ in SOM showed that SOM in SGB was derived from the same marine source in both seasons. The reason for this could be that sediments were receiving OM from autochthonous sources originating from diatoms, bacteria, and green macroalgae (Gao et al. 2012). The significant difference between SOM and POM in the wet season shows less exchange between the 2 OM pools, the reason being either high freshwater inflow or assimilation of terrestrial-derived OM in the upper water column. In both seasons, the $\delta^{15}\text{N}$ values were also close to those reported for marine-derived OM in previous studies (Gearing et al. 1984, Wada et al. 1991). The comparison of our carbon and nitrogen isotopic signatures of the POM in SGB with that of other bays (Table 3) suggests that the water quality of SGB is not significantly impacted by land-based sources of OM. The

Table 3. Ranges of carbon and nitrogen isotope values of the present study compared to previous values reported in the literature from different coastal areas having aquaculture activities or being impacted by various sources of organic matter. nd: not determined

Study area	Activity / source of impact	$\delta^{13}\text{C}$ (‰)	$\delta^{15}\text{N}$ (‰)	References
Southwestern Thailand	Land-based aquaculture	-27.3 to -20.6	3.1 – 8.4	Kuramoto & Minagawa (2001)
Gaeta Gulf (Mediterranean)	Bivalve and cage culture	-25.0 to -19.8	nd	Mazzola & Sarà (2001)
Kat O Bay, Hong Kong	Land-based aquaculture	-21.2 to -20.1	8.5 – 10.2	Wai et al. (2011)
Simon Bay, South Africa	Anthropogenic	-24.8 to -19.3	nd	Filgueira & Castro (2011)
Kosirina Bay, Croatia	Anthropogenic	nd	4.3 – 8.3	Dolenec et al. (2011)
Sanggou Bay	Bivalve and cage culture	-27.4 to -19.0	4.7 – 9.4	Present study

high production of phytoplankton and the $\delta^{13}\text{C}$ values in all cultured species indicate that the bay acts as source of carbon, and that this carbon is utilized by cultured species and removed from the bay at their harvest. However, the high C/N values indicate that SGB may act as a sink for anthropogenic material (river input).

CONCLUSIONS

In SGB, phytoplankton production is one of the main sources of OM to higher trophic levels during the wet season, as indicated by a positive correlation between $\delta^{13}\text{C}$ and POM, the latter of which containing a large proportion of phytoplankton. Trophic relationships showed that cultured fish and oyster take up carbon from different sources while sharing the same trophic level (2.16). On the other hand, oyster and scallop used the same carbon sources in spite of different trophic levels (2.16 and 1.52 respectively). Based on the results of the stable isotope analysis, our conceptual model for the wet season suggested that ~80% of the OM including faecal material and riverine OM in the form of POM is extracted by oyster and scallop. In the dry season, these species still mainly rely on POM but to some extent also use rotten kelp. C/N values >11 for POM indicate the partly terrestrial origin of OM in SGB; however, in the wet season the bay also functions as a source of carbon due to the high phytoplankton production and aquaculture activities, while high C/N values indicate that SGB may also be a sink of anthropogenic material (river input). Therefore, both culture areas SF+F (avg. C/N = 12.69) and SF+SW (avg. C/N = 13.11) in SGB are highly impacted by OM from river inflow and human activities in the wet season, as indicated by average C/N ratios in POM. In the dry season, POM in the near-shore SF+F culture area showed high C/N values of 11.97 ± 2.08 (mean \pm SD) relative to the other 2 areas with C/N values (<10) indicative of more marine-derived OM. The outer SW culture area (near YS) is highly impacted by YS water. However, C/N values (<10, typical of a marine source) indicate the influence of YS, but the $\delta^{13}\text{C}$ values show the signature of terrestrial OM that may result from river input and degraded OM. Results from the 2 end-member mixing model revealed that for POM an average of 72% OM is derived from land during the wet season. $\delta^{13}\text{C}$ and $\delta^{15}\text{N}$ signatures show that OM in SOM during both the wet and dry seasons is mostly of marine origin. However, a detailed study on terrestrial organic

input from rivers into the SGB is required to better understand the sources of OM and its influence on the water quality of the bay. In addition, studies investigating the role of benthic, non-aquaculture organisms and seagrass could further the understanding of the detailed food web structure of the bay.

Acknowledgements. This study was supported by the Ministry of Science and Technology of China (MoST-China) through 'Sustainability of Marine Ecosystem Production under Multi-stressors and Adaptive Management (MEco-PAM)' Project 973-3 (No. 2011CB409801) in the period of 2011–2015. The authors are very grateful to colleagues from the Ocean University of China and East China Normal University for their help with the fieldwork and laboratory experiment. T.M. thanks the China Scholarship Council (CSC) for providing a PhD scholarship and the National Institute of Oceanography Pakistan for granting study leave and moral support.

LITERATURE CITED

- Alabaster JS (1982) Report of the EIFAC workshop on fish-farm effluents. Silkeborg, Denmark, 26–28 May 1981. EIFAC Tech Rep 41
- Bale A, Morris A (1998) Organic carbon in suspended particulate material in the North Sea: effect of mixing resuspended and background particles. *Cont Shelf Res* 18: 1333–1345
- Barros GV, Martinelli LA, Novais TMO, Ometto JPHB, Zuppi GM (2010) Stable isotopes of bulk organic matter to trace carbon and nitrogen dynamics in an estuarine ecosystem in Babitonga Bay (Santa Catarina, Brazil). *Sci Total Environ* 408:2226–2232
- Bates NR, Dennis A, Hansell DA, Moran SB, Codispoti LA (2005) Seasonal and spatial distribution of particulate organic matter (POM) in the Chukchi and Beaufort Seas. *Deep-Sea Res II* 52:3324–3343
- Buschmann AH, Varela DA, Hernández-González MC, Huovinen P (2008) Opportunities and challenges for the development of an integrated seaweed-based aquaculture activity in Chile: determining the physiological capabilities of *Macrocystis* and *Gracilaria* as biofilters. *J Appl Phycol* 20:571–577
- Calder JA, Parker PL (1968) Stable carbon isotope ratios as indices of petrochemical pollution of aquatic systems. *Environ Sci Technol* 2:535–539
- Chanton JP, Lewis FG (1999) Plankton and dissolved inorganic carbon isotopic composition in a river-dominated estuary: Apalachicola Bay, Florida. *Estuaries* 22:575–583
- Costanzo SD, O'Donohue MJ, Dennison WC, Loneragan NR, Thomas M (2001) A new approach for detecting and mapping sewage impacts. *Mar Pollut Bull* 42:149–156
- Cui Y, Wu Y, Zhang J, Wang N (2012) Potential dietary influence on the stable isotopes and fatty acid compositions of jellyfishes in the Yellow Sea. *J Mar Biol Assoc UK* 92: 1325–1333
- Dame R (1996) Ecology of marine shellfish: an ecosystem approach. CRC Press, Boca Raton, FL
- Dolenec M, Žvab P, Mihelčić G, Lambaša Belak Ž and others (2011) Use of stable nitrogen isotope signatures of anthropogenic organic matter in the coastal environ-

- ment: a case study of the Kosirina Bay (Murter Island, Croatia). *Geol Croatica* 64:143–152
- Duarte C (1995) Submerged aquatic vegetation in relation to different nutrient regimes. *Ophelia* 41:87–112
- Evgenidou A, Valiela I (2002) Response of growth and density of a population of *Geukensia demissa* to land-derived nitrogen loading, in Waquoit Bay, Massachusetts. *Estuar Coast Shelf Sci* 55:125–138
- Fang JG, Funderud J, Qi ZH, Zhang JH, Jiang ZJ, Wang W (2009) Sea cucumbers enhance IMTA system with abalone, kelp in China. *Global Aquacult Advocate* July/August 2009:49–51
- Fang JG, Kuang SH, Sun HL, Sun Y (1996a) Study on the carrying capacity of Sanggou Bay for the culture of scallop *Chlamys farreri*. *Mar Fish Res* 17:18–31 (in Chinese with English Abstract)
- Fang JG, Sun HL, Kuang SH, Sun Y (1996b) Assessing the carrying capacity of Sanggou Bay for culture of kelp *Laminaria japonica*. *Mar Fish Res* 17:7–17 (in Chinese with English Abstract)
- Feng JX, Gao QF, Dong SL, Sun ZL, Zhang K (2014) Trophic relationships in a polyculture pond based on carbon and nitrogen stable isotope analyses: a case study in Jinghai Bay, China. *Aquaculture* 428–429:258–264
- Ferreira G, Andersson HC, Corner RA, Desmit X and others (eds) (2007) SPEAR: sustainable options for people, catchment and aquatic resources. EU 6th framework programme FP6-2002-INCO-DEV-1, IMAR—Institute of Marine Research, Coimbra
- Filgueira R, Castro BG (2011) Study of the trophic web of San Simón Bay (Ría de Vigo) by using stable isotopes. *Cont Shelf Res* 31:476–487
- Gao X, Yang Y, Wang C (2012) Geochemistry of organic carbon and nitrogen in surface sediments of coastal Bohai Bay inferred from their ratios and stable isotopic signatures. *Mar Pollut Bull* 64:1148–1155
- Gearing GN, Gearing PL, Rudnick DT, Requejo AG, Hutchins MJ (1984) Isotope variability of organic carbon in a phytoplankton based temperate estuary. *Geochim Cosmochim Acta* 48:1089–1098
- Gowen RJ, Weston DP, Ervik A (1991) Aquaculture and the benthic environment: a review. In: Cowey CB, Cho CY (eds) *Nutritional strategies and aquaculture waste*. Fish Nutrition Research Laboratory, University of Guelph, Guelph, p 187–205
- Hall POJ, Holby O, Kollberg S, Samuelsson MO (1992) Chemical fluxes and mass balances in a marine fish cage farm. IV. Nitrogen. *Mar Ecol Prog Ser* 89:81–91
- Hayes JM (2004) An introduction to isotopic calculations. Woods Hole Oceanographic Institution, Woods Hole, MA, p 1–10
- Hedges JI, Oades JM (1997) Comparative organic geochemistries of soils and marine sediments. *Org Geochem* 27:319–361
- Holby O, Hall POJ (1991) Chemical fluxes and mass balances in a marine fish cage farm. II. Phosphorus. *Mar Ecol Prog Ser* 70:263–272
- Holligan PM, Harris RP, Newell RC, Harbour DS and others (1984) Vertical distribution and partitioning of organic carbon in mixed, frontal and stratified waters of the English Channel. *Mar Ecol Prog Ser* 14:111–127
- Hu J, Peng P, Jia G, Mai B, Zhang G (2006) Distribution and sources of organic carbon, nitrogen and their isotopes in sediments of the subtropical Pearl River estuary and adjacent shelf, Southern China. *Mar Chem* 98:274–285
- Jiang ZJ, Wang GH, Fang JG, Mao YZ (2012) Growth and food sources of Pacific oyster *Crassostrea gigas* integrated culture with sea bass *Lateolabrax japonicus* in Ailian Bay, China. *Aquacult Int* 21:45–52
- Karakassis I, Tsapakis M, Hatziyanni E, Papadopoulou KN, Plaiti W (2000) Impact of cage farming of fish on the seabed in three Mediterranean coastal areas. *ICES J Mar Sci* 57:1462–1471
- Khodse VB, Fernandes L, Gopalkrishna VV, Bhosle NB, Fernandes V, Matondkar SGP, Bhushan R (2007) Distribution and seasonal variation of concentrations of particulate carbohydrates and uronic acids in the northern Indian Ocean. *Mar Chem* 103:327–346
- Kuramoto T, Minagawa M (2001) Stable carbon and nitrogen isotopic characterization of organic matter in a mangrove ecosystem on the southwestern coast of Thailand. *J Oceanogr* 57:421–431
- Lamb AL, Wilson GP, Leng MJ (2006) A review of coastal palaeoclimate and relative sea-level reconstructions using $\delta^{13}\text{C}$ and C/N ratios in organic material. *Earth Sci* 75: 29–57
- Lehmann M, Bernasconi SM, Mckenzie JA, Barbieri A, Simona M, Veronesi M (2004) Seasonal variation of the $\delta^{13}\text{C}$ and $\delta^{15}\text{N}$ of particulate and dissolved carbon and nitrogen in Lake Lugano: constraints on biogeochemical cycling in a eutrophic lake. *Limnol Oceanogr* 49:415–429
- Marin Leal JC, Dubois S, Orvain F, Galois R, Blin JL and others (2008) Stable isotopes ($\delta^{13}\text{C}$, $\delta^{15}\text{N}$) and modeling as tools to estimate the trophic ecology of cultivated oysters in two contrasting environments. *Mar Biol* 153:673–688
- Mays S (2000) New directions in the analysis of stable isotopes in excavated bones and teeth. In: Cox M, Mays S (eds) *Human osteology in archaeology and forensic science*. Greenwich Medical Media, London, p 425–438
- Mazzola A, Sarà G (2001) The effect of fish farming organic waste on food availability for bivalve molluscs (Gaeta Gulf, Central Tyrrhenian, MED): stable carbon isotopic analysis. *Aquaculture* 192:361–379
- McClelland JW, Valiela I, Michener RH (1997) Nitrogen stable isotope signatures in estuarine food webs: a record of increasing urbanization in coastal watersheds. *Limnol Oceanogr* 42:930–937
- Meksumpun S, Meksumpun C, Hoshika A, Mishima Y, Tanimoto T (2005) Stable carbon and nitrogen isotope ratios of sediment in the gulf of Thailand: evidence for understanding of marine environment. *Cont Shelf Res* 25: 1905–1915
- Meyers PA (1994) Preservation of elemental and isotopic source identification of sedimentary organic matter. *Chem Geol* 114:289–302
- Meyers PA (1997) Organic geochemical proxies of paleoceanographic, paleolimnologic, and paleoclimatic processes. *Org Geochem* 27:213–250
- Michener RH, Schell DM (1994) Stable isotope ratios as tracers in marine aquatic food webs. In: Lajtha K, Michener RH (eds) *Stable isotopes in ecology*. Blackwell Scientific Publications, Oxford, p 138–157
- Middelburg JJ, Nieuwenhuize J (1998) Carbon and nitrogen stable isotopes in suspended matter and sediments from the Schelde Estuary. *Mar Chem* 60:217–225
- Miller TW, Omori K, Hamaoka H, Shibata JY, Hidejiro O (2010) Tracing anthropogenic inputs to production in the Seto Inland Sea, Japan—a stable isotope approach. *Mar Pollut Bull* 60:1803–1809
- Miller TW, Jaquinto G, McGlone M, Isobe A, Shibata JY,

- Hamaoka H, Omori K (2011) Tracing dynamics of organic material flow in coastal marine ecosystems: results from Manila Bay (Philippines) and Kyushu Ingression (Japan). In: Omori K, Guo X, Yoshie N, Fujii N, Handoh IC, Isobe A, Tanabe S (eds) Interdisciplinary studies on environmental chemistry: marine environmental modeling and analysis. Terrapub, Tokyo, p 95–104
- Minagawa M, Wada E (1984) Stepwise enrichment of ^{15}N along food chains: further evidence and the relation between $\delta^{15}\text{N}$ and animal age. *Geochim Cosmochim Acta* 48:1135–1140
- Mishima Y, Hoshika A, Tanimoto T (1996) Movement of terrestrial organic matter in the Osaka Bay, Japan. In: Proc 3rd Int Symp ETERNET-APR: conservation of the hydro-spheric environment, Bangkok, Thailand, 3–4 December 1996. Environmental Research Institute, Chulalongkorn University, Bangkok, p 20–25
- Peters KE, Sweeney RE, Kaplan IR (1978) Correlation of carbon and nitrogen stable isotopes in sedimentary organic matter. *Limnol Oceanogr* 23:598–604
- Pillay TVR (1991) Aquaculture and the environment. Blackwell Scientific, London
- Post DM (2002) Using stable isotopes to estimate trophic position: models, methods, and assumptions. *Ecology* 83: 703–718
- Raikow DF, Hamilton SK (2001) Bivalve diets in a mid-western U.S. stream: a stable isotope enrichment study. *Limnol Oceanogr* 46:514–522
- Redfield AC, Ketchum BH, Richards FA (1963) The influence of organisms on the composition of seawater. In: Hill MN (ed) The sea, Vol 2. Wiley Interscience, New York, NY, p 26–77
- Risk MJ, Erdmann MV (2000) Isotopic composition of nitrogen in stomatopod (Crustacea) tissues as an indicator of human sewage impacts on Indonesian coral reefs. *Mar Pollut Bull* 40:50–58
- Shpigel M, Neori A (1996) The integrated culture of seaweed, abalone, fish and clams in modular intensive land-based systems: I. Proportions of size and projected revenues. *Aquacult Eng* 15:313–326
- Shpigel M, Neori A, Gordin H (1991) Oyster and clam production in the outflow water of marine fish pond in Israel. *EAS Spec Publ* 14:295
- Tan FC, Cai DL, Edmond JM (1991) Carbon isotope geochemistry of the Changjiang Estuary. *Estuar Coast Shelf Sci* 32:395–403
- Vizzini S, Mazzola A (2004) Stable isotope evidence for the environmental impact of a land-based fish farm in the western Mediterranean. *Mar Pollut Bull* 49:61–70
- Vollenweider RA (1992) Coastal marine eutrophication: principles and control. In: Vollenweider RA, Marchetti R, Viviani R (eds) Marine coastal eutrophication. Elsevier, Amsterdam, p 1–20
- Wada E, Hattori A (1991) Nitrogen in the sea: forms, abundances and rate processes. CRC Press, Boca Raton, FL
- Wada E, Minagawa M, Mizutani H, Tsuji T, Imaizumi R, Karasawa K (1987) Biogeochemical studies on the transport of organic matter along the Otsuchi River watershed, Japan. *Estuar Coast Shelf Sci* 25:321–336
- Wada E, Mizutani H, Minagawa M (1991) The use of stable isotopes for food web analysis. *Crit Rev Food Sci Nutr* 30: 361–371
- Wai TC, Leung KMY, Wu RSS, Shin PKS, Cheung SG, Li XY, Lee JHW (2011) Stable isotopes as a useful tool for revealing the environmental fate and trophic effect of open-sea-cage fish farm wastes on marine benthic organisms with different feeding guilds. *Mar Poll Bull* 63:77–85
- Wan RJ, Wu Y, Huang L, Zhang J, Gao L, Wang N (2010) Fatty acids and stable isotopes of a marine ecosystem: study on the Japanese anchovy (*Engraulis japonicus*) food web in the Yellow Sea. *Deep-Sea Res II* 57: 1047–1057
- Xu Q, Yang H (2007) Food sources of three shellfish living in two habitats of Jiaozhou Bay (Qingdao, China): indicated by lipid biomarkers and stable isotope analysis. *J Shellfish Res* 26:561–567
- Ye L, Ritz DA, Fenton GE, Lewis ME (1991) Tracing the influence on sediments of organic waste from a salmonid farm using stable isotope analysis. *J Exp Mar Biol Ecol* 145:161–174
- Yokoyama H (2013) Growth and food source of the sea cucumber *Apostichopus japonicus* cultured below fish cages—potential for integrated multi-trophic aquaculture. *Aquaculture* 372–375:28–38
- Yokoyama H, Abo K, Ikuta K, Kamiyama T, Higano J, Toda S (2006) Country scenarios for ecosystem approaches for aquaculture. 4. Japan. In: McVey JP, Lee CS, O'Bryen PJ (eds) Aquaculture and ecosystems: an integrated coastal and ocean management approach. The World Aquaculture Society, Baton Rouge, LA, p 71–89
- Yokoyama H, Ishihi Y, Abo K, Takashi T (2010) Quantification of waste feed and fish feces using stable carbon and nitrogen isotopes. *Bull Fish Res Agen* 31:71–76
- Zhao J, Zhou S, Sun Y, Fang J (1996) Research on Sanggou Bay aquaculture hydro-environment. *Mar Fish Res* 17: 68–79



Impacts of an integrated multi-trophic aquaculture system on benthic nutrient fluxes: a case study in Sanggou Bay, China

Zhiming Ning¹, Sumei Liu^{1,2,*}, Guoling Zhang¹, Xiaoyan Ning¹, Ruihuan Li^{1,5},
Zengjie Jiang³, Jianguang Fang³, Jing Zhang⁴

¹Key Laboratory of Marine Chemistry Theory and Technology MOE, Ocean University of China/
Qingdao Collaborative Innovation Center of Marine Science and Technology, Qingdao 266100, PR China

²Laboratory of Marine Ecology and Environmental Science, Qingdao National Laboratory for Marine Science
and Technology, Qingdao 266100, PR China

³Key Laboratory of Sustainable Utilization of Marine Fisheries Resources, Ministry of Agriculture,
Yellow Sea Fisheries Research Institute, Chinese Academy of Fishery Sciences, Qingdao 266071, PR China

⁴State Key Laboratory of Estuarine and Coastal Research, East China Normal University, Shanghai 200062, PR China

⁵Present address: State Key Laboratory of Tropical Oceanography, South China Sea Institute of Oceanology,
Chinese Academy of Sciences, Guangzhou 510301, PR China

ABSTRACT: Benthic nutrient fluxes in an integrated multi-trophic aquaculture (IMTA) bay—Sanggou Bay, China—were measured in June and September 2012. The benthic nutrient fluxes and total organic carbon (TOC) of sediment in this IMTA system were significantly lower than in monoculture bays. This was due to the efficient recycling of organic matter in the IMTA system, as revealed by historical data of annual production, dissolved inorganic nitrogen (DIN) concentration in seawater and TOC in sediment. Benthic nutrient fluxes in the IMTA system were mainly controlled by seawater temperature, dissolved oxygen (DO) and nutrient concentrations, which were strongly related to aquaculture activities. In June, the early growth phase of cultured finfish and bivalves contributed little to biodeposition, and benthic nutrient fluxes tended to be from the sediment to the seawater and contributed to algal growth. In September, the active growth of finfish and bivalves resulted in high concentrations of nutrients in the seawater and TOC in the sediment; 64 % of the nitrogen and 25 % of the phosphorus metabolized by bivalves were transferred from the seawater to the sediment.

KEY WORDS: Benthic nutrient fluxes · Pore water · Core incubation · Integrated multi-trophic aquaculture · IMTA · Sanggou Bay

INTRODUCTION

World fisheries and aquaculture production has grown rapidly to meet increasing market demand (FAO 2012), and consequently ecosystem biodiversity, productivity and health of marine organisms have been negatively affected. An approach termed 'integrated multi-trophic aquaculture' (IMTA, Fig. 1) was proposed to mitigate these environmental pressures (Tang & Fang 2012) and was implemented in shallow

coastal bays including the Bay of Fundy (Canada), and Sanggou Bay and Ailian Bay (China) (Troell et al. 2009, Tang & Fang 2012, Chopin 2013). In terms of production and economic performance, the clear benefits of employing IMTA as opposed to monoculture have been reported (Tang & Fang 2012). However, no sufficient evaluation of the environmental effects of IMTA in comparison to monoculture has been made. Despite the increasing recognition that nutrients are fundamental to the food web in aquaculture eco-

*Corresponding author: sumeiliu@ouc.edu.cn

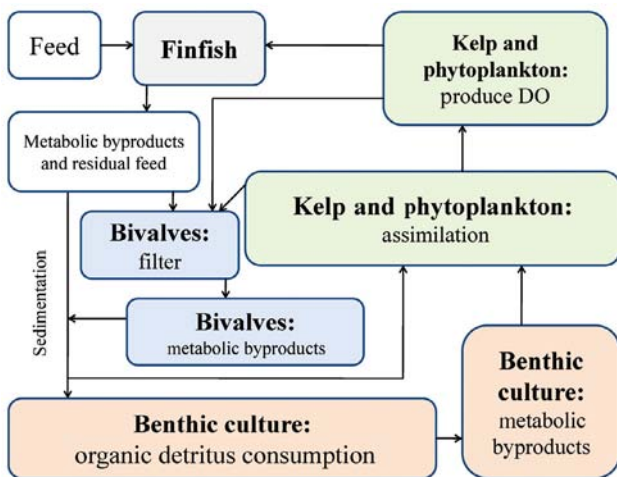


Fig. 1. Diagrammatic representation of the integrated multi-trophic aquaculture (IMTA) system in Sanggou Bay, China, modified from Tang & Fang (2012). DO: dissolved oxygen

systems, information about the internal nutrient cycles in IMTA systems is still unavailable (Sequeira et al. 2008, Troell et al. 2009, Tang & Fang 2012, Chopin 2013). Benthic nutrient regeneration is a significant source of nutrients for primary production in coastal waters (Liu et al. 2003, Sundbäck et al. 2003, Lee et al. 2011). Conversely, nutrients can be stored in the sediments via burial and denitrification (Aller et al. 1985, Song et al. 2013). Hence, an accurate account of nutrient fluxes across the sediment–water interface and the roles of these processes in IMTA systems are of significance to fisheries management.

Many studies have focused on seawater conditions, nutrient uptake efficiency of bivalves, and aquaculture capacity and impacts in Sanggou Bay (Nunes et al. 2003, Mao et al. 2006, Zhang et al. 2009, Lu et al. 2015), but knowledge of the benthic nutrient fluxes in the IMTA system and comparisons of the environmental impacts of IMTA and monoculture are insufficient (Zhang et al. 2006). The aim of this study was to investigate the impacts of aquaculture on benthic nutrient fluxes in the IMTA system, and sedimentary mineralization processes based on nutrient data in pore water, to evaluate the environmental effects of IMTA with respect to benthic nutrient fluxes.

MATERIALS AND METHODS

Study area

Sanggou Bay is a typical IMTA bay located on the western margin of the Yellow Sea (Fig. 2). It is semi-enclosed, with a mean depth of 7.5 m, a total area of 144 km², and a mean salinity of 31 (Zhang et al. 2009). Kelp is cultivated mainly outside the mouth of the bay; bivalves are near the end of the bay. Polyculture of kelp and bivalves occurs centrally between the former 2, and sea cage culture of finfish occurs along the southwest coast. The annual production of kelp, finfish, scallop and oyster were 84 500, 535, 15 000 and 60 000 t in 2012 (the statistical data from the Rongcheng Fishery Technology Extension Sta-

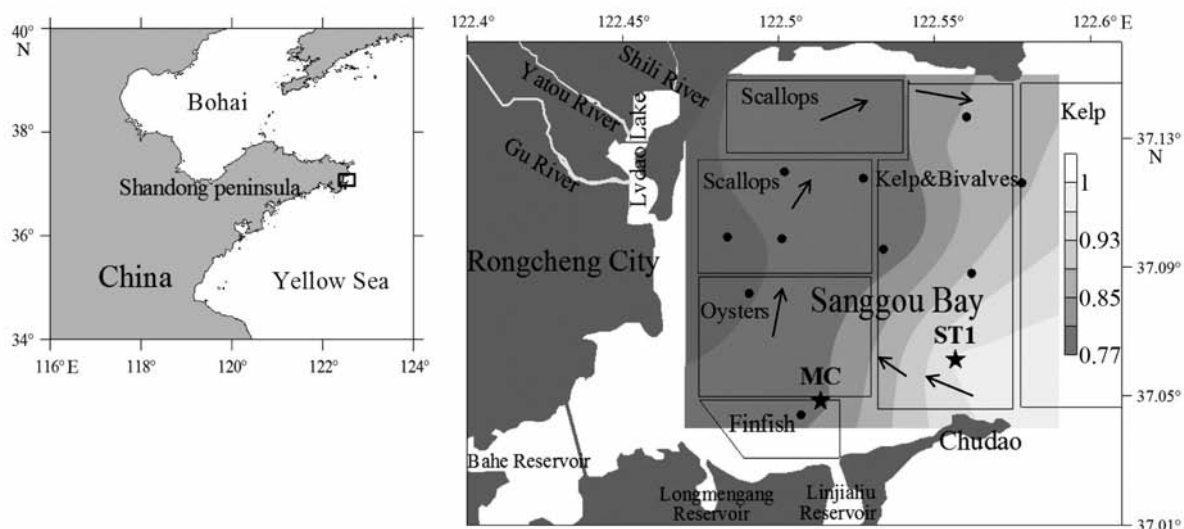


Fig. 2. Aquaculture areas (rectangles, cultured organisms indicated) and study sites in Sanggou Bay, China. ★: stations used for core incubation; ●: stations used for surface sediment sampling. Contours indicate dissolved oxygen saturation levels in bottom seawater in September 2012. Arrows represent current direction at one time of the tidal cycle modified from Bacher et al. (2003)

tion 2012). In an IMTA system (Fig. 1) the bivalves filter suspended particulate matter, including the feces of finfish and phytoplankton; kelp assimilates nutrients from metabolic byproducts generated by the bivalves and finfish, and provides dissolved oxygen (DO) to finfish and bivalves; benthic animals are able to utilize phytoplankton and sedimentary organic detritus from aquaculture occurring in the water column, facilitating maximum nutrient recovery efficiency (Tang & Fang 2012, Chopin, 2013). The sediments are predominantly composed of clayey silt (Zhang et al. 2006).

Seawater and sediment sampling

Field observations were carried out in Sanggou Bay in 2012, 1–2 June and 24–27 September. Surface sediments for analysis of total organic carbon (TOC) and porosity were collected from 12 stations (Fig. 2), and 2 stations located in different aquaculture conditions (polyculture vs. fish culture) were chosen for pore water extraction and core incubation to investigate benthic nutrient fluxes. Diffusion fluxes were derived from the nutrient profiles in original (i.e. at sampling of cores and before incubation) pore water obtained in the field; incubation fluxes were directly measured from core incubation, and sedimentary mineralization processes were evaluated based on nutrient data in pore water before and after incubation.

At each station, bottom seawater was collected using a Plexiglas sampler; sediments were collected using a box-sampler; 2 sediment cores were obtained with Plexiglas tubes (i.d. = 7 cm) and sectioned at 1 or 2 cm intervals within 0.5 h. The resulting sediment sections from one core were put into plastic bag and then frozen at -20°C for later analysis, and sections from the other core were used for pore water extraction (i.e. original pore water). Pore water was extracted and filtered with Rhizon soil moisture samplers (19.21.23F Rhizon CSS) to vacuum tubes (Song et al. 2013) and then frozen at -20°C .

Core incubation

Each core (i.d. = 5 cm) was sealed with a gas-tight lid attached and was pre-incubated in the dark at room temperature (21°C in June and 24°C in September 2012) for 8–12 h in the presence of bottom water recirculated using a peristaltic pump (Song et al. 2015). During the following incubation period the seawater was mixed using a magnetic stirrer turning

a Teflon-coated magnetic stir bar at 60 rpm. At each sampling time, seawater from triplicate cores was sampled for measurement of DO and nutrients, and a sample was taken from the black bucket as a blank. Seawater for nutrient analysis was filtered with a $0.45\text{ }\mu\text{m}$ pore-size syringe filter (Song et al. 2013), and the filtrate was frozen at -20°C . At the first and last sampling time of incubation, sediment cores were sectioned at 2 cm intervals for pore water extraction (i.e. pore water before and after incubation).

Physical and chemical analysis

Each frozen sediment sample was freeze dried (ALPHA 1–4 LD plus freeze dryer; Martin Christ). The water content of the sediment was calculated by determining the weight difference before and after freeze-drying (Song et al. 2013), and porosity was calculated with Berner's equation (Berner 1971). The total organic carbon (TOC) content of sediment was determined using a CHNOS Elemental Analyzer (Vario EL III, Elemental Analyzer) following removal of the carbonate fraction via reaction with $4\text{ mol l}^{-1}\text{ HCl}$; this procedure had a precision $<6\%$ CV (Liu et al. 2010).

Temperature and salinity were measured by a multi-parameter instrument (Multi 350i/SET, WTW GmbH). DO concentration in seawater was measured using the Winkler titration method with a precision better than 0.5% CV (Song et al. 2015). Nutrient concentrations were determined using an autoanalyzer (AutoAnalyzer 3, SEAL Analytical). The measurement precisions for the NO_3^- , NO_2^- , NH_4^+ , PO_4^{3-} , Si(OH)_4 , total dissolved nitrogen (TDN) and total dissolved phosphorus (TDP) analyses were 1, 1, 2, 1, 0.2, 3 and 5% CV, respectively. Dissolved organic phosphorus (DOP) concentration was calculated as TDP concentration minus PO_4^{3-} concentration, and dissolved organic nitrogen (DON) concentration was calculated as TDN concentration minus dissolved inorganic nitrogen (DIN; sum of the NO_3^- , NO_2^- and NH_4^+) concentration.

Flux calculations and statistical analysis

Diffusion fluxes were derived from the nutrient profiles in pore water using Fick's first law of diffusion (Berner 1980, Liu et al. 2003):

$$F = -\phi D_s (\partial C / \partial x)$$

where F is the diffusion flux in $\text{mmol m}^{-2} \text{ d}^{-1}$, ϕ is the porosity of the surface sediment, D_s is the whole

Table 1. Biogeochemical properties of the bottom seawater and the sediment at Stns MC and ST1, during June and September 2012. TOC: total organic carbon; S: salinity; DO: dissolved oxygen; DON: dissolved organic nitrogen; DOP: dissolved organic phosphorus

Date	Stn	Water depth (m)	Porosity in sediment	TOC (%) in sediment	Bottom seawater								
					Temp. (°C)	S	DO saturation (%)	NH ₄ ⁺ (μM)	NO _x ⁻ (μM)	DON (μM)	PO ₄ ³⁻ (μM)	DOP (μM)	Si(OH) ₄ (μM)
Jun 1	MC	9.2	0.70	0.35	17.7	31.1	96.5	1.50	0.19	12.76	0.08	0.21	3.87
Jun 2	ST1	13.8	0.72	0.40	13.8	31.1	97.4	3.23	1.09	21.38	0.27	0.25	3.49
Sep 24	MC	7.8	0.84	0.68	25.0	30.0	79.2	4.14	5.73	28.83	1.19	0.21	24.45
Sep 27	ST1	11.0	0.80	0.62	23.9	29.9	97.5	5.04	5.49	29.59	0.72	0.26	16.31

sediment diffusion coefficient and $\partial C/\partial x$ is the concentration gradient close to sediment–water interface.

Incubation fluxes, which are a direct measure of net solute fluxes across the sediment–water interface, were calculated from the slope of concentrations versus time (Song et al. 2015).

Standard deviation of the linear rate was derived from the slope standard deviation given by the regression statistic; Pearson correlation was applied to discuss the correlation analysis. Statistical significance was judged using the criterion $p < 0.05$. Incubation fluxes were corrected to the *in situ* temperature using the Arrhenius equation (Aller et al. 1985, Song et al. 2015). In the present study, a positive flux (efflux) value represents a flux into the overlying water from the sediment, and a negative flux (influx) value represents a flux into the sediment from the overlying water.

RESULTS

Sediment and bottom seawater parameters

The TOC in surface sediments at both stations in September were approximately twice the level measured in June; porosities had a similar trend to that of TOC and were higher in September than in June but the values were similar at the different stations (Table 1). The bottom seawater temperature in September was higher than in June and was lower at Stn ST1 than at Stn MC because the water was depth greater at the former station. The salinity at both stations in September was slightly lower than in June. The nutrient concentrations in September were higher than in June. The DO concentrations showed saturated conditions at both stations in June, whereas in September the bottom seawater DO concentration was below saturation in the finfish and bivalve culture areas (Fig. 2).

Benthic fluxes from core incubations and their stoichiometric ratios

The DO content decreased linearly over time during incubations, and the linear slopes of the DO–time plots were similar in the various seasons (Fig. 3), although the TOC content was greater in September than in June. However, the higher *in situ* temperature in September resulted in greater DO influxes than in June (Fig. 4). The DO influx at Stn MC was higher than at Stn ST1 in June but was lower at Stn MC than at Stn ST1 in September.

In June, nutrients were released from the sediment to the seawater (the exception was PO₄³⁻, which was transferred from seawater into the sediment), and the magnitudes of benthic nutrient flux at 2 stations were similar (Fig. 5). In September: NH₄⁺ was largely released at Stn MC, but no NH₄⁺ flux was detected at Stn ST1 (Fig. 5a); NO₃⁻ was largely released at Stn ST1 but was transferred to sediment at Stn MC; NO₂⁻ was transferred to sediment at Stn ST1 but was released at Stn MC; DON and TDN were transferred to sediment at both stations (Fig. 5b); PO₄³⁻ was transferred to the sediment at both stations, particularly at Stn MC; DOP was strongly released at Stn MC, while DOP and TDP were transferred to sediments at Stn ST1 (Fig. 5c), and the Si(OH)₄ efflux was less at Stn MC than at Stn ST1 and was lower in September than in June (Fig. 5d). The O₂:DIN flux ratio was higher in September than in June, and the DIN:PO₄³⁻ flux ratio was lower in September than in June, while the Si(OH)₄:DIN flux ratio was higher in September than in June at Stn ST1 but was lower in September than in June at Stn MC (Table 2).

Diffusion fluxes and nutrient profiles in pore water

The concentrations of NH₄⁺, NO_x⁻ (NO₂⁻ + NO₃⁻), PO₄³⁻ and Si(OH)₄ in pore water were measured

Fig. 3. Time course of dissolved oxygen (DO) concentration during incubation at room temperature at Stns MC and ST1 in June and September 2012. O: DO concentration in the control bucket; ●: DO concentration in the water overlying the sediment

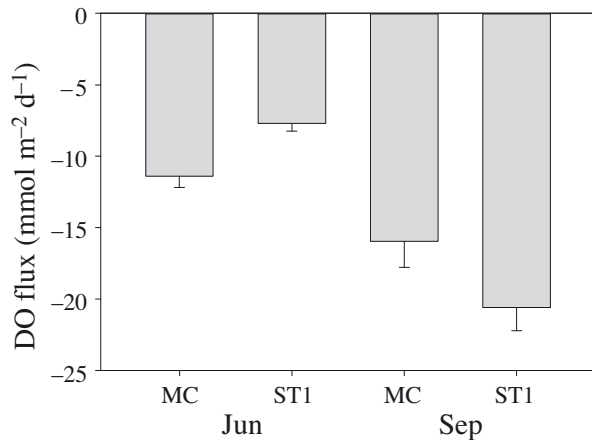
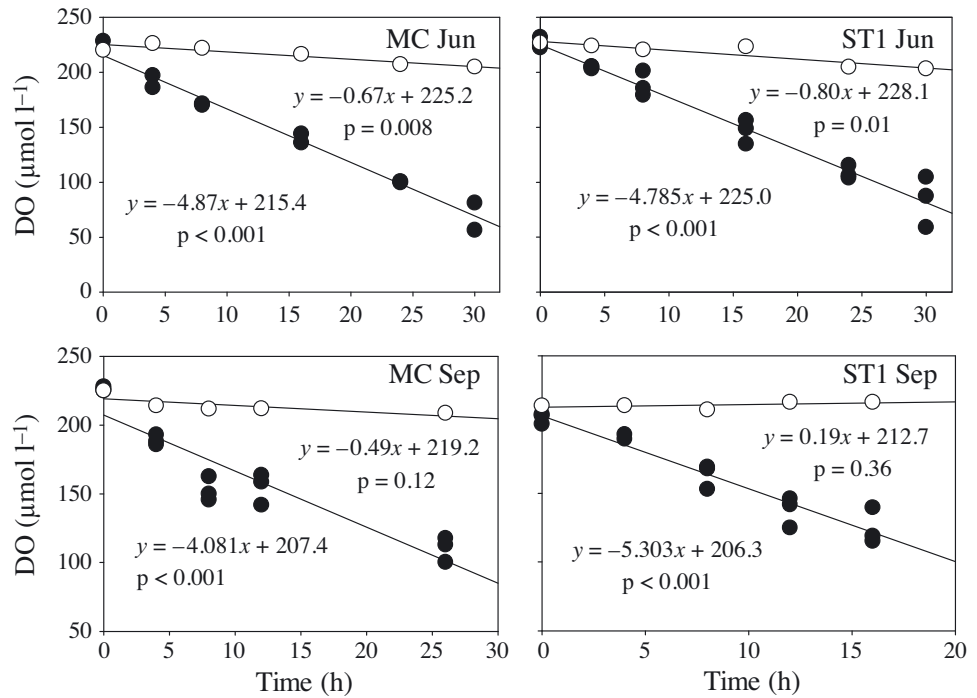


Fig. 4. Temperature-calibrated incubation fluxes of dissolved oxygen (DO) at Stns MC and ST1, during June and September 2012. Error bars show SD

when the core sediments were sampled (original) and before and after incubation (Fig. 6). The nutrient concentrations generally increased with sediment depth; the exception was the NO_x^- concentration. The nutrient diffusion effluxes were supposed to be greater in September than in June as porosities of sediment were higher in September than in June, but the result was opposite. The average diffusion fluxes of DO, NH_4^+ , NO_x^- , PO_4^{3-} and $\text{Si}(\text{OH})_4$ were 1650, 1405, 7, 14 and 932 $\mu\text{mol m}^{-2} \text{d}^{-1}$, respectively, in June and were 6470, 718, -59, 4 and 818 $\mu\text{mol m}^{-2} \text{d}^{-1}$, respectively, in September.

The nutrient profiles of NH_4^+ were substantially greater after incubation, especially at Stn MC, but there was no difference in NH_4^+ concentrations before and after incubation at Stn ST1 in September; NO_x^- was depleted in deep pore water and increased in surface pore water after incubation, but in September the NO_x^- in surface pore water at Stn MC decreased after incubation; there were minor variations in the PO_4^{3-} profiles for surface pore water, but in deep pore water a significant release of PO_4^{3-} was observed after incubation; the differences in $\text{Si}(\text{OH})_4$ concentration before and after incubation were less in September than in June.

DISCUSSION

Environmental factors controlling benthic fluxes

A most important use of DO flux is in the indirect estimation of the total benthic organic carbon mineralization rate (CO_2 flux), which is based on the Redfield ratio; the reported ratio between DO flux and CO_2 flux varies from 0.8 to 1.2, and a $\text{O}_2:\text{C}$ ratio of 1:1 was used in the present study since this ratio has been widely used for studies involving shallow waters (Glud 2008, Song et al. 2015). The quantity and quality of organic matter, temperature, DO concentration and macrofauna abundance have been suggested to be factors controlling benthic DO fluxes

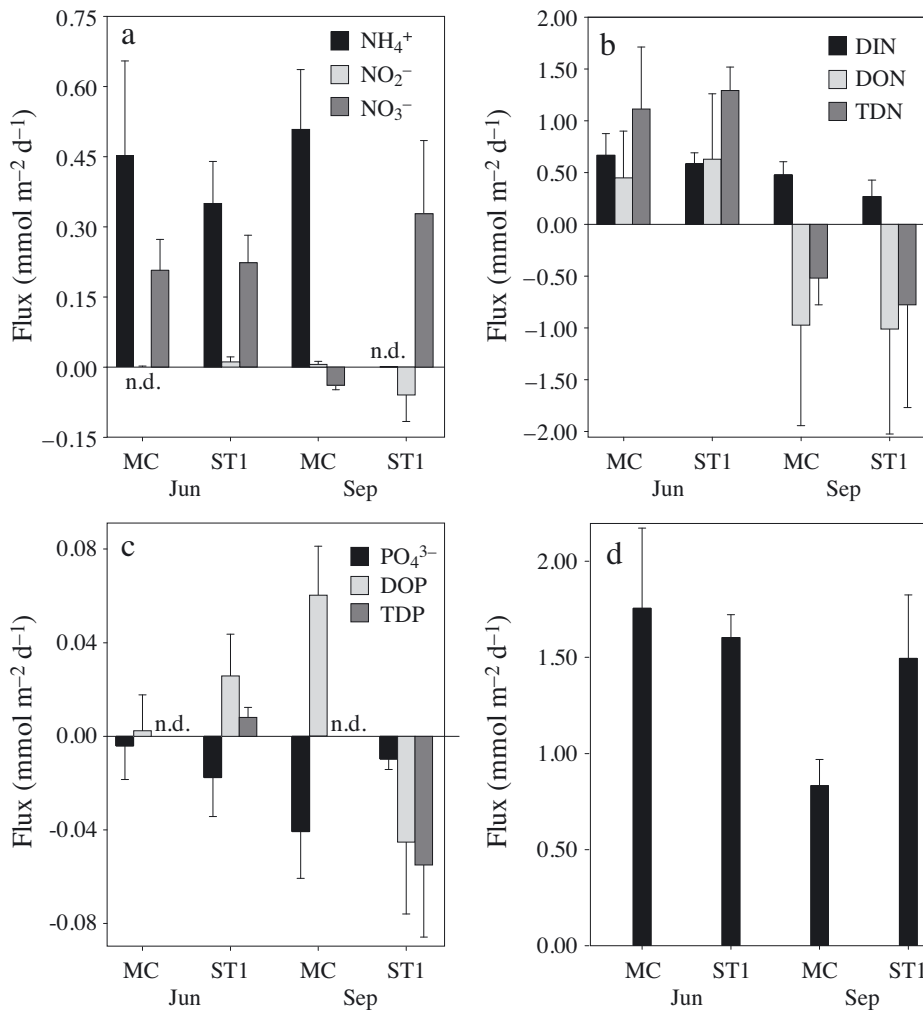


Fig. 5. Incubation fluxes of (a,b) dissolved nitrogen, (c) phosphorus and (d) Si(OH)₄ at Stns MC and ST1 in June and September 2012. Positive flux values denote fluxes into the overlying water from the sediment; negative flux values indicate fluxes into the sediment from overlying water. DIN: dissolved inorganic nitrogen; DON: dissolved organic nitrogen; TDN: total dissolved nitrogen; DOP: dissolved organic phosphorus; TDP: total dissolved phosphorus. n.d.: not detectable. Error bars show SD

(Cowan & Boynton 1996). Benthic DO fluxes were similar under similar incubation temperatures (Fig. 3), although the TOC values were higher in September than in June. The positive correlation between calibrated DO influx (F_{DO}) and seawater temperature (T) ($F_{DO} = -0.99T + 0.36$, $R^2 = 0.79$) indicated that temperature rather than TOC is one factor controlling CO₂ fluxes in Sanggou Bay sediment. This was consistent with another IMTA bay, i.e. Ailian Bay, China, in that the contribution rates of biodeposits by the shellfish

and kelp to the sediments in the IMTA area were very low (Ren et al. 2014), but benthic DO fluxes were positively correlated to TOC sedimentation in monoculture areas (Carlsson et al. 2012). Moreover, the low DO saturation level at Stn MC in September resulted in a lesser DO influx than that of Stn ST1 (Fig. 4), suggesting that DO in bottom seawater is also one factor controlling CO₂ fluxes in Sanggou Bay. Benthic CO₂ fluxes removed 12 and 6% of C input via sedimentation in June and September, respectively, but other parts of the sedimentary matter were mainly transported by horizontal fluxes including bioturbation and resuspension (Fig. 7). In Jiaozhou Bay (China) the polychaete bioturbation resulted in a 25% greater DO flux than that in the absence of bioturbation (Zhang et al. 2006). Hung et al. (2013) also reported resuspension may have contributed 27–93% of the POC flux in the East China Sea. However, the sedimentation fluxes may have been overestimated, as it is possible that their values included materials transported horizontally and re-

Table 2. Stoichiometric ratios of benthic fluxes at Stns MC and ST1, during June and September 2012. PO₄³⁻ fluxes were diffusion fluxes. DIN: dissolved inorganic nitrogen

Date	Stn	O ₂ :DIN	DIN:PO ₄ ³⁻	Si(OH) ₄ :DIN
Jun 1	MC	17	40	3
Jun 2	ST1	13	60	3
Sep 24	MC	33	34	2
Sep 27	ST1	76	17	6

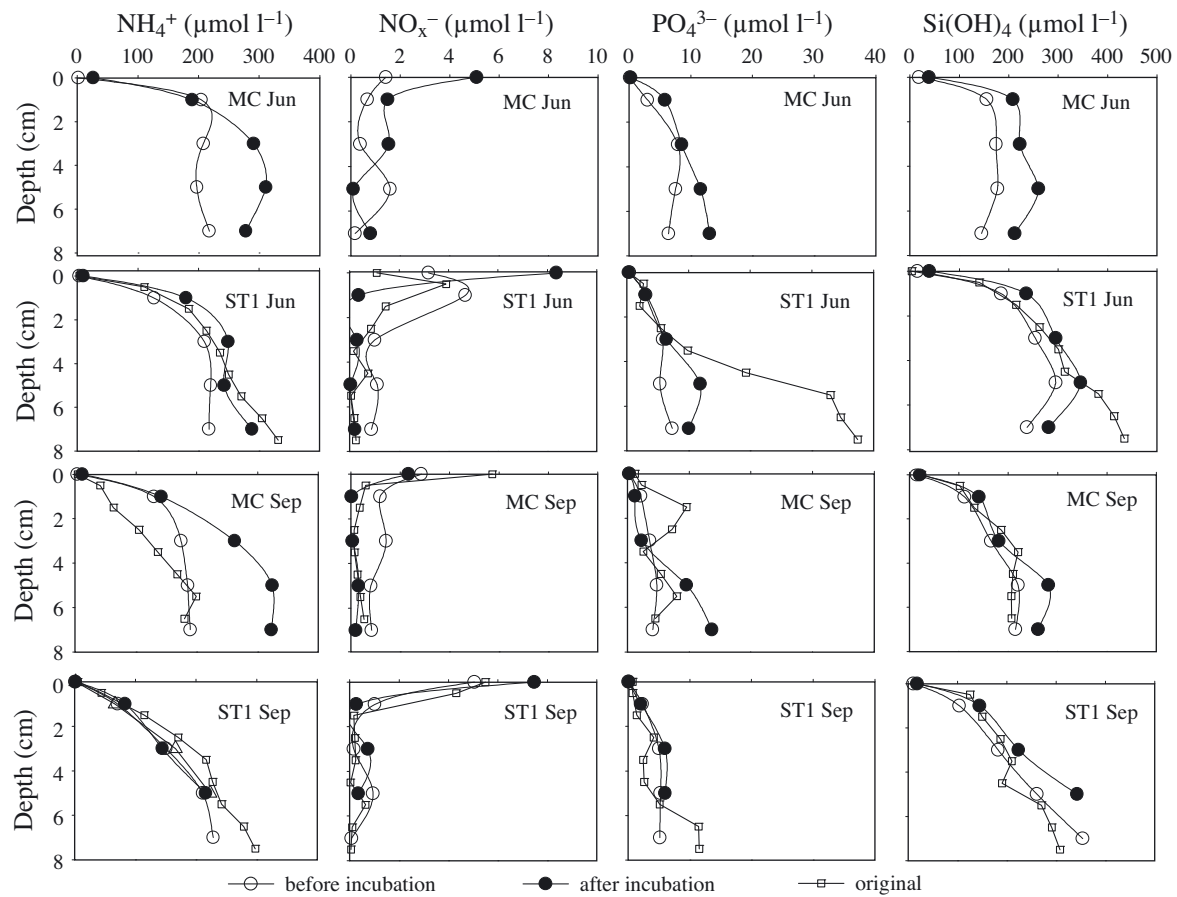


Fig. 6. Nutrient profiles in pore water when the core sediments were sampled (original) and before and after incubation. MC and ST1 are the sampling stations; sampling was done in June and September 2012. Core sediment for original pore water was not sampled at Stn MC in June

mobilized particulates (Hatcher et al. 1994); therefore, these estimated values need confirmation.

Benthic N fluxes are affected by the microbial activities including nitrification and denitrification (Jansen et al. 2012). The elevated O_2 :DIN flux ratio (Table 2) was much higher than the Redfield ratio (i.e. 6.6), which suggests that substantial coupled nitrification–denitrification (Cowan & Boynton 1996) occurred in September. The denitrification rate in Sanggou Bay was $0.19\text{--}0.37\text{ mmol m}^{-2}\text{ d}^{-1}$ (Z. Ning et al. unpubl. data), but the high O_2 :(DIN+N₂) flux ratio (10–29) (which still exceeded the Redfield ratio) indicated that 30–77% of the mineralized NH_4^+ was retained in the Sanggou Bay sediment. The porosity of the sediment should positively relate to the benthic nutrient diffusion flux (Berner 1980); nevertheless, benthic nutrient fluxes were greater in June than in September, although porosity was higher in September than in June (Fig. 7). Although grain size was not determined in this study, grain sizes at different stations should be similar, since the porosities were sim-

ilar at the 2 stations (Table 1). Hence, neither porosity nor grain size were the main factors controlling benthic nutrient fluxes in the IMTA system.

Fluxes of PO_4^{3-} depend on the PO_4^{3-} production rate, the adsorption–desorption equilibrium in the sediment, and the thickness of the diffusion boundary layer at the sediment–water interface (Sundby et al. 1992). Adsorption of PO_4^{3-} by MnO_2 /FeOOH (Woulds et al. 2009) may explain why PO_4^{3-} was transferred to the sediment at both stations (Fig. 5c). Although the N loss by coupled nitrification–denitrification and NH_4^+ adsorption onto clay minerals contributed to the low DIN efflux, the high DIN: PO_4^{3-} flux ratios (Table 2) indicated the degree to which PO_4^{3-} is retained by adsorption in Sanggou Bay. Hence, PO_4^{3-} sorption widely occurred in monoculture (Hyun et al. 2013) and IMTA areas. The DOP fluxes were mainly affected by aquaculture activities (see ‘Aquaculture activities and benthic nutrient fluxes in different seasons’).

The benthic $Si(OH)_4$ fluxes in Sanggou Bay were higher than the nitrogen and phosphorus fluxes

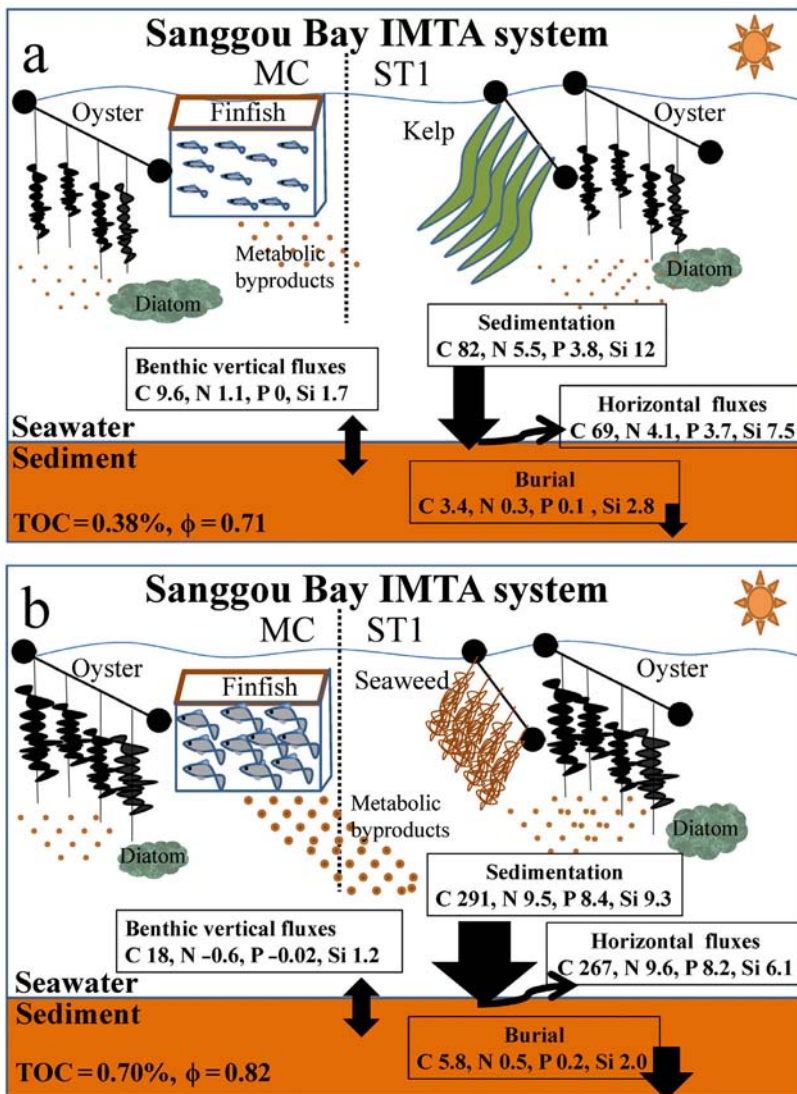


Fig. 7. Sedimentary cycles of C, N, P, Si in (a) June and (b) September 2012 in the Sanggou Bay integrated multi-trophic aquaculture (IMTA) system. Benthic vertical fluxes were measured from core incubation; C fluxes were calculated from the Redfield ratio using dissolved oxygen fluxes. Sedimentation fluxes measured by sediment traps were sourced from Cai et al. (2003); burial fluxes were sourced from Song et al. (2012); horizontal fluxes including resuspension and bioturbation were calculated by difference. All units of fluxes in the boxes are $\text{mmol m}^{-2} \text{d}^{-1}$. IMTA: integrated multi-trophic aquaculture; TOC: total organic carbon; ϕ : porosity of the surface sediment. MC and ST1 are the sampling stations

(Fig. 5). Biogenic silica reaches the sediment surface mainly in the form of skeletons or skeletal fragments of silica-secreting microorganisms (Zabel et al. 1998), and dissolution of sedimentary biogenic silica dominates the dissolved silicate content of pore water (Aller et al. 1985, Liu et al. 2003). Diatoms were predominant in the phytoplankton community in Sanggou Bay (Yuan et al. 2014). Consequently, tempera-

ture and the biomass of diatoms in seawater are the main factors controlling benthic Si(OH)_4 fluxes. The seawater temperature was higher in September than in June, and therefore the Si(OH)_4 fluxes were expected to be higher in September but were found to be higher in June (Fig. 5d). The higher Si(OH)_4 concentration in seawater in September (Table 1) was related to a lesser biomass of diatoms in the seawater, because the abundance of phytoplankton was tightly controlled by filter-feeding oysters (Hyun et al. 2013); therefore, heavy grazing by oysters may result in the reduction of the Si(OH)_4 flux at Stn MC in September. In comparison to other monoculture areas, competition with co-cultivated kelp resulted in lower diatom biomass in the IMTA system (Yuan et al. 2014), resulting in lower benthic Si(OH)_4 fluxes in the IMTA than in monoculture (Table 3).

Aquaculture activities and benthic nutrient fluxes in different seasons

In June the concentrations of nutrients in seawater were quite low because the kelp *Saccharina japonica* assimilated substantial nutrients in spring (Shi et al. 2011), and the metabolic byproducts of finfish and oysters in the early growth stages produced low levels of nutrients in seawater (Fig. 7a). In September the seaweed *Gracilaria lemaneiformis* replaced kelp, and finfish and oysters were in active growth stages and generated large quantities of metabolic byproducts (Fig. 7b). The maximum metabolic rates from Pacific oyster were recorded in July and August (Mao et al. 2006), and

decomposition resulted in high nutrient concentrations in the seawater. In addition to assimilation by kelp, Si(OH)_4 concentration was tightly related to the biomass of diatoms, as diatoms were predominant in the phytoplankton community in Sanggou Bay (Yuan et al. 2014). Hence, ratios of Si(OH)_4 :DIN concentrations were higher in September than in June, especially at Stn MC due to heavy grazing by oysters

(Hyun et al. 2013). When discussing the impacts of aquaculture on benthic nutrient fluxes, it is important to clarify the sources of biodeposits by the marine organisms to the sediments using sediment traps or natural isotopic tracers, etc. However, TOC was not a directly controlling factor of benthic fluxes in an IMTA system as discussed in 'Environmental factors controlling benthic fluxes'; therefore, the sources of biodeposits by the marine organisms to the sediment were not an object of this study.

In June, the decrease in nutrient concentrations in seawater enlarges the concentration gradient in the sediment–water interface, which may result in larger diffusion effluxes (Berner 1980). Hence, all nutrients are released from the sediments to the seawater except PO_4^{3-} , and the effluxes in June were greater than in September (Fig. 5). The benthic effluxes of DIN and Si(OH)_4 contributed 4 and 11 %, respectively, of gross primary productivity (GPP) (including the GPP of kelp). DON can be assimilated by seagrass and macroalgae (Vonk et al. 2008). Assuming DIN and DON released from the sediment was completely consumed by phytoplankton and kelp, the benthic TDN efflux contributed 8 % of GPP. The benthic nutrient contributions to GPP were much smaller than that in the Mandovi Estuary (Pratihary et al. 2009), on the west coast of Sweden (Sundbäck et al. 2003) and in Jinhae Bay (Lee et al. 2011), since substantial cultivation of kelp made the highest contribution to GPP in the IMTA system. If only the GPP of kelp is taken into account, the benthic effluxes of DIN and Si(OH)_4 contributed 7 and 18 % of algal N and Si demands. The low contribution of benthic mineralization may be due to efficient recycling of organic matter in the IMTA system, which will be discussed in 'Benthic nutrient fluxes in different aquaculture modes'. The fact that benthic PO_4^{3-} fluxes made no contribution to GPP in Sanggou Bay is consistent with the finding of Hatcher et al. (1994) that suspended mussel culture had little impact on sediment phosphorus dynamics in Upper South Cove (Nova Scotia, Canada). The sedimentation flux of carbon was $82 \text{ mmol m}^{-2} \text{ d}^{-1}$ in June (Cai et al. 2003), which was much lower than that in September, and therefore the TOC in sediment remained at a low level (0.30 %). With respect to nutrient feedback in pore water (Fig. 6), large amounts of DIN and Si(OH)_4 were generated after incubation, suggesting large potential DIN and Si(OH)_4 effluxes, while the generated PO_4^{3-} was not released to the seawater; the decrease in surface PO_4^{3-} after incubation was probably caused by adsorption by Mn/Fe oxides (Woulds et al. 2009). However, this was offset by the release of DOP.

Table 3. Comparison of benthic fluxes in Sanggou Bay, China, with other regions. Ranges or means \pm SD. TOC: total organic carbon; DO: dissolved oxygen. CO_2 fluxes represent total benthic organic carbon mineralization rate, calculated from the Redfield ratio ($\text{C}:\text{O}_2 = 1:1$) using DO fluxes. DON: dissolved organic nitrogen. nd: no data

Sites	TOC in sediment (%)	Fluxes (mmol m ⁻² d ⁻¹)						References	
		DO	CO ₂	NH ₄ ⁺	NO _x ⁻	DON	PO ₄ ³⁻		Si(OH) ₄
Aquaculture bays									
Sanggou Bay	0.35 to 0.68	-21 to -7.7	7.7 to 21	0 to 0.51	-0.030 to 0.27	-1.01 to 0.63	-0.04 to 0	0.83 to 1.76	Present study
Stn MC	nd	-13 ± 1.0	13 ± 1.0	0.48 ± 0.12	0.090 ± 0.030	-0.26 ± 0.16	-0.02 ± 0.01	1.29 ± 0.22	Present study
Stn ST1	nd	-14 ± 0.86	14 ± 0.86	0.35 ± 0.04	0.25 ± 0.084	-0.19 ± 0.44	-0.01 ± 0.01	1.55 ± 0.18	Present study
Tolo Harbour	nd	-39 to -15	15 to 39	3.3 to 5.9	0.010 to 0.025	0.64 to 1.5	0.070 to 0.098	nd	Chau (2002)
Horsens Fjord	8	-300 to 0	0 to 300	-0.7 to 12	-5 to 0.2	nd	0 to 5	nd	Christensen et al. (2000)
Rio San Pedro creek	1.44 to 2.67	-79 to -16	16 to 79	3.4 to 21.5	-5.0 to 5.6	nd	0.2 to 2.4	0.7 to 10.2	Ferron et al. (2009)
Upper South Cove	7.13	-50 to 10	0 to 50	0 to 30	-2 to 3	-20 to 30	-3 to -2	nd	Hatcher et al. (1994)
Jinhae Bay	1.97 to 4.15	-328 to -58	58 to 328	6 to 41	-5.4 to 0.37	nd	0.90 to 3.0	15 to 45	Lee et al. (2011), Hyun et al. (2013)
Non-aquaculture areas									
East China Sea	0.2 to 0.5	nd	3 to 13	-0.10 to 0.54	-0.04 to 0.02	-1.2 to 0.15	-0.04 to 0	0.55 to 2.6	Qi et al. (2006), Hung et al. (2013)
Yellow Sea	nd	nd	nd	-1.1 to 0	-0.44 to 0.02	-0.42 to 1.3	-0.02 to 0	0.65 to 2.9	Qi et al. (2006)

In September, an intense biodeposition resulted in high levels of TOC accumulation in sediment and high DO and DON influxes (Hatcher et al. 1994). Based on the metabolic rates of NH_4^+ (57 t N) and PO_4^{3-} (11 t P) from the Pacific oyster (Mao et al. 2006) and benthic influxes of TDN and TDP in September, sediment may be able to take up 64 % of the N and 25 % of the P metabolized by oysters. With respect to nutrient feedback in pore water (Fig. 6), at Stn MC the NH_4^+ level in pore water was significantly increased and the NO_x^- was depleted after incubation, which is consistent with high levels of NH_4^+ efflux and NO_x^- influx at high biodeposition sites (Gilbert et al. 1997, Christensen et al. 2000). When NO_x^- is depleted, $\text{MnO}_2/\text{FeOOH}$ were reduced and the adsorption of PO_4^{3-} substantially decreased, which explains why a marked increase in the PO_4^{3-} concentration was observed in deep pore water after incubation at Stn MC. At Stn ST1 there was no obvious increase in the NH_4^+ concentration in pore water after incubation, probably because of the removal of N by coupled nitrification–denitrification or adsorption (discussed in ‘Environmental factors controlling benthic fluxes’).

Benthic nutrient fluxes in different aquaculture modes

Increased biodeposits produced by the actively growing animals can result in a substantial increase in the organic content of sediment (Hatcher et al. 1994, Christensen et al. 2000, Ferrón et al. 2009, Lee et al. 2011); the mineralization of sedimentation can release substantial nutrients from the sediment to the seawater, which may result in the deterioration of seawater quality (Chau 2002). Hence, the TOC in the sediment and benthic effluxes of nutrients in traditional aquaculture areas were extremely high (Table 3). Monoculture was implemented in Sanggou Bay in the 1970s; the extremely high TOC in the sediment and the low DIN concentration in the seawater may have resulted in great benthic nutrient fluxes in this monoculture period (Fig. 8). Since 1980 the introduction of polyculture in Sanggou Bay has resulted in the reduction of TOC in the sediment (Song et al. 2012). And the high DIN concentration in the seawater indicated that substantial organic matter was recycling in the seawater during the polyculture period. The efficient recycling of organic matter and nutrients explains why the TOC of sediment and

the benthic effluxes in Sanggou Bay were significantly less than in other monoculture areas. During the polyculture period, the annual gross yield of seafood increased especially in the 2000s, and the proportion of different species changed continuously so that the optimal aquatic environment was obtained (Zhang et al. 2009). Once the IMTA was widely implemented in Sanggou Bay, the DIN concentration dropped to a moderate level; the TOC of sediment and the benthic effluxes in Sanggou Bay are comparable with that in non-aquaculture areas such as the East China Sea (Table 3), though substantial aquaculture activities have been implemented in Sanggou Bay.

In Sanggou Bay, the benthic mineralization rates (CO_2 fluxes) at the 2 different stations were similar, but the benthic nutrient fluxes were different, which reflected the impacts of different aquaculture modes (Table 3). In September, DO was at near saturation levels at Stn ST1 (polyculture area of kelp and oyster) but below saturation at Stn MC (the fish culture area, and near the oyster area) (Fig. 2; contours of DO saturation); the lower DO level at Stn MC led to an increase in the NH_4^+ efflux and a decrease in the NO_x^- efflux. Hyun et al. (2013) reported DO concentrations less than saturation in bottom waters at an oyster farm, presumably because of the combination of DO consumption at the sediment–water interface and the dense suspended culture that limits seawater exchange and the replenishment of DO. Conversely, at Stn ST1, DO provided by kelp helps to maintain the DO saturation level. Hence, greater NO_x^- efflux was observed at Stn ST1 than at Stn MC. The influxes of DON and PO_4^{3-} were higher at Stn MC

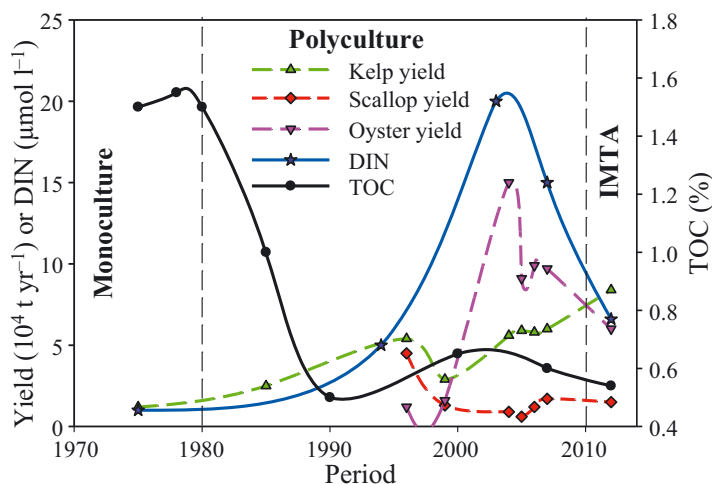


Fig. 8. Historical data of yield, dissolved inorganic nitrogen (DIN) concentration in seawater and total organic carbon (TOC) in sediment, which were sourced from Zhang et al. (2009), Li et al. (2016, this Theme Section) and Song et al. (2012), respectively. IMTA: integrated multi-trophic aquaculture

than at Stn ST1, probably due to the greater metabolic rates from bivalves in the oyster culture area than in the polyculture area of kelp and oyster (Cai et al. 2003). More filtration of diatoms by bivalves in the oyster culture than in the kelp and oyster polyculture area may explain why Si(OH)_4 efflux at Stn MC was lower than at Stn ST1.

In summary, the benthic nutrient fluxes were significantly lower in the IMTA system than in other monoculture areas and were impacted by DO levels at different culture stations rather than by sedimentary TOC generated from aquaculture species. Seasonal variations in benthic fluxes were controlled by temperature and nutrient concentrations related to aquaculture.

Acknowledgements. This study was supported financially by the Ministry of Science & Technology of China (2011 CB409802) and the National Science Foundation of China (40925017). Additional financial support was provided by SKLEC/ECNU for TOC determination. We sincerely thank Senlin Wang, Director of the Chudao Fisheries Corporation, for his cooperation, and thank Guodong Song, Xuming Kang, Shuhang Dong and Mingshuang Sun for their help in the field. We are grateful to the 3 anonymous reviewers and the editor for their comments.

LITERATURE CITED

- Aller RC, Mackin JE, Ullman WJ, Wang CH and others (1985) Early chemical diagenesis, sediment–water solute exchange, and storage of reactive organic matter near the mouth of the Changjiang, East China Sea. *Cont Shelf Res* 4:227–251
- Bacher C, Grant J, Hawkins AJS, Fang JG, Zhu MY, Besnard M (2003) Modelling the effect of food depletion on scallop growth in Sungo Bay (China). *Aquat Living Resour* 16:10–24
- Berner RA (1971) Principles of chemical sedimentology. McGraw-Hill, New York, NY
- Berner RA (1980) Early diagenesis: a theoretical approach. Princeton University Press, Princeton, NJ
- Cai LS, Fang JG, Liang XM (2003) Natural sedimentation in large-scale aquaculture areas of Sungo Bay, north China Sea. *J Fish Sci China* 10:305–310 (in Chinese with English Abstract)
- Carlsson MS, Engström P, Lindahl O, Ljungqvist L, Petersen JK, Svanberg L, Holmer M (2012) Effects of mussel farms on the benthic nitrogen cycle on the Swedish west coast. *Aquacult Environ Interact* 2:177–191
- Chau KW (2002) Field measurements of SOD and sediment nutrient fluxes in a land-locked embayment in Hong Kong. *Adv Environ Res* 6:135–142
- Chopin T (2013) Aquaculture, integrated multi-trophic (IMTA). In: Christou P, Savin R, Costa-Pierce B, Misztal I, Whitelaw B (eds) Sustainable food production. Springer, New York, NY, p 184–205
- Christensen PB, Rysgaard S, Sloth NP, Dalsgaard T, Schwærter S (2000) Sediment mineralization, nutrient fluxes, denitrification and dissimilatory nitrate reduction to ammonium in an estuarine fjord with sea cage trout farms. *Aquat Microb Ecol* 21:73–84
- Cowan JLW, Boynton WR (1996) Sediment–water oxygen and nutrient exchanges along the longitudinal axis of Chesapeake Bay: seasonal patterns, controlling factors and ecological significance. *Estuaries* 19:562–580
- FAO (Food and Agriculture Organization of the United Nations) (2012) The state of world fisheries and aquaculture. FAO, Rome
- Ferrón S, Ortega T, Forja JM (2009) Benthic fluxes in a tidal salt marsh creek affected by fish farm activities: Río San Pedro (Bay of Cádiz, SW Spain). *Mar Chem* 113:50–62
- Gilbert F, Souchu P, Bianchi M, Bonin P (1997) Influence of shellfish farming activities on nitrification, nitrate reduction to ammonium and denitrification at the water–sediment interface of the Thau lagoon, France. *Mar Ecol Prog Ser* 151:143–153
- Glud RN (2008) Oxygen dynamics of marine sediments. *Mar Biol Res* 4:243–289
- Hatcher A, Grant J, Schofield B (1994) Effects of suspended mussel culture (*Mytilus* spp.) on sedimentation, benthic respiration and sediment nutrient dynamics in a coastal bay. *Mar Ecol Prog Ser* 115:219–235
- Hung CC, Tseng CW, Gong GC, Chen KS, Chen MH, Hsu SC (2013) Fluxes of particulate organic carbon in the East China Sea in summer. *Biogeosciences* 10:6469–6484
- Hyun JH, Kim YT, Mok JS, Lee JS, An SU, Lee WC, Jung RH (2013) Impacts of long-line aquaculture of Pacific oysters (*Crassostrea gigas*) on sulfate reduction and diffusive nutrient flux in the coastal sediments of Jinhae–Tongyeong, Korea. *Mar Pollut Bull* 74:187–198
- Jansen HM, Verdegem MCJ, Strand Ø, Smaal AC (2012) Seasonal variation in mineralization rates (C–N–P–Si) of mussel *Mytilus edulis* biodeposits. *Mar Biol* 159:1567–1580
- Lee JS, Kim YT, Shin KH, Hyun JH, Kim SY (2011) Benthic nutrient fluxes at longline sea squirt and oyster aquaculture farms and their role in coastal ecosystems. *Aquacult Int* 19:931–944
- Li R, Liu S, Zhang J, Jiang Z, Fang J (2016) Sources and export of nutrients associated with integrated multi-trophic aquaculture in Sanggou Bay, China. *Aquacult Environ Interact* 8:285–309
- Liu SM, Zhang J, Jiang WS (2003) Pore water nutrient regeneration in shallow coastal Bohai Sea, China. *J Oceanogr* 59:377–385
- Liu SM, Zhu BD, Zhang J, Wu Y and others (2010) Environmental change in Jiaozhou Bay recorded by nutrient components in sediments. *Mar Pollut Bull* 60:1591–1599
- Lu JC, Huang LF, Luo YR, Xiao T, Jiang ZJ, Wu LN (2015) Effects of freshwater input and mariculture (bivalves and macroalgae) on spatial distribution of nanoflagellates in Sungo Bay, China. *Aquacult Environ Interact* 6:191–203
- Mao YZ, Zhou Y, Yang HS, Wang RC (2006) Seasonal variation in metabolism of cultured Pacific oyster, *Crassostrea gigas*, in Sanggou Bay, China. *Aquaculture* 253:322–333
- Nunes JP, Ferreira JG, Gazeau F, Lencart-Silva J, Zhang XL, Zhu MY, Fang JG (2003) A model for sustainable management of shellfish polyculture in coastal bays. *Aquaculture* 219:257–277
- Pratihary AK, Naqvi SWA, Naik H, Thorat BR, Narvenkar G, Manjunatha BR, Rao VP (2009) Benthic fluxes in a tropical estuary and their role in the ecosystem. *Estuar Coast Shelf Sci* 85:387–398
- Qi XH, Liu SM, Zhang J (2006) Sediment–water fluxes of nutrients in the Yellow Sea and the East China Sea. *Mar*

- Sci 30:9–15 (in Chinese with English Abstract)
- Ren L, Zhang J, Fang J, Tang Q, Zhang M, Du M (2014) Impact of shellfish biodeposits and rotten seaweed on the sediments of Ailian Bay, China. *Aquacult Int* 22:811–819
 - Sequeira A, Ferreira JG, Hawkins AJS, Nobre A and others (2008) Trade-offs between shellfish aquaculture and benthic biodiversity: a modelling approach for sustainable management. *Aquaculture* 274:313–328
 - Shi J, Wei H, Zhao L, Yuan Y, Fang JG, Zhang JH (2011) A physical–biological coupled aquaculture model for a suspended aquaculture area of China. *Aquaculture* 318: 412–424
 - Song XL, Yang Q, Sun Y, Yin H, Jiang SL (2012) Study of sedimentary section records of organic matter in Sanggou Bay over the last 200 years. *Acta Oceanol Sin* 34: 120–126 (in Chinese with English Abstract)
 - Song GD, Liu SM, Marchant H, Kuypers MMM, Lavik G (2013) Anammox, denitrification and dissimilatory nitrate reduction to ammonium in the East China Sea sediment. *Biogeosciences* 10:6851–6864
 - Song GD, Liu SM, Zhu ZY, Zhai WD, Zhu CJ, Zhang J (2015) Sediment oxygen consumption and benthic organic carbon mineralization on the continental shelves of the East China Sea and the Yellow Sea. *Deep-Sea Res II*, doi: 10.1016/j.dsr2.2015.04.012
 - Sundbäck K, Miles A, Hulth S, Pihl L, Engström P, Selander E, Svenson A (2003) Importance of benthic nutrient regeneration during initiation of macroalgal blooms in shallow bays. *Mar Ecol Prog Ser* 246:115–126
 - Sundby B, Gobeil C, Silverberg N, Mucci A (1992) The phosphorus cycle in coastal marine sediments. *Limnol Oceanogr* 37:1129–1145
 - Tang QS, Fang JG (2012) Review of climate change effects in the Yellow Sea large marine ecosystem and adaptive actions in ecosystem based management. In: Sherman K, McGovern G (eds) *Frontline observations on climate change and sustainability of large marine ecosystems*. UNDP, New York, NY, p 170–187
 - Troell M, Joyce A, Chopin T, Neori A, Buschmann AH, Fang JG (2009) Ecological engineering in aquaculture—potential for integrated multi-trophic aquaculture (IMTA) in marine offshore systems. *Aquaculture* 297:1–9
 - Vonk JA, Middelburg JJ, Stapel J, Bouma TJ (2008) Dissolved organic nitrogen uptake by seagrasses. *Limnol Oceanogr* 53:542–548
 - Woulds C, Schwartz MC, Brand T, Cowie GL, Law G, Mowbray SR (2009) Porewater nutrient concentrations and benthic nutrient fluxes across the Pakistan margin OMZ. *Deep-Sea Res II* 56:333–346
 - Yuan ML, Zhang CX, Jiang ZJ, Guo SJ, Sun J (2014) Seasonal variations in phytoplankton community structure in the Sanggou, Ailian, and Lidao Bays. *J Ocean Univ China* 13:1012–1024
 - Zabel M, Dahmke A, Schulz HD (1998) Regional distribution of diffusive phosphate and silicate fluxes through the sediment–water interface: the eastern South Atlantic. *Deep-Sea Res I* 45:277–300
 - Zhang XL, Zhu MY, Chen S, Grant J, Martin JLM (2006) Study on sediment oxygen consumption rate in the Sanggou Bay and Jiaozhou Bay. *Adv Mar Sci* 24:91–96 (in Chinese with English Abstract)
 - Zhang JH, Hansen PK, Fang JG, Wang W, Jiang ZJ (2009) Assessment of the local environmental impact of intensive marine shellfish and seaweed farming—application of the MOM system in Sungo Bay, China. *Aquaculture* 287:304–310

*Editorial responsibility: Simone Mirto, (Guest Editor)
Castellammare del Golfo, Italy*

*Submitted: May 8, 2015; Accepted: July 30, 2015
Proofs received from author(s): October 6, 2015*



Reduced inorganic sulfur in sediments of the mariculture region of Sanggou Bay, China

Xuming Kang¹, Sumei Liu^{1,2,*}, Xiaoyan Ning¹

¹Key Laboratory of Marine Chemistry Theory and Technology MOE, Ocean University of China/
Qingdao Collaborative Innovation Center of Marine Science and Technology, Qingdao 266100, PR China

²Laboratory of Marine Ecology and Environmental Science,
Qingdao National Laboratory for Marine Science and Technology, Qingdao, PR China

ABSTRACT: Reduced inorganic sulfur (RIS) and organic matter (OM) in a mariculture region (Sanggou Bay, China; SGB) and at a reference station without mariculture were determined to assess the influence of mariculture on sulfide accumulation and the benthic environment. To this end, sediment acid-volatile sulfide (AVS), pyrite sulfur (pyrite-S), elemental sulfur (ES), OM, porosity, reactive iron, and pore water sulfate were measured. The results indicate that the concentration of RIS was negatively correlated with dissolved oxygen concentration. Principal component analysis showed that sulfide distribution was influenced by sediment porosity, OM, and reactive iron concentration. In addition, sulfide distribution was influenced by water current and water depth. More sulfide content accumulated at an oyster monoculture site than at a scallop/kelp polyculture site and a kelp monoculture site. We found no significant difference in ES concentration among the 3 mariculture types. While no significant influence on benthic OM accumulation was observed, except slightly enhanced reactivity of the OM (making it easily decomposable), mariculture activities in SGB significantly promoted sulfide accumulation compared to the reference station. However, there was no potential threat of toxic sulfide to the benthic biomass in SGB.

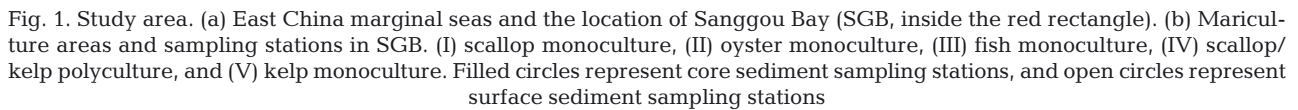
KEY WORDS: Acid volatile sulfide · Pyrite-S · Elemental sulfur · Sediment · Mariculture · Sanggou Bay

INTRODUCTION

World aquaculture output increased continuously from 1950 to 2011, and now accounts for 41.3% of the global supply of fish, crustaceans, and mollusks (FAO 2012). However, despite improved production efficiency, scallop and oyster mariculture generates massive quantities of biological deposits enriched with organic matter (OM) (Carlsson et al. 2009). The accumulation of these organic-rich deposits in sediments of mariculture regions stimulates benthic mineralization and oxygen depletion (Carlsson et al. 2009), and consequently promotes dissimilatory sulfate reduction. Major environmental and ecological

issues arising from sulfate reduction include the accumulation of toxic sulfide (e.g. H₂S), acid-volatile sulfide (AVS), pyrite sulfide (pyrite-S), and elemental sulfur (ES) in the impacted sediments (Otero et al. 2006, Gao et al. 2013) and nutrient release to the overlying water (Hyun et al. 2013). The toxic sulfide can threaten benthic macrofauna and its diversity (Yokoyama 2003). Moreover, the dissolved sulfide in sediments is highly reactive and is rapidly re-oxidized by oxygen, nitrate, or oxidized Fe and Mn, resulting in the deterioration of anoxic conditions. In addition, studies of reduced inorganic sulfur (RIS, e.g. AVS, pyrite-S, and ES) in sediments can contribute to better understanding of benthic miner-

*Corresponding author: sumeiliu@ouc.edu.cn



Environmental responses of Sanggou Bay (SGB), Shandong Province, China, to mariculture have received more attention in recent years (Zhang et al. 2009), including nutrient conditions and benthic nutrient fluxes (Sun et al. 2010, Ning et al. 2016, this Theme Section), natural sedimentation (Cai et al. 2003), and phytoplankton (Lu et al. 2015). However, reports about the impact of mariculture on benthic biogeochemistry, especially sulfur chemistry in SGB, still remains poor. Considering that the concentration and distribution of RIS species are strongly influenced by OM inputs and thus by mariculture, high concentrations of AVS, pyrite-S, and ES in sediments receiving high OM inputs may be well coupled to each other, and the spatial coupling may be used to trace mariculture influence. To test this hypothesis,

SGB, a semi-enclosed bay located in the western Yellow Sea (YS) (Fig. 1a), occupies a total area of approximately 144 km² and has a mean depth of 7.5 m. SGB is the most important integrated multi-trophic aquaculture location in northern China. Suspended multi-species aquaculture of Farrer's scallop *Chlamys farreri*, Pacific oyster *Crassostrea gigas*, and kombu kelp *Saccharina japonica* is well developed in SGB, occupying almost 67% of the total aquaculture area (Zhang et al. 2009), and annually supplies 15 000 and 84 500 t of scallop and kelp, respectively. Three mariculture models for scallop and kelp are currently employed in SGB, viz. monoculture of scallop, monoculture of kelp,

and polyculture of scallop/kelp. The scallop-dominant polyculture system was implemented to maximise economic gains from aquaculture. The culture ratio for scallop and kelp is 2:1, and details of the maricultural facilities can be found in Fang et al. (1996). Mariculture densities for scallop and kelp are reduced to 2/3 and 2/5 compared to their monoculture densities, respectively. Biodeposition rates have increased rapidly along with the expansion of maricultural activities, and can be up to $278.8 \text{ g m}^{-2} \text{ d}^{-1}$ (Cai et al. 2003). In integrated multi-trophic aquaculture systems, kelp assimilates nutrients and CO_2 , converting them into potentially valuable biomass. Scallop cultivation can stimulate carbon migration from the water column to the sediment through filter-feeding and biodeposition (Chopin et al. 2008). Thus, SGB provides an excellent opportunity to investigate the influence of integrated multi-trophic aquaculture systems on RIS in sediments.

Sampling

Field expeditions aboard the RV 'Lurong Fisher 65580' were conducted during April 2013 in SGB. To elucidate the impacts of mariculture on RIS accumulation, 27 surface and 2 core sediments in different mariculture regions were sampled using a box corer (Fig. 1b), and a station without mariculture in the YS from Kang et al. (2014) was selected as a reference station (Stn A02; Fig. 1a). The physico-chemical characteristics were fairly similar between SGB and the YS. Previous studies showed that the nutrient conditions (Sun et al. 2010), OM and biogenic elements (e.g. matrix-bound phosphine) (Li et al. 2010), and total organic carbon (TOC) concentrations in sediment and benthic effluxes in SGB (Ning et al. 2016) are comparable to those in the YS. During the sampling process, each sediment core was sectioned on board in a nitrogen atmosphere (to prevent oxidation) at 1 cm intervals in the top 10 cm, and at 2 cm intervals in the remainder of the core (cores from Stn MC were sectioned only at 2 cm intervals for pore water extraction). The subsamples were immediately placed in plastic ziplock bags with air excluded. Pore water was extracted using Rhizon soil moisture samplers (Liu et al. 2011) and placed in polypropylene plastic bottles. All samples were stored in the dark at -20°C (Lasorsa & Casas 1996) and analyzed immediately upon return to the laboratory. The near-bottom water (1 m distance to bottom) was sampled for temperature and salinity determination.

Analyses

Temperature and salinity of near-bottom water were determined *in situ* using a multi-parameter water quality analyzer (Multi 350i, WTW). The concentration of dissolved oxygen (DO) in near-bottom water was measured using the Winkler titration method (Bryan et al. 1976). OM content in sediments was determined by weight loss upon ignition of the dried sediment at 550°C for 4 h (Santisteban et al. 2004), with a precision (relative standard deviation, RSD) of 1.0% ($n = 5$). Porosity was determined by weight change before and after freeze-drying the sediment. The determination of reactive Fe (Fe_R) followed Zhu et al. (2012), using 0.2 g of dry sediment with 25 ml of 50 g l^{-1} sodium dithionite (buffered with 0.2 M sodium citrate and 0.35 M acetic acid to pH 4.8), and shaking for 2 h for Fe_R extraction. The extracts were measured by inductively coupled plasma-atomic emission spectrometry (Thermo 6300). The relative deviations of parallel determinations were less than 5.0% ($n = 5$). The RIS concentration in sediments comprised the combined concentrations of AVS, pyrite-S, and ES, which were measured using the cold diffusion method followed by iodometric titration of the sulfide collected in alkaline zinc solution (Hsieh et al. 2002); the analytical precision was 4.3, 1.8, and 1.7% ($n = 5$) for the 3 measurements, respectively (Kang et al. 2014). The pore water sulfate was determined using an indirect titration method (Howarth 1978) that had an analytical precision of 0.2% ($n = 5$).

Calculations

The rate constant of OM decomposition, which was calculated according to Wei et al. (2005), has been used to discuss the impact of OM reactivity (ease of decomposition) on sulfate reduction in the YS and the East China Sea (Kang et al. 2014).

To calculate the sulfate reduction rates (SRRs), we assumed that the OM in sediments was oxidized by sulfate-reducing bacteria based on first-order kinetics, which was performed on the rate function. The sulfate profile was best expressed by assuming that the sulfate concentration decreased exponentially with depth (Jørgensen 1978, Bowles et al. 2014). The rate function ($f(x) = a \cdot e^{-bx}$, where a and b are constants and x is depth) was obtained by fitting the sulfate profile using an exponential decay (Jørgensen 1978, Bowles et al. 2014). The SRR at a given depth was then calculated based on the rate function, and the depth-integrated SRR was calculated. To facili-

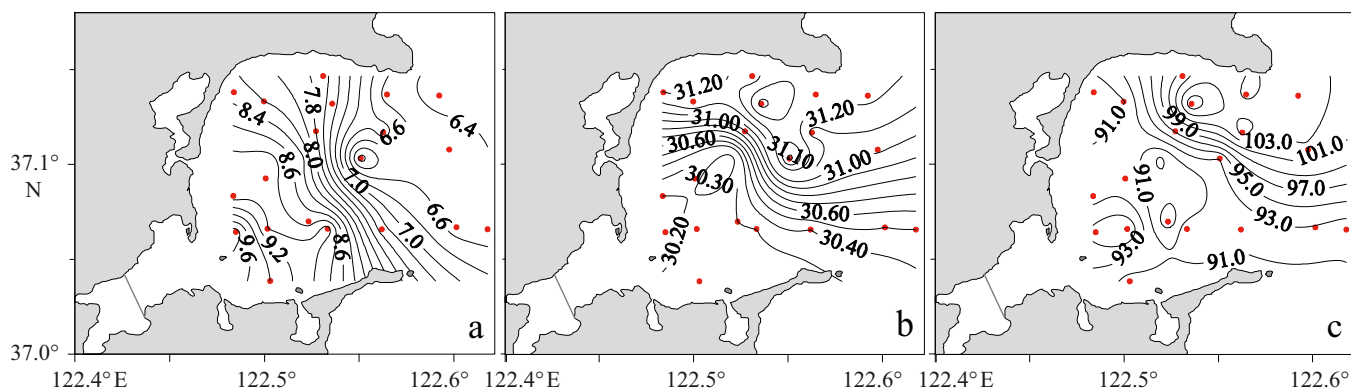


Fig. 2. Horizontal distributions of (a) temperature (°C), (b) salinity, and (c) the degree of dissolved oxygen (DO) saturation (%) in near-bottom seawater of Sanggou Bay (see Fig. 1 for station locations, red dots)

tate consistent comparisons, the SRR was integrated to the bottom of the sulfate reduction zone (the integrated depth determined from extrapolations according the rate function).

Statistics

All statistical tests were performed using SPSS 19 software. Prior to each statistical analysis, the normality and homoscedasticity of the data were tested. One-way ANOVAs were applied to normalized data showing homogeneous variance. A 1-way ANOVA was used to assess differences in the OM and sulfide concentrations among various mariculture areas in the SGB. For all statistical tests, a probability of 0.05 was used to determine statistical significance. In factor analysis, principal component analysis (PCA) with varimax rotation was used to study the relationship among measured parameters. The number of principal components in the PCA model was established by considering only those with an eigenvalue > 1.0 (Reid & Spencer 2009).

RESULTS

Physical and chemical parameters of near-bottom water in SGB

The spatial distribution of temperature, salinity, and the degree of DO saturation in near-bottom water is shown in Fig. 2. The temperature of near-bottom water ranged from 6.1 to 9.9°C (mean \pm SD $7.8 \pm 1.2^\circ\text{C}$) and decreased from the inner bay to the mouth. Salinity ranged from 30.10 to 31.44 (30.71 ± 0.49) and decreased from the mouth to the inner bay.

There was a low-salinity zone in the west and southwest of the bay, near the Guhe River and Bahe reservoir. DO saturation ranged from 87.6 to 108.6% (mean 95.5%), and was higher at the mouth than in the inner bay. There was a slightly lower DO zone from southeast to northwest of the bay.

Quality and quantity of OM in sediments of SGB and YS

The OM concentration ranged from 0.9 to 9.2% (mean 5.4%) in surface sediment of SGB, and increased from the mouth of the bay ($4.08 \pm 0.95\%$) to the inner bay ($6.26 \pm 2.08\%$; Table 1), particularly in the scallop and oyster monoculture areas (Fig. 3a). The OM concentration decreased to a minimum of 3.5% with increasing depth in the deep layer at Stns MC and ST1 (Fig. 3b). The OM rapidly decreased in the upper 7 cm and then remained stable with depth at Stn A02. The rate constant of OM decomposition was 0.072, 0.033, and 0.001 yr^{-1} at Stns MC, ST1, and A02, respectively, which indicated that the OM reactivity of Stn MC was the highest among the 3 stations.

Sulfate in pore waters and sulphate reduction rate in SGB and YS

The pore water sulfate concentration was high and fluctuated with increasing depth at Stns ST1, MC, and A02 (Fig. 4). The depth-integrated SRR was 1.89 and 0.54 $\text{mmol m}^{-2} \text{d}^{-1}$ (X. Kang et al. unpubl. data) at Stns ST1 and A02, respectively. The SRR at Stn MC was not calculated because of the limited available pore water sulfate data.

Table 1. Dissolved oxygen (DO) concentration in near-bottom water and organic matter (OM) and sulfide concentrations in sediments at stations in areas involved in 4 major types of mariculture in Sanggou Bay. We did not compile the data from fish monoculture regions, as only a limited number of stations were available. AVS: acid-volatile sulfide, ES: elemental sulfur, RIS: reduced inorganic sulfur

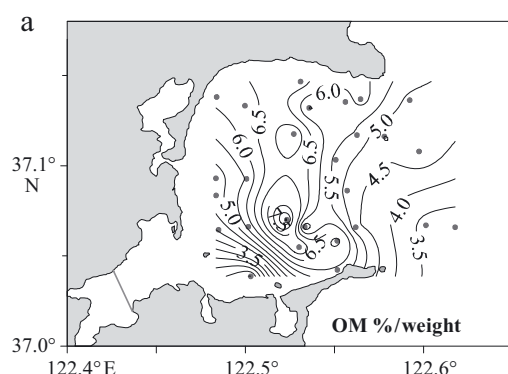
Parameters	Unit	Scallop monoculture		Oyster monoculture		Scallop/kelp polyculture		Kelp monoculture	
		Range	Mean (SD)	Range	Mean (SD)	Range	Mean (SD)	Range	Mean (SD)
DO	mg l ⁻¹	8.53–10.60	9.20 (0.85)	8.38–9.22	8.82 (0.35)	8.77–10.49	9.58 (0.75)	9.22–10.43	9.81 (0.63)
OM	% by dry wt	4.71–7.48	6.06 (0.93)	4.09–9.18	6.26 (2.08)	4.47–7.25	5.49 (0.83)	3.20–4.95	4.08 (0.95)
AVS	μmol g ⁻¹	0.58–5.00	2.54 (1.83)	2.51–12.56	5.87 (5.79)	0.20–5.00	1.57 (1.63)	0.22–3.34	1.12 (1.49)
Pyrite-S	μmol g ⁻¹	8.78–51.52	21.63 (14.65)	15.06–24.01	21.40 (4.18)	5.45–38.52	16.04 (9.59)	7.03–14.50	11.06 (3.17)
ES	μmol g ⁻¹	0.24–1.10	0.65 (0.34)	0.28–0.86	0.52 (0.28)	0.16–0.88	0.48 (0.21)	0.24–0.34	0.29 (0.04)
RIS	μmol g ⁻¹	12.68–53.19	24.82 (13.62)	18.02–37.06	25.71 (7.20)	5.81–39.91	18.09 (9.56)	7.78–18.08	12.46 (4.33)

Distribution of reactive Fe in surface and core sediments of SGB and YS

Content of Fe_R in surface sediments of SGB showed a wide range from 20.7 to 102.1 μmol g⁻¹. A peak value was observed in the scallop monoculture region (Fig. 5a). This spatial distribution was generally coupled to OM (Fig. 3a). The concentrations (in μmol g⁻¹) of Fe_R were 26.0–93.6 (mean 60.6) at Stn MC, 18.0–148.3 (mean 62.0) at Stn ST1, and 29.8–126.1 (mean 82.5) at Stn A02, and all exhibited a decrease with greater core depth (Fig. 5b).

Sediment porosity of surface and core sediments of SGB and YS

The porosity of surface sediment ranged from 0.40 to 0.77 in SGB, presenting higher values in the inner bay with oyster or scallop monoculture and lower values in the mouth of the bay with kelp monoculture (Fig. 6a). The porosity at Stns ST1, MC, and A02 all exhibited a decrease with greater core depth, especially at Stn MC. The porosity of Stn ST1 decreased in the upper 5 cm and then remained stable with depth (Fig. 6b).



Sulfur species in surface and core sediments of SGB and YS

The concentrations (in μmol g⁻¹) of AVS, pyrite-S, and ES in surface sediments of SGB were 0.20–12.56 (mean 2.20), 0.57–51.52 (mean 17.17), and 0.16–1.10 (mean 0.49), respectively. The differences in AVS, ES, and pyrite-S between stations in the SGB were significant at the 95% confidence level. The AVS showed high concentrations in the southwest part of the bay (with oyster monoculture; Fig. 7). Compared

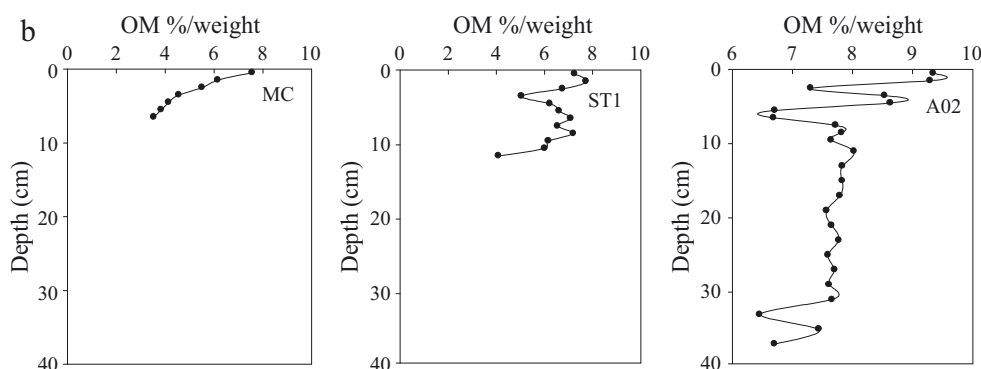


Fig. 3. Distribution of organic matter (OM) concentrations (% by weight) in (a) surface and (b) core sediments of Sanggou Bay and the Yellow Sea (see Fig. 1 for station locations)

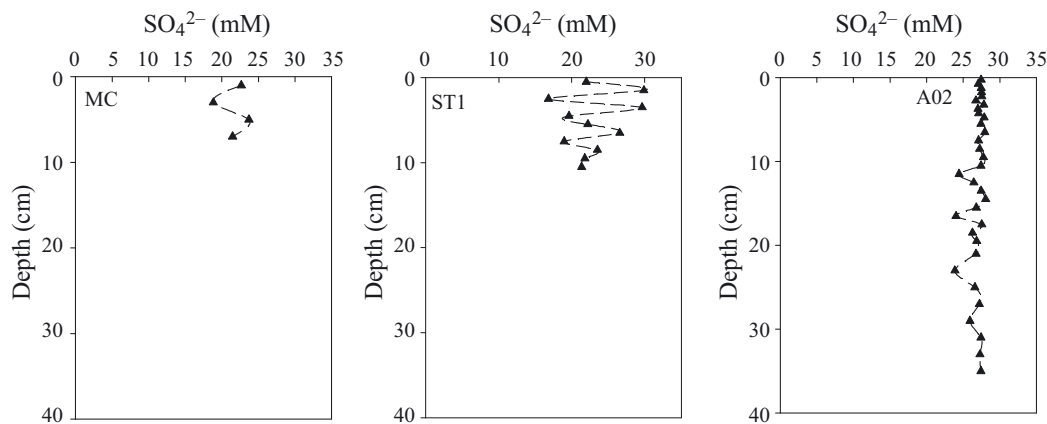


Fig. 4. Pore water profiles of sulfate at Stns ST1, MC, and A02 in Sanggou Bay (see Fig. 1 for station locations)

with AVS and pyrite-S, the concentrations of ES were lower throughout the bay, especially at the mouth. Pyrite-S was the predominant sulfide mineral in sediments of the bay, accounting for 58.2 to 96.9% (mean 85.0%) of the RIS, and its concentration was particularly high in the northwest (with scallop monoculture) and south part (with oyster monoculture) of the bay.

The variations in AVS, ES, and pyrite-S with depth were significant at the 95% confidence level. The AVS concentration was $<12.56 \mu\text{mol g}^{-1}$ in core sedi-

ments of SGB, as its accumulation was limited by transformation to pyrite-S. At Stn ST1, the AVS concentration gradually increased in the upper 7 cm and then stabilized, while the pyrite-S concentration peaked at 2–3 cm depth, then leveled off below this depth (Fig. 8). At Stn MC, we observed 2 peaks of AVS and pyrite-S concentration. The ES concentration was stable with increasing depth at Stns ST1 and MC; pyrite-S was the primary sulfide at these 2 stations. For Stn A02, the AVS concentration was low and only peaked at 8 cm. ES and pyrite-S increased with depth at this station and were comparable to SGB. The distribution of ES was similar to that of pyrite-S at Stn A02. Pearson's correlation analysis revealed a significant positive correlation between the ES and pyrite-S concentrations ($r = 0.62$, $p < 0.001$).

PCA

We performed PCAs of sulfur speciation, OM, Fe_R and porosity. The total variances explained by the first 3 and 2 principal components were 86.45% and

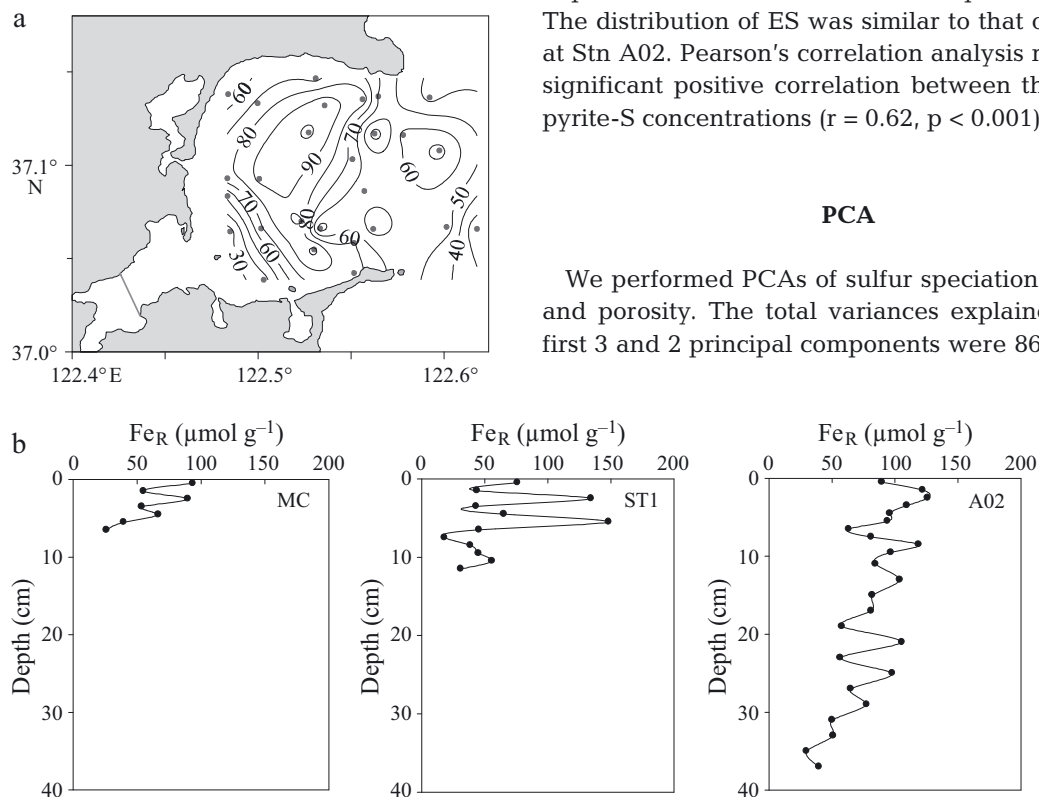


Fig. 5. Distribution of reactive iron (Fe_R ; $\mu\text{mol g}^{-1}$) in (a) surface and (b) core sediments of Sanggou Bay and the Yellow Sea (see Fig. 1 for station locations)

78.04 %, respectively, for surface and core sediments. The degree of association between each variable and each principal component was given by its loading on that principal component.

For surface sediments (Table 2), PC1 accounted for 38.17 % of the total variance and was correlated primarily with ES, pyrite-S, and RIS. PC2 accounted for 32.83 % of the total variance and correlated with Fe_R, OM, and porosity. PC3 accounted for 15.45 % of the

total variance and was primarily characterized by a positive loading of AVS and a negative loading of ES.

For core sediments (Table 3), PC1 accounted for 55.20 % of the total variance, and was positively associated with AVS, pyrite-S, and RIS, and negatively correlated with OM, Fe_R, and porosity. PC2 accounted for 22.84 % of the total variance and was positively correlated with ES and negatively correlated with AVS.

DISCUSSION

Factors controlling RIS partitioning and spatial distribution

Sulfide formation is influenced by many factors, including oxygen concentration, reactivity and quantity of OM, sediment grain size (Martinez-Garcia et al. 2015), presence of reactive iron buried in sediments, the amount of sulfate in pore water (Berner 1984), and other factors.

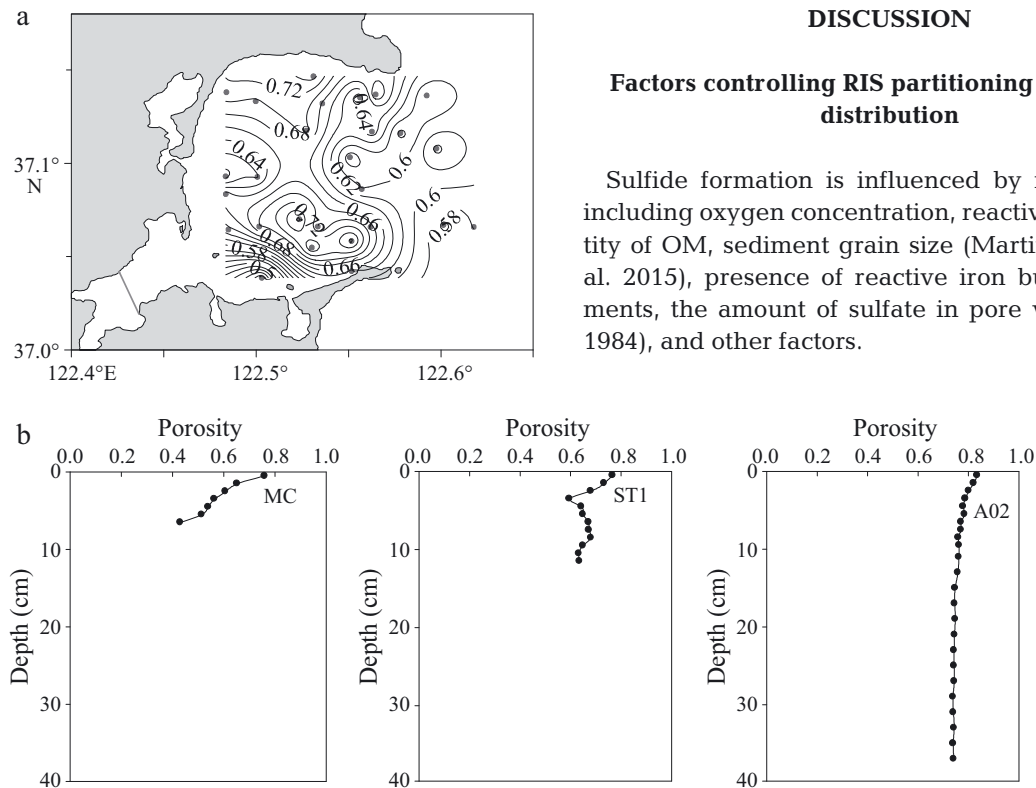


Fig. 6. Porosity of (a) surface and (b) core sediments of Sanggou Bay and the Yellow Sea (see Fig. 1 for station locations)

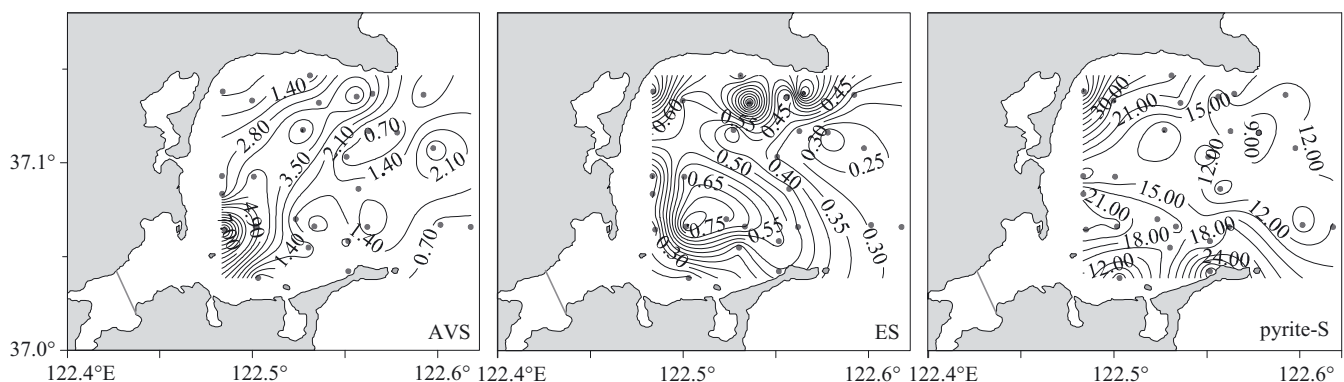


Fig. 7. Horizontal distributions of acid-volatile sulfide (AVS), elemental sulfur (ES), and pyrite-S ($\mu\text{mol g}^{-1}$) in surface sediments of Sanggou Bay

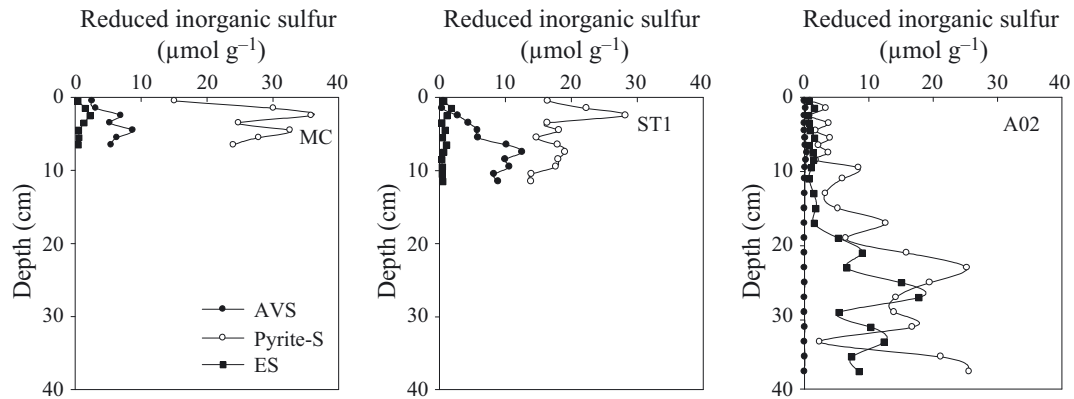


Fig. 8. Vertical distribution of reduced inorganic sulfur in sediments of Sanggou Bay and the Yellow Sea (see Fig. 1 for station locations)

Table 2. Principal component analysis for surface sediments of Sanggou Bay. AVS: acid-volatile sulfide, ES: elemental sulfur, RIS: reduced inorganic sulfur, OM: organic matter

	PC1	PC2	PC3	Communalities
AVS	0.05	0.05	0.98	0.97
ES	0.67	0.42	-0.25	0.69
Pyrite-S	0.97	0.07	-0.01	0.95
RIS	0.96	0.09	0.22	0.97
OM	0.29	0.90	-0.02	0.90
Fe	-0.11	0.87	0.07	0.77
Porosity	0.52	0.74	0.02	0.81
Eigenvalue	2.67	2.30	1.08	—
% of variance	38.17	32.83	15.45	—
Cumulative % of variance	38.17	71.00	86.45	—

Table 3. Principal component analysis for core sediments of the study sites. AVS: acid-volatile sulfide, ES: elemental sulfur, RIS: reduced inorganic sulfur, OM: organic matter

	PC1	PC2	Communalities
AVS	0.65	-0.58	0.75
ES	0.14	0.94	0.90
Pyrite-S	0.89	0.06	0.80
RIS	0.94	0.19	0.93
OM	-0.79	0.41	0.79
Fe	-0.65	-0.01	0.42
Porosity	-0.84	0.42	0.88
Eigenvalue	3.86	1.60	—
% of variance	55.20	22.84	—
Cumulative % of variance	55.20	78.04	—

Oxygen concentration

Sulfate reduction is a strictly anaerobic process and mainly occurs in anoxic environments (Berner 1982, Jørgensen 1982, Aller & Rude 1988). However, the

primary effects of aerobic environments on sulfate reduction are through the re-oxidation of sulfide and the activity of sulfate-reducing bacteria (SRB). Aerobic mineralization may take place in oxic surface sediments in SGB. The extent of aerobic mineralization depends on the DO concentration in bottom water, which subsequently influences the extent of sulfate reduction (Brüchert et al. 2003). The SRR has been shown to be negatively correlated with bottom water oxygen concentration in the seasonally hypoxic Eckernförde Bay in the Baltic Sea (Bertics et al. 2013). In the present study, slightly lower DO concentrations were found in the scallop and oyster monoculture areas of SGB (Fig. 2c), which were related to the relatively high oxygen consumption associated with the process of OM decomposition. Low DO concentrations would have facilitated the activity of SRB and reduced the possibility of sulfide re-oxidation, leading to high concentrations of sulfide (especially the AVS and pyrite-S) in the scallop and oyster monoculture areas of SGB (Table 1). Thus, the DO concentration might regulate the distribution of RIS. Pearson's correlation analysis indicated a significant negative correlation between the DO concentration and the RIS concentration ($r = -0.48$, $p < 0.05$), indicating that the RIS concentration increased with decreasing DO concentration.

Reactivity of OM

The reactivity and quantity of OM are important factors controlling sulfate reduction (Berner 1984). The labile OM in mariculture regions would favor sulfate reduction (Otero et al. 2006). Although the reactivity of OM in SGB was not measured directly, it can be evaluated by calculating the TOC:total nitrogen (TN) ratio. Holmer & Kristensen (1992) noted

that OM with a low TOC:TN ratio (5.7–7.0) can be decomposed rapidly, within several months of closure of a fish farm. The TOC:TN ratio of OM in sediments of SGB has been reported to be in the range of 7.04 to 8.93 (Zhang et al. 2006), which is similar to the mean TOC:TN ratio (6.6) of labile OM in the ocean (Babbin et al. 2014). The decreased OM concentration in the top 4 cm of sediment at Stn ST1 might be related to decomposition of kelp mariculture debris and scallop fecal material. Compared to Stn ST1, a continuous decline in the OM concentration from the sediment surface to 7 cm depth was found at Stn MC, suggesting somewhat higher reactivity of OM in oyster monoculture areas. The high OM decomposition rate constant found at Stn MC also confirmed this phenomenon. The low decomposable characteristics of OM at Stn A02 are also confirmed by the low OM decomposition rate constant (0.001 yr^{-1}).

Sulfate reduction

Sulfate reduction is independent of the sulfate concentration until the concentration is $<3 \text{ mM}$ (Boudreau & Westrich 1984). High concentrations of sulfate in pore water of the sediments of SGB and the reference station (A02) showed that sulfate was not a limiting factor for sulfate reduction. The SRR at Stn ST1 was higher than that at Stn A02, which might be related to the high reactivity of OM in the mariculture regions (Otero et al. 2006). The SRR in sediments of SGB was much lower than that in a marine fish farm ($9\text{--}34 \text{ mmol m}^{-2} \text{ d}^{-1}$) in Kolding Fjord, Denmark, with higher OM concentration (up to 23%) in sediments (Holmer & Kristensen 1992).

Other factors that influence sulfide distribution

Sediment grain size often influences the OM decomposition and sulfide accumulation in marine ecosystems (Martinez-Garcia et al. 2015). The grain size was not determined in this study, and data of the porosity were used here because finer-grain sediments tend to have higher porosities than coarser materials (Buckingham 2005). Our PCA results showed that porosity could influence the distribution of Fe_R and OM in surface and core sediments, and subsequently affected the profiles of AVS and pyrite-S. In addition, Fe_R was closely associated with OM-rich sediments. AVS could oxidize to ES, and the latter had a significant influence on the accumulation of pyrite-S in surface sediments, as highlighted by the

PCA results (Table 2). The high ratio (>3) of pyrite-S to AVS in the core sediments and the PCA results both showed that the AVS could convert to pyrite-S effectively.

The current velocity can also influence the sulfide distribution; for example, the decreased current velocity (up to 54%) (Grant & Bacher 2001) caused by the presence of dense mariculture restricted the DO exchange between SGB and the water outside the bay. In addition, the movement of OM could also be influenced by the current. These 2 cases can influence the sulfate reduction, and consequently influence the sulfide distribution. Our results showed that high concentrations of sulfide distribution coupled well with lower current velocity (Grant & Bacher 2001). Furthermore, the sulfide distribution could also be influenced by water depth, and there was a significant negative correlation between the RIS concentration and water depth (Pearson $r = -0.41$, $p < 0.05$).

Mariculture impacts on sulfide accumulation and the benthic environment

Mariculture impacts on sulfide accumulation

Although in addition to mariculture, natural factors can also impact the sulfide accumulation in sediments, the weak impact of natural factors could be ignored in our study area. For example, river input carries an annual sediment load of up to $17.1 \times 10^4 \text{ t}$, with a mean OM concentration of 4.5% in sediment of rivers around SGB (Xia 1991), which was lower than that in SGB (5.4%). RIS concentration in sediment of the Xiaoluo River (the second largest river around SGB) was determined in our previous study (X. Kang et al. unpubl.), and concentrations of AVS, pyrite-S, and ES were 0.56, 6.63, and $0.66 \mu\text{mol g}^{-1}$, respectively, much lower than those in SGB. Thus, natural factors were not considered in the current study; instead, we focused on the influence of mariculture on sulfide accumulation.

The concentrations of sulfide in various mariculture areas are shown in Table 1. We found no significant difference in the AVS concentration between any 2 regions, except between the oyster monoculture and the scallop/kelp polyculture areas. The AVS concentration in the oyster monoculture areas was significantly higher (by a factor of 3.74) than in the scallop/kelp polyculture areas (1-way ANOVA, $p < 0.05$). AVS concentrations accumulated in oyster monoculture areas were 1.5-fold higher than values in the scallop/kelp polyculture areas owing to dense

mariculture. This additional AVS accumulation might be related to the sedimentation rate in the oyster monoculture areas, which was significantly higher than in the scallop/kelp polyculture areas in spring (Cai et al. 2003). High sedimentation rates favor the retention of AVS in sediments (Gagnon et al. 1995). In addition, dense mariculture also influences the current velocity, which consequently influences the AVS accumulation. We observed no significant difference in the pyrite-S and RIS concentrations between 2 randomly selected regions, except between the oyster and kelp monoculture areas. The pyrite-S and RIS concentrations in the oyster monoculture areas were significantly higher than in the kelp monoculture areas (1-way ANOVA, $p < 0.05$), with the mean concentrations in the former areas being higher by a factor of 2.0. The higher concentrations of AVS, pyrite-S, and RIS in the oyster monoculture areas were related to the higher OM and lower DO concentrations (Table 1). In addition, release of DO to the water column through photosynthesis would be occurring in the kelp mariculture areas. There was no significant difference in the ES concentration between 2 randomly selected regions. It may be that as an intermediate form of sulfide, ES is reduced to H_2S under reducing conditions, and oxidized to sulfate in oxic environments (Lovley & Phillips 1994).

Mariculture also influences sulfur accumulation in core sediments. Pyrite-S and RIS were significantly higher at Stn MC than Stn ST1 (1-way ANOVA, $p < 0.05$), although the OM was significantly lower at MC compared to ST1 (1-way ANOVA, $p < 0.05$). This phenomenon may have been induced by the higher reactivity of OM at Stn MC. However, there was no significant difference in AVS, ES, and Fe_R between Stns ST1 and MC (1-way ANOVA, $p > 0.05$). AVS, pyrite-S, and RIS concentrations at Stns ST1 and MC were significantly higher than at the reference station (A02) (1-way ANOVA, $p < 0.05$). However, there was no significant difference of Fe_R among Stns ST1, MC, and A02 (1-way-ANOVA, $p > 0.05$). In addition, the OM at ST1 and MC was significantly lower than at A02 (1-way ANOVA, $p < 0.05$). The relatively lower OM at Stns ST1 and MC induced high concentrations of AVS, pyrite-S, and RIS and may be related to its high reactivity owing to mariculture. ES was significantly higher at A02 than at MC and ST1 (1-way ANOVA, $p < 0.05$), which might be related to the AVS oxidation.

Compared with the RIS concentration in other mariculture areas (Table 4), the AVS concentration in SGB was in the same range as reported for Laizhou Bay, Zhangzi Island, for scallop and sea cucumber

mariculture (Gao et al. 2013), Bohai Bay for clam mariculture (Jiang et al. 2005), and Jiaozhou Bay for clam and shrimp mariculture (Huo et al. 2001). Hyun et al. (2013) compiled the SRRs for various mariculture regions, and noted that SRR was related to sedimentation rates of organic carbon, hanging mussel biomass, the length of time a farm had been in operation, and temperature. It is difficult to say which factor(s) accounts for the similar concentrations of RIS among these mariculture areas. In general, the RIS concentrations in shellfish farms (including scallop, oyster, and clam farms) were lower than in fish farms, including the Dapengao Bay fish cage mariculture farm (Gan et al. 2003). The difference in RIS concentration between shellfish and fish farms is largely because of the higher sedimentation rate of food pellets in fish farms, which provide additional OM. Compared with non-mariculture regions, such as the adjacent YS (Pu et al. 2008, Kang et al. 2014), there was no significant accumulation of AVS in SGB. The RIS concentration in SGB was lower than that in the East China Sea (Lin et al. 2002, Kang et al. 2014), the Black Sea (Holmkvist et al. 2011), and the Mediterranean Sea (Henneke et al. 1997). As SGB is an integrated multi-trophic aquaculture bay, kelp may assimilate nutrients and release DO into the water column through photosynthesis. The lower TOC concentrations and aerobic environment may explain the lower RIS concentrations in SGB.

Mariculture impacts on the benthic environment

One of the main impacts of mariculture on the benthic environment is OM enrichment of sediments through biodeposition. The OM concentration in the scallop monoculture and the scallop/kelp polyculture areas were slightly higher (by factors of 1.49 and 1.35, respectively) than in the kelp monoculture areas (1-way ANOVA, $p < 0.05$). However, the OM concentration in the surface sediments of SGB was comparable to that in the adjacent YS (Fig. 3) (Kang et al. 2014). Crawford et al. (2003) noted that the effect of shellfish farming on organic enrichment of the seabed was small, and much less than that caused by finfish farming. In addition, the resuspension of surface sediment, driven by wind, waves, and currents, can be observed in spring in SGB (Jiang et al. 2012); these factors can resuspend and move most of the accumulated OM (Holmer & Kristensen 1992). Dissimilatory sulfate reduction through OM decomposition may also be responsible for the low OM concentration in SGB.

Table 4. Concentrations of various sulfur species in the sediments of Sanggou Bay in comparison to other sea regions. AVS: acid-volatile sulfide, ES: elemental sulfur, TOC: total organic carbon, ND: no data

Location	AVS ($\mu\text{mol g}^{-1}$)	Pyrite-S ($\mu\text{mol g}^{-1}$)	ES ($\mu\text{mol g}^{-1}$)	TOC (%/weight)	Reference
Mariculture present					
Sanggou Bay	0.20–12.56	0.57–51.52	0.16–1.10	0.48–0.70 ^a	This study
Northern of Bohai Bay	1.02–13.68	ND	ND	ND	Jiang et al. (2005)
Laizhou Bay	1.22–7.60	ND	ND	0.12–2.18	Gao et al. (2013)
Zhangzi Island	0.71–11.03	ND	ND	0.12–2.18	Gao et al. (2013)
Jiaozhou Bay	5.06–19.11	ND	ND	ND	Huo et al. (2001)
Dapengao Bay	4.44–29.66	ND	ND	ND	Gan et al. (2003)
Mariculture absent					
Yellow Sea	0.02–17.14	0.61–113.1	0–44.4	0.22–0.94	Kang et al. (2014)
East China Sea	0.01–25.02	0.61–54.82	0.14–16.84	0.32–1.05	Kang et al. (2014)
Southern Yellow Sea	0–11.14	ND	ND	ND	Pu et al. (2008)
Southern East China Sea	0–25	0–240	ND	0.50–0.80	Lin et al. (2002)
Black Sea	0–36	0–380	0–16	0.33–15.00	Holmkvist et al. (2011)
Mediterranean Sea	5–25	50–350	0–25	0.50–9.50	Henneke et al. (1997)

^aData from Song et al. (2012)

The mean benthic carbon oxidation rate in SGB was $8.97 \text{ mmol C m}^{-2} \text{ d}^{-1}$ (Z. Ning et al. unpubl. data), calculated from the Redfield stoichiometric C:O₂ ratio (1:1) and oxygen utilization (Ning et al. 2016). Similarly, from the stoichiometric conversion of sulfate reduction to C oxidation (i.e. C:S = 2:1) (Hyun et al. 2013), the contribution of sulfate reduction to total C oxidation was estimated. Calculation of the C oxidation rate, based on the SRR at Stn ST1 and its proportion of the total carbon oxidation rate, suggests that 42.1 % of total C oxidation occurs via sulfate reduction in sediments of SGB. In addition, the contribution of denitrification to total C oxidation ranges from 4 to 10 % in SGB (Ning et al. 2016). The remaining C oxidation may be a consequence of aerobic respiration, iron reduction, manganese reduction, and methanogenesis in SGB. However, the contribution of sulfate reduction to C oxidation in SGB may be underestimated, because Stn ST1 was located in the polyculture area, where sulfate reduction was relatively weak, in part as a result of the low OM concentration. The contribution of sulfate reduction to C oxidation in SGB is higher than that at Stn A02 (30.0 %) and lower than that found in July in the Jinhae–Tongyeong coastal mariculture region (64.4 %) (Hyun et al. 2013) and that found in May in marine fish farm sediments of Kolding Fjord, Denmark (59.0 %) (Holmer & Kristensen 1992).

Among the environmental and ecological issues arising from sulfate reduction in OM-enriched coastal sediments is the release of nutrients, including phosphate and ammonium, into the overlying water (Hyun et al. 2013). The benthic fluxes were -21 to

-7.7 , 7.7 to 21 , 0 to 0.51 , -0.030 to 0.27 , -1.01 to 0.63 , and 0.83 to $1.76 \text{ (mmol m}^{-2} \text{ d}^{-1})$ for DO, CO₂, NH₄, NO_x⁻ (NO₂⁻+NO₃⁻), dissolved organic nitrogen, PO₄³⁻, and Si(OH)₄, respectively, in SGB (Ning et al. 2016), and the benthic nutrient fluxes were significantly lower in polyculture areas than in the monoculture areas.

Ecological implications of sulfide accumulation in SGB

Sulfide tolerance (e.g. H₂S) of benthic fauna has previously been used to study the ecological significance of sulfide in sediment (Vismann 1991). The viability of fish farming can be at risk from the release of H₂S via sulfate reduction from sediments to the water column (Yokoyama 2003). Thus, we evaluated the ecological state of SGB according the sulfide distribution. The direct determination of H₂S was difficult in SGB as a result of the low concentrations of sulfide in the marginal East China Sea of China (Zhu et al. 2013, Kang et al. 2014). The AVS concentration can be used as a key index for evaluating aquaculture environments (Sanz-Lázaro & Marin 2006). Therefore, we used AVS variations instead of H₂S to analyze the ecological state of SGB. Previous studies have indicated that the macrobenthic biomass decreases with increasing AVS concentration in the sediments, and little macrobenthic biota occurs in sediments when the concentration of AVS is higher than $53.1 \mu\text{mol g}^{-1}$ (Yokoyama 2003). However, the concentration of

AVS (range 0.20–12.56 $\mu\text{mol g}^{-1}$) in sediments never exceeded this critical value in SGB.

Sulfur is also of ecological significance in the energy dynamics of sediments in SGB. The following discussion is based on calculations and assumptions detailed by Howarth (1984). During the process of sulfate reduction, generally 75 % of the energy in the OM is transferred and fixed as hydrogen sulfide (Howarth 1984). Therefore, given that 42.1 % of the total carbon oxidation was caused by sulfate reduction in SGB sediments, 31.6 % (75 % of 42.1 %) of the energy transferring through the sediment would be conserved as hydrogen sulfide. Most of the hydrogen sulfide quickly forms iron sulfide, of which 80 to 99 % is reoxidized under aerobic conditions (Howarth 1984). Based on the given calculation method of Howarth (1984) in Limfjorden sediments, approximately 10.0 % of reduced sulfur was assumed to be buried in SGB sediments perpetually, and thus the energy released from reduced sulfur reoxidation would account for 28.4 % (90 % of 31.6 %) of the benthic OM decomposition here. Thus, the released energy would total $1.3 \text{ KJ m}^{-2} \text{ d}^{-1}$, corresponding to a total respiration of $4.6 \text{ KJ m}^{-2} \text{ d}^{-1}$ ($0.11 \text{ g C m}^{-2} \text{ d}^{-1}$) in SGB sediments. This released energy could be used by chemolithoautotrophs for CO_2 fixation, with energy utilization efficiency ranging from 21 to 37 % in sediments (Howarth 1984). Subsequently, new organic carbon (0.007 to $0.012 \text{ g C m}^{-2} \text{ d}^{-1}$) was input to SGB sediments. This new organic carbon produced at the oxic–anoxic interface by chemolithoautotrophic production could be used as food for benthic animals (Howarth 1984).

CONCLUSION

We found that under the combined effects of mariculture activities and physical factors, the RIS was affected in the study area. RIS concentration showed spatial differences with mariculture species. Compared with the oyster monoculture area, the relatively low OM and RIS accumulation in the scallop/kelp polyculture areas demonstrated the environmental benefits of this culture practice. We observed no significant influence of mariculture on the benthic environment after several years of mariculture in SGB, although it promoted sulfide accumulation to some extent compared to the reference station. The lower intensity of culture activities, better hydrodynamic conditions, and the polyculture of scallops and kelp might explain the healthy benthic environment in SGB (Zhang et al. 2009). In addition,

the ecological state of SGB can be assessed using the RIS concentration in sediment.

Although we investigated the effect of mariculture activities on RIS accumulation, the seasonal evolution of the system was not considered in this study, and should therefore be assessed in future research. In addition, the mariculture facilities should be considered further to better evaluate the influence of mariculture.

Acknowledgements. We thank Zhaomeng Xu and Wangwang Ye for help in sample collection, and Zhiming Ning for help with DO measurements and suggestions during revisions to this paper. We thank the editor and 4 anonymous reviewers for comments on an earlier version of this paper. This research was funded by the Ministry of Science & Technology of China (2011CB409802), and the National Science Foundation of China (40925017 and 41221004).

LITERATURE CITED

- Aller RC, Rude PD (1988) Complete oxidation of solid phase sulfides by manganese and bacteria in anoxic marine sediments. *Geochim Cosmochim Acta* 52:751–765
- Babbin AR, Keil RG, Devol AH, Ward BB (2014) Organic matter stoichiometry, flux, and oxygen control nitrogen loss in the ocean. *Science* 344:406–408
- Berner RA (1982) Burial of organic carbon and pyrite sulfur in the modern ocean: its geochemical and environmental significance. *Am J Sci* 282:451–473
- Berner RA (1984) Sediment pyrite formation: an update. *Geochim Cosmochim Acta* 48:605–615
- Bertics VJ, Löscher CR, Salonen I, Dale AW, Gier J, Schmitz RA, Treude T (2013) Occurrence of benthic microbial nitrogen fixation coupled to sulfate reduction in the seasonally hypoxic Eckernförde Bay, Baltic Sea. *Biogeochemistry* 10:1243–1258
- Boudreau BP, Westrich JT (1984) The dependence of bacterial sulfate reduction on sulfate concentration in marine sediments. *Geochim Cosmochim Acta* 48:2503–2516
- Bowles MW, Mogollón JM, Kasten S, Zabel M, Hinrichs K (2014) Global rates of marine sulfate reduction and implications for sub-sea-floor metabolic activities. *Science* 344:889–891
- Brüchert V, Jørgensen BB, Neumann K, Riechmann D, Schlösser M, Schulz H (2003) Regulation of bacterial sulfate reduction and hydrogen sulfide fluxes in the central Namibian coastal upwelling zone. *Geochim Cosmochim Acta* 67:4505–4518
- Bryan JR, Riley JP, Williams PJL (1976) A Winkler procedure for making precise measurements of oxygen concentration for productivity and related studies. *J Exp Mar Biol Ecol* 21:191–197
- Buckingham MJ (2005) Compressional and shear wave properties of marine sediments: comparisons between theory and data. *J Acoust Soc Am* 117:137–152
- Burton ED, Bush RT, Sullivan LA (2006) Fractionation and extractability of sulfur, iron and trace elements in sulfide sediments. *Chemosphere* 64:1421–1428
- Cai LS, Fang JG, Liang XP (2003) Natural sedimentation in large scale aquaculture areas of Sungo Bay, north

- China Sea. *J Fish Sci China* 10:305–310 (in Chinese with English Abstract)
- Carlsson MS, Holmer M, Petersen JK (2009) Seasonal and spatial variations of benthic implications of mussel long-line farming in a eutrophic Danish fjord, Limfjorden. *J Shellfish Res* 28:791–801
- Chopin T, Robinson SMC, Troell M, Neori A, Buschmann AH, Fang JG (2008) Multitrophic integration for sustainable marine aquaculture. In: Jørgensen SE, Fath BD (eds) *Encyclopedia of ecology*. Elsevier, Oxford, p 2463–2475
- Crawford CM, Macleod CKA, Mitchell IM (2003) Effects of shellfish farming on the benthic environment. *Aquaculture* 224:117–140
- Fang JG, Sun HL, Yan JP, Kuang SH, Li F (1996) Polyculture of scallop *Chlamys farreri* and kelp *Laminaria japonica* in Sungo Bay. *Chin J Oceanol Limnol* 14:322–329
- FAO (Food and Agriculture Organization of the United Nations) (2012) The state of world fisheries and aquaculture. FAO, Rome
- Gagnon C, Mucci A, Pelletier É (1995) Anomalous accumulation of acid volatile sulphides (AVS) in a coastal marine sediment, Saguenay Fjord, Canada. *Geochim Cosmochim Acta* 59:2663–2675
- Gan JL, Lin Q, Huang HH, Cai WG and others (2003) Distribution, variation and pollution of the sulfide in surficial sediment at cage culture area in Dapengao Bay. *J Fish Sci China* 27:570–574 (in Chinese with English Abstract)
- Gao XL, Li PM, Chen CT (2013) Assessment of sediment quality in two important areas of mariculture in the Bohai Sea and the northern Yellow Sea based on acid-volatile sulfide and simultaneously extracted metal results. *Mar Pollut Bull* 72:281–288
- Grant J, Bacher C (2001) A numerical model of flow modification induced by suspended aquaculture in a Chinese bay. *Can J Fish Aquat Sci* 58:1003–1011
- Henneke E, Luther GW III, De Lange GJ, Hoefs J (1997) Sulphur speciation in anoxic hypersaline sediments from the Eastern Mediterranean Sea. *Geochim Cosmochim Acta* 61:307–321
- Holmer M, Kristensen E (1992) Impact of marine fish cage farming on metabolism and sulfate reduction of underlying sediments. *Mar Ecol Prog Ser* 80:191–201
- Holmkvist L, Kamysny A Jr, Vogt C, Vamvakopoulos K, Ferdelman TG, Jørgensen BB (2011) Sulfate reduction below the sulfate methane transition in Black Sea sediments. *Deep-Sea Res I* 58:493–504
- Howarth RW (1978) A rapid and precise method for determining sulfate in seawater, estuarine waters, and sediment pore waters. *Limnol Oceanogr* 23:1066–1069
- Howarth RW (1984) The ecological significance of sulfur in the energy dynamics of salt marsh and coastal marine sediments. *Biogeochemistry* 1:5–27
- Hsieh YP, Chung SW, Tsau YJ, Sue CT (2002) Analysis of sulfide in the presence of ferric minerals by diffusion methods. *Chem Geol* 182:195–201
- Huerta-Diaz MA, Tessier A, Carignan R (1998) Geochemistry of trace metals associated with reduced sulfur in freshwater sediments. *Appl Geochem* 13:213–233
- Huo WY, Li QS, Ma XN (2001) Study on acid volatile sulfide (AVS) of sediment in mariculture region of Jiaozhou Bay. *Sci Geog Sin* 21:135–139 (in Chinese with English Abstract)
- Hyun J, Kim S, Mok J, Lee JS, An S, Lee WC, Jung R (2013) Impacts of long-line aquaculture of Pacific oysters (*Crassostrea gigas*) on sulfate reduction and diffusive nutrient flux in the coastal sediments of Jinhae-Tongyeong, Korea. *Mar Pollut Bull* 74:187–198
- Jiang ZH, Ma QM, Wang XL, Zhang YY (2005) Study on the AVS in surface sediment in the north area of the Bohai Bay. *Mar Environ Sci* 24:6–8 (in Chinese with English Abstract)
- Jiang ZJ, Wang GH, Fang JG (2012) Sediment resuspension mechanisms in aquaculture area, Sanggou Bay. *J Environ Sci Eng A1*:295–302
- Jørgensen BB (1978) A comparison of methods for the quantification of bacterial sulfate reduction in coastal marine sediments. *Geomicrobiol J* 1:29–47
- Jørgensen BB (1982) Mineralization of organic matter in the sea bed—the role of sulfate reduction. *Nature* 296:643–645
- Kang XM, Liu SM, Zhang GL (2014) Reduced inorganic sulfur in sediments of the Yellow and East China Seas. *Acta Oceanol Sin* 33:100–108
- Kraal P, Burton ED, Bush RT (2013) Iron monosulfide accumulation and pyrite formation in eutrophic estuarine sediments. *Geochim Cosmochim Acta* 122:75–88
- Lasorsa BM, Casas A (1996) A comparison of sample handling and analytical methods for determination of acid volatile sulfide in sediment. *Mar Chem* 52:211–220
- Li JB, Zhang GL, Zhang J, Liu SM, Ren JL (2010) Matrix bound phosphine in sediments of the Yellow Sea and its coastal areas. *Cont Shelf Res* 30:743–751
- Lin S, Huang KM, Chen SK (2002) Sulfate reduction and iron sulfide mineral formation in the southern East China Sea continental slope sediment. *Deep-Sea Res I* 49:1837–1852
- Liu SM, Li LW, Zhang ZN (2011) Inventory of nutrients in the Bohai. *Cont Shelf Res* 31:1790–1797
- Lovley DR, Phillips EJP (1994) Novel process for anaerobic sulfate production from elemental sulfur by sulfate-reducing bacteria. *Appl Environ Microbiol* 60:2394–2399
- Lu J, Huang L, Luo Y, Xiao T, Jiang Z, Wu L (2015) Effects of freshwater input and mariculture (bivalves and macroalgae) on spatial distribution of nanoflagellates in Sungo Bay, China. *Aquacult Environ Interact* 6:191–203
- Lückge A, Ercegovac M, Strauss H, Littke R (1999) Early diagenetic alteration of organic matter by sulfate reduction in quaternary sediments from the northeastern Arabian Sea. *Mar Geol* 158:1–13
- Martinez-Garcia E, Carlsson MS, Sanchez-Jerez P, Sanchez-Lizaso JL, Sanz-Lazaro C, Holmer M (2015) Effect of sediment grain size and bioturbation on decomposition of organic matter from aquaculture. *Biogeochemistry* 125:133–148
- Ning Z, Liu S, Zhang G, Ning X and others (2016) Impacts of an integrated multi-trophic aquaculture system on benthic nutrient fluxes: a case study in Sanggou Bay, China. *Aquacult Environ Interact* 8:221–232
- Otero XL, Calvo de Anta RM, Macías F (2006) Sulfur partitioning in sediments and biodeposits below mussel rafts in the Ría de Arousa (Galicia, NW Spain). *Mar Environ Res* 61:305–325
- Pu XQ, Li F, Zhong SJ, Xu LJ (2008) Acid volatile sulfides in sediments of South Yellow Sea. *Proc 2nd International Conference on Bioinformatics and Biomedical Engineering*, 16–18 May 2008, Shanghai. Institute of Electrical and Electronics Engineers, Piscataway, NJ, p 1058–1061
- Reid MK, Spencer KL (2009) Use of principal components analysis (PCA) on estuarine sediment datasets: the effect of data pre-treatment. *Environ Pollut* 157:2275–2281

- Santisteban JI, Mediavilla R, López-Pamo E, Dabrio CJ and others (2004) Loss on ignition: a qualitative or quantitative method for organic matter and carbonate mineral content in sediments? *J Paleolimnol* 32:287–299
- Sanz-Lázaro C, Marin A (2006) Benthic recovery during open fish farming abatement in western Mediterranean, Spain. *Mar Environ Res* 62:374–387
- Song XL, Yang Q, Sun Y, Yin H, Jiang SL (2012) Study of sedimentary section records of organic matter in Sanggou Bay over the last 200 years. *Acta Oceanol Sin* 34: 120–126 (in Chinese with English Abstract)
- Sun S, Liu SM, Ren JL, Zhang JH, Jiang ZJ (2010) Distribution features of nutrients and flux across the sediment-water interface in the Sanggou Bay. *Acta Oceanol Sin* 32: 108–117 (in Chinese with English Abstract)
- Vismann B (1991) Sulfide tolerance: physiological mechanisms and ecological implications. *Ophelia* 34:1–27
- Wei ZQ, Liu CQ, Liang XB, Wang FS, Wang SF (2005) Degradation of organic matter in the sediments of Hongfeng Reservoir. *Chin Sci Bull* 50:2377–2380
- Xia DX (1991) The record of Chinese bays, Book Three (The northern and eastern bay of Shandong peninsula). Ocean Press, Beijing
- Yokoyama H (2003) Environmental quality criteria for fish farms in Japan. *Aquaculture* 226:45–56
- Zhang XL, Zhu MY, Chen S, Grant J, Martin JL (2006) Study on sediment oxygen consumption rate in the Sanggou Bay and Jiaozhou Bay. *Adv Mar Sci* 24:91–96 (in Chinese with English Abstract)
- Zhang JH, Hansen PK, Fang JG, Wang W, Jiang ZJ (2009) Assessment of the local environment impact of intensive marine shellfish and seaweed farming—application of the MOM system in the in the Sungo Bay, China. *Aquaculture* 287:304–310
- Zhu MX, Liu J, Yang GP, Li T, Yang RJ (2012) Reactive iron and its buffering capacity towards dissolved sulfide in sediments of Jiaozhou Bay, China. *Mar Environ Res* 80:46–55
- Zhu MX, Shi XN, Yang GP, Hao XC (2013) Formation and burial of pyrite and organic sulfur in mud sediments of the East China Sea inner shelf: constraints from solid-phase sulfur speciation and stable sulfur isotope. *Cont Shelf Res* 54:24–36

*Editorial responsibility: Peter Cranford,
Dartmouth, Nova Scotia, Canada*

*Submitted: May 13, 2015; Accepted: October 13, 2015
Proofs received from author(s): November 9, 2015*



Influence of mariculture on the distribution of dissolved inorganic selenium in Sanggou Bay, northern China

Yan Chang^{1,2,*}, Jing Zhang², Jianguo Qu², Zengjie Jiang³, Ruifeng Zhang²

¹School of Ecological and Environmental Sciences, East China Normal University, Shanghai 200062, PR China

²State Key Laboratory of Estuarine and Coastal Research, East China Normal University, Shanghai 200062, PR China

³Key Laboratory for Sustainable Utilization of Marine Fisheries Resources, Ministry of Agriculture, Yellow Sea Fisheries Research Institute, Chinese Academy of Fishery Sciences, Qingdao 266071, PR China

ABSTRACT: Selenium is known as a 'double-edged sword' element on account of its dual beneficial and toxic effects on organisms, depending on its concentration and chemical form. Dissolved inorganic selenium (DISE) concentration in the water column and selenium content in biological species were investigated in a typical aquacultural area in Sanggou Bay, China. In addition to sampling within Sanggou Bay, the main sources of DISE into Sanggou Bay were sampled to estimate selenium transport from different sources. Results showed that DISE and selenite [Se(IV)] concentrations averaged, respectively, 0.69 nmol l^{-1} and 0.28 nmol l^{-1} , with ranges 0.21 to 1.36 nmol l^{-1} and 0.07 to 0.58 nmol l^{-1} , in the surface water of Sanggou Bay. The DISE in Sanggou Bay remained well below the toxic levels. The DISE and Se(IV) concentrations varied temporally, with lows in summer and highs in spring and autumn. Concentrations showed strong horizontal gradients from the coast to offshore areas within the bay, as significantly influenced by the intensive and widespread seaweeds and bivalves aquaculture activity in the bay. The highest selenium content (mean \pm SD) was observed in scallops ($3.6 \pm 0.7 \text{ } \mu\text{g g}^{-1}$), followed by oyster ($1.6 \pm 0.4 \text{ } \mu\text{g g}^{-1}$), phytoplankton ($0.9 \pm 0.3 \text{ } \mu\text{g g}^{-1}$), *Gracilaria lemaneiformis* ($0.063 \pm 0.008 \text{ } \mu\text{g g}^{-1}$) and kelp ($0.032 \pm 0.005 \text{ } \mu\text{g g}^{-1}$). The main source of DISE in Sanggou Bay was water exchange with the Yellow Sea, whereas the most important sink was biological activity, which removed $53 \pm 12 \%$ of the incoming selenium from bay waters.

KEY WORDS: Dissolved inorganic selenium · Aquaculture · Seaweed · Bivalve · Sanggou Bay

INTRODUCTION

Selenium is known to be a 'double-edged sword' element, having one of the narrowest ranges of beneficial effects of all elements, varying between dietary deficiency ($<40 \text{ } \mu\text{g d}^{-1}$) and toxicity ($>400 \text{ } \mu\text{g d}^{-1}$) (Price et al. 1987, Fernández-Martínez & Charlet 2009). Selenium is an essential trace element required in the diets of many organisms for normal growth and physiological functions (Lin & Shiau 2005, Lobanov et al. 2009). It serves as a component of the enzyme glutathione peroxidase to protect cell

membranes against oxidative damage (Rotruck et al. 1973). However, excess dietary selenium behaves as an analogue to sulfur, erroneously replacing sulfur atoms in proteins; this leads to distortion of the structure and eventual dysfunction of enzymes and proteins (Simmons & Wallschläger 2005). The biogeochemical cycle of selenium in aquatic systems has attracted considerable attention in recent decades (Cutter & Bruland 1984, Cutter & Cutter 1995, 2001, Abdel-Moati 1998, Yao & Zhang 2005).

Similar to other trace elements, the chemical form has an important influence on the fate of the sele-

*Corresponding author: cyyc2010@126.com

nium. To understand the biological function of selenium in aquatic organisms, it is necessary to know the levels of different selenium species in the water column. The behavior of selenium in natural waters is complicated by the presence of several oxidation states (–II, IV, VI) and organic species (Conde & Sanz Alaejos 1997). Selenite [Se(IV)] and selenate [Se(VI)] are depleted in surface water and enriched in deep water, and exhibit a nutrient-type profile consistent with other bioactive trace elements in the ocean (Cutter & Bruland 1984, Cutter & Cutter 1995, 2001).

China is one of the largest marine shellfish and seaweed producers in the world (Zhang et al. 2009). Sanggou Bay, located in Shandong Province, is an important aquacultural production area in China (Guo et al. 1999) (see Fig. 1), and is mainly used to culture seaweed and bivalves (Fang et al. 1996). Sanggou Bay has been the focus of research for ~20 yr, and extensive studies have been conducted on hydrodynamic characteristics (Zhao et al. 1996), sediment chemistry (Cai et al. 2003), nutrients (Liu et al. 2004), heavy metals (Jiang et al. 2008), ecosystem services (Zheng et al. 2009), and the sustainable management of aquaculture (Zhang et al. 2009, Shi et al. 2011). Until now, however, little research has been conducted on selenium in the aquacultural areas. Studies have indicated that selenium can stimulate the growth of seaweed (Fries 1982, Horne 1991) and that, through metabolism, seaweed can accumulate over 50 times more inorganic selenium in Se(IV) enriched culture medium than in seawater (Yan et al. 2004). In addition, the selenium assimilation efficiency of bivalves can be as high as 70 to 95 % when feeding on the cytoplasm of the prey alga (Wang & Fisher 1996, Reinfelder et al. 1997); these levels may be threatening to upper trophic level birds and fish (Lemly 1995). Further studies are necessary to investigate the distributions of selenium species in aquaculture areas like Sanggou Bay, and to understand the mechanisms controlling the speciation of selenium in natural waters more generally.

The goal of this research was to investigate the distribution of dissolved inorganic selenium (DISE), selenite [Se(IV)] and selenate [Se(VI)] in Sanggou Bay, and in the river and groundwater along the coastline of the bay, in order to (1) determine the distribution of inorganic selenium species under different aquaculture conditions, and (2) estimate the input and output fluxes of selenium species. The results of this study will improve understanding of how the mariculture of seaweed and bivalves affects selenium biogeochemistry in aquacultural areas.

MATERIALS AND METHODS

Study area

Sanggou Bay is situated on the eastern tip of Shandong Peninsula to the northwest of the Yellow Sea (37° 01' to 37° 09' N, 122° 24' to 122° 35' E), with a total area of approximately 144 km² and mean depth of 7.5 m (Zhang et al. 2009). The bay has been used for aquaculture with seaweed and bivalves in different regions for >30 yr. Monoculture of seaweeds, including kelp *Saccharina japonica* and *Gracilaria lemaneiformis*, occurs mainly near the mouth of the bay (hereafter 'S-region') from December to May (winter and spring) and from June to November (summer and autumn), respectively. Monoculture of bivalves (in the 'B-region'), including scallops (*Chlamys farreri*) and oysters (*Crassostrea gigas*), is mainly located near the end of the bay, while the middle part of the bay is occupied by seaweed–bivalve polyculture ('SB-region') (Fig. 1). The annual production of kelp and *G. lemaneiformis* is approximately 84.5 × 10³ and 25.4 × 10³ t dry weight, respectively, while the annual production of bivalves is approximately 75 × 10³ t (Rongcheng Fisheries Technology Extension Station 2012). The rivers that enter the bay include the Gu (Chinese name: Guhe), Yatou (Yatouhe), Sanggan (Sangganhe), and Shili (Shilihe) rivers, as well as several other smaller creeks. The annual discharge of these seasonal rivers is from 0.17 × 10⁹ to 0.23 × 10⁹ m³ (Editorial Board of Annals of Bays in China 1991).

Sample collection

Samples were collected from marine areas in and adjacent to Sanggou Bay and from major rivers and groundwater along the coastline of the bay. Marine samples were collected during cruises in Sanggou Bay from 22 to 26 April (spring), 21 to 29 July (summer), and 17 to 20 October (autumn) of 2013, to investigate selenium levels in different seasons and various aquacultural activities. During each cruise, approximately 21 marine stations (Stns SG1 to SG19) were sampled (Fig. 1). Surface water was collected upstream and to the side of the boat while the boat moved forward, using a plastic pole sampler 3 to 4 m in length with an acid-cleaned polyethylene bottle attached to the end. Near-bottom water samples were taken with a 5 l organic glass hydrophore. Sediment cores (about 0 to 4 cm depth) were collected using a box core (15 × 15 cm) at Stns SG5 and SG6 in July 2013. Porewaters were extracted and filtered

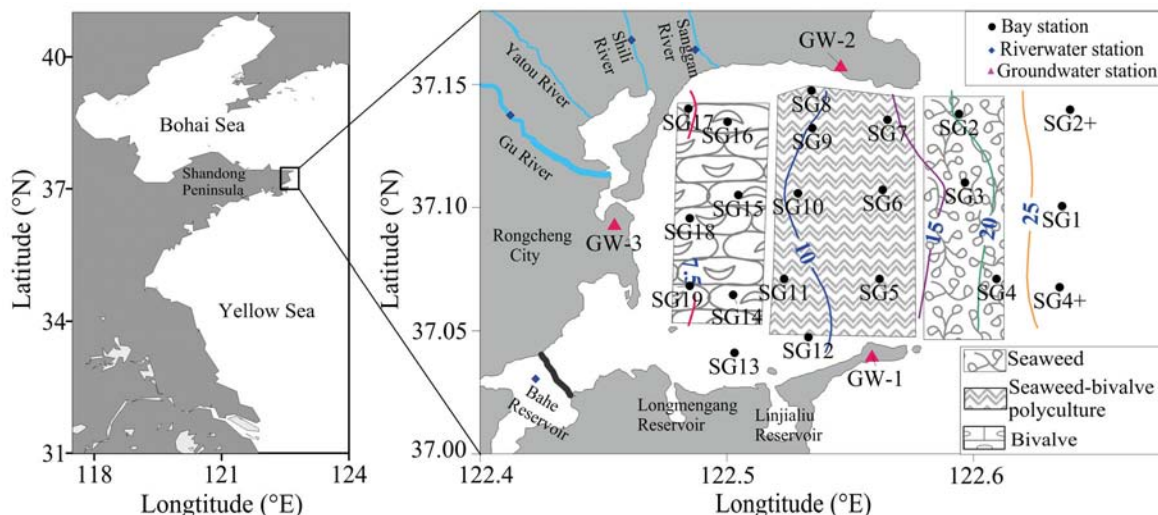


Fig. 1. Locations of field sampling and observation sites in Sanggou Bay in April, July and October 2013

from the sediment cores using 19.21.23F Rhizon CSS soil moisture samplers (Liu et al. 2011) and were frozen until analysis. River water and groundwater sampling was undertaken in April and July 2013 (Fig. 1). On each occasion, a total of 5 river water samples (from the Gu River [2 stations], Shili River, Yatou River, and Bahe Reservoir; Fig. 1) were collected using a 5 l clean plastic bucket from relatively fast-moving areas located away from urban regions. Three groundwater samples (from Stns GW-1, GW-2 and GW-3; Fig. 1) were collected from wells along the coastline of Sanggou Bay. Water temperature and salinity were measured *in situ* using an YSI Professional Plus meter at the time of sample collection. Water samples were filtered in the laboratory within 8 h of collection through precleaned 0.40 μm Nucleopore filters on a class 100 clean bench. The filtrates were placed in acid-cleaned polyethylene bottles and kept frozen until analysis.

Phytoplankton were collected by net tows using a net with a mesh size of 70 μm in April 2015. After the trawl, the plankton were filtered through a 200 μm mesh to remove the zooplankton and then were stored in plastic bottles previously decontaminated with dilute HCl solution. These bottles were kept from the sun and heat in an insulated box containing ice throughout the sampling process and transported to the laboratory. Phytoplankton were collected on the weighed 0.40 μm Nucleopore filters and freeze dried until analysis. Kelp, *G. lemaneiformis*, scallops and oysters samples were also collected in the bay during April, July, July and October 2013, respectively, stored in zip-closure plastic bags and kept in an insulated box containing ice throughout the sampling process. The seaweeds were washed with distilled water

to remove salts and small invertebrates and freeze dried. The muscle was collected from bivalves and freeze dried. Dried samples were ground into powder to pass through an 80 mesh (180 μm) sieve before analysis.

Analytical methods

Measurement of dissolved selenium concentrations

The analytical techniques for Se(IV) and Se(VI) by hydride generation combined with sector field inductively coupled plasma mass spectrometry (HG-ICP-MS) (Element 2™ ICP-MS, Thermol) have been described elsewhere (Zhang & Combs 1996, Chang et al. 2014). Briefly, Se(IV) at an acidity of 2 mol l⁻¹ HCl was reacted with NaBH₄ to produce hydrogen selenide and was then quantified using HG-ICP-MS. Se(VI) was quantitatively reduced to Se(IV) by heating a sample acidified with 3 mol l⁻¹ HCl to 97°C for 75 min, then quickly cooling the sample to room temperature using an ice-water bath, and finally following the steps for Se(IV) determination to yield the concentration of dissolved inorganic selenium (DISE). The reduction recovery ranged from 95 to 103%. This reduction method avoided the problematic variation in Se(VI) reduction behavior with different matrices, and kept the reduction rate at nearly 100% for a longer period of time than previous methods (e.g. Cutter et al. 1978, Yao & Zhang 2003). The Se(VI) concentration was calculated as the difference between DISE and Se(IV). The detection limits for Se(IV) and Se(VI) were 0.025 and 0.030 nmol l⁻¹, respectively. The measurement precisions for Se(IV) and Se(VI) in

river water were 3.4 and 3.9%, respectively, and those in seawater were 3.1 and 3.4%, respectively. The spiked standard Se(IV) or Se(VI) recovery ranged from 97 to 103%. The accuracy of the methods was tested with standard solutions, Se(IV) 50031-94 and Se(VI) GBW10032, and showed differences within −3.0 and 0.7%, respectively. The concentration of chlorophyll *a* (chl *a*) was measured using an ACLW-RS chlorophyll turbidity temperature sensor.

Measurement of selenium content of biological tissues

For total selenium content determination, complete digestion of the biological species tissues was performed with a microwave digestion system (MARSXpress, CEM). Samples (about 0.2 g) of dry tissue were soaked in 6 ml concentrated HNO₃. The digestion program was as follows: the sample was heated to 100°C for 10 min, held for 5 min, and then heated to 150°C for 5 min, held for 5 min, and finally heated to 180°C within 5 min and held for 45 min. After cooling, the solution was evaporated at 150°C to dryness using a heating block within about 2.5 h. Subsequently, the residue was dissolved in 5 ml 4 mol l^{−1} HCl, and heated in 110°C using the heating block to reduce Se(VI) to Se(IV) for 45 min. After cooling, samples were added 15 ml H₂O and diluted with 1 mol l^{−1} HCl to 50.0 ml in volumetric flask. The selenium concentration was determined by HG-ICP-MS. The biological standard reference materials GBW010024 (sea scallop), GBW010025 (spiral algae) and GBW010050 (prawn) were measured, with results of 1.49 ± 0.05, 0.23 ± 0.008 and 5.12 ± 0.05 µg g^{−1} (2σ, n = 6), respectively, with relative error −0.6, +3.8, and +0.3%, respectively, confirming the accuracy of the method.

Data statistics and analysis

The statistics software package Statistical Package for the Social Sciences version 16.0 (SPSS) was used for all data analyses. Differences were tested for significance using 1-way and 2-way analysis of variance (ANOVA), and *p* < 0.05 was taken to indicate significant difference. Mean values are presented with standard deviation throughout.

Flux estimates

A steady-state box model based on the Land-Ocean Interactions in the Coastal Zone (LOICZ) Biogeo-

chemical Modeling Guidelines was used to construct a DISe budget for Sanggou Bay from water budgets and non-conservative distribution of DISe, which were in turn constrained by the salt balance under steady-state conditions (Gordon et al. 1996).

The vertical diffusional flux of dissolved selenium from the bottom sediment was estimated using a modified form of Fick's first law (Meseck & Cutter 2012):

$$J = \theta^m D_o \left(\frac{\Delta Se}{\Delta z} \right) \quad (1)$$

where *J* is the diffusional flux, *θ* is the porosity, *m* has a value of 3 for surface sediments (Ullman & Aller 1982), *D_o* is the effective diffusion coefficient (−4.87 × 10¹⁰ m² s^{−1}) (Meseck & Cutter 2012), and Δ*Se*/Δ*z* is the observed concentration gradient of porewater selenium. The selenium concentration at *z* = 0 m (*Se*₀) in water from the near-bottom of the core was used as the initial point in the concentration gradient. A negative value of *J* indicates that dissolved selenium is fluxing out of the sediments, while a positive *J* results from dissolved selenium fluxing into the sediments. The value of *θ* in Sanggou Bay was 0.7 (Ning et al. 2016, this Theme Section).

RESULTS

Hydrographic properties in Sanggou Bay

The water temperature in the Sanggou Bay displayed a significant horizontal gradient, decreasing from the coast to offshore in spring and summer, with a reversed gradient occurring in autumn (Fig. 2a–c). Mean water temperatures ranged from 7.7 to 20.7°C between seasons, reflecting a remarkable seasonal variation (Table 1). The salinity increased from the coast to offshore (Fig. 2d–f) as a result of water exchange with the Yellow Sea. The mean salinity varied slightly, from 28.3 to 31.4, with lows in July and October due to rainfall and freshwater discharge (Table 1). The average concentrations of phytoplankton biomass, measured as chl *a*, varied between 0.83 µg l^{−1} in spring and autumn, and 6.9 µg l^{−1} in summer (Table 1).

Seasonal variations of inorganic selenium species

Concentrations of DISe ranged from 0.21 to 1.36 nmol l^{−1} for all surface water samples in the bay, with a mean of 0.69 nmol l^{−1} (Table 1). The critical selenium limit in water is classified as 126 nmol l^{−1} in China,

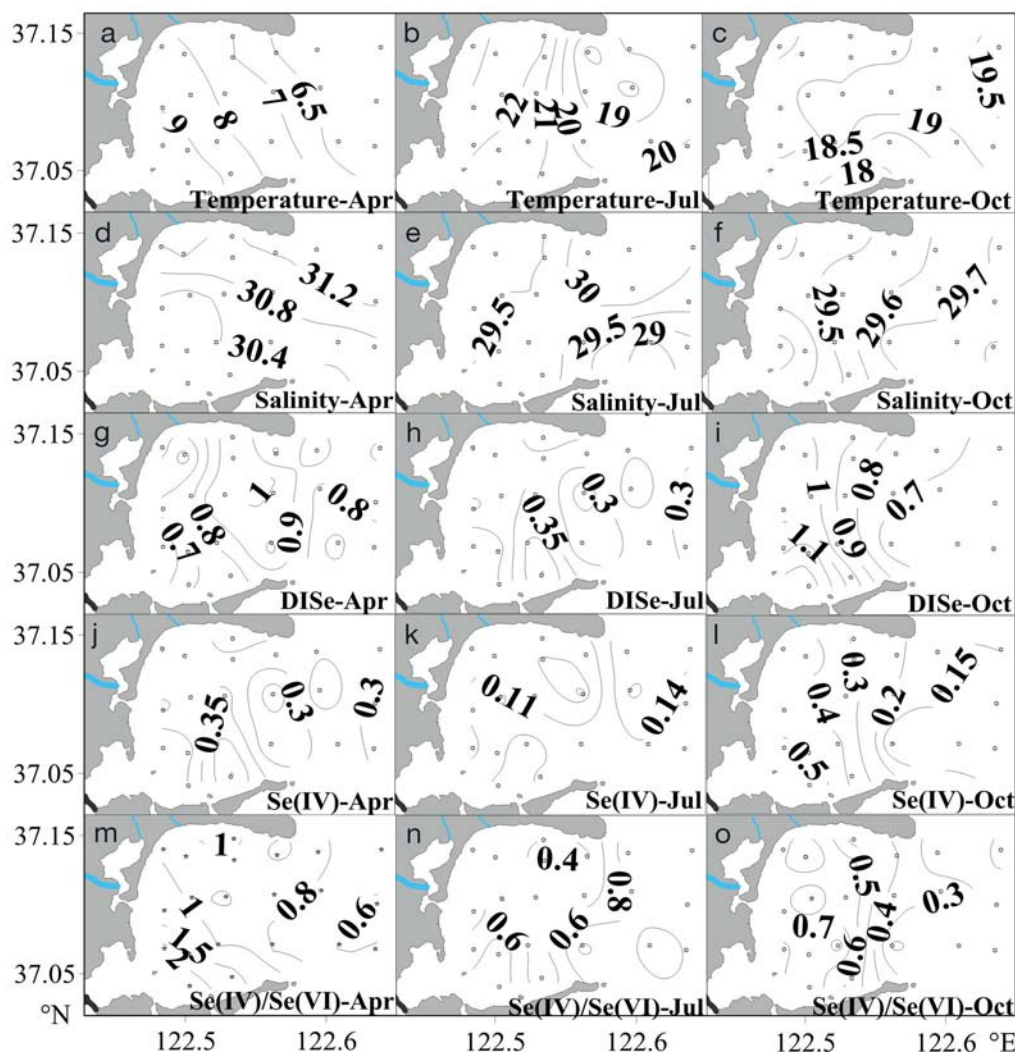


Fig. 2. (a–c) Temperature, (d–f) salinity, (g–i) dissolved inorganic selenium (DISe) concentration, (j–l) Se(IV) concentration and (m–o) Se(IV)/Se(VI) ratio distributions at the surface of Sanggou Bay in April, July, and October 2013 (left, centre and right columns, respectively)

Table 1. Mean values (with ranges in parentheses) of temperature, salinity, chl *a*, dissolved inorganic selenium (DISe) and Se(IV) concentration and Se(IV)/Se(VI) ratio in the surface water of Sanggou Bay in April, July and October 2013

	Spring (April)	Summer (July)	Autumn (October)
Temperature (°C)	7.7 (6.0–9.9)	20.7 (17.7–24.5)	18.5 (16.6–19.6)
Salinity	30.7 (30.1–31.4)	29.6 (28.3–30.5)	29.5 (29.3–29.8)
Chl <i>a</i> (µg l ⁻¹)	0.83 (0.59–2.3)	6.9 (0.86–20)	0.83 (0.36–2.0)
DISe (nmol l ⁻¹)	0.79 (0.47–1.02)	0.33 (0.21–0.46)	0.89 (0.61–1.36)
Se(IV) (nmol l ⁻¹)	0.39 (0.24–0.51)	0.12 (0.07–0.18)	0.30 (0.10–0.58)
Se(IV)/Se(VI) ratio	1.07 (0.59–2.30)	0.64 (0.30–1.06)	0.51 (0.18–0.85)

(State Environmental Protection Administration of China 2002); the dissolved selenium in Sanggou Bay remained 2 orders of magnitude below toxic levels.

The minimum mean concentrations of DISe occurred during summer (0.33 nmol l⁻¹), while the maximum occurred during autumn (0.89 nmol l⁻¹) (Table 1). The minimum mean concentrations of Se(IV) also occurred during summer (0.12 nmol l⁻¹), but the maximum occurred during spring (0.39 nmol l⁻¹) (Table 1). One-way ANOVA showed that the concentrations of DISe and Se(IV) were not significantly different between spring and autumn ($p > 0.05$), but that the values in summer were significantly lower than those in spring and autumn ($p < 0.0001$). It is clear from Table 1 that mean concentrations of DISe and Se(IV)

showed similar seasonal patterns, with low values in summer and high values in spring and autumn. The mean Se(IV)/Se(VI) ratios for spring, summer, and autumn were 1.07, 0.64, and 0.51, respectively (Table 1). One-way ANOVA showed that the Se(IV)/Se(VI) ratio was not significantly different between summer and autumn ($p = 0.25$), whereas values in spring were significantly higher than those in summer and autumn ($p < 0.0001$). The Se(IV)/Se(VI) ratio indicated that Se(VI) was the dominant species of inorganic selenium in the bay during summer and autumn, but Se(IV) was the dominant species in the large proportion along the coast of the bay during spring.

Horizontal distributions of inorganic selenium species

The horizontal distributions of DISE, Se(IV), and the Se(IV)/Se(VI) ratio in surface waters of Sanggou bay show similar features, such as a strong horizontal gradient from the coast to offshore (Fig. 2g–o). The concentrations of DISE along the coast during spring were lower than concentrations in the rest of the bay (Fig. 2g). While DISE showed a strong zonal distribution along the coast during autumn, decreasing offshore from 1.2 to 0.6 nmol l⁻¹, it was rather evenly distributed in summer (Fig. 2h,i). The distribution of Se(IV) in the bay exhibited a similar pattern to DISE in spring, summer, and autumn (Fig. 2j–l). The Se(IV)/Se(VI) ratio had a zonal distribution along the coast during spring and autumn, decreasing offshore from 2 to 0.6 and 0.7 to 0.3, respectively (Fig. 2m,o); however, during summer, the ratio was higher along the coast and at the mouth of the bay (0.8) as compared with in the central region (0.4) (Fig. 2n).

A 2-way ANOVA was conducted that examined the effect of season and space (i.e. S-region, B-region and SB-region, representing the 3 main types of aquaculture in Sanggou Bay) on Se(IV) and Se(VI) distribution. Both season and space significantly affected Se(IV) and Se(VI) concentrations ($p = 0.0001$). There was also significant interaction between season and space ($p = 0.0001$). Se(IV) concentrations in the S-region and B-region were significantly less than those in the SB-region in spring ($p = 0.046$) (Fig. 3a). In contrast, Se(VI) concentrations during spring in the B-region were significantly lower than those in the S-region and SB-region ($p = 0.007$) (Fig. 3b). During summer, Se(IV) concentrations in the S-region were slightly higher than those in the SB-region and B-region ($p = 0.015$) (Fig. 3a). There was no significant difference in Se(VI) concentrations between different regions during summer ($p = 0.235$). In autumn, Se(IV) concentrations in the bay increased in the following order: S-region, SB-region and B-region ($p < 0.0001$) (Fig. 3a). Se(VI) concentrations shared the same pattern ($p < 0.02$), with low values in the S-region and high values in the B-region (Fig. 3b).

Riverine input of selenium to Sanggou Bay

As shown in Table 2, the DISE and Se(IV) concentrations in 4 riverine waters were not significantly different between spring and summer ($p > 0.2$). Overall, DISE concentrations in riverine water ranged from 0.69 to 1.5 nmol l⁻¹ with a mean of 1.0 nmol l⁻¹; these were slightly higher than those observed in the water column in Sanggou Bay (0.68 ± 0.29 nmol l⁻¹) during this study (Tables 1 & 2). The mean concentration of Se(IV) was 0.14 nmol l⁻¹ in both spring and

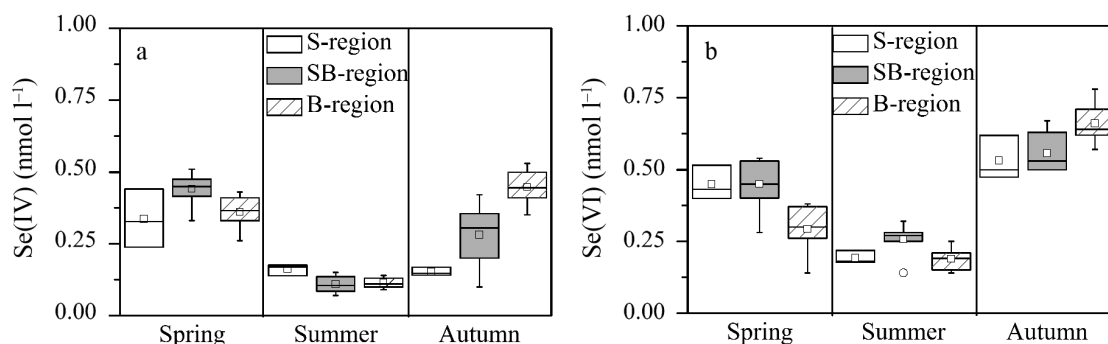


Fig. 3. Box plots of (a) Se(IV) and (b) Se(VI) concentrations in seaweed monoculture (S-region), seaweed-bivalve polyculture (SB-region) and bivalve monoculture (B-region) in spring, summer and autumn of 2013. The ends of the box and the ends of the whiskers, and the line across the box represent the 25th and 75th percentiles, the 1st and 99th percentiles and the median, respectively; the open square inside the box indicates the mean value. A circle represents an outlier

Table 2. Concentrations of dissolved inorganic selenium (DISE) and Se(IV) and Se(IV)/Se(VI) ratio in major rivers that enter into Sanggou Bay and in groundwater (GW) along the coastline of Sanggou Bay, measured in April and July 2013

Water source	Sampling location / station number	DISE (nmol l ⁻¹)	Se(IV) (nmol l ⁻¹)	Se(IV)/Se(VI) ratio
Spring (April 2013)				
River	Gu River	1.21	0.18	0.17
	Sanggan River	0.69	0.17	0.21
	Shili River	1.12	0.08	0.18
	Bahe Reservoir	0.91	0.12	0.10
Groundwater	GW-1	34.9	1.36	0.04
	GW-2	3.14	0.60	0.24
	GW-3	3.49	0.26	0.08
Summer (July 2013)				
River	Gu River	1.49	0.11	0.08
	Sanggan River	0.84	0.21	0.18
	Shili River	1.03	0.12	0.25
	Bahe Reservoir	1.16	0.13	0.11
Groundwater	GW-1	27.5	2.76	0.11
	GW-2	5.45	0.49	0.10
	GW-3	3.54	0.89	0.34

Groundwater input of selenium to Sanggou Bay

The salinity values of groundwater samples were <0.1, indicating that they are freshwater. The DISE and Se(IV) concentrations in groundwater showed little temporal variation and were not significantly different between spring and summer ($p > 0.1$). DISE was >25 nmol l⁻¹ in the sample from Stn GW-1, while it was <6 nmol l⁻¹ in samples from Stns GW-2 and GW-3 (Table 2). The low concentrations of ²²⁶Ra in sample GW-1 (Wang et al. 2014) indicates the low activity of rock–water interactions. Moreover, the dissolved inorganic arsenic concentration was nearly 10 times higher in sample GW-1 than samples GW-2 and GW-3 (Li et al. 2014). Stn GW-1 was

excluded from the calculation of average selenium concentration. The mean DISE and Se(IV) concentrations were 3.91 ± 1.05 nmol l⁻¹ and 0.56 ± 0.26 nmol l⁻¹, respectively. The mean Se(IV)/Se(VI) ratio was 0.15, indicating that Se(VI) was the predominant species in the groundwater. The mean DISE concentration in groundwater (3.91 nmol l⁻¹) was nearly 4 times higher than that in riverine water (1.0 nmol l⁻¹). Compared with surface water, groundwater usually contains higher content due to greater contact time for rock–water interactions (Fordyce 2013).

Selenium content in aquaculture species

The lowest content of Se was present in kelps (0.032 ± 0.005 µg g⁻¹), followed by *G. lemaneiformis* (0.063 ± 0.008 µg g⁻¹) (Fig. 4) these values were in the range of selenium content (0.01 to 0.6 µg g⁻¹) reported elsewhere in seaweed (Liu et al. 1987, Maher et al. 1992, Barwick & Maher 2003). These seaweeds accumulated selenium to concentrations 3 to 4 orders of magnitude above the ambient concentration in the seawater. The Se content for phytoplankton (0.9 ± 0.3 µg g⁻¹) was 10 to 30 times higher than for seaweeds (Fig. 4), and the value was within the range of those previously published for marine phytoplankton (0.5 to 4.5 µg g⁻¹) (Liu et al. 1987, Baines & Fisher 2001, Sherrard et al. 2004). The highest mean Se contents were observed in bivalves, i.e. scallops (3.6 ± 0.7 µg g⁻¹) and oysters (1.6 ± 0.4 µg g⁻¹); these values were consistent with

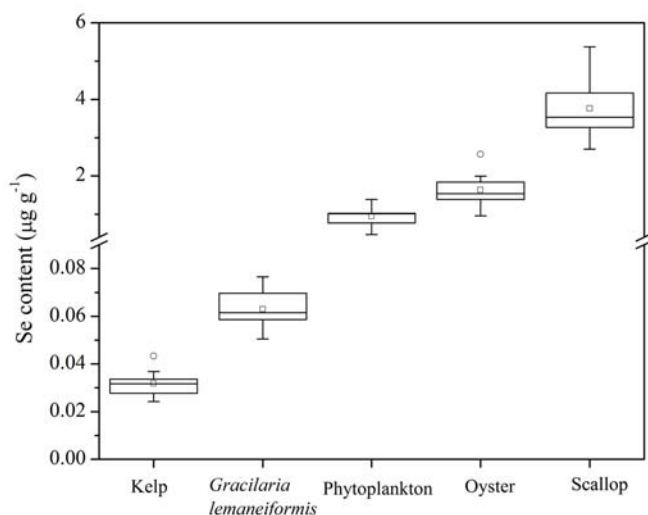


Fig. 4. Selenium (Se) content in kelp (n = 11), *G. lemaneiformis* (n = 9), phytoplankton (n = 6), oysters (n = 9) and scallops (n = 9). Box plot details as in Fig. 3

summer; this concentration was comparable to the one observed in the water column in Sanggou Bay during summer, but was lower than those observed during spring and autumn (Tables 1 & 2). The mean Se(IV)/Se(VI) ratio was 0.16, with a range of 0.08 to 0.25, indicating that Se(VI) was the major inorganic species in riverine water. The DISE concentrations in the Sanggan River during spring and summer were lower than those in the Gu River, the Shili River and Bahe Reservoir; however, concentrations of DISE and Se(IV) varied only slightly among rivers.

the range in bivalves reported elsewhere (0.24 to $4.6 \mu\text{g g}^{-1}$) (Liu et al. 1987, Baldwin & Maher 1997, He & Wang 2013).

DISCUSSION

Influence of phytoplankton on selenium distribution

As shown in Table 1, Se(IV) concentrations were lower in summer and higher in spring, while the opposite was true for chl *a* concentrations. Studies have indicated that Se(IV) and Se(VI) can both be assimilated by phytoplankton, with Se(IV) being the preferred species for phytoplankton uptake (Apte et al. 1986, Vandermeulen & Foda 1988, Baines & Fisher 2001). Moreover, as illustrated in Fig. 2m,o, Se(IV)/Se(VI) ratios along the coast decreased towards offshore. In the coastal regions of the bay, the ratio was >0.5 during all 3 seasons, while the ratio in the freshwater end member (river and groundwater) was normally <0.2 (Table 2). There has been a paucity of investigations on selenium species in the Yellow Sea; the mean Se(IV)/Se(VI) ratio for Bohai Sea is 0.45 (Yao & Zhang 2005) and the value for East China Sea was 0.32 (Y. Chang et al. unpubl.). The relatively high Se(IV)/Se(VI) ratios in the bay compared to rivers and surrounding marine basins suggest that either Se(IV) is produced or Se(VI) is preferentially consumed in the bay. Both anions can be assimilated into biomass, but phytoplankton usually has a higher affinity for Se(IV) than for Se(VI) (Fig. 5). Therefore, preferential uptake of Se(VI)

probably cannot explain the observed pattern. However, the organic selenium is later released into the water column where it oxidizes to Se(IV) (Cutter & Bruland 1984), as dissolved oxygen is high in the bay. In contrast, the rate constant of the oxidation from Se(IV) to Se(VI) was $8.7 \times 10^{-4} \text{ yr}^{-1}$, which means it takes $>1000 \text{ yr}$ to oxidize Se(IV) to Se(VI) (Cutter & Bruland 1984); therefore, this process can be ignored. This may also be the reason why Se(IV)/Se(VI) ratios are elevated at the mouth of the bay during summer, as large amounts of algae would release organic selenium, which would then be oxidized to Se(IV) (Fig. 2n).

Influence of mariculture species on selenium distribution

The distribution of selenium was greatly affected by the mariculture species, as shown in Fig. 3. Laboratory studies have indicated that both Se(IV) and Se(VI) can increase the growth of macroalgae, with Se(IV) taken up more readily than Se(VI) (Fries 1982, Horne 1991). Kelp can bioaccumulate >50 times more inorganic selenium in a Se(IV) enriched culture medium than in seawater (Yan et al. 2004). The kelp in the bay is generally cultivated in November and is harvested in late May. Thus, due to the fast growth of kelp, Se(IV) would be preferentially taken up by the seaweed (Fries 1982). This would explain the relatively low concentrations of Se(IV) in the kelp monoculture region (S-region) in spring (Fig. 3a). Utilization of Se(VI) is more limited compared with Se(IV) (Fries 1982), resulting in the high levels of Se(VI) present in the S-region during spring (Fig. 3b). Moreover, the elevated Se(VI) may be caused by the Yellow Sea input. The *G. lemaneiformis* monoculture is planted after the harvest of kelp in late May. The assimilation of selenium by *G. lemaneiformis* is similar to that of kelp (Fries 1982).

Bivalves mainly accumulate selenium from particulate sources by ingestion and assimilation, while passive uptake from dissolved phases is negligible (Wang & Fisher 1996, Griscom & Fisher 2004, Luoma & Presser 2009). Bivalves have been observed to accumulate ingested selenium to concentrations markedly higher than those present in the algal diet, due to high assimilation rates of cytosolic selenium (Wang & Fisher 1996, Reinfelder et al. 1997). After ingestion, bivalves excrete selenium as dissolved phases probably in the forms of inorganic selenium, including Se(IV) and Se(VI), and organic selenium (Wang & Fisher 1996), and the organic selenium can then be

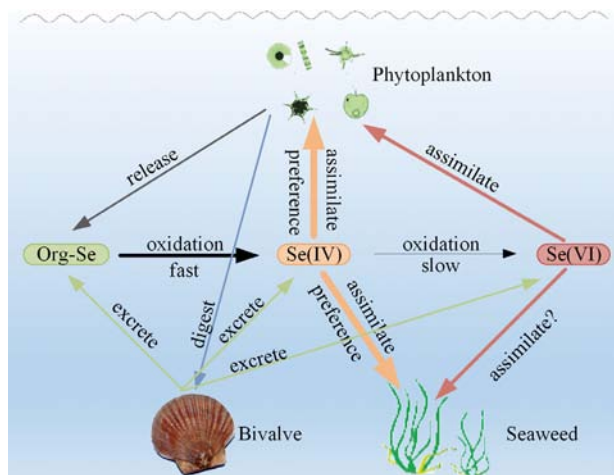


Fig. 5. A conceptual diagram of the biological effects of phytoplankton, seaweed and bivalves on selenium speciation (based on Vandermeulen & Foda 1988, Besser et al. 1994, Hu et al. 1997, Baines & Fisher 2001, present study)

oxidized to Se(IV) (Cutter & Bruland 1984). These processes probably resulted in the high Se(IV) and Se(VI) concentrations in the bivalve monoculture region (B-region) during autumn (Fig. 3a,b). Another possible reason for elevated Se(VI) concentrations in B-region was the input from river or groundwater.

The intensive kelp and bivalve aquaculture activities occurring over large areas of Sanggou Bay have a significant influence on the distribution of selenium in the bay. A conceptual diagram of the biological effects of phytoplankton, seaweed and bivalves on the selenium species in Sanggou Bay is shown in Fig. 5. Phytoplankton and seaweeds (kelp and *G. lemaneiformis*) preferentially assimilate Se(IV) and convert it to organic selenium (Fries 1982, Vandermeulen & Foda 1988, Horne 1991, Besser et al. 1994, Hu et al. 1997, Baines & Fisher 2001). Dissolved organic selenium regenerated from biogenic particles (as phytoplankton cells die and/or bivalves excrete) is quickly oxidized to Se(IV) in the oxygenated water (Cutter & Bruland 1984, Wang & Fisher 1996, Luoma & Presser 2009). However, neither Se(IV) nor organic selenium are reconverted to Se(VI), as these reactions have a half reaction time of hundreds of years (Cutter & Bruland 1984). Thus, the seaweeds assimilate both Se(IV) and Se(VI), resulting in low levels in the water column, while the bivalves assimilate particulate selenium but excrete dissolved selenium, replenishing selenium levels in the water column.

DISE budget for Sanggou Bay

Inputs of selenium to Sanggou Bay

The riverine input of DISE into Sanggou Bay (Y_Q) can reach $15 \pm 4 \text{ kg yr}^{-1}$ (see Fig. 6) by multiplying the mean DISE concentrations with the annual mean river water discharge.

The submarine groundwater discharge into the bay during summer is $(9.45 \text{ to } 11.20) \times 10^9 \text{ m}^3 \text{ yr}^{-1}$, as determined by calculation based on the non-conservative inventory of ^{226}Ra and ^{228}Ra (Wang et al. 2014). As submarine groundwater discharge includes recycled seawater (75 to 90%) as well as fresh groundwater (Moore 1996), the hypothesis of groundwater discharge over the whole bay—instead of just along the shoreline—overestimates the discharge volume. Therefore, we assumed that 5% of the submarine groundwater discharge represented a best estimate of the fresh groundwater discharge, resulting in a value of $0.47 \times 10^9 \text{ m}^3 \text{ yr}^{-1}$. The annual

input of DISE from fresh groundwater (Y_G) into the bay was then estimated by multiplying the mean DISE concentrations of groundwater and annual fresh groundwater discharge, giving a value of $146 \pm 39 \text{ kg yr}^{-1}$.

The diffusional flux of DISE from the sediment was calculated for the bay using Eq. (1). The DISE concentrations in near-bottom water and porewater for Stn SG5 were 0.32 nmol l^{-1} and 0.45 nmol l^{-1} , respectively, and DISE concentrations in near-bottom water and porewater for Stn SG6 were 0.3 and 0.41 nmol l^{-1} , respectively. Calculations demonstrate that there can be a -0.68 and a $-0.58 \text{ nmol m}^{-2} \text{ yr}^{-1}$ flux of DISE between the sediment and water column at Stns SG5 and SG6, respectively. The negative values indicate flux of DISE out of the sediment. The diffusional flux from the sediment to the water column in the bay was estimated by averaging the diffusional flux from each of the different regions. The DISE flux from the sediments (Y_S) was $(7.2 \pm 0.8) \times 10^{-3} \text{ kg yr}^{-1}$.

The selenium concentration in rainwater ranges from 1.3 to 2.6 nmol l^{-1} in China (Zhu & Tan 1988). A rainwater sample was collected during summer in the Bay with a selenium concentration of 1.7 nmol l^{-1} , which is within the range of rainwater values in China (Zhu & Tan 1988). Thus, the annual wet deposition of DISE was estimated to be 17.5 kg yr^{-1} , by multiplying the selenium concentration in rainwater with the amount of annual rainfall. The amount of selenium in dry deposition is not known for this region; therefore, the value for the East China Sea (soluble dry deposition of $0.27 \pm 0.48 \mu\text{g m}^{-2} \text{ d}^{-1}$) (Hsu et al. 2010) has been adopted to estimate the annual dry deposition of selenium into the bay. Accordingly, the total atmospheric input (wet and dry deposition) of selenium into the bay (Y_P) was $32 \pm 25 \text{ kg yr}^{-1}$.

Biological utilization of selenium

The elemental Se:C ratio for phytoplankton in seawater was $(8.5 \pm 3.0) \times 10^{-6}$, which were within the range of those previously published for marine phytoplankton (Liu et al. 1987, Baines & Fisher 2001, Sherrard et al. 2004), and the carbon fixed by phytoplankton in Sanggou Bay is $9.5 \times 10^6 \text{ kg yr}^{-1}$ (Jiang et al. 2015). Utilization of selenium by phytoplankton in Sanggou Bay was estimated to be $-81 \pm 29 \text{ kg yr}^{-1}$ (negative values indicate removal of selenium from the bay through assimilation by biological organisms; see Fig. 6) by multiplying the carbon fixed by phytoplankton and the elemental Se/C ratio for phytoplankton in Sanggou Bay.

Intensive aquaculture activities have a large influence on selenium levels in Sanggou Bay. The amount of selenium removed from the bay by aquaculture activities was calculated by multiplying aquacultural production in the bay (Rongcheng Fisheries Technology Extension Station 2012) and the selenium content in the cultured species, including kelp, *G. lemaneiformis*, scallops, and oysters. Thus, the amount of selenium fixed by kelp, *G. lemaneiformis*, scallops and oysters was 2.7 ± 0.4 , 1.6 ± 0.2 , 54 ± 11 , and 98 ± 54 kg yr⁻¹, respectively. The highest selenium utilization was by scallops and oysters (151 ± 30 kg yr⁻¹), followed by phytoplankton (81 ± 29 kg yr⁻¹) and seaweed (4.31 ± 0.5 kg yr⁻¹), and the total selenium utilization was estimated to be about 236 ± 42 kg yr⁻¹ (see Fig. 6).

Selenium budget for Sanggou Bay

The steady-state box model, illustrated in Fig. 6, calculates the water and salt budgets, and then estimates the mass balance of DISe in Sanggou Bay, including exchange with the Yellow Sea. Freshwater inputs from river discharge (V_Q), groundwater discharge (V_G) and precipitation (V_P) are 0.19×10^9 (Editorial Board of Annals of Bays in China 1991), 0.47×10^9

(Wang et al. 2014) and 0.13×10^9 m³ yr⁻¹ (Shandong province Rongcheng City the Local Chronicles Compilation Committee 1999), respectively. These inputs are reduced by evaporation (V_E), which is 0.15×10^9 m³ yr⁻¹ (Shandong province Rongcheng City the Local Chronicles Compilation Committee 1999). From the water mass balance, net water exchange (V_R) is from Sanggou Bay to the Yellow Sea, with a residual flow of -0.64×10^9 m³ yr⁻¹ (positive values indicate transport into the bay, negative values export from the bay to the Yellow Sea). Using a salinity of 0 for freshwater input, and salinities of 30 and 32 for Sanggou Bay and the Yellow Sea (Lin et al. 2005), respectively, the water exchange flow from the Yellow Sea to Sanggou Bay (V_X) is 9.96×10^9 m³ yr⁻¹, based on the salt balance in the bay. When calculating the net DISe transport from the Yellow Sea to Sanggou Bay, the mean the DISe concentration (1 ± 0.44 nmol l⁻¹) of Bohai Sea (Yao & Zhang 2005) and the East China Sea (Y. Chang et al. unpubl. data) was used as the value for the Yellow Sea, where DISe data are lacking. The net transport (Y_R) from Sanggou Bay to the Yellow Sea is -42 ± 12 kg yr⁻¹ (positive values indicate transport into the bay, negative values export from the bay to the Yellow Sea), and the exchange (Y_X) between the Yellow Sea and Sanggou Bay is 253 ± 71 kg yr⁻¹. The data obtained in this study allow for the calculation of

selenium budgets in Sanggou Bay (Fig. 6). Atmospheric dry and wet depositions (Y_P), riverine input (Y_Q), groundwater influx (Y_G), exchange between Yellow Sea and Sanggou Bay (Y_X), net transport from the Yellow Sea to Sanggou Bay (Y_R), sediment diffusion (Y_S), and biological fluxes are all shown in Fig. 6. The exchange between Sanggou Bay and the Yellow Sea (Y_X) was the major source of selenium to Sanggou Bay, contributing $57 \pm 19\%$ of total DISe inputs. Groundwater discharge (Y_G) accounted for $33 \pm 10\%$ of the total DISe input, making it the second largest source of selenium into the bay. However, the exchange of DISe flux ($0.002 \pm 0.0004\%$) between the sediment and the water column was negligible compared with other sources. The sediment–water exchange of selenium is also a negligible source in San Francisco Bay, as indicated by stable isotope ratios (Johnson et al. 2000) and sediment porewater values (Mesheck & Cutter 2012). The net transport of DISe from Sanggou Bay to the Yellow Sea accounted for $10 \pm 3\%$ of the DISe export.

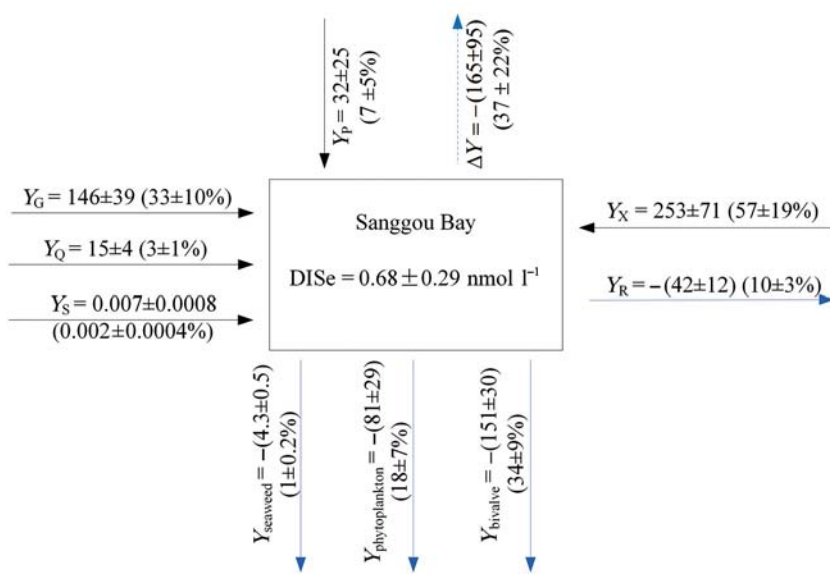


Fig. 6. Selenium budget in Sanggou Bay, showing inputs and outputs (Y) as absolute values (kg yr⁻¹; mean \pm SD) and as percentages of total input. Positive values of Y indicate transport into Sanggou Bay; negative values indicate export of dissolved inorganic selenium (DISe) from Sanggou Bay or assimilation by biological organisms. Y_P : atmospheric deposition; Y_Q : riverine input; Y_G : groundwater input; Y_X : exchange between Sanggou Bay and Yellow Sea; Y_R : net transport from Yellow Sea to Sanggou Bay; Y_S : sediment/diffusion; ΔY : net internal sink

The amount of selenium utilized by bivalves was $151 \pm 30 \text{ kg yr}^{-1}$. This amount was $34 \pm 9\%$ of the total DISe input (Fig. 6), making bivalves the most important selenium sink. Phytoplankton assimilation was another sink of selenium, using $18 \pm 7\%$ of the total DISe input, while the seaweed assimilated only $1 \pm 0.2\%$ of the total DISe input (Fig. 6). Thus, biological activity removed nearly $53 \pm 12\%$ of the DISe out of the water column and was the major sink of DISe in Sanggou Bay. This means with the harvesting of marine products, nearly half of the selenium was removed out of the bay.

The input of DISe was $445 \pm 85 \text{ kg yr}^{-1}$, and output of DISe was $280 \pm 42 \text{ kg yr}^{-1}$ in the bay. There was a net imbalance between the input and output of dissolved selenium, however. The selenium budgets in Sanggou Bay are only approximations, which depend on the accuracy of the freshwater, water exchange fluxes between Sanggou Bay and the Yellow Sea. If these flux estimates are valid, however, there is a net internal sink of $-165 \pm 95 \text{ kg yr}^{-1}$ ($37 \pm 22\%$) in the bay (Fig. 6). Studies have shown that algae can form dimethylselenide and dimethyldiselenide, which can be volatilized and released into the atmosphere (Ansede & Yoch 1997). The selenium flux of dimethylselenide to the atmosphere was estimated to be 60 to 260 kg yr^{-1} in Gironde Estuary (Ansede & Yoch 1997), and methylation was estimated to account for 10 to 30% of the selenium removed from San Francisco Bay (Hansen et al. 1998). Thus, internal sinks of DISe in Sanggou Bay might include emission from the water column into the atmosphere as volatile selenium, dissimilatory reduction of Se(VI) and Se(IV) to inorganic reduced phases (Se0, Se-II) (Stüeken et al. 2015), and/or transformation to other organic and particulate forms of selenium. To better constrain the uncertainty of budget calculations, more observations are required to understand the biogeochemical process of selenium in Sanggou Bay.

Sensitivity analysis

Box model sensitivity analysis were exemplified by changing model parameters by 10% in order to evaluate model response. The sensitivity was quantified by calculating a normalized sensitivity defined as the percentage change in a variable produced by a percentage change in the parameter.

Table 3. Normalized parameter sensitivity of the net internal sink of dissolved inorganic selenium (DISe) (ΔY) for each parameter

Parameter	Treatment (%)	Normalized sensitivity (%)
River discharge (V_Q)	10	4.7
Groundwater discharge (V_G)	10	18
Precipitation (V_P)	10	3.6
Evaporation (V_E)	10	-3.0
DISe concentration in Yellow Sea	10	47
DISe concentration in Sanggou Bay	10	-33
DISe concentration in rivers	10	0.9
DISe concentration in groundwater	10	8.8
DISe concentration in rainwater	10	1.1
Soluble dry deposition	10	0.9
DISe flux in sediments (Y_S)	10	1.1
Se content in phytoplankton	10	-4.9
Se content in kelp	10	-0.2
Se content in <i>G. lemaneiformis</i>	10	-0.1
Se content in oysters	10	-5.9
Se content in scallops	10	-3.3
Carbon fixed by phytoplankton	10	-4.9
Production of kelp	10	-0.2
Production of <i>G. lemaneiformis</i>	10	-0.1
Production of oysters	10	-5.9
Production of scallops	10	-3.3

Ten percentage changes in parameters of DISe concentration for Yellow Sea, DISe concentration for Sanggou Bay and groundwater discharge result in changes in net internal sink (ΔY) yield of 47, -32 and 18%, respectively, while changes in other parameters result in changes in ΔY yield of $<10\%$ (Table 3). There has been a paucity of investigations on selenium species in the Yellow Sea; the DISe concentration in Yellow Sea which was used to calculate the net DISe transport from the Yellow Sea to Sanggou Bay (Y_X) was obtained by averaging the values of Bohai Sea (Yao & Zhang 2005) and the East China Sea (Y. Chang et al. unpubl. data). The sensitivity analysis showed that DISe concentration in the Yellow Sea was the most critical parameter and therefore in cases where selenium data are available, it would be worth using a more accurate parameterization of DISe concentration in the Yellow Sea. The DISe concentrations in Sanggou Bay presented significantly variation between seasons and the relative annual mean variation was 42%, which is greater than the 10% changes for sensitivity analysis. Therefore, in future selenium budget calculation, it may be possible to reduce uncertainty in calculating the budget in seasonal levels. Moreover, the box model's sensitivity to changes in groundwater discharge suggested that any improvement in estimates of groundwater discharge is likely to improve the model accuracy. Finally, the budgets were relatively insensitive to riverine input (Y_G), atmospheric

deposition (Y_p), sediment diffusion (Y_s), and to biological fluxes. This suggested that inaccuracies in riverine, atmospheric deposition, sediment diffusion and biological data sets have relatively minor impacts on selenium budget calculation, especially in comparison with inaccuracies associated with other model inputs.

CONCLUSION

Distributions of dissolved inorganic selenium species observed in Sanggou Bay provide relevant information that can be linked to the dynamics and biological reactions that take place in the region. Average concentrations of DISe and Se(IV) in surface waters of the bay were 0.67 and 0.28 nmol l^{-1} , respectively, with ranges of 0.21 – 1.36 and 0.07 – 0.58 nmol l^{-1} , respectively. The average Se(IV)/Se(VI) ratio was 0.74 , indicating that Se(VI) was the predominate inorganic selenium species in large proportion of the bay. DISe concentrations in Sanggou Bay remained 2 orders of magnitude below the critical selenium limit for water in China. The highest selenium content was observed in scallops ($3.6 \pm 0.7 \mu\text{g g}^{-1}$), followed by oyster ($1.6 \pm 0.4 \mu\text{g g}^{-1}$), phytoplankton ($0.9 \pm 0.3 \mu\text{g g}^{-1}$), *G. lemaneiformis* ($0.063 \pm 0.008 \mu\text{g g}^{-1}$) and kelp ($0.032 \pm 0.005 \mu\text{g g}^{-1}$).

The DISe and Se(IV) concentrations were low in summer and high in spring and autumn. The distribution of DISe and Se(IV) in the bay showed strong horizontal gradients from the coast to offshore. The intensive seaweed and bivalve aquaculture present over large areas had a strong influence on selenium distribution. The Se(IV) concentrations in the seaweed monoculture region were low in spring due to the uptake by the seaweed. While the Se(IV) and Se(VI) concentrations in the bivalve monoculture region were high in autumn, probably caused by the bivalves assimilating particulate selenium but excreting dissolved selenium, thereby replenishing selenium levels in the water column.

A simple budget for DISe in Sanggou Bay was estimated in this study. The major source of DISe into Sanggou Bay was water exchange with the Yellow Sea. Groundwater discharge was the second largest source of selenium into the bay. However, intensive bivalve aquaculture removed $34 \pm 9\%$ of the DISe input, making it the most important sink.

Acknowledgements. This study was supported by the National Basic Research Program of China (No. 2011CB409801). The authors thank Chudao and Xunshan Fisheries Corporations for the help in the field work and providing

laboratory. We thank colleagues from Yellow Sea Fisheries Research Institute, East China Normal University and Ocean University of China for the assistance in field observations. Anonymous reviewers and the editor are especially acknowledged for their constructive suggestions, which greatly improved the manuscript.

LITERATURE CITED

- Abdel-Moati M (1998) Speciation of selenium in a Nile Delta Lagoon and SE Mediterranean Sea mixing zone. *Estuar Coast Shelf Sci* 46:621–628
- Ansede JH, Yoch DC (1997) Comparison of selenium and sulfur volatilization by dimethylsulfoniopropionatelyase (DMSP) in two marine bacteria and estuarine sediments. *Microb Ecol* 23:315–324
- Apte S, Howard A, Morris R, McCartney M (1986) Arsenic, antimony and selenium speciation during a spring phytoplankton bloom in a closed experimental ecosystem. *Mar Chem* 20:119–130
- Baines SB, Fisher NS (2001) Interspecific differences in the bioconcentration of selenite by phytoplankton and their ecological implications. *Mar Ecol Prog Ser* 213:1–12
- Baldwin S, Maher W (1997) Spatial and temporal variation of selenium concentration in five species of intertidal molluscs from Jervis Bay, Australia. *Mar Environ Res* 44: 243–262
- Barwick M, Maher W (2003) Biotransference and biomagnification of selenium copper, cadmium, zinc, arsenic and lead in a temperate seagrass ecosystem from Lake Macquarie Estuary, NSW, Australia. *Mar Environ Res* 56:471–502
- Besser JM, Huckins JN, Clark RC (1994) Separation of selenium species released from Se-exposed algae. *Chemosphere* 29:771–780
- Cai LS, Fang JG, Liang XM (2003) Natural sedimentation in large-scale aquaculture areas of Sungo Bay, North China Sea. *J Fish Sci China* 10:305–310 (in Chinese with English Abstract)
- Chang Y, Qu JG, Zhang RF, Zhang J (2014) Determination of inorganic selenium speciation in natural water by sector field inductively coupled plasma mass spectrometry combined with hydride generation. *Chin J Anal Chem* 42:753–758 (in Chinese with English Abstract)
- Conde JE, Sanz Alaejos M (1997) Selenium concentrations in natural and environmental waters. *Chem Rev* 97: 1979–2004
- Cutter GA (1978) Species determination of selenium in natural waters. *Anal Chim Acta* 98:59–66
- Cutter GA, Bruland KW (1984) The marine biogeochemistry of selenium: a re-evaluation. *Limnol Oceanogr* 29: 1179–1192
- Cutter GA, Cutter LS (1995) Behavior of dissolved antimony, arsenic, and selenium in the Atlantic Ocean. *Mar Chem* 49:295–306
- Cutter GA, Cutter LS (2001) Sources and cycling of selenium in the western and equatorial Atlantic Ocean. *Deep-Sea Res II* 48:2917–2931
- Editorial Board of Annals of Bays in China (1991) *Annals of bays in China*. Ocean Press, Beijing (in Chinese)
- Fang JG, Kuang SH, Sun HL, Li F, Zhang AJ, Wang XZ, Tang TY (1996) Mariculture status and optimising measurements for the culture of scallop *Chlamys farreri* and kelp *Laminaria japonica* in Sanggou Bay. *Mar Fish Res*

- 17:95–102 (in Chinese with English Abstract)
- Fernández-Martínez A, Charlet L (2009) Selenium environmental cycling and bioavailability: a structural chemist point of view. *Rev Environ Sci Biotechnol* 8:81–110
 - Fordyce FM (2013) Selenium deficiency and toxicity in the environment. In: Selinus O (ed) *Essentials of medical geology*. Springer, Amsterdam, p 375–416
 - Fries L (1982) Selenium stimulates growth of marine macroalgae in axenic culture. *J Phycol* 18:328–331
 - Gordon DC, Boudreau P, Mann K, Ong J and others (1996) LOICZ biogeochemical modelling guidelines, Vol 5. LOICZ Core Project, Netherlands Institute for Sea Research, Texel
 - Griscom SB, Fisher NS (2004) Bioavailability of sediment-bound metals to marine bivalve molluscs: an overview. *Estuaries* 27:826–838
 - Guo XM, Ford SE, Zhang FS (1999) Mollusca aquaculture in China. *J Shellfish Res* 18:19–31
 - Hansen D, Duda PJ, Zayed A, Terry N (1998) Selenium removal by constructed wetlands: role of biological volatilization. *Environ Sci Technol* 32:591–597
 - He M, Wang WX (2013) Bioaccessibility of 12 trace elements in marine molluscs. *Food Chem Toxicol* 55:627–636
 - Horne AJ (1991) Selenium detoxification in wetlands by permanent flooding: I. Effects on a macroalga, an epiphytic herbivore, and an invertebrate predator in the long-term mesocosm experiment at Kesterson Reservoir, California. *Water Air Soil Pollut* 57:43–52
 - Hsu SC, Wong GTF, Gong GC, Shiah FK, and others (2010) Sources, solubility, and dry deposition of aerosol trace elements over the East China Sea. *Mar Chem* 120: 116–127
 - Hu MH, Yang YP, Martin JM, Yin K, Harrison PJ (1997) Preferential uptake of Se(IV) over Se(VI) and the production of dissolved organic Se by marine phytoplankton. *Mar Environ Res* 44:225–231
 - Jiang ZJ, Fang JG, Zhang JH, Mao YZ, Wang W (2008) Distribution features and evaluation on potential ecological risk of heavy metals in surface sediments of Sungo Bay. *J Agro-Environ Sci* 27:0301–0305 (in Chinese with English Abstract)
 - Jiang ZJ, Li J, Qiao XD, Wang GH, Bian DP and others (2015) The budget of dissolved inorganic carbon in the shellfish and seaweed integrated mariculture area of Sanggou Bay, Shandong, China. *Aquaculture* 446:167–174
 - Johnson TM, Bullen TD, Zawislanski PT (2000) Selenium stable isotope ratios as indicators of sources and cycling of selenium: results from the northern reach of San Francisco Bay. *Environ Sci Technol* 34:2075–2079
 - Lemly AD (1995) A protocol for aquatic hazard assessment of selenium. *Ecotoxicol Environ Saf* 32:280–288
 - Li L, Ren JL, Liu SM, Jiang ZJ, Du JZ, Fang JG (2014) Distribution, seasonal variation and influence factors of dissolved inorganic arsenic in the Sanggou Bay. *Environ Sci* 35:2705–2713 (in Chinese with English Abstract)
 - Lin CL, Ning XR, Su JL, Lin Y, Xu B (2005) Environmental changes and the responses of the ecosystems of the Yellow Sea during 1976–2000. *J Mar Syst* 55:223–234
 - Lin YH, Shiau SY (2005) Dietary selenium requirements of juvenile grouper, *Epinephelus malabaricus*. *Aquaculture* 250:356–363
 - Liu DL, Yang YP, Hu MH, and others (1987) Selenium content of marine food chain organisms from the coast of China. *Mar Environ Res* 22:151–165
 - Liu H, Fang J, Zhu J, Dong S, and others (2004) Study on limiting nutrients and phytoplankton at long-line-culture areas in Laizhou Bay and Sanggou Bay, northeastern China. *Aquat Conserv* 14:551–574
 - Liu SM, Ling WL, Zhang ZN (2011) Inventory of nutrients in the Bohai. *Cont Shelf Res* 31:1790–1797
 - Lobanov AV, Hatfield DL, Gladyshev VN (2009) Eukaryotic selenoproteins and selenoproteomes. *Biochim Biophys Acta* 1790:1424–1428
 - Luoma SN, Presser TS (2009) Emerging opportunities in management of selenium contamination. *Environ Sci Technol* 43:8483–8487
 - Maher W, Baldwin S, Deaker M, Lrving M (1992) Characteristics of selenium in Australian marine biota. *Appl Organomet Chem* 6:103–112
 - Meseck S, Cutter G (2012) Selenium behavior in San Francisco Bay sediments. *Estuaries Coasts* 35:646–657
 - Moore WS (1996) Large groundwater inputs to coastal waters revealed by ²²⁶Ra enrichments. *Nature* 380:612–614
 - Ning Z, Liu S, Zhang G, Ning X and others (2016) Impacts of an integrated multi-trophic aquaculture system on benthic nutrient fluxes: a case study in Sanggou Bay, China. *Aquacult Environ Interact* 8:221–232
 - Price NM, Thompson PA, Harrison PJ (1987) Selenium: an essential element for growth of the coastal marine diatom *Thalassiosira pseudonana* (bacillariophyceae). *J Phycol* 23:1–9
 - Reinfelder J, Wang W, Luoma S, Fisher N (1997) Assimilation efficiencies and turnover rates of trace elements in marine bivalves: a comparison of oysters, clams and mussels. *Mar Biol* 129:443–452
 - Rongcheng Fisheries Technology Extension Station (2012) Marine fishery statistics data. Fishery Technology Station of Rongcheng City, Rongcheng
 - Rotruck JT, Pope A, Ganther H, Swanson A, Hafeman DG, Hoekstra W (1973) Selenium: biochemical role as a component of glutathione peroxidase. *Science* 179:588–590
 - Shandong Flourish the Local Chronicles Compilation Committee (1999) *Records Rongcheng*. Qilu, Jinan (in Chinese)
 - Sherrard JC, Hunter KA, Boyd PW (2004) Selenium speciation in subantarctic and subtropical waters east of New Zealand: trends and temporal variations. *Deep-Sea Res I* 51:491–506
 - Shi J, Wei H, Zhao L, Yuan Y, Fang J, Zhang J (2011) A physical-biological coupled aquaculture model for a suspended aquaculture area of China. *Aquaculture* 318: 412–424
 - Simmons DB, Wallschläger D (2005) A critical review of the biogeochemistry and ecotoxicology of selenium in lotic and lentic environments. *Environ Toxicol Chem* 24: 1331–1343
 - State Environmental Protection Administration of China (2002) *Environmental quality standards for surface water (GB 3838-2002)*. China Environmental Science Press, Beijing (in Chinese)
 - Stüeken EE, Buick R, Bekker A Catling D and others (2015) The evolution of the global selenium cycle: secular trends in Se isotopes and abundances. *Geochim Cosmochim Acta* 162:109–125
 - Ullman WJ, Aller RC (1982) Diffusion coefficients in near-shore marine sediments. *Limnol Oceanogr* 27:552–556
 - Vandermeulen J, Foda A (1988) Cycling of selenite and selenate in marine phytoplankton. *Mar Biol* 98:115–123
 - Wang WX, Fisher NS (1996) Assimilation of trace elements and carbon by the mussel *mytilus edulis*: effects of food

- composition. *Limnol Oceanogr* 41:197–207
- Wang XL, Du JZ, Ji T, Wen TY, Liu SM, Zhang J (2014) An estimation of nutrient fluxes via submarine groundwater discharge into the Sanggou Bay—a typical multi-species culture ecosystem in China. *Mar Chem* 167:113–122
 - Yan X, Zheng L, Chen H, Lin W, Zhang W (2004) Enriched accumulation and biotransformation of selenium in the edible seaweed *Laminaria japonica*. *J Agric Food Chem* 52:6460–6464
 - Yao QZ, Zhang J (2003) Salt effect on the determination of inorganic selenium in natural water and its modified method. *J Ocean Univ Qingdao* 33:765–880 (in Chinese with English abstract)
 - Yao QZ, Zhang J (2005) The behavior of dissolved inorganic selenium in the Bohai Sea. *Estuar Coast Shelf Sci* 63: 333–347
 - Zhang LS, Combs SM (1996) Using the installed spray chamber as a gas–liquid separator for the determination of germanium, arsenic, selenium, tin, antimony, tellurium and bismuth by hydride generation inductively coupled plasma mass spectrometry. *J Anal At Spectrom* 11:1043–1048
 - Zhang J, Hansen PK, Fang J, Wang W, Jiang Z (2009) Assessment of the local environmental impact of intensive marine shellfish and seaweed farming—application of the MOM system in the Sungo Bay, China. *Aquaculture* 287:304–310
 - Zhao J, Zhou S, Sun Y, Fang J (1996) Research on Sanggou Bay aquaculture hydro-environment. *Mar Fish Res* 17: 68–79 (in Chinese with English Abstract)
 - Zheng W, Shi H, Chen S, Zhu M (2009) Benefit and cost analysis of mariculture based on ecosystem services. *Ecol Econ* 68:1626–1632
 - Zhu F, Tan J (1988) Selenium, iodine and fluorine in rainwater and dustfall in China. *Acta Sci Circumst* 8:428–437 (in Chinese with English Abstract)

Editorial responsibility: Sebastien Lefebvre, (Guest Editor)
Wimereux, France

Submitted: June 3, 2015; Accepted: December 9, 2015
Proofs received from author(s): January 20, 2016



Distribution and seasonal variation of picoplankton in Sanggou Bay, China

Li Zhao^{1,2}, Yuan Zhao^{1,2,*}, Jianhong Xu^{1,2}, Wuchang Zhang^{1,2}, Lingfeng Huang³,
Zengjie Jiang^{4,5}, Jianguang Fang^{4,5}, Tian Xiao^{1,2}

¹Key Laboratory of Marine Ecology and Environmental Sciences, Institute of Oceanology, Chinese Academy of Sciences, Qingdao 266071, PR China

²Laboratory of Marine Ecology and Environmental Science, Qingdao National Laboratory for Marine Science and Technology, Qingdao 266071, PR China

³Key Laboratory of the Ministry of Education for Coastal and Wetland Ecosystem, Xiamen University, Xiamen 361102, PR China

⁴Key Laboratory of Sustainable Development of Marine Fisheries, Ministry of Agriculture, Yellow Sea Fisheries Research Institute, Chinese Academy of Fishery Sciences, Qingdao 266071, PR China

⁵Function Laboratory for Marine Fisheries Science and Food Production Processes, Qingdao National Laboratory for Marine Science and Technology, Qingdao 266071, PR China

ABSTRACT: Picoplankton abundance and biomass in Sanggou Bay, China, were investigated in 4 successive seasons (April, August and October 2011, January 2012). Different distribution patterns of picoplankton abundance and biomass were observed according to season and culture areas (bivalves or macroalgae). *Synechococcus*, picoeukaryotes and heterotrophic prokaryotes exhibited higher abundance and biomass in warm seasons (summer and autumn) than in cold seasons (spring and winter). Over all 4 seasons, picoplankton abundance was higher in the bivalve culture area than in the macroalgae culture area. Among picoplankton, picoeukaryotes contributed most to the carbon standing stock in summer and autumn. In spring and winter, the heterotrophic component biomass exceeded that of the autotrophic picoplankton. Picoeukaryotes were an important contributor (21–27 %) to total phytoplankton carbon biomass in spring to autumn. In spring, heterotrophic prokaryote biomass accounted for more than 56 % of total phytoplankton biomass, and even exceeded phytoplankton biomass at some stations. As revealed by multiple stepwise regression analysis, physicochemical factors and protist grazing were the most important variables that controlled picoplankton distribution and variation. The reduction in grazing pressure, as well as phosphorus release by bivalves, is likely to explain the higher abundance of picoplankton in the bivalve culture area of Sanggou Bay.

KEY WORDS: *Synechococcus* · Picoeukaryotes · Heterotrophic prokaryotes · Sanggou Bay

INTRODUCTION

Marine picoplankton are generally defined as plankton in the size range $\leq 2 \mu\text{m}$ in diameter. Picoplankton consist mostly of cyanoprokaryotes of the genera *Synechococcus* (SYN) (Johnson & Sieburth 1979, Waterbury et al. 1979) and *Prochlorococcus* (Chisholm et al. 1988); picoeukaryotes (PEUK), a very diverse assemblage of eukaryotes; and hetero-

trophic prokaryotes (HP). Picoplankton have a ubiquitous distribution and contribute significantly to phytoplankton biomass and primary production in the ocean (Agawin et al. 2000, Bell & Kalff 2001). Picophytoplankton are major contributors to phytoplankton biomass in oligotrophic oceanic ecosystems (Li et al. 1983, Morán et al. 2004). SYN is present in inshore or coastal waters (Jochum 1988) and could account for 20 % of the biomass of all living organ-

*Corresponding author: yuanzhao@qdio.ac.cn

isms in the ocean (Caron et al. 1991). In some areas, PEUK are major biomass contributors (Worden et al. 2004). HP play a central role in the carbon flux in aquatic ecosystems. It is estimated that HP could consume ~50 % of primary production and be responsible for 10–20 % of daily organic matter production (Ducklow & Carlson 1992, Ducklow 2000).

The aquaculture of bivalves depends on the natural production of plankton. Suspension-feeding bivalves clear seston particles $>3\ \mu\text{m}$ in diameter from the water column (Newell 2004), and therefore adult bivalves cannot efficiently capture picoplankton. Although picoplankton do not directly contribute to the growth of bivalves, they can provide a large proportion of the food source for heterotrophic nanoflagellates and ciliates in the water column (Sherr & Sherr 2002). By quantifying the ingestion of protists feeding on picoplankton, it is possible to determine how bivalves can use the microbial energy indirectly (Le Gall et al. 1997). Furthermore, some bivalve larvae can use picoplankton as part of their food source (Gallager et al. 1994), and therefore the study of picoplankton abundance and biomass is considered to provide useful information on the microbial food web in aquacultural regions such as Sanggou Bay.

Sanggou Bay is a semi-circular bay on the north-eastern coast of China, with a large entrance towards the Yellow Sea in the east. Sanggou Bay has been used for aquaculture for >20 yr (Guo et al. 1999). Nearly 2/3 of the area has been used for bivalves and seaweed aquaculture since 1983. The main cultivated species include the seaweed *Laminaria japonica* and longline culture of Chinese scallops *Chlamys farreri* and Pacific oysters *Crassostrea gigas* (Zhang et al. 2009). Although Sanggou Bay is one of the most important aquaculture areas for shellfish and seaweed in northern China, picoplankton distribution

and seasonal variation, as well as their contribution to total phytoplankton biomass in Sanggou Bay, remain poorly documented. In the present study, we investigated picoplankton distribution over 4 successive seasons to gain insights into the factors and processes that regulate picoplankton abundance in Sanggou Bay.

MATERIALS AND METHODS

Study area and sampling strategy

Four cruises were conducted in Sanggou Bay (Fig. 1) over 4 successive seasons: April 2011 (spring), August 2011 (summer), October 2011 (autumn) and January 2012 (winter) using the fishing boat 'Lu Rong Yu Yang 65536'. The bivalve culture areas (collectively referred to as 'B-area' here) are located at the head of the bay, and the macroalgae culture areas ('M-area') are located at the mouth of Sanggou Bay (Lu et al. 2015a). During each cruise, seawater samples were collected from the sea surface (0.5 m depth) at 19 stations (Fig. 1) using a Ruttner sampler (HYDRO-BIOS). *In situ* parameters such as water temperature and salinity were determined with a YSI® Professional Plus series multiprobe water quality meter.

Sample analysis

Seawater samples ($5\ \text{cm}^3$) for picoplankton flow cytometry analysis were fixed with paraformaldehyde (final concentration 1 %) immediately after collection. After 15 min at room temperature, the samples were frozen in liquid nitrogen until analysis was carried out in the laboratory (Marie et al. 2000b).

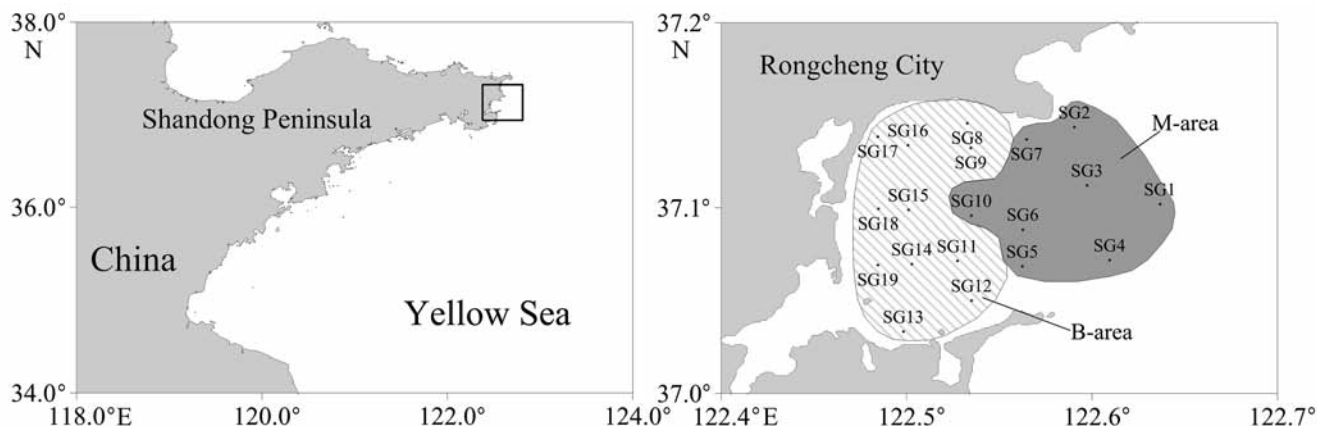


Fig. 1. Study area and location of sampling stations in Sanggou Bay, China. Grey area: macroalgae culture (M-area), dashed area: bivalve culture (B-area)

Picoplankton flow cytometry analyses were run with a FACS Vantage SE flow cytometer (Becton Dickinson) equipped with a water-cooled Argon laser (488 nm, 1 W; Coherent). Protocols were adapted from the literature (Marie et al. 2000a,b). Fluorescent beads (2 μm ; Polysciences; concentration unknown) were used as the internal standard for the instrument set-up and enumeration of picoplankton cells (Olson et al. 1993).

For SYN and PEUK analysis, forward scatter, side scatter and 2 fluorescence signals (red, range: 695 ± 20 nm; orange, range: 585 ± 21 nm) were recorded. Signals were triggered on red fluorescence to discard signals from heterotrophic organisms and inorganic particles. SYN and PEUK were distinguished on the basis of their scatter and fluorescence signals.

For HP analysis, seawater sub-samples were diluted 5-fold with TE buffer (Tris-EDTA, 100 mM Tris-Cl, mM EDTA, pH 8.0; Sigma), and then stained with the nucleic acid dye SYBR Green I (Molecular Probes; final dilution 10^{-4} , v/v) and kept in the dark at room temperature for 20 min before analysis. HP cell groups were resolved on the basis of their green (range: 530 ± 15 nm) fluorescence signal in the green fluorescence vs. sideward scatter cytogram.

For the determination of chlorophyll (chl) *a* concentration, 50–200 cm^3 seawater samples were filtered onto GF/F glass-fibre filters (Whatman) under low vacuum. The filters were wrapped in aluminium foil and kept frozen at -80°C until analysis in the laboratory. Chl *a* was extracted with 90% acetone at 4°C in the dark for 20 h. Chl *a* concentrations were determined by the acidification method using a Turner Design (Model Trilogy 040) fluorometer, which was calibrated with pure chl *a* (Sigma) (Parsons et al. 1984).

Seawater samples for determining nutrient concentration were filtered through acid-washed, pre-cleaned (with ultrapure water), 0.45 μm pore-size acetate cellulose filters (Development Center of Water Treatment Technology, Hangzhou, PR China). The filtrates were poisoned by the addition of saturated HgCl_2 (ca. 1.5×10^{-3} v/v), preserved in low-density polyethylene bottles at room temperature and then analysed in the laboratory.

Nutrient concentrations including those of NO_3^- and NO_2^- were determined spectrometrically using a SKALAR SAN plus autoanalyser, while NH_4^+ and PO_4^{3-} concentrations were determined by manual methods (Parsons et al. 1984). The concentration of dissolved inorganic nitrogen (DIN) was calculated as the sum of NO_3^- , NO_2^- and NH_4^+ .

The enumeration of heterotrophic nanoflagellates (HNF) followed specifications by Lu et al. (2015a). The enumeration of ciliates was carried out according to

Yu et al. (2013). Picoplankton biomass was derived from the abundance of the cell groups resolved by flow cytometry. The abundance/biomass conversion factors used for SYN, PEUK and HP were $250 \text{ fg C cell}^{-1}$ (Li et al. 1992), $1500 \text{ fg C cell}^{-1}$ (Zubkov et al. 1998) and $20 \text{ fg C cell}^{-1}$ (Lee & Fuhrman 1987), respectively. Total phytoplankton biomass per unit volume was estimated from the chl *a* concentration assuming a constant C:chl *a* ratio of 50 (mg:mg) (Krempin & Sullivan 1981).

Flow cytometry data were collected and analysed with CellQuest software (version 3.3, Becton Dickinson). Contour plots were generated using Surfer (version 8.0, Golden Software). Statistical analysis was conducted using SPSS (version 19, IBM SPSS Statistics). Two independent-sample *t*-tests were used to compare picoplankton abundance between the B- and M-areas. Spearman correlation analysis was used to detect significant relationships between variables. As an attempt to explain the variation in picoplankton distribution, stepwise multiple regression analysis was performed to assess the relative influence of potential factors controlling picoplankton abundance (temperature, salinity, nutrient and chl *a* concentrations and other biological components). The abundance data of picoplankton, HNF and ciliates used for statistical analysis were log-transformed to achieve homogeneity of the variance.

RESULTS

Physicochemical conditions

The seasonal distribution of seawater variables is shown in Fig. 2. The average surface water temperature of Sanggou Bay was 9.00, 21.36, 16.47 and 3.76°C in spring, summer, autumn and winter, respectively (Table 1). In spring and summer, water temperature decreased from inside Sanggou Bay to the open sea, while the opposite trend was observed in autumn and winter. Salinity increased from inside the bay to the open sea in summer, autumn and winter. Minimum average salinity was found in summer. In summer and autumn, high chl *a* concentrations were observed, especially at coastal stations inside the bay. Maximum chl *a* concentration reached 38.74 mg m^{-3} at Stn SG13 in summer. Average DIN varied from $4.83 \text{ }\mu\text{M}$ in summer to $10.44 \text{ }\mu\text{M}$ in autumn. The season-averaged PO_4^{3-} concentration was much lower than that of DIN with a maximum ($0.11 \text{ }\mu\text{M}$) in spring and a minimum ($0.02 \text{ }\mu\text{M}$) in autumn and winter. At some stations in autumn and winter, PO_4^{3-} concentration was below the detection limit (Fig. 2).

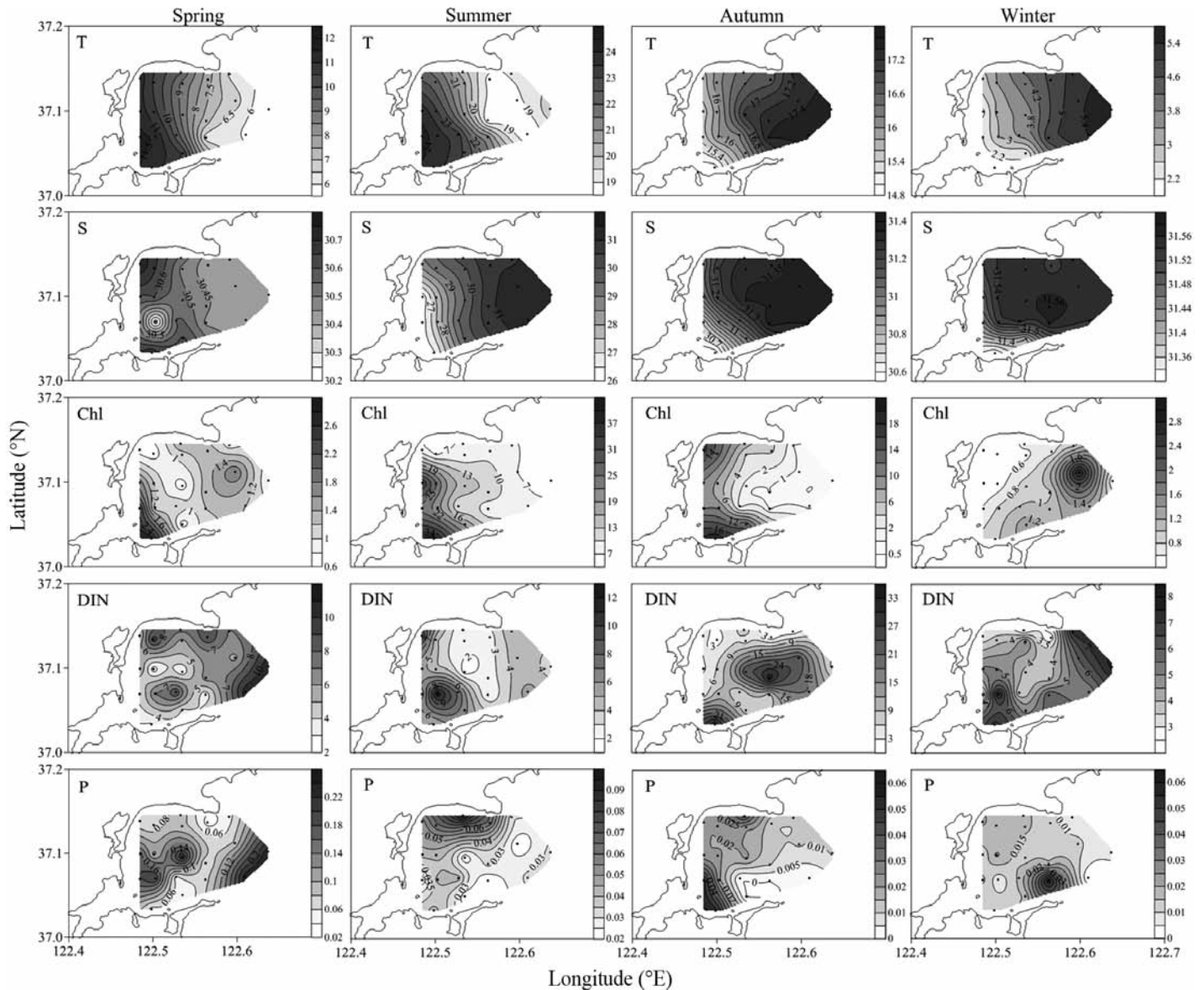


Fig. 2. Spatial distribution of environmental variables in Sanggou Bay and adjacent area over 4 successive seasons. Black dots: sampling stations; T: temperature (°C); S: salinity; Chl: chl a concentration (mg m^{-3}); DIN: dissolved inorganic nitrogen (represents the sum of NO_3^- , NO_2^- and NH_4^+ , μM); P: PO_4^{3-} (μM)

Distribution patterns of picoplankton abundance

Depending on seasons, different distribution patterns of picoplankton abundances were observed in Sanggou Bay (Fig. 3). In spring, SYN abundance was lower at the centre of the bay than at other stations. In summer and autumn, SYN abundance decreased from coastal stations inside the bay to the open sea; however, the opposite trend was observed in winter. Average SYN abundance varied from 0.05×10^3 cells cm^{-3} in spring to 84.06×10^3 cells cm^{-3} in autumn, with a difference of about 4 orders of magnitude (Table 1). The season-averaged SYN abundance was

significantly higher in summer and autumn than in spring and winter ($p < 0.01$).

PEUK and HP had similar abundance distribution patterns in Sanggou Bay, with seasonal variation in the order winter < spring < autumn < summer. Over all seasons, PEUK and HP abundances decreased from coastal stations inside the bay to the open sea. Both PEUK and HP abundances fluctuated less than that of SYN, with values from 1.80×10^3 cells cm^{-3} and 3.00×10^5 cells cm^{-3} in winter to 82.57×10^3 cells cm^{-3} and 40.77×10^5 cells cm^{-3} in summer, respectively (Table 1). The abundances of PEUK and HP were significantly higher in summer than in other seasons ($p < 0.01$).

Table 1. Summary of environmental factors, abundance and biomass of picoplankton in Sanggou Bay (SGB) and macroalgae and bivalve culture areas (M- and B-areas, respectively). DIN: dissolved inorganic nitrogen; SYN: *Synechococcus*; PEUK: picoeukaryotes; HP: heterotrophic prokaryotes. SYN C, PEUK C, HP C: carbon biomass of SYN, PEUK and HP, respectively. Diff.: Significant difference between values of M- and B-areas, * $p < 0.05$, ** $p < 0.01$, t -test; /: test was not performed; NS: not significant

	Spring				Summer			
	SGB	M-area	B-area	Diff.	SGB	M-area	B-area	Diff.
Temperature (°C)	9.00 ± 2.12	6.82 ± 1.06	10.58 ± 0.88	/	21.36 ± 2.02	19.49 ± 1.06	22.73 ± 1.30	/
Salinity	30.51 ± 0.12	30.44 ± 0.04	30.56 ± 0.14	/	29.39 ± 1.78	30.87 ± 0.63	28.31 ± 1.55	/
Chl <i>a</i> (mg m ⁻³)	1.27 ± 0.55	1.15 ± 0.35	1.35 ± 0.67	/	14.41 ± 9.74	9.23 ± 3.31	18.18 ± 11.23	/
DIN (μM)	6.24 ± 2.63	7.00 ± 2.92	5.68 ± 2.38	/	4.83 ± 2.69	3.39 ± 1.43	5.87 ± 2.96	/
PO ₄ ³⁻ (μM)	0.11 ± 0.07	0.12 ± 0.09	0.10 ± 0.06	/	0.04 ± 0.02	0.03 ± 0.01	0.05 ± 0.02	/
SYN abund. (10 ³ cells cm ⁻³)	0.05 ± 0.03	0.06 ± 0.03	0.04 ± 0.02	NS	33.20 ± 12.19	27.08 ± 5.45	37.65 ± 13.96	NS
PEUK abund. (10 ³ cells cm ⁻³)	9.15 ± 7.99	1.49 ± 1.15	14.72 ± 5.74	**	82.57 ± 31.66	77.71 ± 16.70	86.09 ± 39.71	NS
HP abund. (10 ⁵ cells cm ⁻³)	15.43 ± 4.17	11.61 ± 3.58	18.22 ± 1.44	**	40.77 ± 17.90	24.54 ± 9.05	52.58 ± 12.47	**
SYN C (mg C m ⁻³)	0.01 ± 0.01	0.01 ± 0.01	0.01 ± 0.01	/	8.27 ± 3.04	6.74 ± 1.36	9.37 ± 3.48	/
PEUK C (mg C m ⁻³)	13.73 ± 11.99	2.24 ± 1.72	22.09 ± 8.62	/	123.85 ± 47.49	116.57 ± 25.04	129.14 ± 59.56	/
HP C (mg C m ⁻³)	30.87 ± 8.34	23.21 ± 7.17	36.43 ± 2.88	/	81.54 ± 35.81	49.08 ± 18.10	105.16 ± 24.94	/
	Autumn				Winter			
	SGB	M-area	B-area	Diff.	SGB	M-area	B-area	Diff.
Temperature (°C)	16.47 ± 0.79	17.25 ± 0.26	15.91 ± 0.49	/	3.76 ± 1.22	4.89 ± 0.66	2.95 ± 0.79	/
Salinity	31.18 ± 0.23	31.36 ± 0.02	31.06 ± 0.23	/	31.52 ± 0.06	31.55 ± 0.01	31.50 ± 0.08	/
Chl <i>a</i> (mg m ⁻³)	6.49 ± 6.01	1.38 ± 1.21	10.20 ± 5.29	/	0.90 ± 0.55	1.17 ± 0.72	0.71 ± 0.30	/
DIN (μM)	10.44 ± 10.10	13.90 ± 11.72	7.93 ± 8.43	/	4.88 ± 1.72	5.26 ± 1.77	4.61 ± 1.70	/
PO ₄ ³⁻ (μM)	0.02 ± 0.02	0.01 ± 0.01	0.02 ± 0.02	/	0.02 ± 0.01	0.02 ± 0.02	0.02 ± 0.00	/
SYN abund. (10 ³ cells cm ⁻³)	84.06 ± 80.74	11.04 ± 11.85	137.16 ± 65.34	**	0.51 ± 0.20	0.62 ± 0.07	0.42 ± 0.22	*
PEUK abund. (10 ³ cells cm ⁻³)	57.42 ± 66.40	8.75 ± 12.88	92.82 ± 67.42	**	1.80 ± 1.45	1.34 ± 0.49	2.14 ± 1.82	NS
HP abund. (10 ⁵ cells cm ⁻³)	23.35 ± 17.26	8.22 ± 3.24	34.36 ± 14.58	**	3.00 ± 0.62	2.66 ± 0.46	3.25 ± 0.61	NS
SYN C (mg C m ⁻³)	21.01 ± 20.19	2.76 ± 2.96	34.29 ± 16.34	/	0.13 ± 0.05	0.16 ± 0.02	0.10 ± 0.06	/
PEUK C (mg C m ⁻³)	86.13 ± 99.60	13.12 ± 19.32	139.23 ± 101.13	/	2.70 ± 2.17	2.01 ± 0.73	3.21 ± 2.73	/
HP C (mg C m ⁻³)	46.71 ± 34.53	16.43 ± 6.49	68.72 ± 29.15	/	6.00 ± 1.23	5.32 ± 0.92	6.50 ± 1.23	/

The relationships between picoplankton abundance and environmental and biological factors were complex. In spring, PEUK and HP abundances were positively correlated with each other (Table 2). Both PEUK and HP abundances were positively correlated with water temperature, salinity and ciliate abundance. No significant correlation was found between SYN abundance and the other parameters. In summer, SYN abundance was positively correlated with PEUK and negatively correlated with salinity. HP abundance was positively correlated with HNF abundance, temperature and DIN, and negatively correlated with salinity. The abundances of all 3 picoplankton groups were positively correlated with chl *a* concentration. In autumn, SYN, PEUK and HP abundances were positively correlated with each other, as well as with HNF and ciliate abundances, and chl *a* and PO₄³⁻ concentrations, while they were negatively correlated with temperature and salinity. In winter, no significant correlation was found between picoplankton groups. SYN abundance was positively correlated with tem-

perature and chl *a* and negatively correlated with HNF and ciliate abundances. PEUK abundance was positively correlated with chl *a* concentration. HP abundance was negatively correlated with chl *a* concentration.

Distribution of picoplankton in different aquaculture areas

In warm seasons (summer and autumn), there was an obvious freshwater input to the bay (Fig. 2). All picoplankton groups exhibited higher abundances in the B-area than in the M-area, especially in autumn (Fig. 3, Table 1). In cold seasons (winter and spring), SYN abundance remained low throughout Sanggou Bay, with slightly higher values in the M-area (Fig. 3, Table 1). For PEUK and HP, the abundances were still higher in the B-area, but the difference was not significant in winter.

As revealed by multiple stepwise regression analysis, warm-season grazing by protists was the most

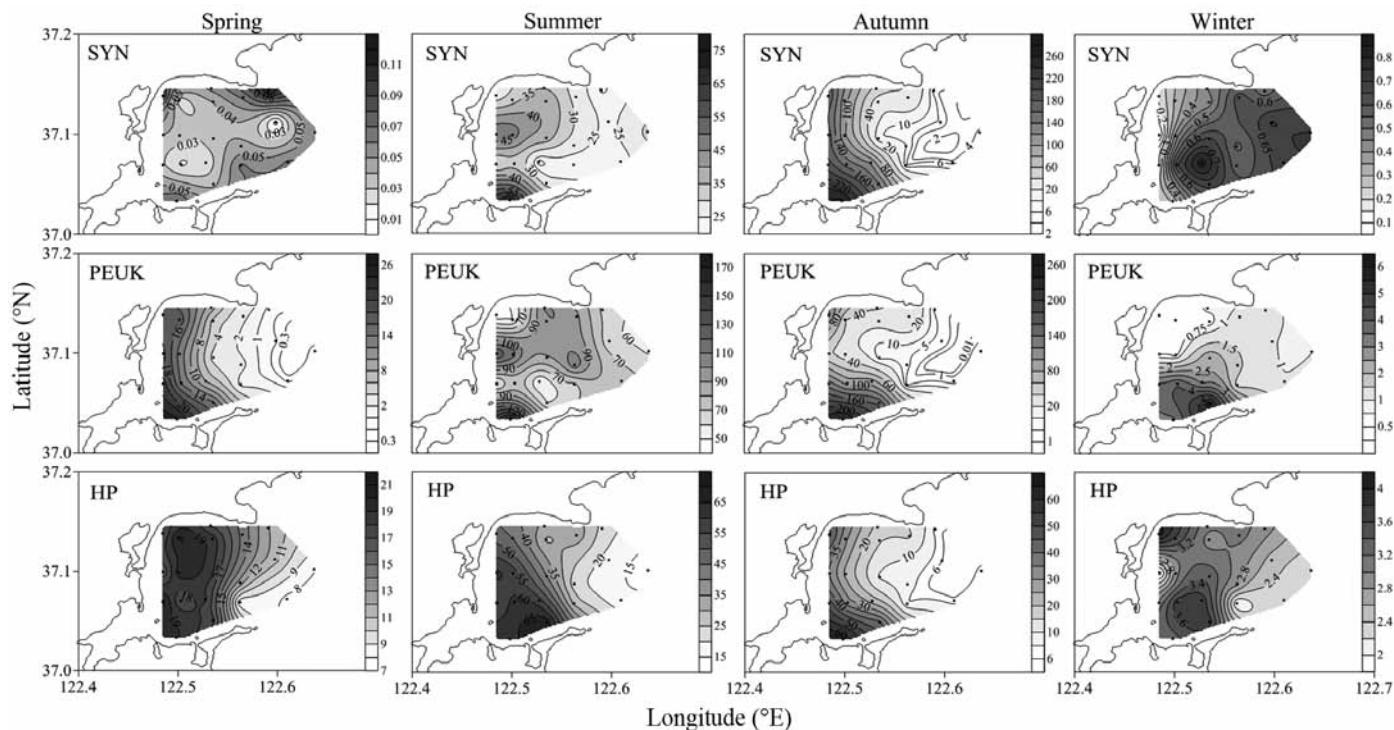


Fig. 3. Spatial distribution of picoplankton abundance in Sanggou Bay and adjacent area over 4 successive seasons. *Synechococcus* (SYN) and picoeukaryotes (PEUK): $\times 10^3$ cells cm^{-3} ; heterotrophic prokaryotes (HP): $\times 10^5$ cells cm^{-3}

Table 2. Spearman's rank correlation coefficient between biological factors and picoplankton abundances in Sanggou Bay over 4 successive seasons (all $n = 19$). SYN: *Synechococcus*; PEUK: picoeukaryotes; HP: heterotrophic prokaryotes; HNF: heterotrophic nanoflagellates; T: temperature; S: salinity; DIN: dissolved inorganic nitrogen. Picoplankton, HNF and ciliate abundances were log transformed prior to analysis. Only correlations that were significant at the **0.01 level (2-tailed) and *0.05 level (2-tailed) are shown

		Log SYN	Log PEUK	Log HP	Log HNF	Log ciliates	T	S	Chl <i>a</i>	DIN	PO ₄ ³⁻
Spring	Log SYN										
	Log PEUK			0.786**		0.774**	0.933**	0.743**			
	Log HP					0.714**	0.765**	0.645**			
Summer	Log SYN		0.604**					-0.553*	0.512*		
	Log PEUK								0.515*		
	Log HP				0.705**		0.861**	-0.865**	0.773**	0.470*	
Autumn	Log SYN		0.961**	0.978**	0.955**	0.899**	-0.961**	-0.964**	0.928**		0.586**
	Log PEUK			0.960**	0.933**	0.828**	-0.899**	-0.946**	0.925**		0.496*
	Log HP				0.960**	0.870**	-0.951**	-0.948**	0.953**		0.581**
Winter	Log SYN				-0.522*	-0.671**	0.608**		0.730**		
	Log PEUK								0.607**		
	Log HP						-0.471*				

important variable that controlled picoplankton abundance and distribution in the M-area (Table 3). HNF abundance explained 66.5 and 80.8% of the variance for SYN and PEUK, respectively. For HP, chl *a* was the most important variable; however, HNF and ciliate abundance also explained about 8.3% of the abundance and distribution of HP. In

the B-area, during warm seasons, physicochemical factors and HNF provided the best explanation for SYN and HP distribution, respectively. No significant variable was found for PEUK. In cold seasons, salinity was the most important variable controlling the distribution of picoplankton in both M- and B-areas (Table 3).

Table 3. Summary of multiple stepwise regression analysis between picoplankton abundances and environmental and biological variables in culture areas of Sanggou Bay and adjacent area (M-area: macroalgae culture, B-area: bivalve culture; see Fig. 1) in warm (summer, autumn) and cold (winter, spring) seasons. Picoplankton, heterotrophic nanoflagellate (HNF) and ciliate abundances were log transformed prior to analysis. R^2 : correlation coefficient of multiple determination. R^2 change: change in multiple R^2 caused by entering a new variable in a single step (hierarchical analysis). Results of $F > 1$ and $p < 0.05$ represent improvements due to fitting the regression model is much greater than the inaccuracy within the model, which means the final model significantly improved our ability to predict the outcome variable. NS: not significant. SYN: *Synechococcus*; PEUK: picoeukaryotes; HP: heterotrophic prokaryotes; Chl: chl a concentration; T: temperature; S: salinity

		Dependent variables	Variables entered	R^2	R^2 change	Beta	F	p
M-area	Warm seasons	Log SYN	Log HNF	0.665	0.665	0.815	27.770	<0.001
		Log PEUK	Log HNF	0.808	0.808	0.899	58.771	<0.001
		Log HP	Chl	0.847	0.847	0.425	77.655	<0.001
			Log HNF	0.902	0.055	0.403	59.884	<0.001
			Log ciliates	0.930	0.028	0.240	53.098	<0.001
	Cold seasons	Log SYN	S	0.813	0.813	0.901	52.011	<0.001
		Log PEUK	Log ciliates	0.342	0.342	0.585	6.236	<0.001
		Log HP	S	0.900	0.900	-0.925	108.293	<0.001
			Log ciliates	0.942	0.042	0.207	89.943	<0.001
B-area	Warm seasons	Log SYN	T	0.625	0.625	-1.594	33.384	<0.001
			S	0.817	0.192	-0.914	42.381	<0.001
		Log PEUK		NS	NS	NS	NS	NS
		Log HP	Log HNF	0.658	0.658	0.811	38.489	<0.001
	Cold seasons	Log SYN	S	0.822	0.822	0.610	83.235	<0.001
			Log HNF	0.873	0.051	-0.373	58.687	<0.001
		Log PEUK	S	0.710	0.170	-0.842	43.988	<0.001
		Log HP	S	0.941	0.941	-0.527	287.344	<0.001
			T	0.967	0.026	0.472	251.419	<0.001

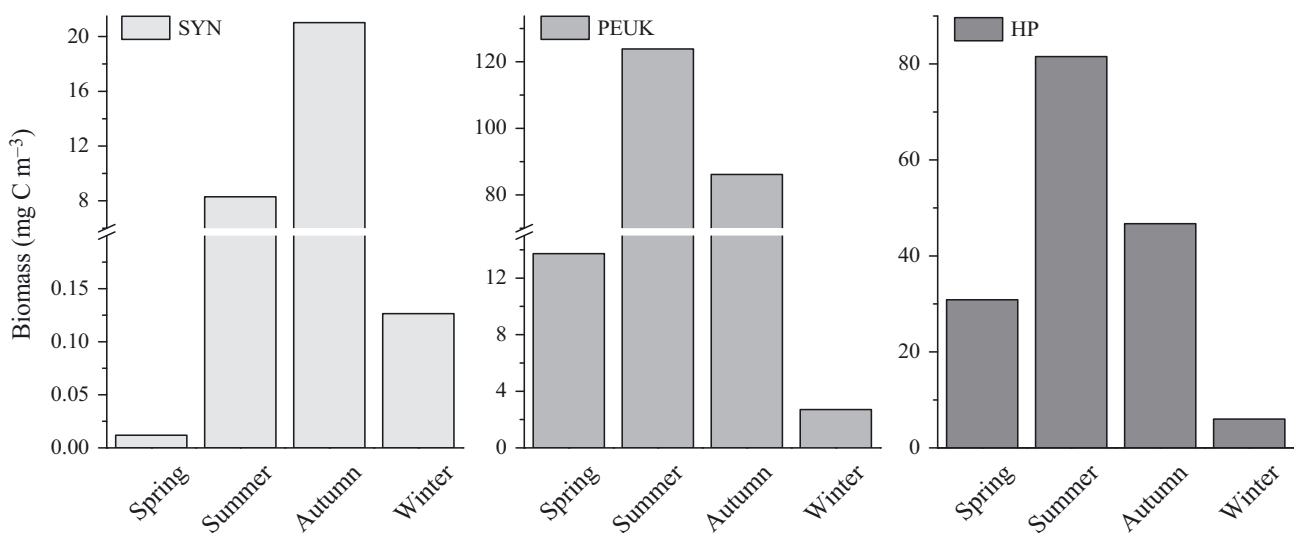


Fig. 4. Depth-averaged biomass (mg C m^{-3}) of picoplankton in Sanggou Bay over 4 successive seasons. SYN: *Synechococcus*; PEUK: picoeukaryotes; HP: heterotrophic prokaryotes. Note different y-axis scales

Carbon biomass contribution of picoplankton to phytoplankton

Among picoplankton, PEUK represented the highest standing stock of carbon biomass in summer and autumn (Fig. 4), contributing to >50 % of picoplankton

biomass (Fig. 5). In spring and winter, the heterotrophic component of biomass exceeded that of autotrophic picoplankton. HP was the major contributor to picoplankton biomass in spring and winter. SYN biomass was relatively low compared with that of PEUK and HP throughout the 4 successive seasons (Fig. 4).

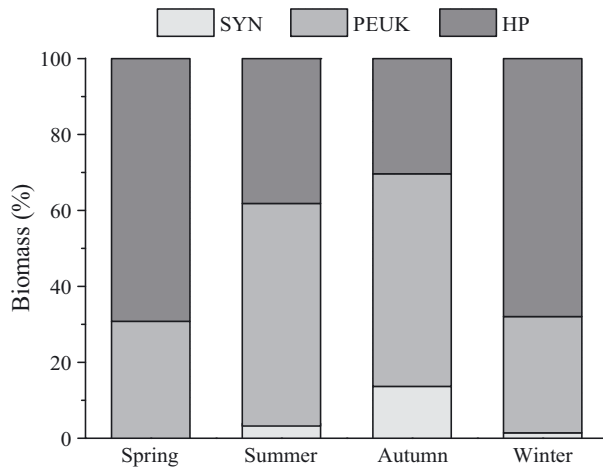


Fig. 5. Biomass contribution of *Synechococcus* (SYN), picoeukaryotes (PEUK) and heterotrophic prokaryotes (HP) to picoplankton biomass in Sanggou Bay over 4 successive seasons

In spring, summer and autumn, PEUK was an important (21.46–27.74%) carbon contributor to total phytoplankton biomass (Fig. 6). This contribution decreased to 6.39% in winter. HP biomass amounted to >50% of total phytoplankton biomass in spring, and at some stations even exceeded phytoplankton biomass. SYN contributed 6.82% to phytoplankton biomass in autumn and <1.5% in other seasons.

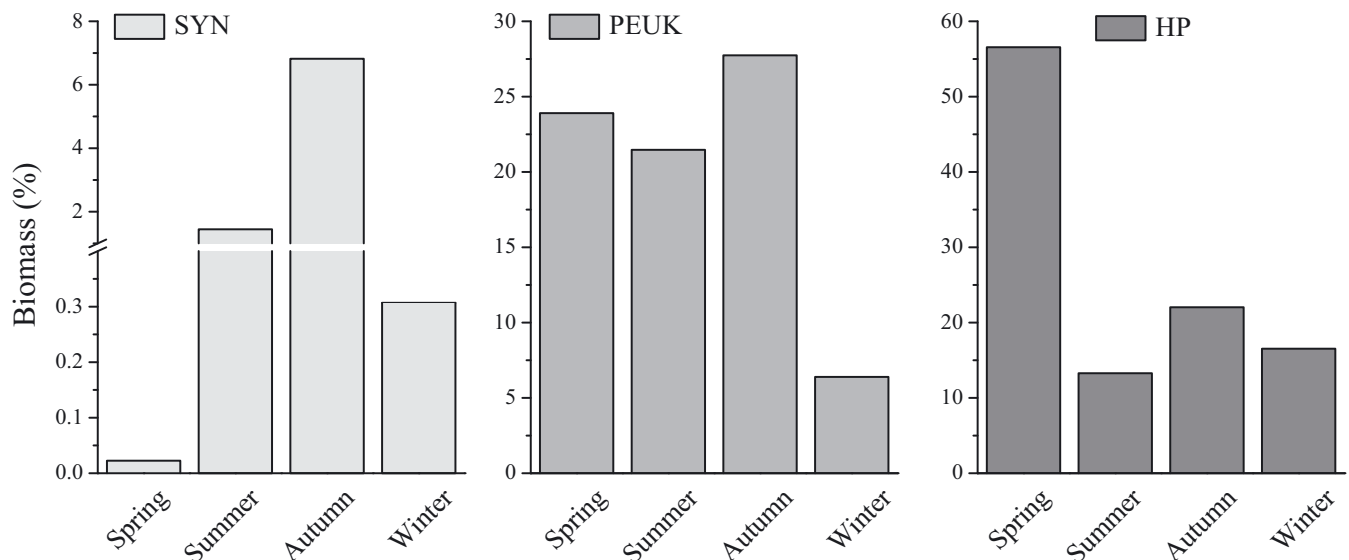


Fig. 6. Biomass contribution of *Synechococcus* (SYN), picoeukaryotes (PEUK) and heterotrophic prokaryotes (HP) to total phytoplankton biomass in Sanggou Bay over 4 successive seasons. The total phytoplankton biomass was derived from chlorophyll *a* concentration. Note different y-axis scales

DISCUSSION

Picoplankton seasonal distribution and variation

This is the first report on picoplankton abundance distribution and its seasonal variation in Sanggou Bay, China, with results comparable to those reported from other coastal waters (Vaquer et al. 1996, Kamiyama 2004, Bec et al. 2005, Kamiyama et al. 2009, Thomas et al. 2010, Bouvy et al. 2012). Picoplankton abundance distribution and its variations depend on both abiotic and biotic factors. Abiotic factors, also called bottom-up controls, include water temperature and salinity, as well as light and nutrient availability. The biotic factors (top-down controls) are essentially predation by nano- and micro-zooplankton, and lysis by virioplankton.

Picoplankton abundance is particularly affected by water temperature and nutrient availability (Agawin et al. 2000). Seasonal variation of SYN and HP abundances in temperate waters usually follows patterns with maxima in summer and minima in winter (Li 1998). In Sanggou Bay, a clear seasonality for picoplankton abundance and biomass was observed, associated with physicochemical features. High abundances and biomasses of SYN, PEUK and HP were found during summer and autumn, in agreement with previous reports (Vaquer et al. 1996, DuRand et al. 2001, Bec et al. 2005). SYN abundance is about 4 orders of magnitude higher in

autumn than in spring in Sanggou Bay. Similar SYN variation was also found in previous studies (DuRand et al. 2001, Li & Dickie 2001, Agawin et al. 2003). A 10 yr monthly observation (2006–2015) in Jiaozhou Bay, China, at a similar longitude and latitude, has revealed the same variation (T. Xiao, L. Zhao unpubl. data).

Picoplankton in the aquaculture area

Being an important component of the aquatic food web, picoplankton feed larger zooplankton that channel their carbon biomass from microbial to higher trophic levels (Azam et al. 1983). The aquaculture of bivalves depends on the production of natural plankton. Picoplankton ($<2\ \mu\text{m}$) are too small to be efficiently retained by most bivalves, including the scallop *Chlamys farreri* and oyster *Crassostrea gigas* (Barillé et al. 1993, Kreeger & Newell 1996, Hawkins et al. 2001). However, the distribution of picoplankton is still affected by bivalves in aquaculture areas. Although picoplankton do not directly contribute to the growth of bivalves, they can provide a large proportion of the food source for HNF and ciliates in the water column (Sherr & Sherr 2002). Most HNF (2–20 μm) and ciliates (mostly $>10\ \mu\text{m}$) are much larger and can be efficiently captured by most bivalves (Riisgård 1988, Fournier et al. 2012). Therefore, bivalves can use the microbial energy indirectly (Le Gall et al. 1997). Nano- and micro-zooplankton grazing are important top-down control factors for picoplankton (Sherr & Sherr 2002). Protists are recognized as the main consumers of SYN, PEUK and HP in similar environments (Kamiyama 2004, Bec et al. 2005). In the macroalgae culture area of Sanggou Bay, grazing by protists was the most important variable controlling picoplankton abundances and distribution in both warm and cold seasons. However, no such correlation could be observed in the bivalve culture area. Physicochemical factors such as temperature and salinity were the main control factors of picoplankton distribution. It is possible that HNF and ciliates in the B-area were efficiently retained by bivalves, alleviating grazing pressure on picoplankton and enabling a significantly higher abundance of picoplankton in this area, especially in warm seasons. We found possible collinearity between some variables used in the stepwise regressions (Table 3). It is possible that the estimates of the multiple regressions may change erratically in response to small changes in the data. To remedy the analysis, data were log transformed prior to analysis to standardize

the variables in our study. Despite its shortcomings, stepwise regression has nevertheless been a suitable method used to predict influential factors in other research (e.g. Kimmel et al. 2012, Oberbeckmann et al. 2012).

A predominance of picoplankton has also been reported in other areas of intense bivalve farming (Dupuy et al. 2000). Traditionally, picophytoplankton has been viewed as having a critical growth dependence on inorganic nutrients. At low nutrient concentrations, picoplankton cells can take up nutrients better than large plankton cells, owing to their higher surface area to volume ratio (Morel et al. 1991, Chisholm 1992). In Sanggou Bay, phosphorus (P) was found to be deficient, whereas DIN was sufficient (Sun et al. 2007). Bivalve culture can release P into the environment (Carlsson et al. 2012, Cranford et al. 2012), and the release of P by bivalves may have induced the high abundance of picoplankton in the Sanggou Bay B-area. Indeed, a 7 d *in situ* enclosure experiment in Sanggou Bay demonstrated that scallop cultivation increased the PO_4^{3-} concentration, as well as the abundance of picoplankton, total nanoflagellates and ciliates (Lu et al. 2015a,b). In addition to P release, bivalves can excrete important amounts of ammonium ions, which also favours picophytoplankton (Chisholm 1992, Courties et al. 1994). Although we lack data on ammonium ion concentration in Sanggou Bay, it is possible that ammonium ions stimulated the growth of picoplankton in the bivalve culture area.

Picoplankton biomass contribution

In cold seasons (winter and spring), heterotrophic picoplankton carbon biomass exceeded that of autotrophic picoplankton. This result is in agreement with observations in the Sargasso Sea, where the microbial carbon biomass was dominated by non-photosynthetic prokaryotes (Fuhrman et al. 1989, Bouvy et al. 2012). When the water temperature rose, PEUK biomass became predominant ($>50\%$) within the picoplankton biomass. These results differ from previous observations in distinct environments such as the northeastern Atlantic Ocean (Partensky et al. 1996), the South Pacific Ocean (Grob et al. 2007) and the Yellow Sea (Zhao et al. 2011), where SYN or HP was predominant in the picoplankton biomass. Bec et al. (2005) reported that PEUK were predominant within picoplankton, and could serve as an important carbon source for the protozoan community. Our observations are in line with these findings, support-

ing the suggestion that PEUK could make a large contribution to the carbon flow towards higher trophic levels in coastal regions.

CONCLUSION

Our study is the first report on picoplankton seasonal abundance distribution and its variations in Sanggou Bay, China. Different distribution patterns of picoplankton abundance and biomass were observed. Physicochemical factors and protist grazing were the most important variables controlling the distribution of and variation in picoplankton abundance in Sanggou Bay. Picoplankton were more abundant in the bivalve culture area than in the macroalgae culture area, especially in warm seasons. Among the picoplankton, PEUK contributed most to the carbon biomass standing stock in summer and autumn. The reduction in protist grazing pressure, as well as P release by bivalves, are likely explanations for the higher picoplankton abundance in the bivalve culture area. In spring and winter, the heterotrophic component of the biomass exceeded that of the autotrophic picoplankton. In spring to autumn, PEUK contributed >20% to the assessed autotrophic biomass. HP biomass amounted to >56% of the assessed autotrophic biomass in spring, and at some stations the percentage was even larger.

Acknowledgements. This work was supported by the Natural Science Foundation of China project 41306161, 973 project 2011CB409804, and Natural Science Foundation of China project 41306160. We are grateful to the crew members of the Rongcheng Marine Science and Technology Bureau for their assistance during the cruises.

LITERATURE CITED

- Agawin NS, Duarte CM, Agustí S (2000) Nutrient and temperature control of the contribution of picoplankton to phytoplankton biomass and production. *Limnol Oceanogr* 45:591–600
- Agawin NS, Duarte CM, Agustí S, McManus L (2003) Abundance, biomass and growth rates of *Synechococcus* sp. in a tropical coastal ecosystem (Philippines, South China Sea). *Estuar Coast Shelf Sci* 56:493–502
- Azam F, Fenchel T, Field JG, Gray JS, Meyer-Reil LA, Thingstad F (1983) The ecological role of water-column microbes in the sea. *Mar Ecol Prog Ser* 10:257–263
- Barillé L, Prou J, Héral M, Bourgrier S (1993) No influence of food quality, but ration-dependent retention efficiencies in the Japanese oyster *Crassostrea gigas*. *J Exp Mar Biol Ecol* 171:91–106
- Bec B, Hussein-Ratrem J, Collos Y, Souchu P, Vaquer A (2005) Phytoplankton seasonal dynamics in a Mediterranean coastal lagoon: emphasis on the picoeukaryote community. *J Plankton Res* 27:881–894
- Bell T, Kalff J (2001) The contribution of picophytoplankton in marine and freshwater systems of different trophic status and depth. *Limnol Oceanogr* 46:1243–1248
- Bouvy M, Dupuy C, Pagano M, Barani A, Charpy L (2012) Do human activities affect the picoplankton structure of the Ahe atoll lagoon (Tuamotu Archipelago, French Polynesia)? *Mar Pollut Bull* 65:516–524
- Carlsson MS, Engström P, Lindahl O, Ljungqvist L, Petersen JK, Svanberg L, Holmer M (2012) Effects of mussel farms on the benthic nitrogen cycle on the Swedish west coast. *Aquacult Environ Interact* 2:177–191
- Caron DA, Lim EL, Miceli G, Waterbury JB, Valois FW (1991) Grazing and utilization of chroococcoid cyanobacteria and heterotrophic bacteria by protozoa in laboratory cultures and a coastal plankton community. *Mar Ecol Prog Ser* 76:205–217
- Chisholm SW (1992) Phytoplankton size. In: Falkowski PG, Woodhead AD (eds) *Primary productivity and biogeochemical cycles in the sea*. Springer, New York, NY, p 213–237
- Chisholm SW, Olson RJ, Zettler ER, Goericke R, Waterbury JB, Welschmeyer NA (1988) A novel free-living prochlorophyte abundant in the oceanic euphotic zone. *Nature* 334:340–343
- Courties C, Vaquer A, Troussellier M, Lautier J and others (1994) Smallest eukaryotic organism. *Nature* 370:255
- Cranford PJ, Kamermans P, Krause G, Mazurié J and others (2012) An ecosystem-based approach and management framework for the integrated evaluation of bivalve aquaculture impacts. *Aquacult Environ Interact* 2:193–213
- Ducklow H (2000) Bacterial production and biomass in the oceans. In: Kirchman DL (ed) *Microbial ecology of the oceans*. Wiley-Liss, New York, NY, p 85–120
- Ducklow HW, Carlson CA (1992) Oceanic bacterial production. In: Marshall KC (ed) *Advances in microbial ecology*. Springer, New York, NY, p 113–181
- Dupuy C, Pastoureaud A, Ryckaert M, Sauriau PG, Montanié H (2000) Impact of the oyster *Crassostrea gigas* on a microbial community in Atlantic coastal ponds near La Rochelle. *Aquat Microb Ecol* 22:227–242
- DuRand MD, Olson RJ, Chisholm SW (2001) Phytoplankton population dynamics at the Bermuda Atlantic Time-series station in the Sargasso Sea. *Deep-Sea Res II* 48:1983–2003
- Fournier J, Dupuy C, Bouvy M, Couraudon-Reale M and others (2012) Pearl oysters *Pinctada margaritifera* grazing on natural plankton in Ahe atoll lagoon (Tuamotu Archipelago, French Polynesia). *Mar Pollut Bull* 65:490–499
- Fuhrman JA, Sleeter TD, Carlson CA, Proctor LM (1989) Dominance of bacterial biomass in the Sargasso Sea and its ecological implications. *Mar Ecol Prog Ser* 57:207–217
- Gallagher S, Waterbury J, Stoecker D (1994) Efficient grazing and utilization of the marine cyanobacterium *Synechococcus* sp. by larvae of the bivalve *Mercenaria mercenaria*. *Mar Biol* 119:251–259
- Grob C, Ulloa O, Li WKW, Alarcón G, Fukasawa M, Watanabe S (2007) Picoplankton abundance and biomass across the eastern South Pacific Ocean along latitude 32.5°S. *Mar Ecol Prog Ser* 332:53–62
- Guo X, Ford S, Zhang F (1999) Molluscan aquaculture in China. *J Shellfish Res* 18:19–31
- Hawkins A, Fang J, Pascoe P, Zhang J, Zhang X, Zhu M (2001) Modelling short-term responsive adjustments in particle clearance rate among bivalve suspension-

- feeders: separate unimodal effects of seston volume and composition in the scallop *Chlamys farreri*. J Exp Mar Biol Ecol 262:61–73
- Jochem F (1988) On the distribution and importance of picocyanobacteria in a boreal inshore area (Kiel Bight, Western Baltic). J Plankton Res 10:1009–1022
- Johnson PW, Sieburth J (1979) Chroococcoid cyanobacteria in the sea: a ubiquitous and diverse phototrophic biomass. Limnol Oceanogr 24:928–935
- Kamiyama T (2004) The microbial loop in a eutrophic bay and its contribution to bivalve aquaculture. Bull Fish Res Agency Jpn Suppl 1:41–50
- Kamiyama T, Yamauchi H, Iwai T, Hamasaki K (2009) Seasonal variations in abundance and biomass of picoplankton in an oyster-farming area of northern Japan. Plankton Benthos Res 4:62–71
- Kimmel DG, Boynton WR, Roman MR (2012) Long-term decline in the calanoid copepod *Acartia tonsa* in central Chesapeake Bay, USA: an indirect effect of eutrophication? Estuar Coast Shelf Sci 101:76–85
- Kreeger DA, Newell RIE (1996) Ingestion and assimilation of carbon from cellulolytic bacteria and heterotrophic flagellates by the mussels *Geukensia demissa* and *Mytilus edulis* (Bivalvia, Mollusca). Aquat Microb Ecol 11:205–214
- Krempin D, Sullivan CW (1981) The seasonal abundance, vertical distribution, and relative microbial biomass of chroococcoid cyanobacteria at a station in southern California coastal waters. Can J Microbiol 27:1341–1344
- Le Gall S, Hassen MB, Le Gall P (1997) Ingestion of a bacterivorous ciliate by the oyster *Crassostrea gigas*: protozoa as a trophic link between picoplankton and benthic suspension-feeders. Mar Ecol Prog Ser 152:301–306
- Lee S, Fuhrman JA (1987) Relationships between biovolume and biomass of naturally derived marine bacterioplankton. Appl Environ Microbiol 53:1298–1303
- Li WKW (1998) Annual average abundance of heterotrophic bacteria and *Synechococcus* in surface ocean waters. Limnol Oceanogr 43:1746–1753
- Li WKW, Dickie P (2001) Monitoring phytoplankton, bacterioplankton, and virioplankton in a coastal inlet (Bedford Basin) by flow cytometry. Cytometry 44:236–246
- Li WKW, Rao S, Harrison W, Smith J, Cullen J, Irwin B, Platt T (1983) Autotrophic picoplankton in the tropical ocean. Science 219:292–295
- Li WKW, Dickie P, Irwin B, Wood A (1992) Biomass of bacteria, cyanobacteria, prochlorophytes and photosynthetic eukaryotes in the Sargasso Sea. Deep-Sea Res A 39:501–519
- Lu J, Huang L, Luo Y, Xiao T, Jiang Z, Wu L (2015a) Effects of freshwater input and mariculture (bivalves and macroalgae) on spatial distribution of nanoflagellates in Sungo Bay, China. Aquacult Environ Interact 6:191–203
- Lu J, Huang L, Xiao T, Jiang Z, Zhang W (2015b) The effects of Zhikong scallop (*Chlamys farreri*) on the microbial food web in a phosphorus-deficient mariculture system in Sanggou Bay, China. Aquaculture 448:341–349
- Marie D, Simon N, Guillou L, Partensky F, Vaulot D (2000a) DNA/RNA analysis of phytoplankton by flow cytometry. Curr Protoc Cytom 11:11.12.11–11.12.14
- Marie D, Simon N, Guillou L, Partensky F, Vaulot D (2000b) Flow cytometry analysis of marine picoplankton. In: Diamond RA, DeMaggio S (eds) In living color. Protocols in flow cytometry and cell sorting. Springer, New York, NY, p 421–454
- Morán XAG, Fernández E, Pérez V (2004) Size-fractionated primary production, bacterial production and net community production in subtropical and tropical domains of the oligotrophic NE Atlantic in autumn. Mar Ecol Prog Ser 274:17–29
- Morel FM, Hudson RJ, Price NM (1991) Limitation of productivity by trace metals in the sea. Limnol Oceanogr 36:1742–1755
- Newell RI (2004) Ecosystem influences of natural and cultivated populations of suspension-feeding bivalve molluscs: a review. J Shellfish Res 23:51–62
- Oberbeckmann S, Fuchs BM, Meiners M, Wichels A, Wiltshire KH, Gerdt G (2012) Seasonal dynamics and modeling of a *Vibrio* community in coastal waters of the North Sea. Microb Ecol 63:543–551
- Olson RJ, Zettler ER, DuRand MD (1993) Phytoplankton analysis using flow cytometry. In: Kemp PF, Cole JJ, Sherr BF, Sherr EB (eds) Handbook of methods in aquatic microbial ecology. Lewis, Boca Raton, FL, p 175–186
- Parsons T, Maita Y, Lalli C (1984) A manual of chemical and biological methods for seawater analysis. Pergamon Press, Oxford
- Partensky F, Blanchot J, Lantoine F, Neveux J, Marie D (1996) Vertical structure of picophytoplankton at different trophic sites of the tropical northeastern Atlantic Ocean. Deep-Sea Res I 43:1191–1213
- Riisgård HU (1988) Efficiency of particle retention and filtration rate in 6 species of Northeast American bivalves. Mar Ecol Prog Ser 45:217–223
- Sherr EB, Sherr BF (2002) Significance of predation by protozoists in aquatic microbial food webs. Antonie Leeuwenhoek 81:293–308
- Sun P, Zhang Z, Hao L, Wang B and others (2007) Analysis of nutrient distributions and potential eutrophication in seawater of the Sangou Bay. Adv Mar Sci 25:436–455 (in Chinese with English abstract)
- Thomas Y, Courties C, El Helwe Y, Herbland A, Lemonnier H (2010) Spatial and temporal extension of eutrophication associated with shrimp farm wastewater discharges in the New Caledonia lagoon. Mar Pollut Bull 61:387–398
- Vaquer A, Troussellier M, Courties C, Bibent B (1996) Standing stock and dynamics of picophytoplankton in the Thau Lagoon (northwest Mediterranean coast). Limnol Oceanogr 41:1821–1828
- Waterbury JB, Watson SW, Guillard RR, Brand LE (1979) Widespread occurrence of a unicellular, marine, planktonic, cyanobacterium. Nature 277:293–294
- Worden AZ, Nolan JK, Palenik B (2004) Assessing the dynamics and ecology of marine picophytoplankton: the importance of the eukaryotic component. Limnol Oceanogr 49:168–179
- Yu Y, Zhang W, Jiang Z, Zhao Y, Feng M, Li H, Xiao T (2013) Seasonal variation of planktonic ciliates in Sanggou Bay, Huanghai Sea. Acta Oceanol Sin 35:215–224 (in Chinese with English abstract)
- Zhang J, Hansen PK, Fang J, Wang W, Jiang Z (2009) Assessment of the local environmental impact of intensive marine shellfish and seaweed farming—application of the MOM system in the Sungo Bay, China. Aquaculture 287:304–310
- Zhao Y, Zhao L, Xiao T, Zhao S, Xuan J, Li C, Ning X (2011) Spatial and temporal variation of picoplankton distribution in the Yellow Sea, China. Chin J Oceanol Limnol 29:150–162
- Zubkov MV, Sleight MA, Tarran GA, Burkill PH, Leakey RJ (1998) Picoplanktonic community structure on an Atlantic transect from 50° N to 50° S. Deep-Sea Res I 45:1339–1355



A model for the growth of mariculture kelp *Saccharina japonica* in Sanggou Bay, China

Jihong Zhang^{1,2,*}, Wenguang Wu¹, Jeffrey S. Ren³, Fan Lin¹

¹Yellow Sea Fisheries Research Institute, Chinese Academy of Fishery Sciences, Qingdao 266071, PR China

²Function Laboratory for Marine Fisheries Science and Food Production Processes,
Qingdao National Laboratory for Marine Science and Technology, Qingdao, PR China

³National Institute of Water and Atmospheric Research, 10 Kyle Street, PO Box 8602, Christchurch 8440, New Zealand

ABSTRACT: The kelp *Saccharina japonica* is one of the most important mariculture species in China. To predict kelp growth and provide a component for a general multitrophic ecosystem model, a dynamic individual growth model was developed to evaluate environmental effects on kelp growth. This model was calibrated and validated using data from 2 annual mariculture cycles (2008–2009, 2011–2012) from Sanggou Bay, China. Gross growth of *S. japonica* was described as functions of temperature, light and nutrient contents in plant tissues (internal nutrients), and nitrogen (N) and phosphorus (P) in seawater. Net growth was defined as gross growth minus respiration. The simulation results showed that nutrients were the key limiting factor for growth throughout the kelp growth cycle, whereas both temperature and light only limited kelp growth during simulation days 60–120, i.e. from 1 January to the end of February. Scenario simulations showed that fertilizing with nitrogen could improve kelp growth by as much as 4.4 times. The model also predicted that individual dry weight of *S. japonica* would increase by 18% when lifting the culture ropes up to the surface. Sensitivity analysis indicates that the empirical coefficient of respiration (r), maximum growth rate (μ_{\max}) and minimum internal quota for nitrogen (N_{\min}) were among the most sensitive parameters. This model shows that the introduction of culture methods such as cage culture, which allows more effective fertilization and depth control, would result in more effective kelp farming.

KEY WORDS: Kelp · *Saccharina japonica* · Suspended long-line culture · Environmental variables · Individual growth model · Sanggou Bay

INTRODUCTION

The kelp *Saccharina japonica* (previously *Laminaria japonica*) is one of the most intensively cultured seaweed species in the world. The annual production of this species was ~5.09 million t in China in 2013 (FAO 2014). For management of kelp mariculture, it is important to understand the environmental effects on growth and production and to be able to estimate the carrying capacity of the culture ecosystems (Liu et al. 2013).

Large-scale seaweed cultivation has been proposed as a method for mitigating eutrophication in

coastal ecosystems (Fei 2004). Co-culture of kelp with other species in integrated multi-trophic aquaculture (IMTA) systems has been shown to improve water quality, daylight oxygen levels were reported to have increased and excreted nutrients decreased (Chopin et al. 2001, Troellet al. 2003, Buschmann et al. 2008). A model of the physiological behaviour and growth of kelp would be an important contribution to a general IMTA model which could be used in optimising production of each trophic species in IMTA systems.

Macroalgal growth modelling is a powerful tool and is being increasingly used in sustainable man-

*Corresponding author: zhangjh@ysfri.ac.cn

agement of coasts and estuaries (Duarte et al. 2003, Aveytua-Alcázar et al. 2008), as a component of ecosystem models to estimate carrying capacity of polyculture ecosystems (Duarte et al. 2003, Nunes et al. 2003, Shi et al. 2011). However, the application of these sub-models of kelp is limited because they are over-simplified and do not consider all the key limiting factors, particularly the effect of the internal state on growth. The recent development of a green-algal model is probably the most comprehensive macroalgal model (Ren et al. 2014) in which most of these factors have been incorporated. To our knowledge, there are no similar models available as yet for kelp.

The objective of this study was to develop a generic growth model of kelp for predicting its response to dynamic environmental conditions, to understand the relationship between potential increases in production and environmental fertilization, and to investigate the effects of climate change (temperature increase) on mariculture. The main purpose of the model is to guide maricultural activity. Fertilization (by the hanging bag method) and adjusting culture depth are the most commonly used techniques in kelp mariculture in China. Using these techniques, the cultivation efficiency can be assessed by comparison with the model prediction.

MATERIALS AND METHODS

Study area

The growth model was developed for Sanggou Bay, which is located at the eastern end of Shandong Peninsula, PR China (37° 01'–09' N, 122° 24'–35' E) (Fig. 1). The total area is 140 km², with an average depth of 7.5 m. The tidal elevation in Sanggou Bay is irregularly semidiurnal with a maximum tidal range of ~2 m. The flooding tide current enters the bay along the northern side, flows anti-clockwise and exits along the southern side; the ebbing tide is in the opposite direction (Shi et al. 2011). There are several seasonal stream rivers for freshwater input to Sanggou Bay, with runoff (approx. $1.7\text{--}2.3 \times 10^8$ m³) accounting for ca. 17% of the total volume of the bay (Li et al. 2014). Temperature ranges from 2 to 26°C and average salinity is 30.6‰. The bay is one of the most intensively cultured bays in China and aquaculture was already introduced in the 1980s. The main cultivated species are kelp (*Saccharina japonica*), scallop (*Chlamys farreri*) and Pacific oyster *Crassostrea gigas*. Annual production of kelp is ~68 000 t in dry weight. Kelp occurs mainly near the

mouth of the bay as a monoculture and integrates with bivalves towards the middle of the bay. Kelp is typically cultivated from November to the end of May in the following year. The sample site was in the northern Sanggou Bay.

Available data and data analysis

Field data were obtained during 2 mariculture cycles of *S. japonica* at the experimental site in Sanggou Bay (Fig. 1B), from November to May for the years 2008–2009 and 2011–2012. Length and dry weight of kelp fronds were measured twice each month, while environmental parameters were measured monthly, including water temperature, salinity, total suspended particulate materials and nutrient concentrations. Total suspended matter concentrations were obtained by filtering a known volume of water onto a pre-weighed and pre-dried (450°C, 5 h) Whatman GF/F glass fiber filter. The filter was then oven-dried at 60°C for 24 h and total suspended solids were calcu-

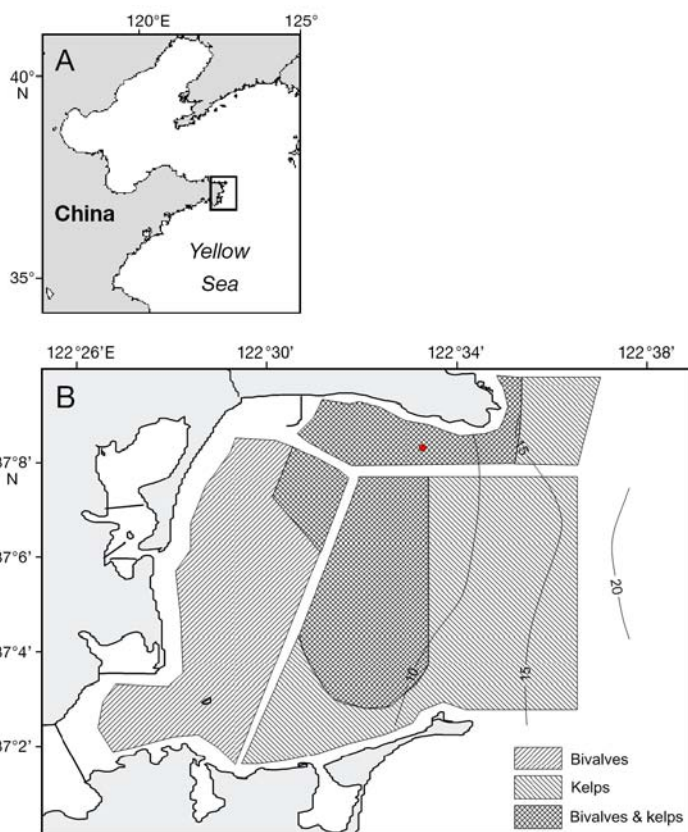


Fig. 1. (A) Location of Sanggou Bay (rectangle) at the eastern end of Shandong Peninsula, China and (B) location of the experimental site (red dot) in the northern part of the bay, within the kelp and bivalve mariculture area. Areas of kelp or bivalve monoculture are also indicated. Contour lines: 10, 15 and 20 m water depth

lated. Dissolved inorganic nitrogen (i.e. $\text{NH}_4\text{-N}$ + $\text{NO}_3\text{-N}$ + $\text{NO}_2\text{-N}$, hereafter called N), and phosphorus (i.e. $\text{PO}_4\text{-P}$, hereafter called P) were analyzed with colorimetric methods (Grasshoff et al. 1983).

Model description

A conceptual diagram of the model is depicted in Fig. 2. The equations for the main parameters are presented below. The environmental variables influencing the growth of kelp in the present model are temperature (T), irradiance (I) and nutrient concentration (N and/or P) in the water. The model was run with STELLA 9.1.3 software using a time step of 1 d for 180 d, which started from the beginning of November to May, corresponding to culture day 1 through 180.

Main processes and state variables

Kelp biomass can be defined as a balance between 2 dynamic processes: gross macroalgal production (growth) and removal of macroalgal biomass by respiration and erosion, or 'apical frond loss'. The biomass of kelp (B , g dry weight [DW] ind.^{-1}) is governed by the following equation:

$$\frac{dB}{dt} = (\text{NGR} - \text{ER}) \times B \quad (1)$$

where NGR is the net growth rate (d^{-1}), ER is the individual erosion rate (d^{-1}) per kelp and t is time (d).

NGR is defined by the difference between gross growth rate (G_{growth} , d^{-1}) and respiration rate (R_{resp} , d^{-1}):

$$\text{NGR} = G_{\text{growth}} - R_{\text{resp}} \quad (2)$$

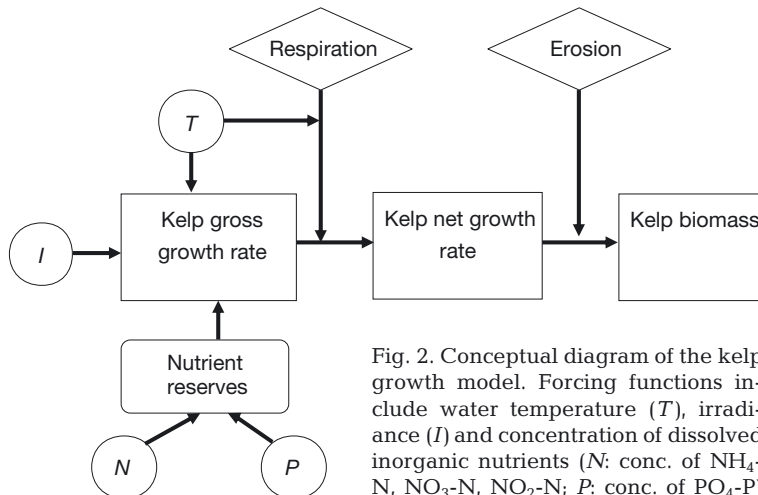


Fig. 2. Conceptual diagram of the kelp growth model. Forcing functions include water temperature (T), irradiance (I) and concentration of dissolved inorganic nutrients (N : conc. of $\text{NH}_4\text{-N}$, $\text{NO}_3\text{-N}$, $\text{NO}_2\text{-N}$; P : conc. of $\text{PO}_4\text{-P}$)

It is generally accepted that respiration, like any other biochemical reaction, is temperature dependent and can be described by an Arrhenius function (Duarte & Ferreira 1997, Martins & Marques 2002):

$$R_{\text{esp}} = R_{\text{max20}} \times r^{(T_w - 20)} \quad (3)$$

where R_{max20} is the maximum respiration rate at 20°C , r is the empirical coefficient and T_w is seawater temperature ($^\circ\text{C}$).

G_{growth} is described as a function of water temperature, irradiance and internal concentration of nutrients (NP) (Solidoro et al. 1997, Duarte & Ferreira 1997, Martins & Marques 2002), with μ_{max} being the maximum growth rate:

$$G_{\text{growth}} = \mu_{\text{max}} \times f(T) \times f(NP) \times f(I) \quad (4)$$

Kelp growth depends on temperature, which is described by a temperature-optimum curve (Duarte et al. 2003). The temperature limitation is expressed as follows:

$$f(T) = \frac{2.0(1 + \beta) \times X_T}{X_T^2 + 2.0 \times \beta \times X_T + 1.0} \quad (5)$$

where $X_T = \frac{T_w - T_{\text{opt}}}{T_{\text{opt}} - T_{\text{max}}}$, T_{max} is the upper temperature limit above which growth ceases ($^\circ\text{C}$), T_{opt} is the optimum temperature for growth ($^\circ\text{C}$), and β is an adjustment parameter ($^\circ\text{C}$).

Light attenuation through a column of water is one of the primary limiting variables in the growth of macroalgae. Kelp production is limited by light intensity. Similar to Shi et al. (2011), the functional response is integrated over depth:

$$f(I) = \frac{I}{I_0} \times e^{\left(1 - \frac{I}{I_0}\right)} \quad (6)$$

where I_0 is the optimum light intensity for growth (W m^{-2}) and I is the light intensity at depth Z defined by the Lambert-Beer law:

$$I = I_s \times e^{-kZ} \quad (7)$$

where k is the coefficient of light attenuation (m^{-1}), Z is the depth of kelp mariculture (m) and I_s is the light intensity at the surface (W m^{-2}), expressed by the following cosine function of time, which is based on Shi et al. (2011):

$$I_s = 200.38 - 116.47 \times \cos[2\pi(t - 1)/365] \quad (8)$$

The light extinction coefficient (k , m^{-1}) is influenced by suspended particles in

the water column. The suspended particles include many different forms such as phytoplankton, and particulate organic and inorganic matter. The k value depends on the type of the particles (Parsons et al. 1984). For simplicity, k was calculated from an empirical relationship with total particulate matter (TPM; the concentration of total suspended particulate materials, mg l^{-1}) (Duarte et al. 2003):

$$k = 0.0484 \text{TPM} + 0.0243 \quad (9)$$

Similar to most macroalgae, kelp store nutrients (N and P) in the tissue for growth, thus buffering the kelp against external nutrient shortage (Chapman & Craigie 1977, Pedersen & Borum 1996). Growth and photosynthesis are directly dependent on internal rather than external nutrient concentrations. Therefore, the model considers kelp growth to be a function of internal concentration of nutrients (NP). Nutrient limitation is calculated as follows:

$$f(NP) = \text{Min}[f(N), f(P)] \quad (10)$$

The preference of kelp for ammonium and nitrate is not considered in the model. Above a threshold level of N-quota, kelp growth increases with an increase of N-quota; below the threshold, growth did not occur. Following Ren et al. (2014), N-quota-dependent growth is calculated as:

$$f(N) = 1 - \frac{N_{\text{imin}}}{N_{\text{int}}} \quad (11)$$

where N_{imin} is the minimum internal cell quota for N and N_{int} the internal content of N in kelp tissue. The relationship between macroalgal growth and P-quota is defined similarly (Ren et al. 2014):

$$f(P) = 1 - \frac{P_{\text{imin}}}{P_{\text{int}}} \quad (12)$$

where P_{imin} is the minimum internal cell quota for P and P_{int} is the internal P concentration. Growth stops ($f(N) = 0$) when $N_{\text{int}} < N_{\text{imin}}$. Also, growth stops ($f(P) = 0$) when $P_{\text{int}} < P_{\text{imin}}$. Variations in internal nutrient concentrations are determined by subtracting consumed nutrients (γ) from the uptake of nutrients (Ψ). The uptake of nutrients is described in Eq. 13, with the amount of consumed nutrients depending on macroalgal growth rate:

$$\Psi_X = \frac{X_{\text{imax}} - X_{\text{int}}}{X_{\text{imax}} - X_{\text{imin}}} \times V_{\text{max}} \times \frac{X_{\text{ext}}}{K_X + X_{\text{ext}}} \quad (13)$$

Ψ_X is the nutrient ($X = \text{N or P}$) uptake rate. The factor $\frac{X_{\text{ext}}}{K_X + X_{\text{ext}}}$ represents simple Michaelis-Menten kinetics (Holling 1959). X_{ext} is the external nutrient con-

centration (in water) and X_{int} is the internal nutrient concentration (within the kelp tissue). K_X is the half-saturation constant for the uptake of the nutrient.

The factor $\frac{X_{\text{imax}} - X_{\text{int}}}{X_{\text{imax}} - X_{\text{imin}}}$ accounts for the internal nutrient reserve concentrations (Solidoro et al. 1997). X_{imax} is the maximum internal concentration, X_{imin} is the minimum internal concentration, and V_{max} is the maximum uptake rate of the nutrient. The use of internal nutrients is described as:

$$\gamma_X = X_{\text{int}} \times G_{\text{growth}} \quad (14)$$

where X_{int} is the internal nutrient concentration (within the plant).

Model parameters

Definitions and values of parameters used in the model are summarized in Table 1. The values for maximum N and P uptake rate were set to $V_{\text{maxN}} = 60 \mu\text{mol gDW}^{-1} \text{d}^{-1}$ and $V_{\text{maxP}} = 7 \mu\text{mol gDW}^{-1} \text{d}^{-1}$, respectively. Ozaki et al. (2001) report V_{maxN} for *S. japonica* to range from 0.54 to 1.95 $\mu\text{g cm}^{-2} \text{h}^{-1}$, leading to 27.8–100 $\mu\text{mol gDW}^{-1} \text{d}^{-1}$, and V_{maxP} from 0.17 to 0.31 $\mu\text{g cm}^{-2} \text{h}^{-1}$, leading to 3.95–7.2 $\mu\text{mol gDW}^{-1} \text{d}^{-1}$. Ozaki et al. (2001) reported K_N values ranging from 1.76 to 3.36 $\mu\text{mol l}^{-1}$, and a value of 3 $\mu\text{mol l}^{-1}$ was chosen for our model. N_{imin} and N_{imax} were set to 500 $\mu\text{mol gDW}^{-1}$ and 3000 $\mu\text{mol gDW}^{-1}$, respectively (Chapman et al. 1978, Sjøtun 1993).

Our P_{imax} and P_{imin} values were set in accordance with the values of Mizuta et al. (2003). K_P was set to 0.1 $\mu\text{mol l}^{-1}$ in our model, but data were limited. For brown macroalgae, the value of K_P varies from 0.14 to 11.17 $\mu\text{mol l}^{-1}$ (Rees 2003). For *Laminaria japonica* (now *Saccharina japonica*), Ozaki et al. (2001) found K_P ranging from 0.09 to 0.18 $\mu\text{mol l}^{-1}$.

I_0 was set to 180, according to the experimental result by Zhu et al. (2004). *S. japonica* is usually cultured on ropes, with farmers adjusting culture depth as kelp weight increases. A depth of 0.2 m was set for Z . The temperature parameters T_e and T_{opt} were obtained from Petrell et al. (1993), Duarte et al. (2003) and Wu et al. (2009).

Chapman et al. (1978) reported the growth rate of the congeneric *S. latissima* (as *Laminaria saccharina*) to be 0.18 d^{-1} . The maximum growth rate value in our model was set to 0.135 d^{-1} , based on our own data (J. Zhang unpubl.). The values for R_{max20} and r were obtained from EPA (1985). Most algal models use empirical equations or set loss rates equal to some constant proportion of seaweed biomass, varying

Table 1. Definitions and values of the parameters used in the kelp growth model. These are final values obtained by experimental procedure, field measurement, literature and/or calibration. DW: dry weight

Symbol	Definition	Unit	Value	Source
$R_{\max 20}$	Maximum respiration rate at 20°C	d^{-1}	0.015	EPA (1985)
r	Empirical coefficient	–	1.07	EPA (1985)
μ_{\max}	Maximum growth rate	d^{-1}	0.135	J. Zhang (unpubl.)
T_{opt}	Optimum temperature for growth	°C	13	Petrell et al. (1993), Duarte et al. (2003)
T_{\max}	Upper temperature limit above which growth ceases	°C	23	Petrell et al. (1993)
I_0	Optimum light intensity for growth	W m^{-2}	180	Tseng (1981)
Z	Water depth of kelp mariculture	m	0.2	This study (adjusted to 0 m in the simulation)
N_{imin}	Minimum internal quota for nitrogen	$\mu\text{mol gDW}^{-1}$	500	Chapman et al. (1978), Sjøtun (1993)
N_{imax}	Maximum internal quota for nitrogen	$\mu\text{mol gDW}^{-1}$	3000	Chapman et al. (1978), Sjøtun (1993)
$V_{\max N}$	Maximum nitrogen uptake rate	$\mu\text{mol gDW}^{-1} \text{d}^{-1}$	90	Ozaki et al. (2001)
K_N	Half-saturation constant for nitrogen uptake	$\mu\text{mol l}^{-1}$	2	Ozaki et al. (2001), Shi et al. (2011)
P_{imin}	Minimum internal phosphorus concentration	$\mu\text{mol gDW}^{-1}$	31	Mizuta et al. (2003)
P_{imax}	Maximum internal phosphorus concentration	$\mu\text{mol gDW}^{-1}$	250	Mizuta et al. (2003)
K_P	Half-saturation constant for phosphate uptake	$\mu\text{mol l}^{-1}$	0.1	Ozaki et al. (2001), Kitadai & Kadowaki (2003)
$V_{\max P}$	Maximum phosphate uptake rate	$\mu\text{mol ngDW}^{-1} \text{d}^{-1}$	7	Kitadai & Kadowaki (2003)
ER	Individual erosion rate	d^{-1}	0.01 % (day 130); 0.015 % (days 130–180)	This study (adjusted)

from 0.0005 to 0.03 d^{-1} (Canale & Auer 1982). With the hole-punching method, Suzuki et al. (2008) measured an erosion rate of *S. japonica* in the range of 0.3–2.3 g wet weight d^{-1} , which corresponds to 1.8–4 % d^{-1} . As temperature increases, rates of erosion of more mature plants also increase. For our simulations, we adjusted ER to 0 for simulation days 0–128, 0.01 % d^{-1} for day 130, and 0.015 % d^{-1} for days 130–180.

Calibration, validation and statistical analysis

Model calibration was conducted using data from the 2011–2012 culture cycle, whereas data from the 2008–2009 culture cycle was used for validation. The goodness-of-fit of model performance was evaluated by linear regression between the observation (on the x-axis) and simulation (on the y-axis), which was tested against the model $y = x$. Limiting factors for growth depended on $f(T)$, $f(I)$ and $f(NP)$, being functions with normalized values between 0 (maximum limitation) and 1 (no limitation).

Following Majkowski (1982) and Ren et al. (2014), we performed sensitivity analyses to assess the responses of the model to changes in model parameters. For each model run, 1 parameter was changed by $\pm 10\%$ (for temperature this is equivalent to a $\pm 3^\circ\text{C}$ shift), and the relative change in model output was

used to calculate sensitivity. The difference (S) between the unperturbed and perturbed results from the model was measured by:

$$S = \frac{1}{n} \sum \frac{x_{i,t} - x_t^0}{x_t^0} \quad (15)$$

where n is the number of simulation days, x_t^0 is the individual dry weight of kelp predicted with the calibrated set of parameters set at time t , and $x_{i,t}$ is the individual mass with 1 perturbed parameter of i at time t . Two model runs were performed for each parameter, differing by $\pm 10\%$. The averaged percentage change in individual dry weight from the 2 model runs was used as a measure of sensitivity of the change in the parameter value.

RESULTS

Fig. 3 shows the environmental data collected during 2008–2009 and 2011–2012. Temperature and nutrient data from November were used for initial model conditions.

During model calibration (using 2011–2012 data), reasonable agreement was achieved between the modelled and observed dry weight of kelp (Fig. 4A), and during validation, simulated DW also matched observed data with significant linear correlation ($R^2 = 0.969$; ANOVA, $p < 0.001$) (Fig. 4B).

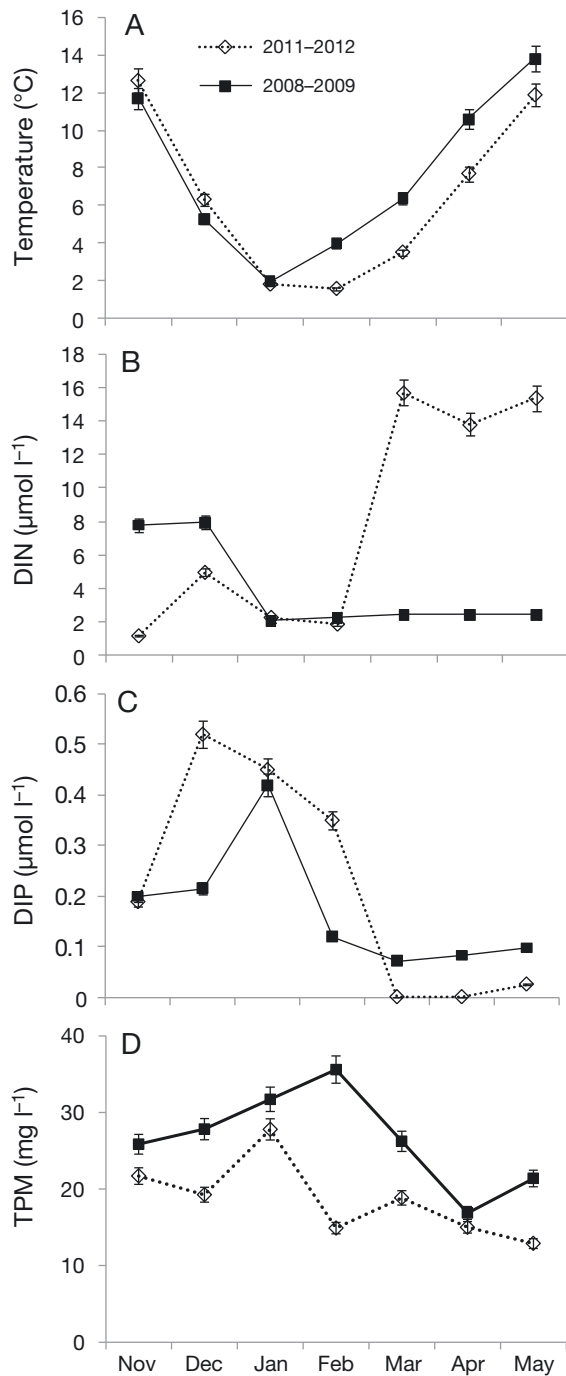


Fig. 3. Observed environmental data (mean \pm SE) for the periods 2008–2009 and 2011–2012 in Sanggou Bay, China, that were used to force the kelp growth model. (A) Temperature, (B) dissolved inorganic nitrogen (DIN), (C) dissolved inorganic phosphorus (DIP), and (D) total suspended particulate materials (TPM)

The simulated and observed values for 2011–2012 and for 2008–2009 were plotted in Fig. 5. For 2001–2012, $y = x$ regression of the data revealed a significant correlation ($R^2 = 0.996$; ANOVA, $p < 0.001$).

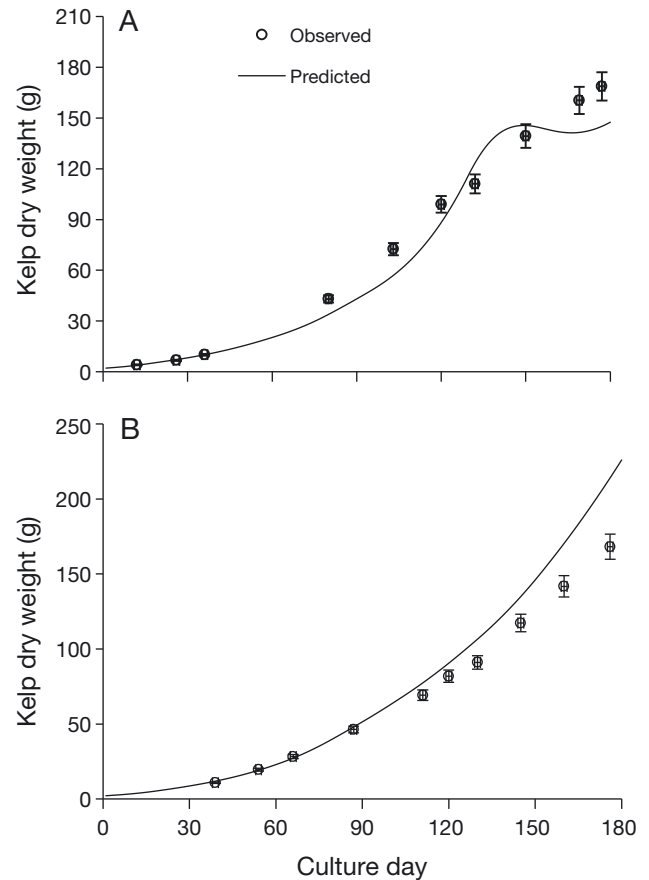


Fig. 4. Comparison of measured and predicted individual dry weight (mean \pm SE) of cultured kelp *Saccharina japonica* in Sanggou Bay, China. (A) 2011–2012, (B) 2008–2009

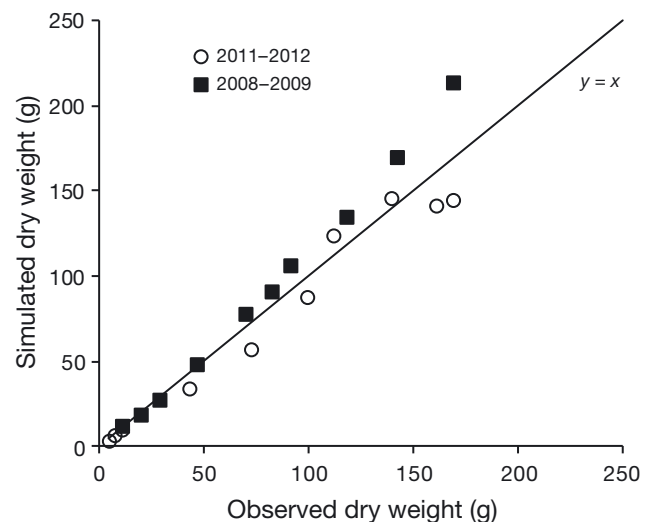


Fig. 5. Observed individual dry weight of cultured kelp vs. values simulated by the kelp growth model for the periods 2011–2012 ($R^2 = 0.995$, $p < 0.001$) and 2008–2009 ($R^2 = 0.969$, $p < 0.001$). For a perfect fit all points would be on the line $y = x$

Statistical analysis showed that predicted values did not significantly differ from observed values (ANOVA, $p > 0.64$). In addition, the model achieved a reasonably low root mean square error (RMSD = 12.4). For 2008–2009, there was no significant difference between prediction and observation (RMSD = 19.0; ANOVA, $p > 0.65$). The model satisfactorily reproduced the growth of kelp in both years, but achieved a much better result for the period 2011–2012 than 2008–2009.

The effects of nutrients, light intensity and temperature on growth are shown in Fig. 6, plotting normalized functions of these parameters (0 = maximum limitation, 1 = no limitation). During the culture cycle (November–May), nutrients were the greatest limiting factor in kelp growth, while there was also substantial light and temperature limitation. The values of $f(NP)$ varied between 0.15 and 0.5 in 2011–2012, and 0.30–0.54 in 2008–2009, with the lowest value on simulation days 150–180 (from mid-March to late April). For $f(I)$ and $f(T)$, the values ranged from 0.66–0.99 and 0.78–1.0, respectively, both with the lowest value on simulation day 60 (the beginning of January).

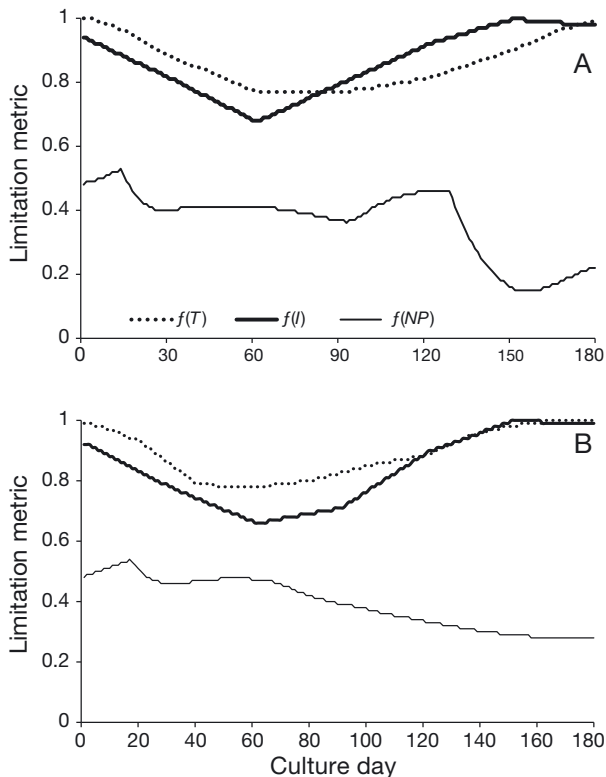


Fig. 6. Comparison among environmental limitation factors for temperature (T), irradiance (I) and nutrients (dissolved inorganic nitrogen or phosphorus; NP) on the growth of cultured kelp *Saccharina japonica*. Results of normalized functions over time are shown; a value close to 1 indicates the absence of limitation. (A) 2011–2012, (B) 2008–2009

The effects of N and P limitation on growth are shown in Fig. 7. At simulation days 15–130 in 2011–2012, $f(N)$ values were lower than $f(P)$ values, whereas $f(P)$ values were lower than $f(N)$ values on days 130–180 (Fig. 7A). While in 2008–2009, the values of $f(N)$ were lower than $f(P)$ from days 15–180 (Fig. 7B).

Sensitivity analysis revealed that the model is relatively sensitive to changes in most model parameters (Table 2). S was $<100\%$ in all cases tested, suggesting that uncertainties in parameters and initial conditions are not amplified in the values of the state variables. The empirical coefficient of respiration (r) was found to exert the greatest influence on the prediction result of the model, in which 10% change resulted in an extensive change in model output (89.45%). Other relatively sensitive parameters were the maximum growth rate (μ_{\max}) and the minimum internal quota for nitrogen (N_{\min}).

The simulations of unlimited nutrient supply showed that in 2011–2012, assuming $f(N) = 1$, DW of kelp increased 3.4 times, and $f(P) = 1$, DW of kelp increased 3.0 times (Fig. 8A). However, in 2008–2009, only fertilization with N resulted in an increase in kelp growth (Fig. 8B). Raising the culture

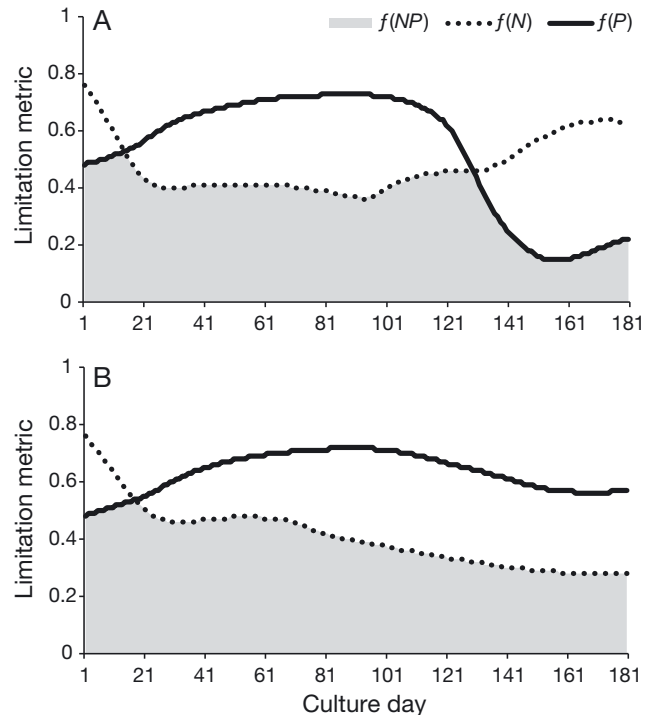


Fig. 7. Nutrient limitation factors on the growth of cultured kelp *Saccharina japonica*. Results of normalized functions for the concentration of dissolved inorganic nitrogen (N), phosphorus (P) or both (NP , grey shaded area) over time are shown; a value close to the gray shaded area indicates growth limitation. (A) 2011–2012, (B) 2008–2009

Table 2. Sensitivity analyses as percent relative change from the baseline of dry weight of cultured *Saccharina japonica* predicted by the kelp growth model after changing each model parameter by $\pm 10\%$ (except T_{\min} changed only $+10\%$ from standard value of $T_{\min} = 0.5^{\circ}\text{C}$). Parameters with very low sensitivity coefficients ($<1\%$) are not presented. See Table 1 for parameter definitions

Model parameter	% change
r	89.45
μ_{\max}	25.97
N_{\min}	18.05
$V_{\max N}$	15.41
T_{opt}	14.93
P_{\min}	14.57
$V_{\max P}$	12.75
$R_{\max 20}$	7.90
K_N	5.75
K_P	6.57
P_{\max}	3.52
N_{\max}	3.33
I_0	1.37

ropes from 0.2 m depth up to the surface would result in the final DW of kelp being increased by 18.8% in 2011–2012 (Fig. 9).

DISCUSSION

The kelp growth model reflects the relationship between productivity and the environment. It is a useful tool for the management of kelp mariculture.

Temperature

Recent research has focused on the influence of increased seawater temperature on the growth of *Saccharina japonica* in cold-water environments (Ohno & Matsuoka 1992, Suzuki et al. 2006). The influence of low temperature on kelp growth is not being concerned about: However, from this study, we found that the growth of *S. japonica* in Sanggou Bay was largely limited by temperature, particularly during culture days 60–120 in January–February. A previous study showed that the uptake rates of nitrate and phosphate by *S. japonica* decreased when water temperature dropped to $<5^{\circ}\text{C}$ (Ozaki et al. 2001). In Sanggou Bay in 2011–2012, water temperature fell $<5^{\circ}\text{C}$ for over 2 mo in winter and became the main limiting factor for *S. japonica* growth in this season.

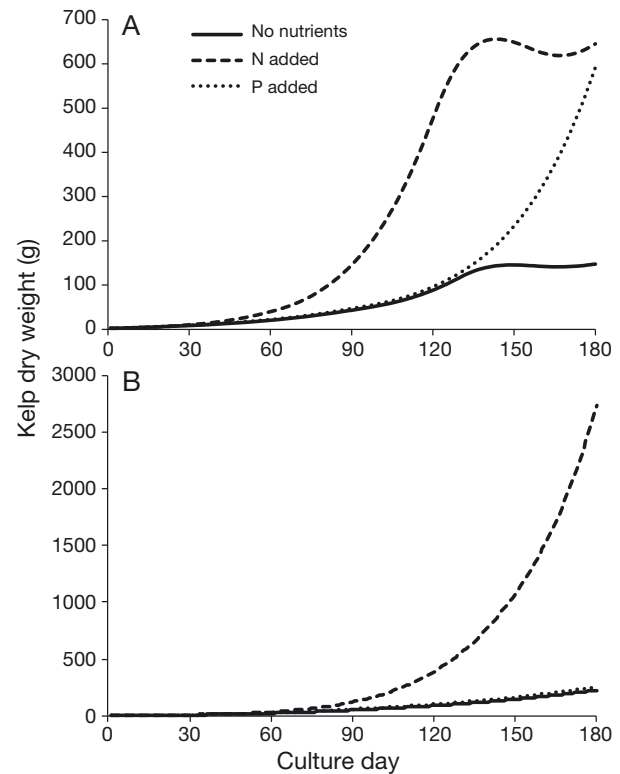


Fig. 8. Simulation results on the potential effect of fertilization with dissolved inorganic nitrogen (N) or phosphorus (P) on the individual dry weight of cultured kelp *Saccharina japonica* in comparison to predicted growth without fertilization. Addition of nutrients to fertilize kelp was implemented by running the model with the normalized functions of N and P set to 1 (i.e. absence of nutrient limitation). (A) 2011–2012, (B) 2008–2009

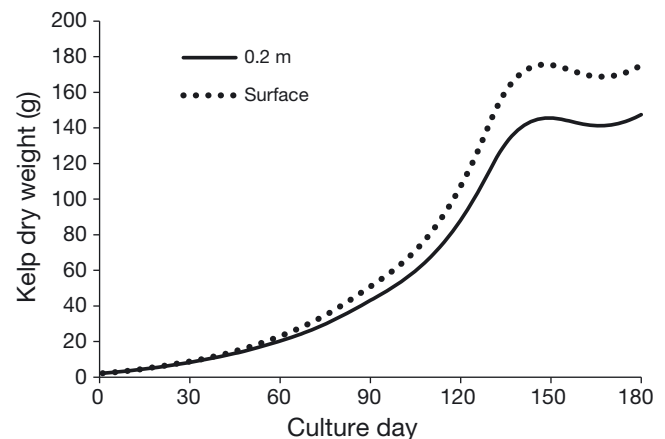


Fig. 9. Simulated growth (individual dry weight) of kelp *Saccharina japonica* when lifting the culture ropes from 0.2 m depth to the surface

Light

The surface radiation and extinction of light in the water column affect the light intensity available to kelp. Although clouds and dust in the atmosphere

could influence the incident surface radiation to some extent, there is considerable variation in the incident surface radiation with geographical position. Our results showed that although kelp was cultured near the water surface in Sanggou Bay, light intensity was still a limiting factor in winter (Fig. 9). Extinction of light depends on depth and suspended particles in the water. Despite diurnal and seasonal variations of the light extinction coefficient (k), the use of total suspended particulate materials to calculate k still achieved reasonable results. In addition, self-shading by macroalgal thalli can also affect k . However, most reports were on natural macroalgae, such as *Ulva*, where the density of a natural population is not uniform and can be very high (e.g. Enriquez et al. 1994, Ren et al. 2014). In maricultural macroalgae, density is controlled. The suspended long-line culture usually allows the kelp fronds to float horizontally, which reduces self-shading. Therefore, in the model, we did not consider the influence of self-shading on the growth of kelp.

Earlier types of models to assess the carrying capacity for kelp (Shi et al. 2011) or for multi-species (kelp and scallop) culture in Sanggou Bay (Duarte et al. 2003) do not consider light to be a limiting factor, because the depth of kelp culture ropes was manually adjusted to overcome light limitation in the past. As kelp weight increases, the culture rope is submerged under water. Farmers adjust the depth of culture ropes by increasing or decreasing the number of floating balls. However, with increasing scale and labor costs of present-day mariculture, this practice is no longer feasible considering the economic value of kelp, although our model shows that the DW of kelp could theoretically be increased by 18% with raising culture ropes to the surface when light is limited.

Nutrients

The availability of nutrients is one of the primary factors regulating macroalgae growth in a marine ecosystem. In this study, we identified nutrient availability to be the key limiting factor for kelp growth and there were seasonal and inter-annual variations of limitations in N or P. N was the main limiting factor in the culture period 2008–2009 and on simulation days 15–130 in 2011–2012. The kelp farming area is not only in the middle area of the bay, but also has been expanded to the mouth and even outside the bay. Therefore, both the rafts and seaweeds impede water exchange of the bay with the Yellow Sea,

which limits influx of supplementary oceanic nutrients. Coupled with the absorption of nutrients by seaweed and little riverine input, nutrient concentrations within Sanggou Bay are usually lower during the kelp cultural season than during the rest of the year (Liu et al. 2003, Sun et al. 2007, Zhang et al. 2011). Consequently, variability in nutrient availability can strongly influence kelp productivity (Rosell & Srivastava 1984, Ahn et al. 1998). In the past, farmers have increased mariculture seaweed yield by fertilizing them with ammonia or urea. On the northern coast of China, Tseng et al. (1955) conducted experiments to investigate the effect of fertilizer application on the growth of *S. japonica*, and found that the harvest could be increased by 3 to 4 times with increasing the DIN concentration. Our model simulations also showed that kelp DW could be increased by 3.4 times in the absence of N limitation. Although the application of nitrogen fertilizers can increase the yield of kelp, few farmers in Sanggou Bay fertilize with N during the kelp culture period.

Recent studies have shown that phosphates and silicates can become limiting factors for phytoplankton growth in Sanggou Bay (Quet et al. 2008, Zhang et al. 2011). However, there are no reports on the influence of phosphates on kelp mariculture. Our results revealed that low P availability was a key limiting factor for kelp growth only on simulation days 130–180 in 2011–2012. As one of few studies reporting on the relationship between P availability and macroalgal growth, Lapointe et al. (1992) found that low availability of P limited macroalgal productivity in oligotrophic waters. Although Sanggou Bay is not known to be oligotrophic, the concentrations of phosphate became too low to support potential growth during March to May in 2012 (Fig. 3). According to our model, enriching waters with phosphates could have improved kelp growth in 2012, but not in 2009. Therefore, whether to fertilize or not and at which seasons depends on the specific circumstances of the environment in a particular year.

The addition of nutrients may improve kelp growth, but it may also cause potentially detrimental ecological responses. Nutrient addition can stimulate the growth of phytoplankton and other macroalgae, increasing the competition for nutrients and causing light limitation; effects that, in concert, could cause more serious ecological problems, such as the formation of red tides.

IMTA is a form of ecological engineering that combines the biological processes of cultured fish and extractive co-cultured species to remove waste loadings associated with intensive aquaculture systems

(Troell et al. 2009). Co-cultures of macroalgae have been successfully used to reduce the amount of aquaculture-derived inorganic nutrients (Yu et al. 2014). Similarly, the IMTA practice could stimulate the growth of kelp, because the release of aquaculture-derived inorganic nutrients is equivalent to kelp fertilization. In view of the observed nutrient limitation in Sanggou Bay, the results of the present modelling study indicate that the introduction of cage culture (in which fish are fed highly nutritious food, resulting in soluble waste materials containing ammonium and soluble P) would be beneficial for kelp growth (Ahn et al. 1998).

Acknowledgements. The study was supported by the National Science and Technology Pillar Program (no. 2011BAD13B06), National Natural Science Foundation of China (no. 41276172), and Special Fund of Basic Research for Central non-profit Scientific Research Institute (no. 2014A01YY01). We thank Mr. Huayao Zhang from Xunshan Fisheries Group for his help in measuring the growth of *Saccharina japonica*.

LITERATURE CITED

- Ahn O, Petrell RJ, Harrison PJ (1998) Ammonium and nitrate uptake by *Laminaria saccharina* and *Nereocystis luetkeana* originating from a salmon sea cage farm. *J Appl Phycol* 10:333–340
- Aveytua-Alcázar L, Camacho-Ibar VF, Souza AL, Allen JI, Torres R (2008) Modelling *Zostera marina* and *Ulva* spp. in a coastal lagoon. *Ecol Modell* 218:354–366
- Buschmann AH, Varela DA, Hernández-González MC, Huovinen P (2008) Opportunities and challenges for the development of an integrated seaweed-based aquaculture activity in Chile: determining the physiological capabilities of *Macrocystis* and *Gracilaria* as biofilters. *J Appl Phycol* 20:571–577
- Canale RP, Auer MT (1982) Ecological studies and mathematical modeling of *Cladophora* in Lake Huron: V. Model development and calibration. *J Gt Lakes Res* 8: 112–125
- Chapman ARO, Craigie JS (1977) Seasonal growth in *Laminaria longicruris*-relations with dissolved inorganic nutrients and internal reserves of nitrogen. *Mar Biol* 40: 197–205
- Chapman ARO, Marklam JW, Luning K (1978) Effect of nitrate concentration on the growth and physiology of *Laminaria saccharina* in culture. *J Phycol* 14:195–198
- Chopin T, Buschmann AH, Halling C, Troell M and others (2001) Integrating seaweeds into marine aquaculture systems: a key toward sustainability. *J Phycol* 37:975–986
- Duarte P, Ferreira JG (1997) A model for the simulation of macroalgal population dynamics and productivity. *Ecol Modell* 98:199–214
- Duarte R, Meneses R, Hawkins AJS, Zhu M, Fang JG, Grant J (2003) Mathematical modelling to assess the carrying capacity for multi-species culture within coastal waters. *Ecol Modell* 168:109–143
- Enriquez S, Agustí S, Duarte C (1994) Light absorption by marine macrophytes. *Oecologia* 98:121–129
- EPA (Environmental Protection Agency) (1985) Rates, constants, and kinetics. In: Bowie GL, Mills WM, Porcellaet DB, Campbell CL and others (eds) Formulations in surface water quality modelling, 2nd edn. EPA, Atlanta, GA, p 188–204
- FAO (Food and Agriculture Organization of the United Nations) (2014) Global Aquaculture Production 1950–2014 database. <http://www.fao.org/fishery/statistics/global-aquaculture-production/query/en>
- Fei XG (2004) Solving the coastal eutrophication problem by large scale seaweed cultivation. *Hydrobiologia* 512: 145–151
- Grasshoff K, Ehrhardt M, Kremling K (eds) (1983) Methods of seawater analysis. Verlag Chemie, Weinheim
- Holling CS (1959) Some characteristics of simple types of predation and parasitism. *Can Entomol* 91:385–398
- Kitadai Y, Kadowaki S (2003) The growth process and N, P uptake rates of *Laminaria japonica* cultured in coastal fish farms. *Aquacult Sci* 51:15–23
- Lapointe BE, Littler MM, Littler DS (1992) Nutrient availability to marine macroalgae in siliclastic versus carbonate-rich coastal waters. *Estuaries* 15:75–82
- Li L, Ren JL, Liu SM, Jiang ZJ, Du JZ, Fang JG (2014) Distribution, seasonal variation and influence factors of dissolved inorganic arsenic in the Sanggou Bay. *Huan Jing Ke Xue* 35:2705–2713 (in Chinese with English abstract)
- Liu H, Fang JG, Dong SL, Wang LC, Lian Y (2003) Annual variation of major nutrients and limiting factors in Laizhou Bay and Sanggou Bay. *J Fish Sci China* 10: 227–234 (in Chinese with English abstract)
- Liu Y, Saitoh SI, Radiarta IN, Isada T, Hirawake T, Mizuta H (2013) Improvement of an aquaculture site-selection model for Japanese kelp (*Saccharina japonica*) in southern Hokkaido, Japan: an application for the impacts of climate events. *ICES J Mar Sci* 70:1460–1470
- Majkowski J (1982) Usefulness and applicability of sensitivity analysis in a multispecies approach to fisheries management. In: Pauly D, Murphy GI (eds) Theory and management of tropical fisheries. *ICLARM Conf Proc* 9: 149–165
- Martins I, Marques JC (2002) A model for the growth of opportunistic macroalgae (*Enteromorpha* sp.) in tidal estuaries. *Estuar Coast Shelf Sci* 55:247–257
- Mizuta H, Ogawa S, Yasui H (2003) Phosphorus requirement of the sporophyte of *Laminaria japonica* (Phaeophyceae). *Aquat Bot* 76:117–126
- Nunes JP, Ferreira JG, Gazeau F, Lencart-Silva J, Zhang XL, Zhu MY, Fang JG (2003) A model for sustainable management of shellfish polyculture in coastal bays. *Aquaculture* 219:257–277
- Ohno M, Matsuoka M (1992) Growth of cultivated *Laminaria japonica*, *Undaria pinnatifida*, and *U. undarioides* in sub-tropical waters of Tosa Bay. *Aquacult Sci* 40: 279–283 (in Japanese with English abstract)
- Ozaki AI, Mizuta H, Yamamoto H (2001) Physiological differences between the nutrient uptakes of *Kjellmaniella crassifolia* and *Laminaria japonica* (Phaeophyceae). *Fish Sci* 67:415–419
- Parsons TR, Takahashi M, Hargrave B (eds) (1984) Biological oceanographic processes. Pergamon Press, New York, NY
- Pedersen MF, Borum J (1996) Nutrient control of algal growth in estuarine waters. Nutrient limitation and the importance of nitrogen requirements and nitrogen

- storage among phytoplankton and species of macroalgae. *Mar Ecol Prog Ser* 142:261–272
- Petrell RJ, Tabrizi KM, Harrison PJ, Druehl LD (1993) Mathematical model of *Laminaria* production near a British Columbian salmon sea cage farm. *J Appl Phycol* 5:1–14
 - Qu KM, Song YL, Xun Y, Fang JG (2008) Experiment on nutrient limitations in cultured areas of Sanggou Bay *in situ* in spring and summer. *Mar Environ Sci* 27:124–127 (in Chinese with English abstract)
 - Rees TAV (2003) Safety factors and nutrient uptake by seaweeds. *Mar Ecol Prog Ser* 263:29–42
 - Ren JS, Barr NG, Scheuer K, Schiel DR, Zeldis J (2014) A dynamic growth model of macroalgae: application in an estuary recovering from treated wastewater and earthquake-driven eutrophication. *Estuar Coast Shelf Sci* 148: 59–69
 - Rosell KG, Srivastava LM (1984) Seasonal variation in the chemical constituents of the brown algae *Macrocystis integrifolia* and *Nereocystis luetkeana*. *Can J Bot* 62: 2229–2236
 - Shi J, Wei H, Zhao L, Yuan Y, Fang JG, Zhang JH (2011) A physical–biological coupled aquaculture model for a suspended aquaculture area of China. *Aquaculture* 318: 412–424
 - Sjøtun K (1993) Seasonal lamina growth in two age groups of *Laminaria saccharina* (L.) Lamour. in western Norway. *Bot Mar* 36:433–441
 - Solidoro C, Pecenic G, Pastres R, Franco D, Dejak C (1997) Modelling macroalgae (*Ulvarigida*) in the Venice Lagoon: model structure identification and first parameters estimation. *Ecol Modell* 94:191–206
 - Sun PX, Zhang ZH, Hao LH, Wang B and others (2007) Analysis of nutrient distributions and potential eutrophication in seawater of the Sanggou Bay. *Adv Mar Sci* 25: 436–445 (in Chinese with English abstract)
 - Suzuki S, Furuya K, Takeuchi I (2006) Growth and annual production of the brown alga *Laminaria japonica* (Phaeophyta, Laminariales) introduced into the Uwa Sea in southern Japan. *J Mar Biol Assoc UK* 339:15–29
 - Suzuki S, Furuya K, Kawai T, Takeuchi I (2008) Effect of seawater temperature on the productivity of *Laminaria japonica* in the Uwa Sea, southern Japan. *J Appl Phycol* 20:833–844
 - Troell M, Halling C, Neori A, Chopin T, Buschmann AH, Kautsky N, Yarish C (2003) Integrated mariculture: asking the right questions. *Aquaculture* 226:69–90
 - Troell M, Joyce A, Chopin T, Neori A, Buschmann AH, Fang JG (2009) Ecological engineering in aquaculture-potential for integrated multi-trophic aquaculture (IMTA) in marine offshore systems. *Aquaculture* 297:1–9
 - Tseng CK, Sun KY, Wu CY (1955) Studies on fertilizer application in the cultivation of Haitai (*Laminaria japonica* Areseh). *Acta Bot Sin* 4:374–392 (in Chinese with English abstract)
 - Tseng CK (1981) Commercial cultivation. In: Lobban CS, Wynne MJ (eds) *The biology of seaweeds*. University of California Press, Berkeley, CA, p 680–725
 - Wu RJ, Zhang XL, Zhu MY, Zheng YF (2009) A model for the growth of Haidai (*Laminaria japonica*) in aquaculture. *Mar Sci Bull* 28:34–40 (in Chinese with English abstract)
 - Yu Z, Zhu X, Jiang Y, Luo P, Hu C (2014) Bioremediation and fodder potentials of two *Sargassum* spp. in coastal waters of Shenzhen, South China. *Mar Pollut Bull* 85: 797–802
 - Zhang JH, Ren LH, Xu D, Zhang ML and others (2011) Analysis of water quality of abalone suspended long-line mariculture area of Sanggou Bay. *J Fish Sci China* 35: 52–58 (in Chinese with English abstract)
 - Zhu MY, Wu RJ, Li RX, Yue GF, Sun PX, Deslous-Paoli JM, Auby I (2004) The impacts of temperature on growth and photosynthesis of *Laminaria japonica* juvenile sporophytes. *Acta Ecol Sin* 24:22–27

Editorial responsibility: Sebastien Lefebvre, (Guest Editor)
Wimereux, France

Submitted: June 1, 2015; Accepted: January 22, 2016
Proofs received from author(s): April 5, 2016



Sources and export of nutrients associated with integrated multi-trophic aquaculture in Sanggou Bay, China

Ruihuan Li^{1,5}, Sumei Liu^{1,2,*}, Jing Zhang³, Zengjie Jiang⁴, Jianguang Fang⁴

¹Key Laboratory of Marine Chemistry Theory and Technology, MOE, Ocean University of China/Qingdao Collaborative Innovation Center of Marine Science and Technology, Qingdao 266100, PR China

²Laboratory for Marine Ecology and Environmental Science, Qingdao National Laboratory for Marine Science and Technology, Qingdao, PR China

³State Key Laboratory of Estuarine and Coastal Research, East China Normal University, Shanghai 200062, PR China

⁴Carbon Sink Fisheries Laboratory, Key Laboratory of Sustainable Utilization of Marine Fisheries Resources, Ministry of Agriculture, Yellow Sea Fisheries Research Institute, Chinese Academy of Fishery Sciences, 106 Nanjing Road, Qingdao 266071, PR China

⁵Present address: State Key Laboratory of Tropical Oceanography, South China Sea Institute of Oceanology, Chinese Academy of Sciences, 164 West Xingang Road, Guangzhou 510301, PR China

ABSTRACT: Field observations were made from 2012 to 2014 at an integrated multi-trophic aquaculture (IMTA) site in Sanggou Bay (SGB), China, to characterize the nutrients associated with aquaculture activities, and to assess the effects of aquaculture on nutrient cycles in the bay. Dissolved inorganic and organic nutrient levels were measured in rivers, groundwater, and SGB. Seasonal variations in nutrient concentrations were detected in the rivers, particularly enrichment of dissolved inorganic nitrogen (DIN) and silicate (DSi). Nutrient concentrations showed considerable seasonal variation, with higher and significantly different concentrations occurring in autumn than in the other seasons. The composition and distribution of nutrients were also affected by the species being cultured. Dissolved organic nitrogen and phosphorus (DON and DOP) accounted for 27 to 87 % of total dissolved nitrogen and 34 to 81 % of total dissolved phosphorus, respectively. Phosphorus may be a potentially limiting nutrient for phytoplankton growth in summer. Nutrient budgets were developed based on a simple steady-state box model. These showed that bivalve aquaculture was the major source of PO_4^{3-} (contributing 64 % of total influx) and led to increased riverine fluxes of PO_4^{3-} . The results indicated that substantial quantities of nitrogen and DSi accumulated in sediments or were transformed into other forms (e.g. phytoplankton cell composition or particles). Large quantities of DIN and PO_4^{3-} were removed from the bay through harvesting of seaweeds and bivalves, which represented up to 64 and 81 % of total outflux, respectively. The results show that aquaculture activities play the most important role in nutrient cycling in SGB.

KEY WORDS: Nutrients · IMTA · Budgets · Aquaculture activities · Sanggou Bay

INTRODUCTION

With an annual average increase of 8.7 % over the past 40 yr, aquaculture is the fastest-growing food production sector in the world, and is overtaking capture fisheries as a source of food fish (Herbeck et al.

2013). The rapid growth of aquaculture has given rise to a wide variety of environmental problems, including ecosystem degradation and water pollution (Neori et al. 2004). One of the largest of impacts of aquaculture effluents to local ecosystems is imbalance created in nutrient dynamics and eutrophic

*Corresponding author: sumeiliu@ouc.edu.cn

conditions (Marinho-Soriano et al. 2009, Bouwman et al. 2011). In addition, excess nutrients cause stress in the cultivated organisms, with deleterious effects including smaller size, reduced production, and mass mortality (Newell 2004, Mao et al. 2006). Due to increasing concerns about the environmental impacts of aquaculture, a new method of aquaculture with a smaller ecological footprint has been developed. Integrated multi-trophic aquaculture (IMTA) has the potential to mitigate the environmental impacts of aquaculture (Buschmann et al. 2008).

IMTA is described as the cultivation of aquatic species from different trophic levels within a shared water system (Bostock et al. 2010). Such systems significantly increase the sustainability of aquaculture and recycle waste nutrients from high trophic-level species into production of lower trophic-level crops of commercial value (Troell et al. 2009). Seaweeds are used in IMTA systems for their nutrient-absorbing and sequestering properties. Nutrients excreted and egested by bivalves can be absorbed by macroalgae and recycled into valuable biomass (Newell 2004, Buschmann et al. 2008), and this amount of nutrient waste can be effectively removed from the ecosystem. In addition, a number of studies have confirmed that suspension-feeding bivalves can exert top-down control on phytoplankton (Newell & Koch 2004, Wall et al. 2008); larger nanoplankton will be removed in comparison with smaller ($<3\ \mu\text{m}$ diameter) picoplankton species, thereby reducing turbidity (Newell 2004). The resulting increased light penetration can potentially enhance the production of benthic plants (Newell & Koch 2004). If high levels of dissolved inorganic nitrogen (DIN) regenerated by bivalves are sufficient to allow the relatively slow-growing nanoplankton to grow fast enough to overcome grazer control, primary production can be stimulated through recycling of nitrogen (Smaal et al. 2001). Some marine IMTA systems have been commercially successful at industrial scales, especially in Asia (China) (Troell et al. 2009).

China is the largest aquaculture producer in the world, with a total production of 34.1 million tons, which accounts for 62% of total global production and 51% of the global value (Yang et al. 2005, FAO 2010, Yuan et al. 2010, Yu et al. 2012). The area devoted to aquaculture increased from 11.2×10^4 ha in 1977 to 218×10^4 ha in 2012 (The People's Republic of China Ministry of Agriculture Fisheries Bureau 2013). The rapid growth of aquaculture has led to eutrophication of coastal waters (Wu et al. 2014), and to the occurrence of aquatic diseases that have resulted in major economic losses (Fei 2004); for

example, in 1998, more than 10 billion Chinese Yuan (approximately US\$ 1.5 billion) were lost because of mariculture disease (Fei 2004). To improve the environmental sustainability of aquaculture and benefit the local economy, IMTA was developed in China. Sea-ranching and suspended aquaculture are the 2 main forms of IMTA in China, and the latter is used in Sanggou Bay.

Sanggou Bay (SGB) is located in northern China and has been used for aquaculture for over 30 yr (Zhang et al. 2009). It has been estimated that more than 300 t of inorganic nitrogen have been excreted into the bay by cultivated and fouling animals (Troell et al. 2009). Studies of core sediments also indicated that the total nitrogen (TN) content has increased in recent decades as a consequence of aquaculture activities (Song et al. 2012). Bivalves clear seston particles $>3\ \mu\text{m}$ in diameter from natural water and are not supplied with additional feed in the bay. The absolute and relative abundances of dinoflagellate cells in the bay are lower inside the scallop culture area than outside (Zhang et al. 2005), and the phytoplankton community has changed as a result; meanwhile, the reduction in phytoplankton biomass has a negative impact on bivalve growth (Duarte et al. 2003, Shi et al. 2011a). In addition, kelp can compete with phytoplankton for nutrients, and 80 000 t of dried kelp can be produced annually through uptake of inorganic nitrogen from the bay (Zhang et al. 2009). In pursuing high levels of productivity, SGB has been subject to a rapid growth in aquaculture, with long-line culture of kelp having expanded to areas more than 8 km away from the coast, where the water depth is between 20 and 30 m (Troell et al. 2009, Fu et al. 2013).

Much attention has been focused on the carrying capacity of shellfish and kelp mariculture (Bacher et al. 2003, Nunes et al. 2003, Shi et al. 2011a), ecology (Song et al. 2007, Hao et al. 2012), nutrient levels (Wang 2012, Zhang et al. 2012), and nutrient fluxes at the sediment–water interface (Jiang et al. 2007, Sun et al. 2010) in SGB, but the effects of aquaculture activities on nutrient cycling have not been well studied in the bay. The objective of this study was to determine the amounts and composition of dissolved nutrients in the bay and associated rivers and groundwater, to assess the sources and transportation of nutrients, to evaluate the impact of aquaculture activities on nutrient cycling, and to discriminate the importance of internal nutrient inputs vs. physical transport, based on the land–ocean interactions in the coastal zone (LOICZ) nutrient model (Gordon et al. 1996).

MATERIALS AND METHODS

Study area

SGB (Fig. 1) is a semi-enclosed water body of approximately 144 km² at the eastern end of Shandong Peninsula, and has an average depth of 7.5 m (Zhang et al. 2009). The bay is characterized by semi-diurnal tides having an average tidal range of 2 m, and is connected to the Yellow Sea through an 11.5 km wide channel (Mao et al. 2006, Jiang et al. 2007). It is dominated by land-ocean climate, with water temperatures ranging from 2 to 26°C (Kuang et al. 1996). Approximately 73.3% of annual precipitation in the area (819.6 mm) occurs during the wet season, from June to September. The average river discharge into the bay is $1.7\text{--}2.3 \times 10^8 \text{ m}^3 \text{ yr}^{-1}$, and this carries an annual sediment load of $17.1 \times 10^4 \text{ t}$.

More than 70% of the area of SGB is currently used for aquaculture (Zhang et al. 2009, 2010, Fu et al. 2013). It is one of the largest aquaculture production sites in China, and is extensively used for the culture

of scallops (*Chlamys farreri*), Pacific oyster *Crassostrea gigas*, and seaweeds (*Saccharina japonica* and *Gracilaria lemaneiformis*) (Zhang et al. 2009). These species are grown in both monoculture and polyculture, from suspended longlines (Fang et al. 1996a) (Fig. 1). *S. japonica* monoculture occurs mainly near the mouth of the bay, bivalves are mainly cultured in the western part of the bay, and kelp and bivalve polyculture occurs in the middle part of the bay (Fig. 1). The co-cultivation of abalone *Haliotis discus hannai* with kelp (*S. japonica*) has also been developed, with the abalones held in lantern nets hanging vertically from the longlines. In 2012, production included approximately 84 500 t dry weight of *S. japonica*, 25 410 t wet weight of *G. lemaneiformis*, and approximately 15 000 and 60 000 t wet weight of *C. farreri* and *C. gigas*, respectively (data from Rongcheng Fishery Technology Extension Station). The main cultured species has shifted from scallop to oyster since 1996 because of reduced scallop production as a consequence of disease (Zhang et al. 2009).

To increase production, aquaculture has expanded from the bay to the open sea since the 1990s (Fang et al. 1996a). However, the total aquaculture production of kelp has not increased (Shi et al. 2011a). This may be related to a reduced supply of nutrients resulting from a decrease in the water exchange rate, which has been a consequence of reduced circulation because of the increase in aquaculture activities (Fang et al. 1996b). The hydrodynamic conditions have changed significantly because of the presence of suspended aquaculture (Shi et al. 2011a). Current speeds can be reduced by aquaculture facilities including rafts, and ropes impose drag (Grant & Bacher 2001, Duarte et al. 2003). The renewal of suspended particles for bivalve culture and nutrient regeneration for kelp have also been reduced (Grant & Bacher 2001, Duarte et al. 2003). Compared with the period of farming activities up to 1983, tidal currents had decreased by 50% by 1994 because of large-scale cultivation (Zhao et al. 1996). Based on a 2-dimensional model, Grant & Bacher (2001) estimated a reduction of 41% in the water exchange rate in SGB because of increased bottom friction with expansion of intensive suspended aquaculture. The vertical current has also changed because of suspended aquaculture (Fan & Wei 2010).

Sample collection

Sampling took place during 31 May to 4 June 2012 (early summer), 20 September to 2 October

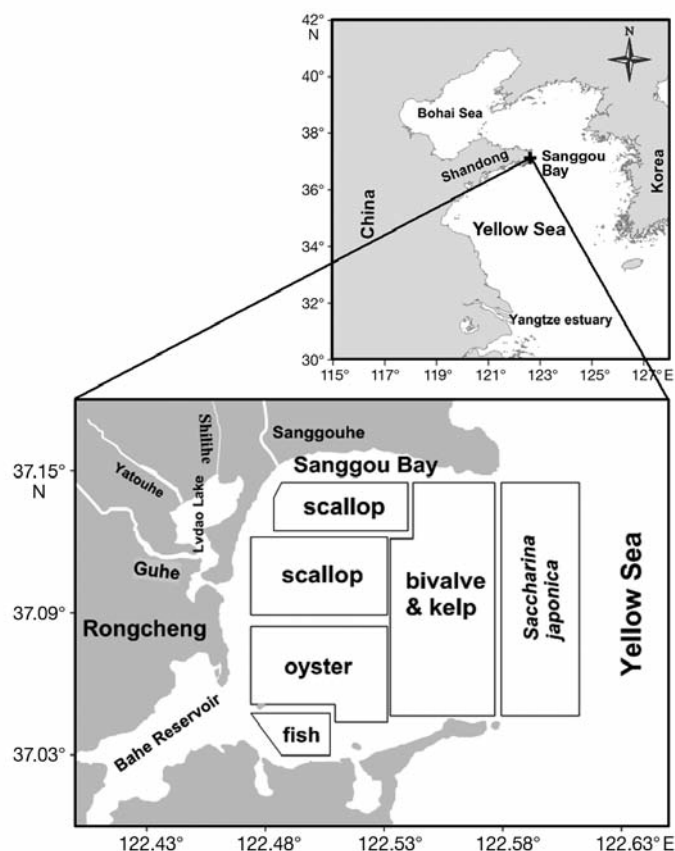


Fig. 1. Location of Sanggou Bay, China, and aquaculture activities, showing the regions of kelp (*Saccharina japonica*) monoculture; scallop, oyster, and fish monoculture; and multi-species aquaculture

2012 (early autumn), 22 to 25 April 2013 (spring), 21 to 25 July 2013 (summer), 16 to 17 October 2013 (autumn), and 15 to 17 January 2014 (winter) (Fig. 2). Two anchor stations for monitoring over complete tidal cycles of 25 h were established, one in April 2013 in the northern mouth of the bay (D1), and the other in October 2013 in the southern mouth (D2) (Fig. 2), respectively. At each station, surface water samples were collected by submersing a 1 l acid-cleaned polyethylene bottle from a boat, and bottom water samples were collected using a 5 l polymethyl methacrylate water sampler. River water samples were collected from the river edge in 0.5 l acid-cleaned polyethylene bottles, and groundwater was collected from wells around the bay (Fig. 2).

Water temperature and salinity were measured *in situ* using a WTW MultiLine F/Set3 multi-parameter

probe. Each water sample was immediately filtered through a 0.45 μm pore size cellulose acetate filters (pre-cleaned with hydrochloric acid, pH = 2) into a polyethylene bottle that had previously been rinsed 3 times with some of the filtered water sample. The filtrates were fixed by the addition of saturated HgCl_2 solution (Liu et al. 2005), and the filters were dried at 45°C and weighed to determine the mass of suspended particulate matter (SPM).

Chemical analysis

Dissolved nutrient concentrations were measured in the laboratory using an Auto Analyzer 3 (Seal Analytical). Total dissolved nitrogen (TDN) and total dissolved phosphorus (TDP) were measured according to the methods of Grasshoff et al. (1999). The DIN

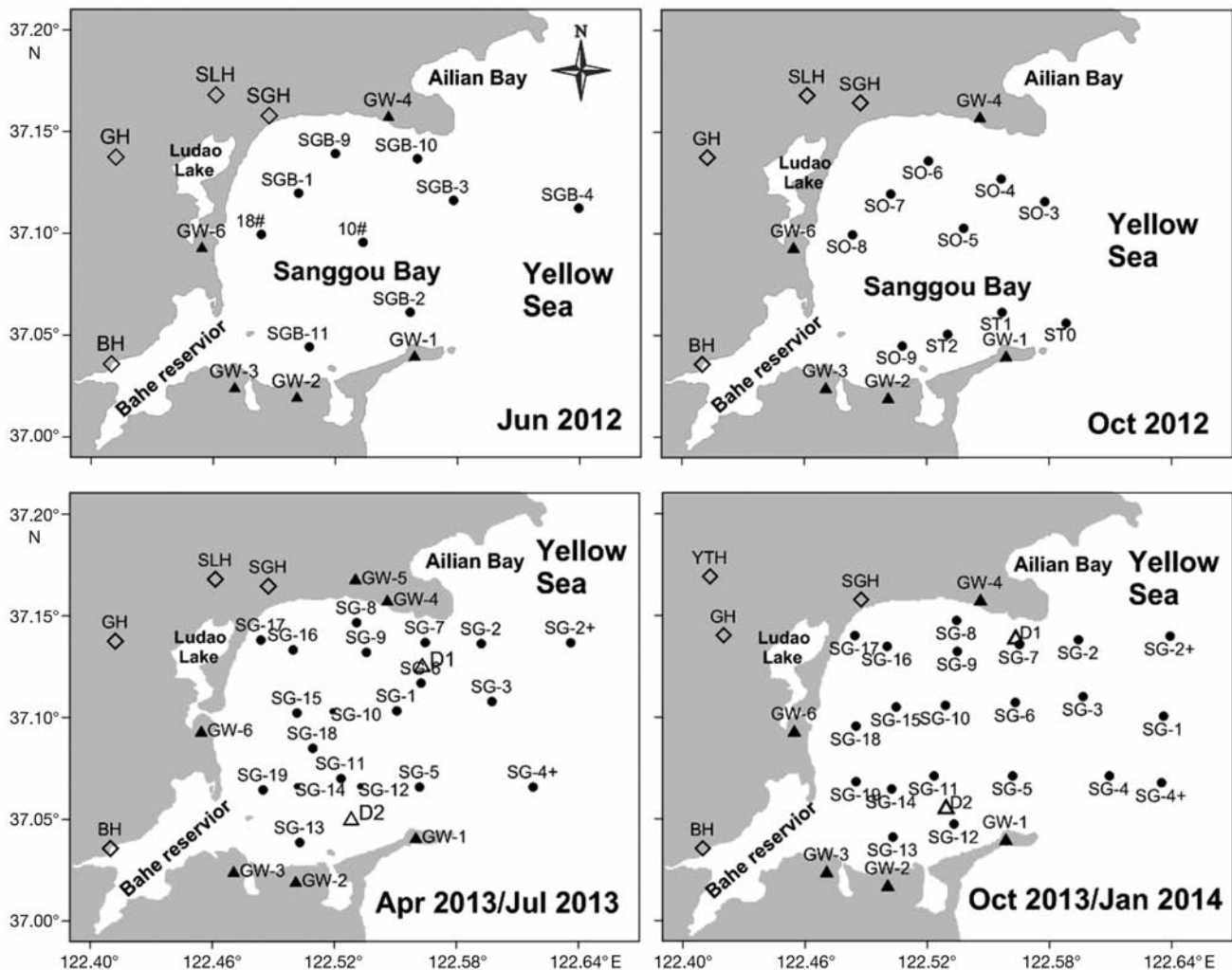


Fig. 2. Sampling stations in Sanggou Bay for the cruises during 2012 to 2014. (◇) River stations; (▲) groundwater stations (BH: Bahe; GH: Guhe; SLH: Shilihe; SGH: Sanggouhe; YTH: Yatouhe); (●) bay stations; (Δ) anchor stations

concentration was determined as the sum of the NO_3^- , NO_2^- , and NH_4^+ concentrations. The concentrations of dissolved organic nitrogen (DON) and dissolved organic phosphorus (DOP) were estimated by subtracting DIN from TDN and PO_4^{3-} from TDP, respectively. The analytical precision of NO_3^- , NO_2^- , NH_4^+ , PO_4^{3-} , dissolved silicate (DSi), TDN, and TDP was <5 %.

Statistical analysis

Statistical analyses were performed using the software SPSS 20.0 by IBM. One-way ANOVAs were used to analyze the individual effects of seasons and particular cultivation area on variations in SPM, and 2-way ANOVAs were used to analyze the combined effects of seasons and cultivation area on variations in SPM. Two-way ANOVAs were also used to analyze the effects of surface/bottom and seasons on variations in nutrient concentrations. Based on *a posteriori* homogeneity tests, Tukey's HSD or Tamhane's T2 comparisons were applied to assess the statistical significance of differences ($p < 0.05$) following ANOVA.

Nutrient budgets

Dissolved nutrient budgets for the study system were constructed based on the LOICZ box model (Gordon et al. 1996). This model has been widely used to construct nutrient budgets defining the internal biogeochemical processes and external nutrient inputs of estuarine and coastal ecosystems (Savchuk 2005, Liu et al. 2009). For our model, we assumed that the study system was in a steady state, and the bay was treated as a single well-mixed box. The water mass balance, salinity balance, and the non-conservative fluxes of nutrient elements based on nutrient concentrations and water budgets were estimated according to Eqs. (1) to (3), respectively:

$$V_R = V_{\text{in}} - V_{\text{out}} = -V_Q - V_P - V_G - V_W + V_E \quad (1)$$

$$V_X(S_1 - S_2) = S_R V_R \quad (2)$$

$$\Delta Y = \text{outflux} - \text{influx} = V_R C_R + V_X C_X - V_Q C_Q - V_P C_P - V_G C_G - V_W C_W \quad (3)$$

where V_R is the residual flow, and V_Q , V_P , V_G , V_W , V_E , V_{in} , V_{out} , V_X , and ΔY are the river discharge, precipitation, groundwater, wastewater, evaporation, inflow of water to the system of interest, outflow of water from the system of interest, the mixing flow between the 2 systems and nonconservative flux of nutrients, respectively. The volume of aquaculture effluent discharged directly into the system of interest was not considered, as the data were limited. We assumed that the salinity of fresh water (V_Q , V_P , and V_E) was 0. In Eq. (2), $S_R = (S_1 + S_2)/2$, where S_1 and S_2 are the average salinity of the system of interest and the adjacent system, respectively. The total water exchange time (τ) of the system of interest was estimated from the ratio of V_S to $(V_R + V_X)$, where V_S is the volume of the system. In Eq. (3), C_Q , C_P , C_G , C_W , C_R , and C_X are the average concentrations of nutrients in the river discharge, the precipitation, groundwater, wastewater, the residual flow, and the mixing flow, respectively. C_R and C_X equate to $(C_1 + C_2)/2$ and $(C_1 - C_2)$, respectively. C_1 and C_2 are the average concentrations of nutrients in the system of interest and the adjacent system, respectively. Outflux and influx are the total nutrient flux out of and into the system of interest, respectively. A negative or positive sign for ΔY indicates that the system of interest was a sink or a source, respectively.

RESULTS

Hydrographical characteristics

The surface water temperature (Table 1) reflected the seasonality of this temperate system. The surface water temperature decreased from the mouth to the

Table 1. Seasonal variations in temperature, salinity, and suspended particulate matter (SPM) in Sanggou Bay, China, during the study. Mean values are given in parentheses

Season	Temperature (°C)		Salinity		SPM (mg l ⁻¹)	
	Surface	Bottom	Surface	Bottom	Surface	Bottom
Spring	6.00–9.60 (7.60)	6.10–9.90 (7.80)	30.2–31.3 (30.8)	30.1–31.4 (30.7)	3.91–31.9 (13.6)	3.59–40.5 (14.9)
Summer	13.3–25.9 (20.0)	13.5–20.6 (17.0)	28.2–30.8 (30.0)	30.2–30.7 (30.4)	3.78–26.4 (13.9)	5.61–92.0 (37.6)
Autumn	17.7–25.0 (20.1)	16.6–23.3 (19.3)	29.1–30.0 (29.6)	29.3–29.9 (29.5)	5.75–29.3 (15.5)	11.9–67.8 (27.4)
Winter	1.80–5.70 (3.50)	0.90–5.30 (3.15)	29.2–30.6 (30.0)	29.2–30.4 (29.9)	2.27–54.0 (15.8)	3.04–54.7 (13.5)

west of the bay in spring and summer, but increased in this direction in autumn and winter. The horizontal distribution of temperature in the near-bottom layer was similar to that in surface water, but the temperatures were generally lower. The salinity of both surface and bottom water gradually increased from the west of the bay to mouth, except in winter. The salinity was lowest in autumn (Table 1).

The SPM concentrations varied considerably among seasons and cultivation areas, as evidenced by the large ranges shown in Table 1 and Fig. 3. The average concentration of SPM showed minor differences between surface and bottom waters in spring and winter, but was significantly less in surface water than in the bottom layer in both summer and autumn between different cultivation areas, especially those involving oyster and scallop monoculture (Fig. 3). A 1-way ANOVA indicated very significant differences in SPM concentration in bottom water of the bay in different seasons ($p < 0.05$). The subsequent post hoc Tamhane's T2 test showed that the concentrations of SPM in bottom water in summer and autumn differed significantly from those in spring and winter. In addition, a 1-way ANOVA indicated highly significant differences between different cultivation areas ($p <$

0.05). The subsequent post hoc Tamhane's T2 test showed that the values of SPM in both bottom and surface waters in the fish, oyster, and scallop cultivation areas differed significantly from those in the kelp, offshore, and bivalve and kelp areas.

Nutrients in rivers

Nutrient concentrations in rivers adjacent to SGB varied greatly during the study period (Table 2). The rivers were generally enriched with DIN relative to PO_4^{3-} (Table 2). The DIN was dominated by NO_3^- , which accounted for 73 to 98% of DIN among all seasons. The NO_2^- concentrations in rivers were generally $>2 \mu\text{M}$ except Bahe river ($0.14\text{--}1.13 \mu\text{M}$; Table 2). The PO_4^{3-} concentration ranged from 0.08 to $6.02 \mu\text{M}$ in the rivers, with an annual average of $1.45 \mu\text{M}$. Seasonal variation of PO_4^{3-} in the Bahe river was similar to that in the Guhe river, and the PO_4^{3-} concentrations in the Bahe and Guhe rivers were lower than in the Shilihe and Sanggouhe rivers (Table 2). The DSi concentrations were high in our study rivers (average $182 \mu\text{M}$; Table 2), indicating a high weathering rate associated with rivers adjacent

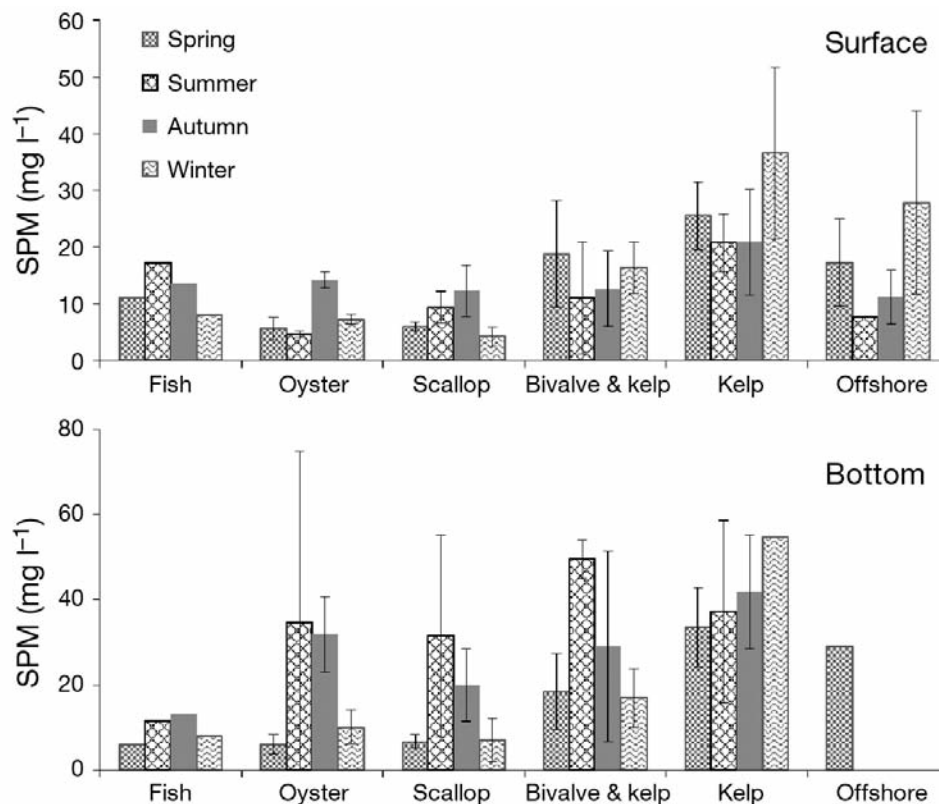


Fig. 3. Suspended particulate matter (SPM) concentrations (mg l^{-1} ; mean \pm SD) in various cultivation areas in different seasons during the study periods

Table 2. Nutrient concentrations (μM) and molar ratios in surface water in rivers adjacent to Sanggou Bay, China, in different seasons during the study. DSi: dissolved silicate. Dates are given as year-month

River	NH_4^+	NO_2^-	NO_3^-	PO_4^{3-}	DSi	N:P	Si:N
Bahe							
2012-06	2.53	0.15	0.48	0.17	29.0	18	9.0
2012-09	0.65	0.04	0.25	0.17	164	5.5	176
2013-04	2.91	0.32	28.9	2.23	47.9	14	0.4
2013-07	0.65	1.13	88.6	0.32	90.4	21	1.0
2013-10	1.41	0.15	10.5	0.56	246	21	20
2014-01	1.68	0.12	18.5	1.78	142	11	7.0
Guhe							
2012-06	36.3	17.5	309	0.19	72.3	1905	0.2
2012-09	9.86	10.4	530	0.08	102	7157	0.2
2013-04	22.5	5.18	288	1.80	55.6	175	0.2
2013-07	2.56	7.60	590	0.16	208	122	0.3
2013-10	12.6	6.40	240	–	143	–	0.6
2014-01	5.71	3.05	455	0.50	130	927	0.3
Shilihe							
2012-06	103	4.38	283	3.23	364	121	0.9
2012-09	17.8	6.70	600	0.22	282	2821	0.5
2013-04	93.0	17.0	503	2.89	243	212	0.4
2013-07	30.3	10.2	199	3.60	199	63	0.3
Sanggouhe							
2012-06	15.4	2.26	169	0.12	172	1505	0.9
2012-09	4.00	17.5	508	2.60	182	204	0.3
2013-04	8.23	10.2	351	1.44	166	256	0.5
2013-07	25.0	16.6	382	6.02	382	106	0.4
2013-10	2.73	4.40	362	–	318	–	0.9
2014-01	7.25	5.65	569	2.00	236	291	0.4
Yatouhe							
2013-10	4.68	3.20	420	–	189	–	–
2014-01	6.50	4.36	687	0.36	211	–	–

to the SGB. Except for Bahe river, the $\text{DIN}:\text{PO}_4^{3-}$ molar ratios in the rivers were significantly higher than the Redfield ratio (Table 2), indicating that phytoplankton might be limited by phosphorus despite high NO_3^- values, especially in summer in the Bahe and Guhe rivers. The high concentrations of DIN led to $\text{DSi}:\text{DIN}$ ratios that were less than or approached a value of 1.

Spatial and temporal variations of nutrients in SGB

The concentrations of dissolved inorganic nutrients decreased gradually from offshore to the inner part of SGB in spring (April 2013; Fig. 4a), while the DON and DOP concentrations showed the opposite horizontal distribution (Fig. 4a). The concentrations of NO_3^- accounted for 53–92% and 56–89% of the DIN in surface and near-bottom layers, respectively. DON contributed 27–46% of TDN in surface water outside the bay, where kelp monoculture occurs, and ac-

counted for 46–87% of TDN inside of the bay. DON represented 40–84% of TDN in the near-bottom layer. For phosphorus compounds, PO_4^{3-} and DOP accounted for approximately 66 and 34% of TDP in the bay, respectively. The molar ratios of $\text{DIN}:\text{PO}_4^{3-}$ ranged from 7.8 to 31 (average 19 ± 7.9 SD) in surface water, and from 9.4 to 69 in the near-bottom layer, respectively. The average $\text{DSi}:\text{DIN}$ ratio was higher than the Redfield ratio in both surface (1.3 ± 0.8) and bottom (1.2 ± 0.6) waters. Studies of nutrient uptake kinetics have shown that the threshold values for phytoplankton growth are $1.0 \mu\text{M}$ DIN and $0.1 \mu\text{M}$ PO_4^{3-} (Justi et al. 1995). In the western part of the bay, DIP concentrations were lower than the threshold values for phytoplankton growth (Fig. 4a). This suggests that phosphorus may be the most limiting element for phytoplankton growth in the following season.

During June 2012 (Fig. 4b), the levels of dissolved inorganic nutrients were lower than those in spring (Fig. 4a). The NO_3^- , NO_2^- , and NH_4^+ concentrations decreased gradually from offshore to the inner part of the bay, while PO_4^{3-} and DSi concentrations showed the opposite horizontal distribution. With respect to nitrogen compounds, NO_3^- comprised 24–78% of DIN in surface water and 34–72% in bottom water. Surface water was depleted in PO_4^{3-} ($0.03\text{--}0.17 \mu\text{M}$), which led to the $\text{DIN}:\text{PO}_4^{3-}$ ratios being significantly higher than the Redfield ratio. The $\text{DIN}:\text{DSi}$ molar ratios ranged from 0.4 to 3.2 (average 1.6 ± 0.7). In July 2013, nutrient concentrations increased significantly from the mouth of the bay to the inner part (Fig. 4c), and were higher in the near-bottom layer than in surface water. The DIN was dominated by NH_4^+ , which contributed 32–89% (mean 62%) and 32–69% (mean 52%) to DIN in surface water and the near-bottom layer, respectively. DON comprised 57–88% of the TDN in the entire bay, and DOP accounted for 34–75% and 46–81% of the TDP in surface water and the near-bottom layer, respectively. The molar ratios of $\text{DIN}:\text{PO}_4^{3-}$ were higher than the Redfield ratio in surface water, and the $\text{DSi}:\text{DIN}$ ratios were higher than or comparable to the Redfield ratio. The PO_4^{3-} concentrations in surface water at 70% of the stations in June 2012 (Fig. 4b), and in the south-eastern part of the bay in July 2013 (Fig. 4c), were lower than the threshold values. This suggested that phytoplankton growth might be limited by P in summer. In the western part of the bay (the main area for bivalve culture) the DIN concentrations were lower than or comparable to the threshold values, suggesting that N might be potentially limiting for phytoplankton growth in this part of the bay.

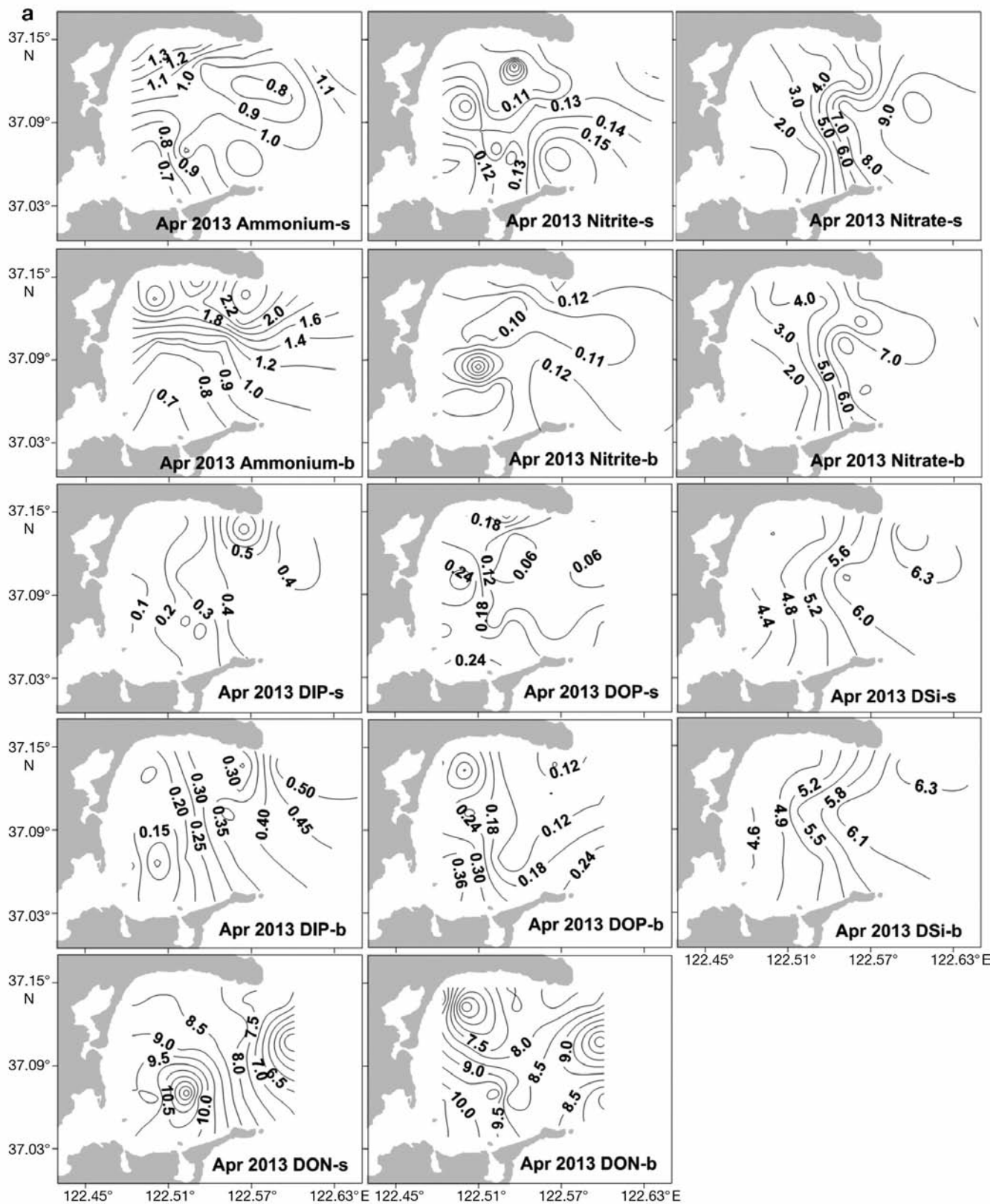


Fig. 4. Horizontal distributions of nutrients (μM) in Sanggou Bay: (a) April 2013; (b) June 2012; (c) July 2013; (d) October 2012; (e) October 2013; (f) January 2014. DIP (DOP): dissolved inorganic (organic) phosphorus, DSi: dissolved silicate, DON: dissolved organic nitrogen. s: surface; b: bottom

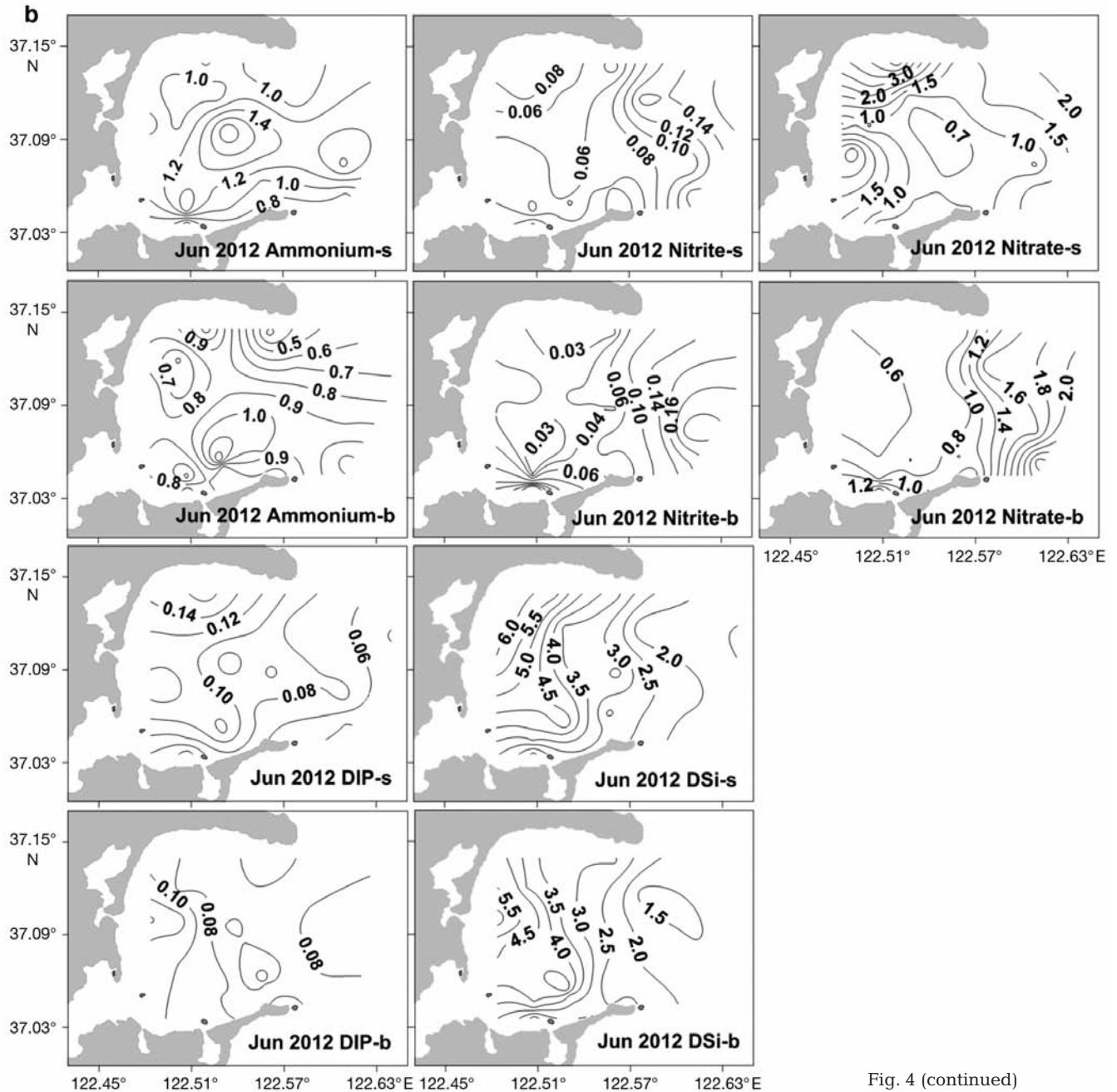


Fig. 4 (continued)

During the September–October 2012 study period, NO_3^- and NH_4^+ concentrations decreased from south to north in the bay; NO_2^- , DSi, and DOP increased gradually from west to east, and the PO_4^{3-} concentration increased from northeast to southwest (Fig. 4d). Throughout the entire bay, NO_3^- comprised 52–86% of DIN, and NH_4^+ comprised 6–38%. In October 2013, the NO_3^- , NO_2^- , DON, DIP, and DSi concentrations decreased from the mouth to the southwestern part of the bay (Fig. 4e). Throughout the entire bay, NO_3^- accounted for 55–84% of DIN. DON comprised

27–48% of TDN inside the bay, and 51–61% in the kelp monoculture area. DOP contributed to 12–36% and 16–50% of TDP in surface water and the bottom layer, respectively. In autumn in both 2012 and 2013, the average DIN: PO_4^{3-} ratios were higher than the Redfield ratio, while the DSi:DIN ratios in the water column were comparable to the Redfield ratio.

In winter, the horizontal distribution of nutrients was similar to that in spring (except for the NO_2^- and NH_4^+ concentrations), with higher concentrations in the near-bottom layer than in surface water (Fig. 4f).

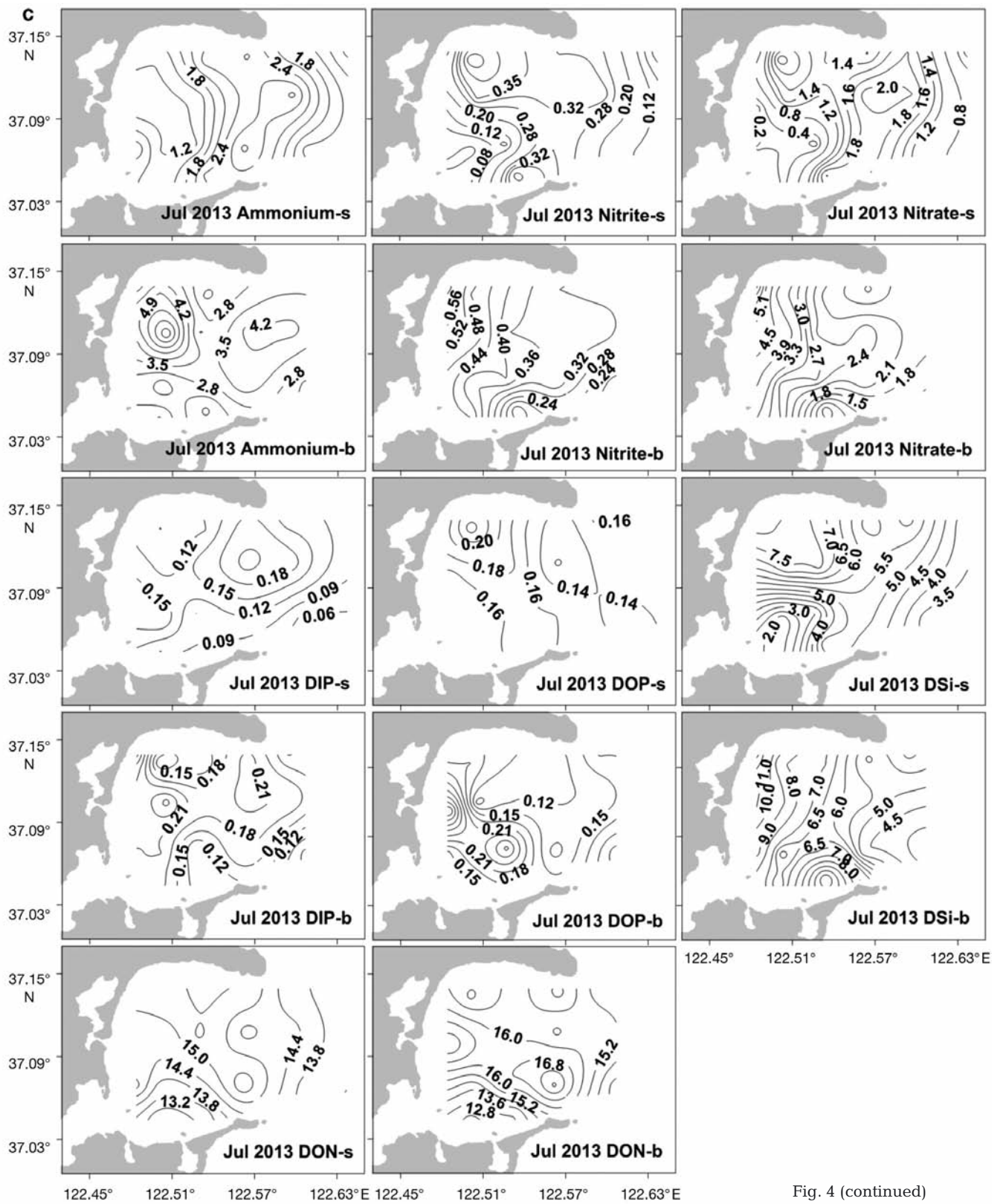


Fig. 4 (continued)

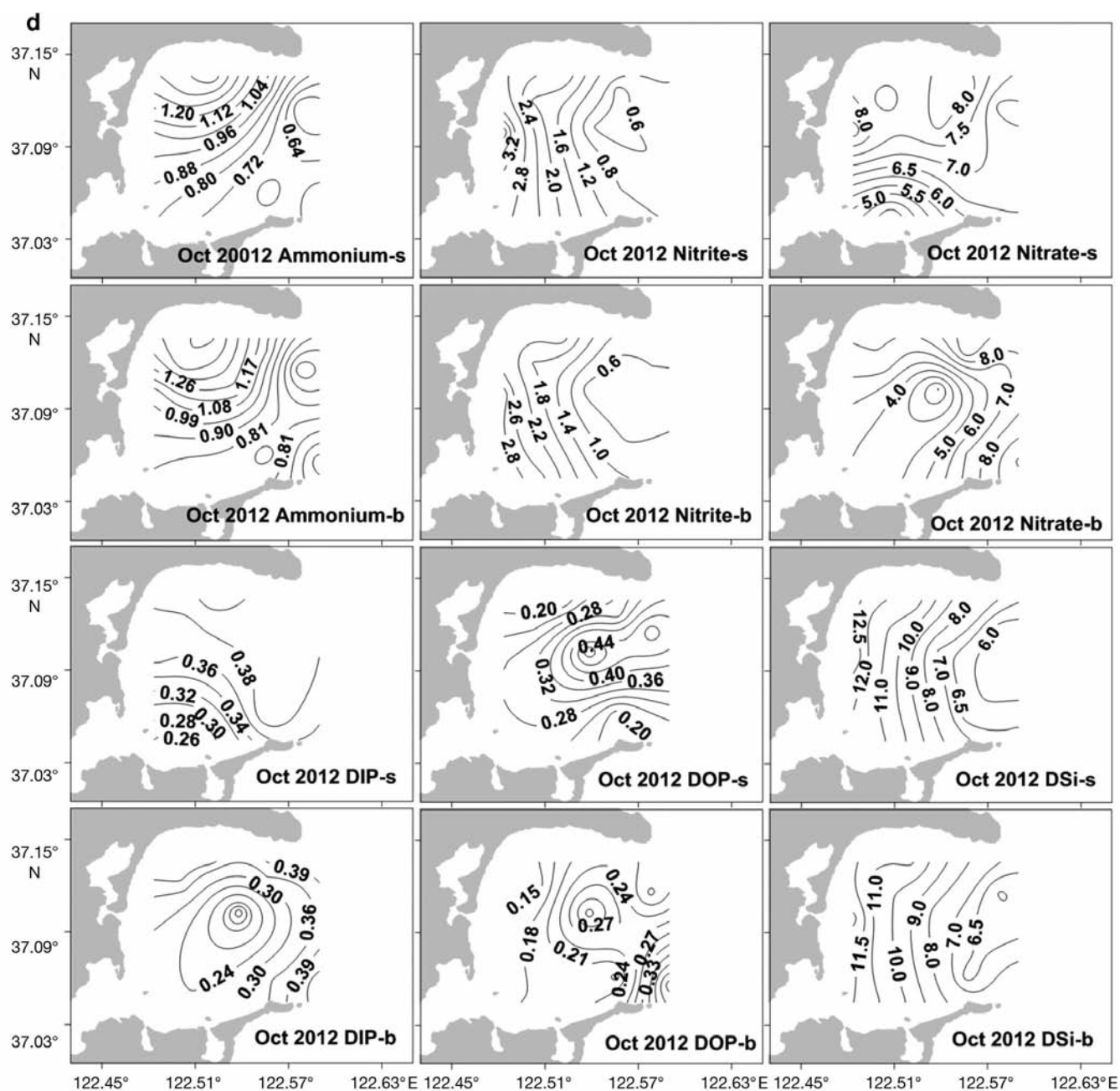


Fig. 4 (continued)

In the entire bay, NO_3^- accounted for 66–92% of DIN. DON was the dominant species of TDN, which represented 53–81% of TDN in the water column, and DOP represented 35–67% of TDP. The molar ratios of $\text{DIN}:\text{PO}_4^{3-}$ ranged from 20 to 62 and 17 to 46 in surface and bottom waters, respectively. The average $\text{DSi}:\text{DIN}$ ratio in surface and bottom waters was comparable and significantly lower than the Redfield ratio. The results suggest that phosphorus may be a limiting element for phytoplankton growth in winter.

Seasonality in nutrient concentrations was evident in SGB (Figs. 4 & 5). At all sites, the NO_3^- , PO_4^{3-} , and DSi concentrations were significantly higher in autumn than in the other seasons. The average NO_3^- concentrations in surface ($9.44 \pm 4.00 \mu\text{M}$) and bottom ($9.72 \pm 4.48 \mu\text{M}$) waters in autumn exceeded those in summer by factors of 7.4 and 5.3, respectively. DIN was dominated by NO_3^- , except in summer. The DON concentrations in winter ($16.0 \pm 1.67 \mu\text{M}$) were comparable to those in summer, and were signifi-

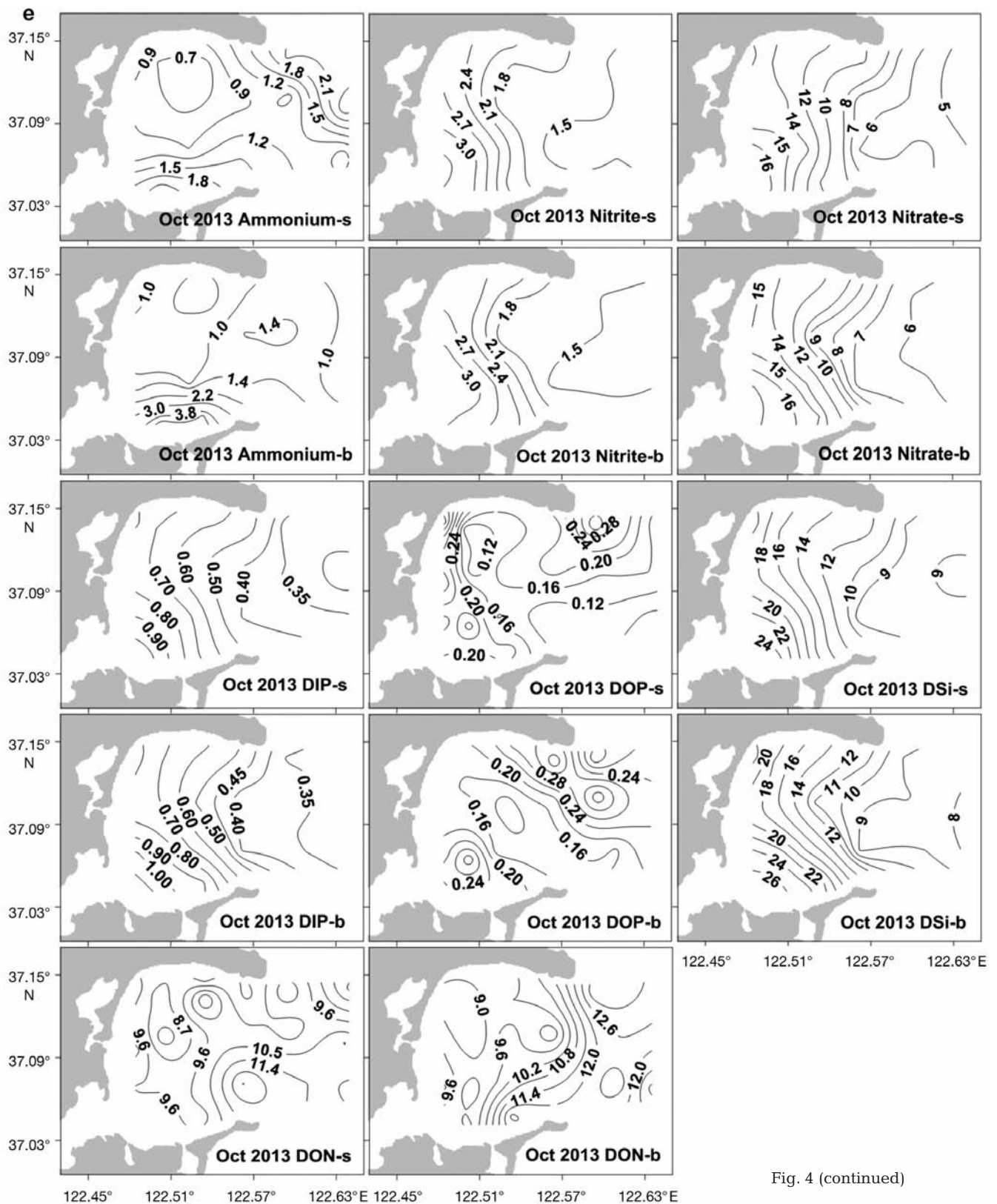


Fig. 4 (continued)

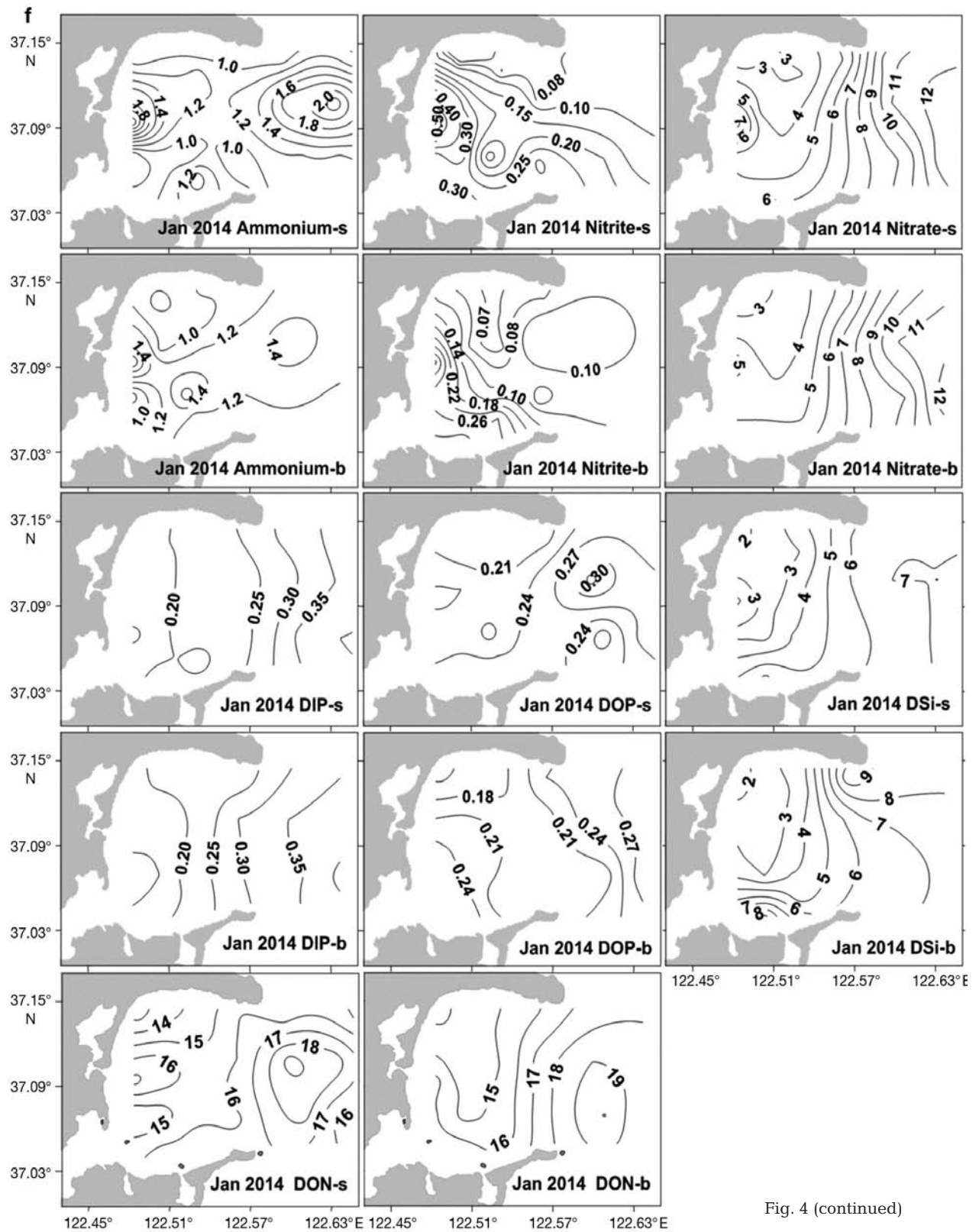


Fig. 4 (continued)

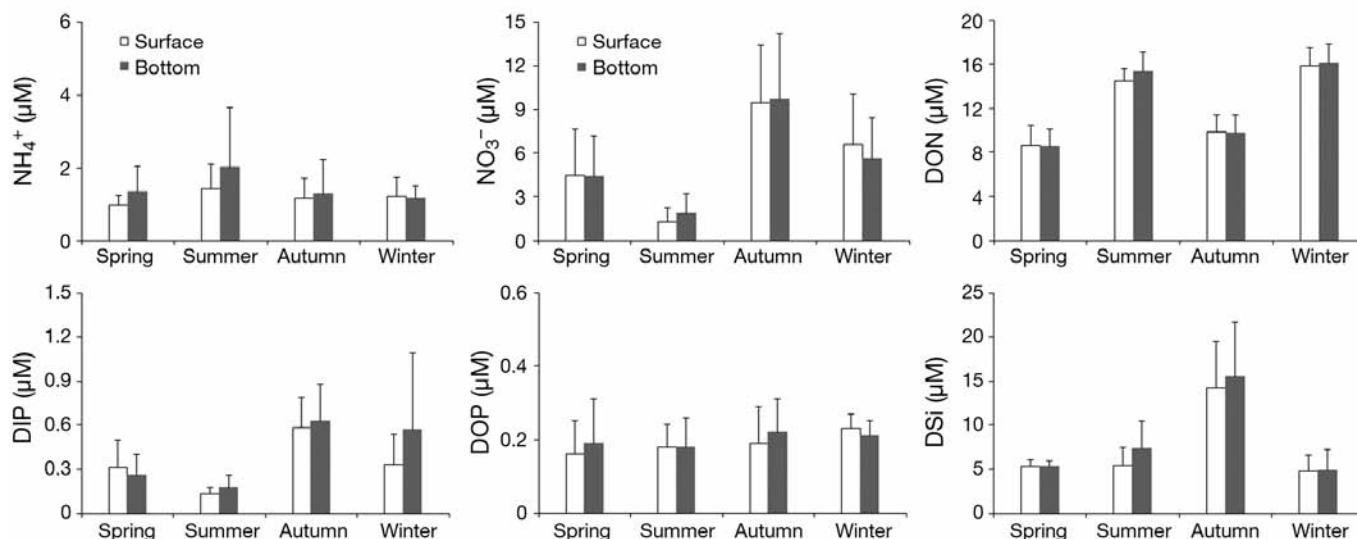


Fig. 5. Seasonal variations in nutrient concentrations (μM) in Sanggou Bay during the study period. DON: dissolved organic nitrogen, DIP (DOP): dissolved inorganic (organic) phosphorus, DSi: dissolved silicate

cantly higher than the concentrations in spring and autumn (Fig. 4). TDN was dominated by DON (59–82%), except in autumn (approximately 40%). Two-way ANOVA indicated highly significant differences in nutrient concentrations among seasons and layers ($p < 0.01$). The subsequent post hoc Tukey's HSD test showed that the nutrient concentrations in autumn differed significantly from those in other seasons ($p < 0.01$). Two-way ANOVA also indicated highly significant differences in nutrient concentrations among seasons and cultivation areas (Fig. 6; $p < 0.01$), suggesting that aquaculture activities significantly affect the nutrient composition in SGB.

Nutrients at the anchor stations

In April 2013, all nutrients changed during the tidal cycle at Stn D1 (Fig. 7a). The maximum concentrations usually occurred during high tide, indicating the outer bay as a nutrient source. The vertical profiles for concentrations of all dissolved inorganic nutrients at Stn D1 showed that the water column was well mixed (Fig. 7a). High concentrations of DON (9.01–13.8 μM) were found throughout the water column, and comprised up to 50% of TDN. The DIN:PO₄³⁻ ratio ranged from 23 to 74 in surface water and from 30 to 132 in near-bottom water, and the DSi:DIN ratio ranged from 0.5 to 0.8 in surface water and from 0.4 to 0.9 in near-bottom water. At Stn D2, the nutrient concentrations were higher in near-bottom waters than in surface water, the exception being NH₄⁺ and DOP (Fig. 7a). The DON (8.26–

10.5 μM) comprised 66–87% of TDN. The concentrations of DOP (0.08–0.35 μM) represented 25–73% of TDP, and indicated a well-mixed profile. The DIN:PO₄³⁻ ratio increased from 8.0–20 in surface water to 11–37 in near-bottom water, while the DSi:DIN ratio decreased from 1.6–3.2 in surface water to 1.0–1.5 in near-bottom water. The nutrient concentrations at Stn D1 were higher than at D2.

Analysis of the concentrations of all nutrients during 18–19 October 2013 showed that the water column at Stn D1 was well mixed (Fig. 7b). No parameter showed significant differences between day and night, indicating that tidal mixing was the main factor affecting concentration changes. The concentrations of DON were 5.38–10.5 μM, which comprised 26–83% of TDN. The DOP concentrations were 0.05–0.34 μM, which represented 8–39% of TDP. The DIN:PO₄³⁻ ratio was 23–36 (average 27) in surface water, and 22–51 (average 28) in bottom water. The DSi:DIN ratio was 0.7–1.0 (average 0.9) in surface water and 0.5–1.0 (average 0.8) in bottom water. At Stn D2, the concentrations of all nutrients in surface water showed a general decrease with increasing tide height. The DIN:PO₄³⁻ and DSi:DIN ratios in surface water ranged from 22 to 32 and 0.8 to 1.0, respectively. The nutrient concentrations at Stn D1 were lower than at D2.

Water and nutrient budgets in SGB

Domestic wastewater is discharged directly into rivers adjacent to SGB, and so in developing a water

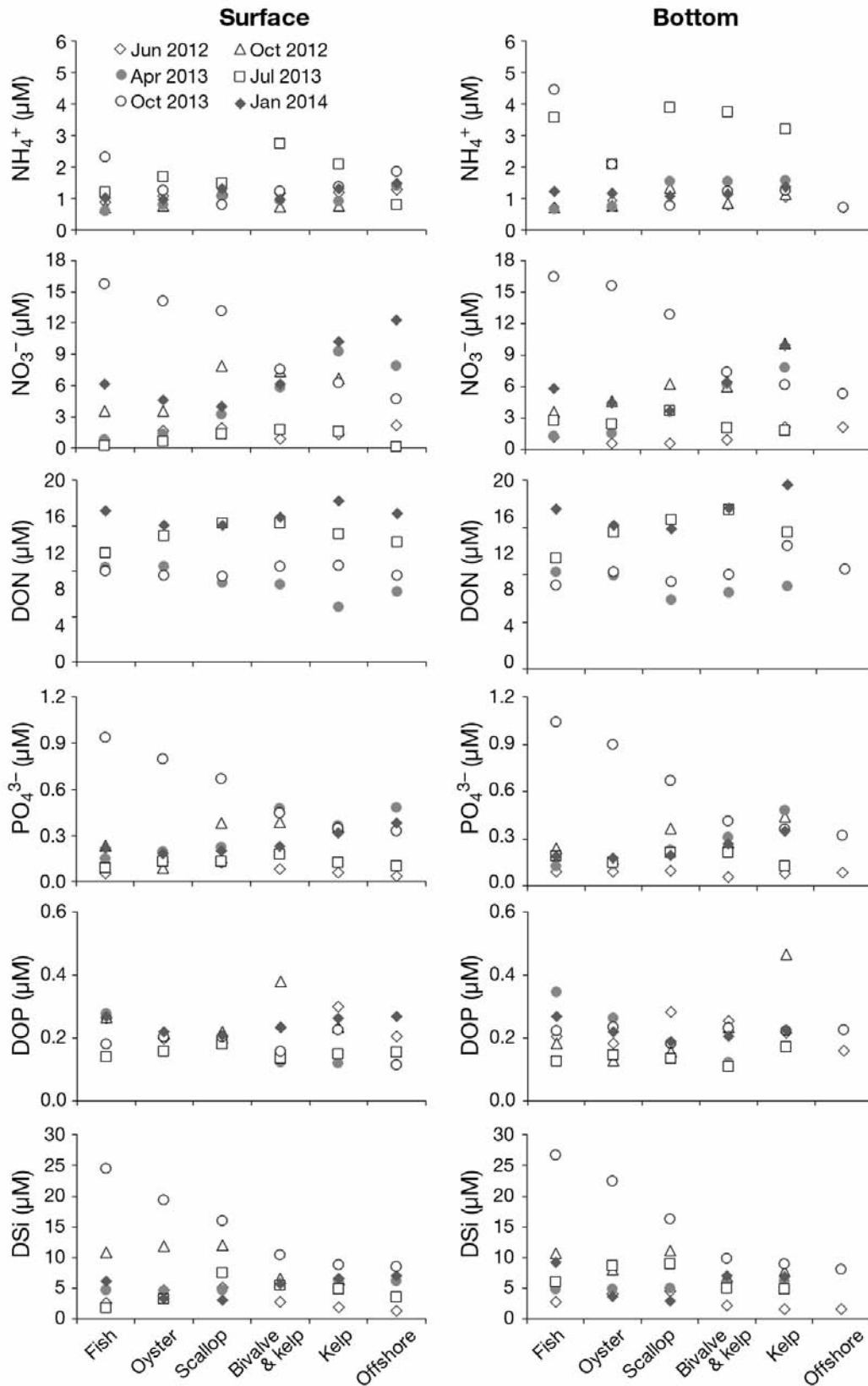


Fig. 6. Nutrient cycles, averaged for various aquaculture regions in Sanggou Bay Left: nutrients in surface water, right: nutrients in the near-bottom layer. DON: dissolved organic nitrogen, DOP: dissolved organic phosphorus, DSi: dissolved silicate

budget for the bay, sewage discharge was included in river discharges. The Guhe is the largest major river that directly empties into SGB. In developing the water budget (Fig. 8), we used the average discharge (V_Q) of the Guhe during 2011. The submarine groundwater discharge (SGD) was estimated based on submarine groundwater measurements made in June 2012. The groundwater discharge into SGB was calculated to be $(2.59\text{--}3.07) \times 10^7 \text{ m}^3 \text{ d}^{-1}$, based on the naturally occurring ^{228}Ra isotope (Wang et al. 2014). Generally, recirculated seawater accounts for 75 to 90 % of total SGD (Moore 1996). Based on Ra isotopes, Beck et al. (2008) reported that recirculated seawater could account for approximately 90 % of total SGD, and could increase as a consequence of precipitation (Guo et al. 2008). In our study, groundwater samples were collected during a summer in which substantial rainfall occurred. Based on the assumption that recirculated seawater could account for 90 % of total SGD in SGB, the SGD was estimated to be $(2.59\text{--}3.07) \times 10^6 \text{ m}^3 \text{ d}^{-1}$. As the volume (V_S) of SGB is $10.8 \times 10^8 \text{ m}^3$, the total water exchange time (τ) for SGB, estimated from the ratio $V_S/(V_R + V_X)$, was 22.4 d.

Scallop (*Chlamys farreri*) and oyster (*Crassostrea gigas*) are the main shellfish cultured in SGB. Aquaculture wastewater effluents are discharged directly into the bay. The minimum individual wet weight of oysters and scallops at harvest are 40 and 23 g (Nunes et al. 2003), respectively, and 60 000 t of oyster (wet weight) and 15 000 t of scallop are harvested annually from the bay (data from Rongcheng Fishery Technology Extension Station). Based on these data, we estimated that bivalve cultivation involved approximately 2.15×10^9 individuals during 2012. Based on excretion rates determined for bivalves and oysters in Sishili Bay (China) (Zhou et al. 2002a), the quantities of DIN and phosphate excreted by scallops were 3.84 and $0.21 \mu\text{mol h}^{-1} \text{ ind.}^{-1}$, respectively, and by oysters were 3.57 and $0.25 \mu\text{mol h}^{-1} \text{ ind.}^{-1}$, respectively. The bivalve growth

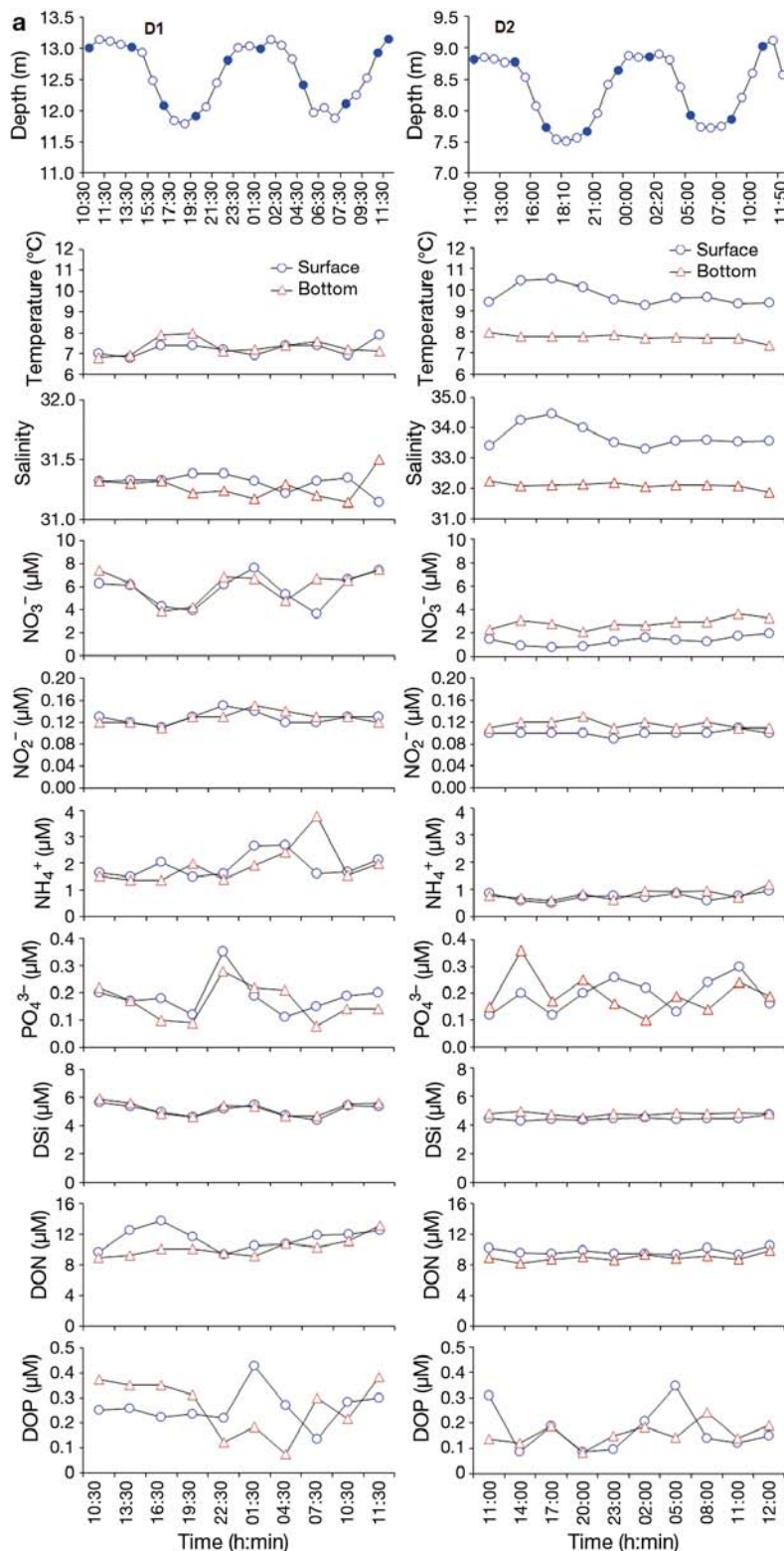


Fig. 7. Concentrations of nutrients (μM) at: (a) the anchor station in April 2013; (b; next page) the anchor station in October 2013. The water depth (m) in April 2013 and tide heights (cm) in October 2013 are provided, and the filled circles represent the nutrient sampling times. DSi: dissolved silicate, DON (DOP): dissolved organic nitrogen (phosphorus)

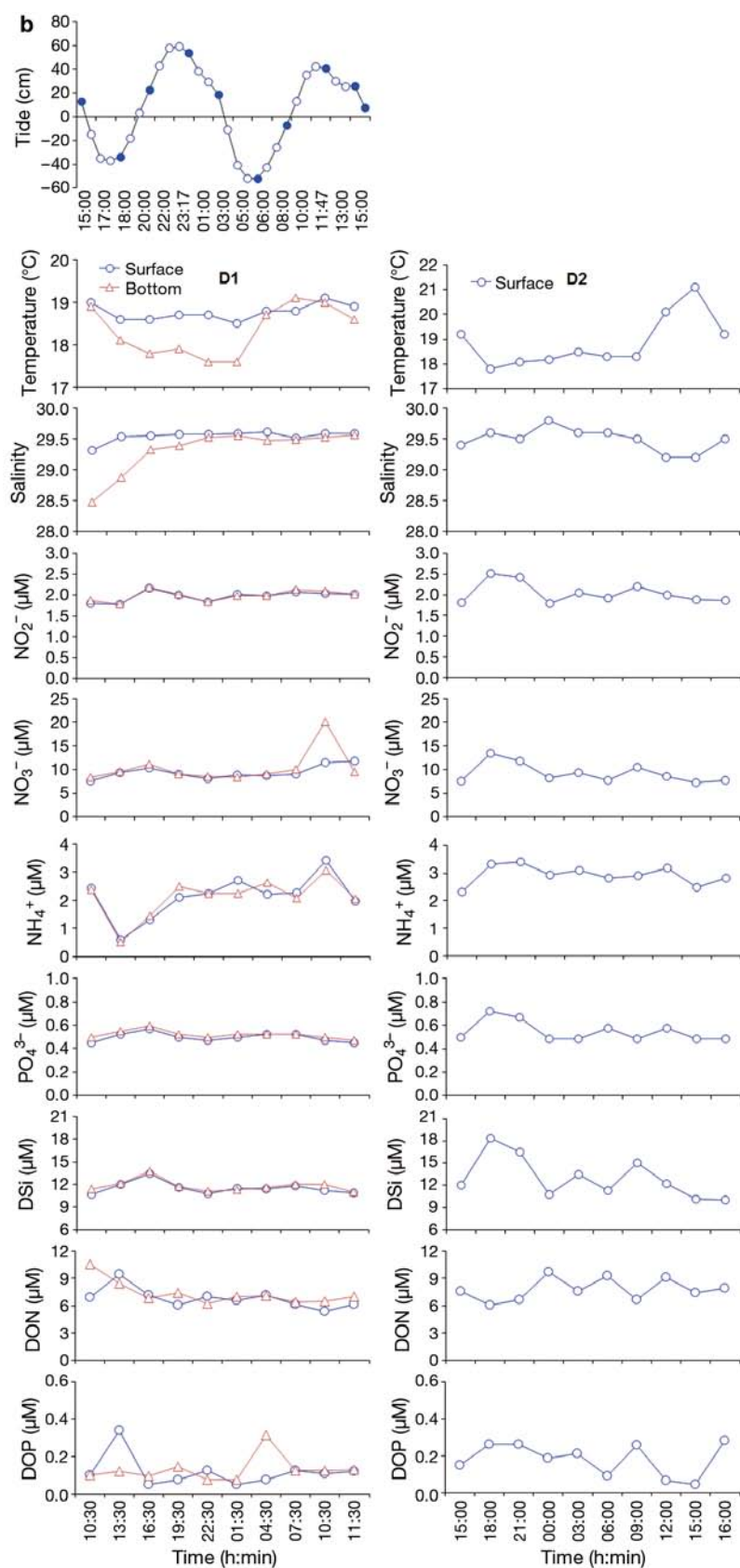


Fig. 7 (continued)

periods were mainly from May in one year to November in the following year (approximately 500 d). Hence, the total DIN and phosphate excreted by scallops and oysters in SGB amounted to 70.9×10^6 and $4.19 \times 10^6 \text{ mol yr}^{-1}$, respectively. Nutrients are removed from the bay as a consequence of bivalve harvest. The dry weight nitrogen content of the soft tissue and shell of *C. gigas* is 8.19 and 0.12 % (Zhou et al. 2002b), respectively, while the phosphorus content is 0.379 and 62.1×10^{-4} % (Zhou et al. 2002b), respectively. The dry weight nitrogen and phosphorus content of the soft tissue of *C. farreri* is 12.36 and 0.839 % (Zhou et al. 2002b), respectively, and in the shell is 0.09 and 62.1×10^{-4} %, respectively. Therefore, in total the harvest of *C. farreri* and *C. gigas* removes 304 t of nitrogen and 16.7 t of phosphorus from the bay.

Saccharina japonica and *Gracilaria lemaneiformis* are the main algae cultivated in SGB. The weight of individual kelp plants at seeding is 1.2 g, and the cultivation area and density are 3331 ha and 12 ind. m⁻², respectively (Nunes et al. 2003). The dry weight:wet weight ratio of kelp is 1:10 (Tang et al. 2013). Hence, the dry weight of kelp at seeding is 48 t, while 87 040 t of dried kelp are produced annually in the bay (data from Rongcheng Fishery Technology Extension Station). The dry weight nitrogen and phosphorus content of kelp is 1.63 and 0.38 % (Zhou et al. 2002b), respectively. Hence, 1419 t of nitrogen and 331 t of phosphorus are removed from the bay as a consequence of kelp harvest. Similarly, 25 410 t wet weight of *G. lemaneiformis* are produced annually in the bay (data from Rongcheng Fishery Technology Extension Station). Therefore, 41.4 t of nitrogen and 9.66 t of phosphorus are removed from the bay as a consequence of *G. lemaneiformis* harvesting.

The nutrient transport fluxes from rivers and groundwater into SGB were determined from surveys undertaken during the period 2012 to 2014. The nutrient concentrations in rainwater were based on measurements at Qianliyan Island, in the western Yellow Sea (Han et al. 2013). Benthic fluxes in SGB were based on surveys undertaken during the same period

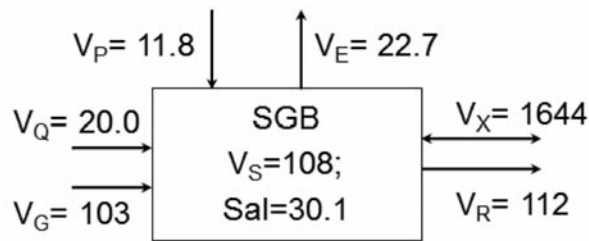


Fig. 8. Water and salt budgets for Sanggou Bay (SGB). Units: water volume, 10^7 m^3 ; water and salt fluxes, 10^7 m^3 and $10^7 \text{ psu m}^3 \text{ mo}^{-1}$, respectively. V_Q , V_P , V_E , V_G , V_S , V_R , and V_X are the mean flow rate of river water, precipitation, evaporation, groundwater, the volume of the system of interest, the residual flow, and the mixing flow between the system of interest and the adjacent system, respectively. For comparison, salinity of the adjacent system = 32.23

(Ning et al. 2016, this Theme Section). For the nutrient budget, estimates of DSi removed through kelp and bivalve harvesting were not included, as no data were available.

The nutrient budgets showed that SGB behaved as a source of PO_4^{3-} and as a sink of DSi and DIN (Table 3). The model results indicated that PO_4^{3-} was mainly derived from bivalve excretion, which accounted for 65% of total influx, while benthic flux contributed 16% of total influx. Bivalve excretion may be an important source of PO_4^{3-} when phytoplankton growth is phosphorus-limited in the bay. The DSi load in the bay was mainly from river input and benthic flux, which contributed 47 and 34% of total influx (Table 3), respectively. Groundwater was the major source of DIN entering SGB, accounting for

41% of total influx. In addition, bivalve excretion accounted for 19% of total DIN influx. DIN and PO_4^{3-} were mainly removed through kelp harvesting, which represented up to 64 and 81% of total outflux, respectively. The results show that aquaculture activities play an important role in nutrient cycling in SGB.

DISCUSSION

Nutrient transport in rivers

Nutrient levels in rivers varied widely (Table 2). The DIN concentrations in the rivers fell between those for polluted waters (110 μM) and severely polluted waters (350 μM) (Smith et al. 2003), except for the Bahe river. The DIN concentrations in the studied rivers were also higher than in most other small to medium-sized rivers in temperate China (Liu et al. 2009), and high relative to major Chinese rivers including the Yellow, Yangtze, and Pearl rivers (Liu et al. 2009). The extremely high DIN concentrations resulted in the high DIN: PO_4^{3-} ratios in these rivers.

The DIN loading to streams is directly related to the extent of agriculture in the catchment (Heggie & Savage 2009). The high NO_3^- concentrations, which dominated the DIN in rivers, is primarily attributable to anthropogenic nutrient sources, particularly to washout of fertilizers not used by target plants (Bellos et al. 2004). Rivers in the study area flow through villages and Rongcheng City, then discharge directly into SGB. Untreated industrial and domestic sewage is also discharged directly into rivers. The drainage

Table 3. Nutrient budgets for Sanggou Bay, China. $V_R C_R$: residual nutrient transport out of the system of interest (Eq. 1); $V_X C_X$: mixing exchange flux of nutrients (Eq. 2); influx (outflux): total nutrient flux into (out of) the system of interest. $\Delta (= \sum \text{outflux} - \sum \text{influx})$ is the non-conservative flux of nutrients. Negative and positive signs of Δ indicate that the system is a sink or a source, respectively. DIP (DIN): dissolved inorganic phosphorus (nitrogen), DSi: dissolved silicate (units: 10^6 mol)

	DIP	DSi	DIN	Reference
River input ($V_Q C_Q$)	0.29	22.4	83.2	Present study
Atmospheric deposition ($V_P C_P$)	0.41	0.87	14.6	Han et al. (2003)
Groundwater discharge ($V_G C_G$)	0.55	8.27	155	Wang et al. (2014)
Benthic fluxes	1.05	16.3	57.8	Ning et al. (2016)
Bivalve excretion	4.19		70.9	Zhou et al. (2002a,b)
Influx	6.49	47.8	382	
Kelp harvest	-10.7		-101	Zhou et al. (2002a,b)
<i>Gracilaria lemaneiformis</i> harvest	-0.32		-2.96	Zhou et al. (2002a,b)
Bivalve harvest	-1.19		-21.7	Zhou et al. (2002a,b), Zhang et al. (2013)
Residual flow ($V_R C_R$)	-0.38	-8.26	-7.31	Present study
Mixing exchange ($V_X C_X$)	-0.65	-16.1	-26.2	Present study
Outflux	13.2	24.4	159	
$\Delta Y (= \sum \text{outflux} - \sum \text{influx})$	6.71	-23.4	223	

areas of the Yatouhe, Sanggouhe, and Shilihe rivers are small ($<30 \text{ km}^2$) and are therefore readily affected by human activities. We conclude that the high NO_3^- concentrations in rivers are derived from agriculture, urban, and industrial wastewater in their drainage basins, as well as surface runoff from Rongcheng City.

The concentrations of PO_4^{3-} in the Bahe and Guhe rivers were between those for pristine ($0.5 \text{ }\mu\text{M}$) and clean ($1.4 \text{ }\mu\text{M}$) water, and apparently lower than in the Shilihe and Sanggouhe rivers (Table 2). The high PO_4^{3-} concentration (up to $6.02 \text{ }\mu\text{M}$) in the Sanggouhe, and industrial and domestic sewage, might be the most important sources of PO_4^{3-} to water bodies. DSi is little affected by human activities (Jennerjahn et al. 2009) and mainly originates from natural sources. The high DSi levels in rivers adjacent to SGB may be related to the underlying rock types and weathering rates.

Rain events can result in nutrient inputs derived from hinterland areas. Approximately 73.3% of annual precipitation occurs during summer (June to September), and the annual rainfall in Rongcheng City is 819.6 mm. River discharges can be enhanced by rainfall, and weathering rates are affected by precipitation and temperature (Liu et al. 2011), which can lead to higher nutrient values during the wet seasons. High nutrient concentrations (especially dissolved silicate) but low salinities were found in the bay (Fig. 4), suggesting that rainfall might be an important factor affecting nutrient supply to SGB in summer.

Nutrient fluxes from the bay to the Yellow Sea

In this study, nutrient budgets were developed to provide an overview of nutrient cycles under the impact of aquaculture activities. Despite some uncertainties, the nutrient budgets indicated that large quantities of nitrogen and silicate would probably be buried in the sediment or transformed into other forms in the bay (Table 3). Seaweeds can absorb large amounts of nutrients from the water column, resulting in the removal of these nutrients from the system when the plants are harvested (Schneider et al. 2005). The budgets indicated that a large proportion of DIN and DIP were removed during seaweed and bivalve harvesting (Table 3), demonstrating that aquaculture activities are a significant sink for nutrients in the bay.

Based on the budgets, nutrient fluxes from SGB to the Yellow Sea were estimated as the sum of the

net residual flux ($V_R C_R$) and mixing flux ($V_X C_X$) (Table 3). With the exception of DIN, nutrient fluxes to the Yellow Sea were 1.1 to 3.6 times the riverine input ($F_{\text{model}} = VC_Q$), indicating that nutrient cycling in the bay (including regeneration, aquaculture effluents) may magnify the riverine fluxes, especially bivalve excretion, which contributed to 65% of the total DIP influx. Additionally, the molar ratios of $\text{DIN}:\text{PO}_4^{3-}$ and $\text{DSi}:\text{DIN}$ were approximately 49 and 0.2 in all external nutrient inputs to the studied system, respectively, while the corresponding flux ratios in the output waters to the Yellow Sea were approximately 35 and 0.7. These ratios deviated significantly from the Redfield ratio, indicating that aquaculture activities have significantly influenced nutrient cycling in the bay.

Wang et al. (2014) estimated that approximately $4.76 \times 10^7 \text{ mol mo}^{-1}$ of DIN and $5.58 \times 10^6 \text{ mol mo}^{-1}$ of PO_4^{3-} are input from fertilizer and feed, based on protein data of shellfish and kelp in the bay during summer being used to construct a mass balance. Based on their data, fertilizer and feed would be the major source of nutrients in the bay. By visiting local farming households, we confirmed that fertilizers were used; however, fertilizer and feed are only used in fish farming during summer in SGB, thus the amounts might be far below the estimated values. If fertilizer and feed for fish farming were taken into account, the uncertainty might rise. Hence, nutrient input from feed was ignored in the box model. Furthermore, aquaculture effluents were not taken into account. Consequently, more studies on nutrient cycling in relation to aquaculture activities in SGB are needed to improve our understanding of the nutrient sink or source function of the bay.

Effects of aquaculture activities on nutrient biogeochemical cycles

The nutrient concentrations varied significantly among seasons in SGB. The dissolved inorganic nutrient levels in SGB in summer were quite low compared with other seasons; they increased from summer to autumn and reached the highest values in October (Figs. 4 & 5), indicating a shift from consumption to autumn accumulation. These seasonal variations corresponded with aquaculture activities in the bay, and this was confirmed by statistical analysis. Zhang et al. (2012) reported that nutrient biogeochemical processes and cycles were significantly affected by intensive kelp and bivalve aquaculture activities in SGB. Shi et al. (2011a) also reported that

Saccharina japonica assimilates substantial nutrients in spring. During the growth period of kelp from November to May, the NO_3^- and PO_4^{3-} concentrations decreased rapidly because of assimilation by kelp (Fig. 6). Nitrogen removed through kelp harvesting accounted for 64 % of total outflux (Table 3). Kelp was a net sink for nutrients during winter and spring, and competed with phytoplankton for nutrient utilization during kelp seeding; as a consequence, phytoplankton growth was restrained. Following the kelp harvest in late May, phytoplankton could grow fast because of adequate solar radiation and temperature. As a result, the dissolved inorganic nutrient concentrations continued to decrease (Figs. 4–6).

Shellfish aquaculture generally commences in May, during the period when kelp is harvested. Bivalves in turn become another source of nutrients through excretion. During early summer, the bivalves are in the early growth stage, and produce only low levels of nutrients. The dissolved nutrients released through bivalve excretion have the potential to stimulate phytoplankton production at local scales and promote the risk of harmful algal blooms (Pietros & Rice 2003, Buschmann et al. 2008). The highest concentrations of chlorophyll *a* have been reported in summer (Hao et al. 2012). The dissolved nutrients in aquaculture effluents, coupled with high solar radiation, result in high phytoplankton production in summer (Shpigel 2005). At this time, *Gracilaria lemaneiformis* replaces kelp, and is cultivated from June to October in SGB; because it can use available nitrogen efficiently (Buschmann et al. 2008), it absorbs nutrients from seawater and probably reduces the nutrient levels in summer. This probably leads to the nutrient levels dropping rapidly to the lowest level in summer (Fig. 6).

In September, the bivalves are in active growth stages and generate large quantities of metabolic byproducts. The maximum metabolic rates for oysters are recorded in July and August (Mao et al. 2006), and lead to high nutrient concentrations in seawater (Fig. 5). Bivalves filter phytoplankton larger than 3 μm in size, thereby reducing their biomass in the water column (Newell, 2004). Phytoplankton growth is also limited by the level of solar radiation (Shi et al. 2011b). Thus, as nutrient utilization by phytoplankton decreased, the dissolved inorganic nutrient concentrations increased as a result, and increased to a greater extent in regions where bivalve monoculture occurred. Based on the nutrient budget in our study, phosphorus released from bivalve excretion could account for 65 % of total influx to SGB. Hence, from June to October, prior to kelp seeding, bivalves and

fish excretion may constitute an important nutrient source in SGB, leading to increased nutrient levels. Particulate waste material (feces or pseudofeces) from bivalves and phytoplankton are consumed by bivalves, and the nutrients involved may be removed through bivalve harvesting (Shpigel 2005, Troell et al. 2009). As top-down grazers, bivalves filter phytoplankton, which results in a reduction in the nutrient turnover time and speeds up nutrient cycling.

Nutrients can be produced indirectly via remineralization and subsequent release from enriched sediments (Forrest et al. 2009). Nutrient release from sediment is also a common phenomenon occurring beneath bivalve farms in SGB (Cai et al. 2004, Sun et al. 2010). The nutrient budgets also show that benthic flux is another important source of nutrients in SGB, especially for DIP and DSi (Table 3), and that this is significantly affected by aquaculture activities in the bay (Ning et al. 2016). Based on studies of other bivalve culture systems and natural or restored oyster reefs, it is evident that benthic fluxes are determined by processes involving filter feeding and excretion of dissolved nutrients, as well as biodeposition and sediment remineralization of nutrients (Newell 2004, Forrest et al. 2009). The TDN in SGB was dominated by DON in both summer and winter (Figs. 4 & 5), as observed in landbased aquaculture (Jackson et al. 2003, Herbeck et al. 2013). Burford & Williams (2001) reported that most of the dissolved nitrogen leaching from feed and shrimp feces was in organic rather than in inorganic forms. Hence, DON leaching from feces or pseudofeces might be an important source of DON in the bivalve cultivation regions in SGB (Fig. 6). Furthermore, increased sedimentation of organic matter from feces and pseudofeces underneath mussel farms can have significant ecosystem effects on the biogeochemical cycles of nitrogen and phosphorus (Stadmark & Conley 2011).

Biogeochemical cycling of DSi can be affected by diatom dissolution, sediment resuspension, and terrigenous input. In our study, the average concentrations of DSi increased by 9.0 μM from July to October, and decreased rapidly from 14.2 to 4.76 μM in January. Phytoplankton abundance was tightly controlled by filter feeding of oysters (Hyun et al. 2013), so the high metabolic rates of oysters may result in a reduction of diatom biomass, leading to high levels of DSi in autumn. In addition, as the water depth in SGB is ≤ 20 m, sediment resuspension and diatom dissolution might be important sources of DSi during the summer to autumn period. The dissolution of diatom frustules depends on a variety of factors, including microbial activity (Olli et al. 2008). Bacteria can

attack the organic matrix protecting the diatom frustule, exposing biogenic silica, and substantially increase the dissolution rate (Bidle & Azam 1999). The maximum biomass in SGB occurred in autumn (Chen 2001), and diatoms dominated in the bay in summer. Consequently, dissolution of diatom frustules may be an important source of DSi in the bay.

Although the aquaculture area and quantities of effluents released in SGB were high (Table 3), nutrient levels in the bay were not significantly elevated compared with other bays used for aquaculture, including Jiaozhou Bay (Liu et al. 2007) and Sishili Bay (Zhou et al. 2002b). This is attributed to the fact that nutrients released from shellfish are taken up by seaweeds during their growth periods. Large-scale kelp cultivation plays an important role in keeping nutrients at low levels and maintaining relatively good water quality.

Effects of physical factors on nutrient changes

The marine IMTA culture system used in SGB is suspended aquaculture. Water exchange between SGB and the Yellow Sea could be hindered by kelp (*S. japonica*), especially during kelp harvesting (Zeng et al. 2015). Our depth study showed that nutrient changes over the tidal cycle generally closely followed changes in water depth at Stn D2 (Fig. 7), indicating that water exchange is greater at Stn D1 (in the northern mouth of SGB), and weaker at Stn D2. Furthermore, in April 2013, the nutrients were well mixed at Stn D1, while at Stn D2, the nutrient concentrations were higher in bottom water than in the surface water (Fig. 7). This indicates that the current was affected by the aquaculture facilities and kelp at Stn D2, which may have led to higher nutrient concentrations in the bottom water than in the surface water. These results are consistent with the *in situ* measurements of Zeng et al. (2015), which showed that the vertical tidal flux at the northern entrance of SGB was much larger than at the southern entrance. In addition, the current structure in SGB has been significantly changed by the presence of aquaculture activities (Shi et al. 2011a). The tidal current in the surface layer is only half that in the middle layer when kelp is at its maximum length (Shi et al. 2011a). As a result, particulate matter and nutrients in bottom waters are constrained from entering the upper water layers because of the influence of aquaculture facilities and species (Wei et al. 2010).

The current flow generally tends to decrease in suspended aquaculture areas because of the extra

drag caused by the presence of aquaculture facilities. In SGB, bivalves and fish are grown in cages, nets, or other containers hung from floats or rafts. Based on a 3-dimensional physical-biological coupled aquaculture model (Shi et al. 2011a), the average current flow speed can be reduced by approximately 63 % by aquaculture facilities and cultured species. Moreover, Grant & Bacher (2001) reported a 20 % reduction in current speed in the main navigation channel in SGB, and a 54 % reduction in the middle of the culture area because of the effects of suspended aquaculture. Nutrients are likely to be retained in the bay because of the weaker current in the bivalve culture areas. The nutrient budgets showed that bivalve excretion was an important source of nutrients (Table 3). Large quantities of nutrients could accumulate in the west of the bay, and red tides have occurred in SGB in recent years (Zhang et al. 2012). The effects of consequent shading and competition pressure from the increased algae biomass on the valuable habitats involved may negatively affect the seagrass meadows in the southwest of the bay, and the production of bivalves may be reduced. To conserve the natural services provided by the bay, aquaculture effluents should be treated before they are released into natural water bodies.

Water exchange can also cause differences in nutrient species inside and outside SGB. Wei et al. (2010) observed that the flow speed declined by approximately 70 % from the mouth to the southwestern part of the bay, and the outflow was slowed by the increased aquaculture activities and infrastructure (Fan & Wei 2010). Thus, movement of nutrients from the southwest of the bay to the open sea may be impeded, which was suggested by the high concentrations of nutrients found in this part of the bay in summer and autumn (Fig. 4).

Long-term trends of nutrients in SGB

Fig. 9 shows compiled data for DIN, DSi, and PO_4^{3-} in SGB, based on historical data and our observations (Song et al. 1996, P. Sun et al. 2007, S. Sun et al. 2010, Zhang et al. 2010, 2012, this study), reflecting the long-term variations for the period 1983 to 2014. No trends in the PO_4^{3-} concentrations were evident because of the high variability in this parameter (Fig. 9). In contrast, the DIN concentrations increased over time and were significantly higher in 2003 to 2011 than in previous years (Fig. 9). Prior to the 1980s, kelp was the main aquaculture species, and the DIN concentration was low in the bay (Fang et al. 1996a,

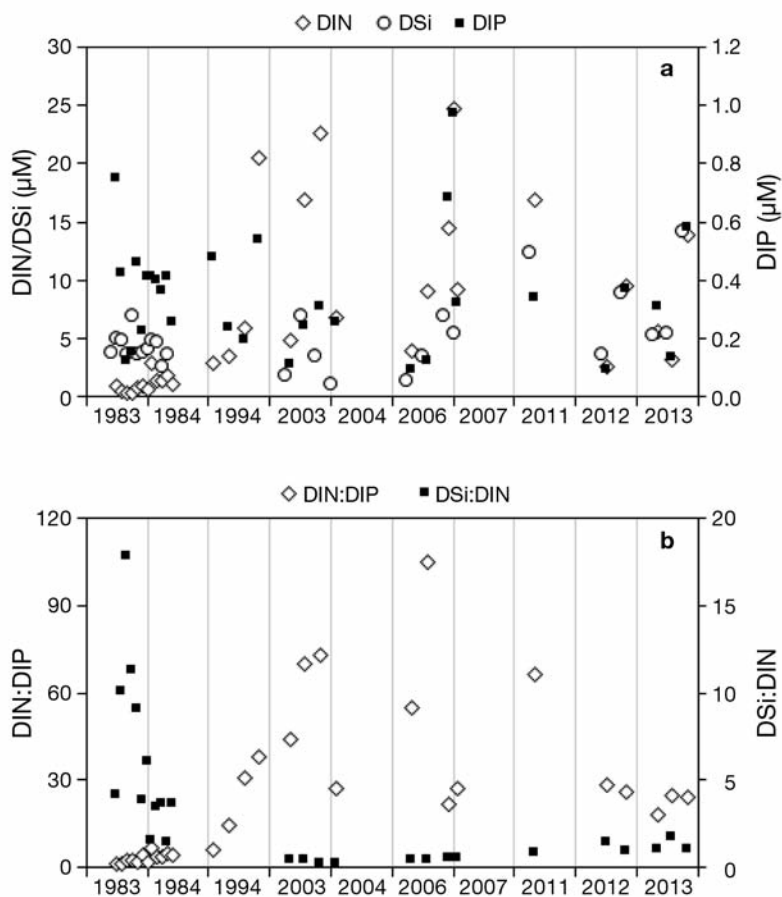


Fig. 9. Long-term changes in (a) the concentrations of dissolved inorganic nitrogen (DIN), dissolved inorganic phosphorus (DIP), and dissolved silicate (DSi) concentrations, and (b) the DIN:PO₄³⁻ and DSi:DIN ratios for the period 1983 to 2013

Ning et al. 2016). Polyculture was introduced into the bay for economic reasons (Fang et al. 1996a), and its rapid development may have been responsible for increasing levels of nutrients in the bay, and resulted in long-term alterations to the nutrient conditions (Shi et al. 2011a, Zhang et al. 2012). In SGB, nutrient-rich aquaculture effluents are released into the natural water body without prior treatment. The high concentrations of nitrogen in aquaculture effluents mainly originate from excess feed or from excretion from the farmed animals (Burford & Williams 2001).

As a result of the increased nitrogen levels, the DIN:DIP ratios in SGB shifted from severe nitrogen limitation in 1983 to the ecologically desirable Redfield ratio (16) in summer 1994, and continued to increase until summer 2006, when the DIN:PO₄³⁻ ratio reached 105; phytoplankton growth is now limited by phosphorus in summer. The increase in the DIN:PO₄³⁻ ratios in SGB is a common phenomenon observed in long-term studies of estuarine and coastal areas affected by human activities, and also in semi-closed

bays used for aquaculture, including Chesapeake Bay in the US (Tango et al. 2005), and Jiaozhou (Shen 2002, Sun et al. 2011) and Daya Bays (Wang et al. 2009) in China. Turner et al. (1998) reported that the risk of harmful algal blooms increases with shifts in the DSi:DIN ratio to values <1, when phytoplankton becomes dominated by non-diatom species. Molar ratios of DSi:DIN in SGB changed from 1.4–18 in 1983 to <1 during the 2003 to 2011 period. Red tides were observed in April 2011 (Zhang et al. 2012), and were apparent in small areas in 2013. In addition, an increase in the DIN concentration will lower the DSi:DIN ratio, and could change ecosystem structure of the bay (Billen & Garnier 2007).

Because of its combination of environmental, economic, and social benefits (Allsopp et al. 2008, Nobre et al. 2010), IMTA has been gaining recognition as a sustainable approach to aquaculture, and the water quality in SGB has remained in good condition compared with other bays affected by aquaculture activities. Environmental management strategies will need to include both reduction of nutrient pollution and monitoring of the relative abundance of nutrients. The ecological and economic health of SGB should be tightly monitored to ensure a rapid response to critical changes.

CONCLUSION

We have reported on the nutrient dynamics of SGB, which represents a typical watershed for IMTA. The results of our investigation show that aquaculture activities play an important role in nutrient cycling in SGB. Nutrients showed considerable seasonal variation in the bay, and nutrient composition and distribution were also affected by the cultured species in the bay. The nutrient budgets showed that SGB behaved as a source of PO₄³⁻ and as a sink of DSi and DIN. The model results indicated that PO₄³⁻ was mainly derived from bivalve excretion. Bivalve excretion may be an important source of PO₄³⁻ when phytoplankton growth is phosphorus-limited in the bay. Seaweed and bivalve harvesting play an important role in removing DIN and PO₄³⁻ from the bay. Under the combined effects of natural processes and aquaculture activities, nutrient biogeochemistry in the bay has been affected.

Acknowledgements. This research was funded by the Chinese Ministry of Science and Technology (2011CB409802), the Natural Sciences Foundation of China (NSFC: 41221004), and the Taishan Scholars Programme of Shandong Province. We thank colleagues at the Yellow Sea Fisheries Research Institute, Chinese Academy of Fishery Sciences, East China Normal University, and the Ocean University of China for their help during field investigations.

LITERATURE CITED

- Allsopp M, Johnston P, Santillo D (2008) Challenging the aquaculture industry on sustainability. Greenpeace International, Amsterdam
- Bacher C, Grant J, Hawkins AJS, Fang JG, Zhu MY, Besnard M (2003) Modelling the effect of food depletion on scallop growth in Sungo Bay (China). *Aquat Living Resour* 16:10–24
- Beck AJ, Rapaglia JP, Kirk Cochran J, Bokuniewicz HJ, Yang SH (2008) Submarine groundwater discharge to Great South Bay, NY, estimated using Ra isotopes. *Mar Chem* 109:279–291
- Bellos D, Sawidis T, Tsekos I (2004) Nutrient chemistry of River Pinios (Thessalia, Greece). *Environ Int* 30:105–115
- Bidle KD, Azam F (1999) Accelerated dissolution of diatom silica by marine bacterial assemblages. *Nature* 39:508–511
- Billen G, Garnier J (2007) River basin nutrient delivery to the coastal sea: assessing its potential to sustain new production of non-siliceous algae. *Mar Chem* 106:148–160
- Bostock J, McAndrew B, Richards R, Jauncey K and others (2010) Aquaculture: global status and trends. *Philos Trans R Soc Lond B Biol Sci* 365:2897–2912
- Bouwman AF, Pawłowski M, Liu C, Beusen AHW, Shumway SE, Glibert PM, Overbeek CC (2011) Global hindcasts and future projections of coastal nitrogen and phosphorus loads due to shellfish and seaweed aquaculture. *Rev Fish Sci* 19:331–357
- Burford MA, Williams KC (2001) The fate of nitrogenous waste from shrimp feeding. *Aquaculture* 198:79–93
- Buschmann AH, Varela DA, Hernández-González MC, Huovinen P (2008) Opportunities and challenges for the development of an integrated seaweed-based aquaculture activity in Chile: determining the physiological capabilities of *Macrocystis* and *Gracilaria* as biofilters. *J Appl Phycol* 20:571–577
- Cai LS, Fang JG, Dong SL (2004) Preliminary studies on nitrogen and phosphorus fluxes between seawater and sediment in Sungo Bay. *Mar Fish Res* 25:57–64 (in Chinese with English abstract)
- Chen HW (2001) Correlation analysis on bacteriological indexes and environmental parameters for surface water of Sanggou Bay. *Mar Environ Sci* 20:29–33 (in Chinese with English abstract)
- Duarte P, Meneses R, Hawkins AJS, Zhu M, Fang J, Grant J (2003) Mathematical modelling to assess the carrying capacity for multi-species culture within coastal waters. *Ecol Model* 168:109–143
- Fan X, Wei H (2010) Modeling studies on vertical structure of tidal current in a typically coastal raft-culture area. *Prog Fish Sci* 31:78–84 (in Chinese with English abstract)
- Fang JG, Sun HL, Yan JP, Kuang SH, Li F, Newkirk GF, Grant J (1996a) Polyculture of scallop *Chlamys farreri* and kelp *Laminaria japonica* in Sungo Bay. *Chin J Oceanol Limnol* 14:322–329
- Fang JG, Kuang SH, Sun HL, Li F, Zhang AJ, Wang XZ, Tang TY (1996b) Mariculture status and optimizing measurements for the culture of scallop *Chlamys farreri* and kelp *Laminaria japonica* in Sungou Bay. *Mar Fish Res* 17:95–102 (in Chinese with English abstract)
- FAO (Food and Agriculture Organization of the United Nations) (2010) The state of world fisheries and aquaculture 2010. Fisheries and Aquaculture Department, FAO, Rome
- Fei XG (2004) Solving the coastal eutrophication problem by large scale seaweed cultivation. *Hydrobiologia* 512: 145–151
- Forrest BM, Keeley NB, Hopkins GA, Webb SC, Clement DM (2009) Bivalve aquaculture in estuaries: review and synthesis of oyster cultivation effects. *Aquaculture* 298: 1–15
- Fu MZ, Pu XM, Wang ZL, Liu XJ (2013) Integrated assessment of mariculture ecosystem health in Sanggou Bay. *Acta Ecol Sin* 33:238–316 (in Chinese with English abstract)
- Gordon DC, Boudreau PR, Mann KH, Ong JE and others (1996) LOICZ biogeochemical modeling guidelines. LOICZ Reports and Studies (5). Land–Ocean Interactions in the Coastal Zone, Texel
- Grant J, Bacher C (2001) A numerical model of flow modification induced by suspended aquaculture in a Chinese Bay. *Can J Fish Aquat Sci* 58:1–9
- Grasshoff K, Kremling K, Ehrhardt M (1999) Methods of seawater analysis. In: Hansen HP, Koroleff F (eds) Determination of nutrients. Wiley-VCH, Weinheim, p 159–228
- Guo ZR, Huang L, Liu HT, Yuan XJ (2008) The estimation of submarine inputs of groundwater to a coastal bay using radium isotopes. *Acta Geosci Sin* 29:647–652 (in Chinese with English abstract)
- Han LJ, Zhu YM, Liu SM, Zhang J, Li RH (2013) Nutrients of atmospheric wet deposition from the Qianliyan Island of the Yellow Sea. *China Environ Sci* 33:1174–1184 (in Chinese with English abstract)
- Hao LH, Sun PX, Hao JM, Du BB, Zhang XJ, Xu YS, Bi JH (2012) The spatial and temporal distribution of chlorophyll-a and its influencing factors in Sanggou Bay. *Ecol Environ Sci* 21:338–345 (in Chinese with English abstract)
- Heggie K, Savage C (2009) Nitrogen yields from New Zealand coastal catchments to receiving estuaries. *N Z J Mar Freshw Res* 43:1039–1052
- Herbeck LS, Unger D, Wu Y, Jennerjahn TC (2013) Effluent, nutrient and organic matter export from shrimp and fish ponds causing eutrophication in coastal and back-reef waters of NE Hainan, Tropical China. *Cont Shelf Res* 57: 92–104
- Hyun JH, Kim SH, Mok JS, Lee JS, An SU, Lee WC (2013) Impacts of long-line aquaculture of Pacific oysters (*Crassostrea gigas*) on sulfate reduction and diffusive nutrient flux in the coastal sediments of Jinhae-Tongyeong, Korea. *Mar Pollut Bull* 74:187–198
- Jackson C, Preston N, Thompson PJ, Burford M (2003) Nitrogen budget and effluent nitrogen components at an intensive shrimp farm. *Aquaculture* 218:397–411
- Jennerjahn TC, Nasir B, Pohlenga I (2009) Spatio-temporal variation of dissolved inorganic nutrients related to hydrodynamics and land use in the mangrove-fringed Segara Anakan Lagoon, Java, Indonesia. *Reg Environ Change* 9:259–274
- Jiang ZJ, Fang JG, Zhang JH, Mao YZ, Wang W (2007) Forms and bioavailability of phosphorus in surface sedi-

- ments from Sungo Bay. Huan Jing Ke Xue (Environ Sci) 28:2783–2788 (in Chinese with English abstract)
- Justić D, Rabalais NN, Turner RE, Dortch Q (1995) Changes in nutrient structure of river-dominated coastal waters: stoichiometric nutrient balance and its consequences. *Estuar Coast Shelf Sci* 40:339–356
- Kuang S, Fang J, Sun H, Li F (1996) Seston dynamics in Sanggou Bay. *Mar Fish Res* 17:60–67 (in Chinese with English abstract)
- Liu SM, Zhang J, Chen HT, Zhang GS (2005) Factors influencing nutrient dynamics in the eutrophic Jiaozhou Bay, North China. *Prog Oceanogr* 66:66–85
- Liu SM, Li XN, Zhang J, Wei H, Ren JL, Zhang GL (2007) Nutrient dynamics in Jiaozhou Bay. *Water Air Soil Pollut Focus* 7:625–643
- Liu SM, Hong GH, Zhang J, Ye XW, Jiang XL (2009) Nutrient budgets for large Chinese estuaries. *Biogeosciences* 6:2245–2263
- Liu SM, Li RH, Zhang GL, Wang DR and others (2011) The impact of anthropogenic activities on nutrient cycling dynamics in the tropical Wenchanghe and Wenjiaohe Estuary and Lagoon system in East Hainan, China. *Mar Chem* 125:49–68
- Mao YZ, Zhou Y, Yang HS, Wang RC (2006) Seasonal variation in metabolism of cultured Pacific oyster, *Crassostrea gigas*, in Sanggou Bay, China. *Aquaculture* 253:322–333
- Marinho-Soriano E, Nunes SO, Carneiro MAA, Pereira DC (2009) Nutrients' removal from aquaculture wastewater using the macroalgae *Gracilaria birdiae*. *Biomass Bioenergy* 33:327–331
- Moore WS (1996) Large groundwater inputs to coastal waters revealed by ^{226}Ra enrichments. *Nature* 380:612–614
- Neori A, Chopin T, Troell M, Buschmann AH and others (2004) Integrated aquaculture: rationale, evolution and state of the art emphasizing seaweed biofiltration in modern mariculture. *Aquaculture* 231:361–391
- Newell RIE (2004) Ecosystem influences of natural and cultivated populations of suspension-feeding bivalve molluscs: a review. *J Shellfish Res* 23:51–61
- Newell RIE, Koch EW (2004) Modeling seagrass density and distribution in response to changes in turbidity stemming from bivalve filtration and seagrass sediment stabilization. *Estuaries* 27:793–806
- Ning Z, Liu S, Zhang G, Ning X and others (2016) Impacts of an integrated multi-trophic aquaculture system on benthic nutrient fluxes: a case study in Sanggou Bay, China. *Aquacult Environ Interact* 8:221–232
- Nobre AM, Robertson-Andersson D, Neori A, Sankar K (2010) Ecological-economic assessment of aquaculture options: comparison between abalone monoculture and integrated multi-trophic aquaculture of abalone seaweeds. *Aquaculture* 306:116–126
- Nunes JP, Ferreira JG, Gazeau F, Lencart-Silva J, Zhang XL, Zhu MY, Fang JG (2003) A model for sustainable management of shellfish polyculture in coastal bays. *Aquaculture* 219:257–277
- Olli K, Clarke A, Danielsson Å, Aigars J, Conley D, Tamminen T (2008) Diatom stratigraphy and long-term dissolved silica concentrations in the Baltic Sea. *J Mar Syst* 73:284–299
- Pietros JM, Rice MA (2003) The impacts of aquacultured oysters, *Crassostrea virginica* (Gmelin, 1791) on water column nitrogen and sedimentation: results of a mesocosm study. *Aquaculture* 220:407–422
- Savchuk OP (2005) Resolving the Baltic Sea into seven sub-basins: N and P budgets for 1991–1999. *J Mar Syst* 56: 1–15
- Schneider O, Sereti V, Eding EH, Verreth JAJ (2005) Analysis of nutrient flows in integrated intensive aquaculture systems. *Aquacult Eng* 32:379–401
- Shen ZL (2002) Long-term changes in nutrient structure and its influences on ecology and environment in Jiaozhou Bay. *Oceanol Limnol Sin* 33:322–331 (in Chinese with English abstract)
- Shi J, Wei H, Zhang L, Yuan Y, Fang JG, Zhang JH (2011a) A physical-biological coupled aquaculture model for a suspended aquaculture area of China. *Aquaculture* 318: 412–424
- Shi HH, Fang GH, Hu L, Zheng W (2011b) Analysis on response of pelagic ecosystem to kelp mariculture within coastal waters. *J Waterway Harbor* 32:213–218
- Shpigel M (2005) Bivalves as biofilters and valuable by-products in land-based aquaculture systems. In: Dame RF, Olenin S (eds) *The comparative roles of suspension feeders in ecosystems*. Springer-Verlag, Dordrecht, p 183–197
- Smaal A, van Stralen M, Schuiling E (2001) The interaction between shellfish culture and ecosystem processes. *Can J Fish Aquat Sci* 58:991–1002
- Smith SV, Swaney DP, Talaue-McManus L, Bartley JD and others (2003) Humans, hydrology, and the distribution of inorganic nutrient loading to the ocean. *Bioscience* 53: 235–245
- Song HJ, Li RX, Wang ZL, Zhang XL, Liu P (2007) Inter-annual variations in phytoplankton diversity in the Sanggou Bay. *Adv Mar Sci* 25:332–339 (in Chinese with English abstract)
- Song XL, Yang Q, Sun Y, Yin H, Jiang SL (2012) Study of sedimentary section records of organic matter in Sanggou Bay over the last 200 years. *Acta Oceanol Sin* 34: 120–126 (in Chinese with English abstract)
- Song YL, Cui Y, Sun Y, Fang JG, Sun HL, Kuang SH (1996) Study on nutrient state and influencing factors in Sanggou Bay. *Mar Fisher Res* 17(2):41–51 (in Chinese with English abstract)
- Stadmark J, Conley DJ (2011) Mussel farming as a nutrient reduction measure in the Baltic Sea: consideration of nutrient biogeochemical cycles. *Mar Pollut Bull* 62:1385–1388
- Sun PX, Zhang ZH, Hao LH, Wang B and others (2007) Analysis of nutrient distributions and potential eutrophication in seawater of the Sanggou Bay. *Adv Mar Sci* 25: 436–445 (in Chinese with English abstract)
- Sun S, Liu SM, Ren JL, Zhang JH, Jiang ZJ (2010) Distribution features of nutrients and flux across the sediment-water interface in the Sanggou Bay. *Acta Oceanol Sin* 32: 108–117 (in Chinese with English abstract)
- Sun S, Li CL, Zhang GT, Sun XX, Yang B (2011) Long-term changes in the zooplankton community in the Jiaozhou Bay. *Oceanol Limnol Sin* 42:625–631 (in Chinese with English abstract)
- Tang QS, Fang JG, Zhang JH, Jiang ZJ, Liu HM (2013) Impacts of multiple stressors on coastal ocean ecosystems and integrated multi-trophic aquaculture. *Prog Fish Sci* 34:1–11 (in Chinese with English abstract)
- Tango PJ, Magnien R, Butler W, Luckett C, Luckenbach M, Lacouture R, Poukish C (2005) Impacts and potential effects due to *Prorocentrum minimum* blooms in Chesapeake Bay. *Harmful Algae* 4:525–531
- The People's Republic of China Ministry of Agriculture Fisheries Bureau (2013) *China Fishery Statistical Yearbook*.

- China Agriculture Press, Beijing (in Chinese)
- Troell M, Joyce A, Chopin T, Neori A, Buschmann AH, Fang JG (2009) Ecological engineering in aquaculture-potential for integrated multi-trophic aquaculture (IMTA) in marine offshore systems. *Aquaculture* 297:1–9
- Turner RE, Qureshi N, Rabalais NN, Dortch Q, Justi D, Shaw RF, Cope J (1998) Fluctuating silicate: nitrate ratios and coastal plankton food webs. *Proc Natl Acad Sci USA* 95:13048–13051
- Wall CC, Peterson BJ, Gobler CJ (2008) Facilitation of seagrass *Zostera marina* productivity by suspension-feeding bivalves. *Mar Ecol Prog Ser* 357:165–174
- Wan L (2012) Effect of shellfish farming on nutrient salts of seawater in Sanggou Bay in spring. *Environ Sci Manag* 2012(6):62–64 (in Chinese with English abstract)
- Wang XL, Du JZ, Ji T, Wen TY, Liu SM, Zhang J (2014) An estimation of nutrient fluxes via submarine groundwater discharge into the Sanggou Bay—a typical multi-species culture ecosystem in China. *Mar Chem* 167:113–122
- Wang ZH, Zhao JG, Zhang YJ, Cao Y (2009) Phytoplankton community structure and environmental parameters in aquaculture areas of Daya Bay, South China Sea. *J Environ Sci (China)* 21:1268–1275
- Wei H, Zhao L, Yuan Y, Shi J, Fan X (2010) Study of hydrodynamics and its impact on mariculture carrying capacity of Sanggou Bay: observation and modeling. *Prog Fish Sci* 31:65–71 (in Chinese with English abstract)
- Wu H, Peng RH, Yang Y, He L, Wang WQ, Zheng TL, Lin GH (2014) Mariculture pond influence on mangrove areas in south China: significantly larger nitrogen and phosphorus loadings from sediment wash-out than from tidal water exchange. *Aquaculture* 426–427:204–212
- Yang YF, Li CH, Nie XP, Tang DL, Chuang EK (2005) Development of mariculture and its impacts in Chinese coastal waters. *Rev Fish Biol Fish* 14:1–10
- Yu HY, Bao LJ, Wong CS, Hu Y, Zeng EY (2012) Sedimentary loadings and ecological significance of polycyclic aromatic hydrocarbons in a typical mariculture zone of South China. *J Environ Monit* 14:2685–2691
- Yuan XT, Zhang MJ, Liang YB, Liu D, Guan DM (2010) Self-pollutant loading from a suspension aquaculture system of Japanese scallop (*Patinopecten yessoensis*) in the Changhai sea area, Northern Yellow Sea of China. *Aquaculture* 304:79–87
- Zeng DY, Huang DJ, Qiao XD, He YQ, Zhang T (2015) Effect of suspended kelp culture on water exchange as estimated by in situ current measurement in Sanggou Bay, China. *J Mar Syst* 149:14–24
- Zhang JH, Hansen PK, Fang JG, Wang W, Jiang ZJ (2009) Assessment of the local environmental impact of intensive marine shellfish and seaweed farming—application of the MOM system in the Songo Bay, China. *Aquaculture* 287:304–310
- Zhang JH, Shang DR, Wang W, Jiang ZJ, Xue SY, Fang JG (2010) The potential for utilizing fouling macroalgae as feed for abalone *Haliotis discus hannai*. *Aquacult Res* 41:1770–1777
- Zhang JH, Wang W, Hang TT, Liu DH and others (2012) The distributions of dissolved nutrients in spring of Songo Bay and potential reason of outbreak of red tide. *J Fish China* 36:132–138 (in Chinese with English abstract)
- Zhang JH, Fang JG, Tang QS, Ren LH (2013) Carbon sequestration rate of the scallop *Chlamys farreri* cultivated in different areas of Sanggou Bay. *Prog Fish Sci* 34:12–16 (in Chinese with English abstract)
- Zhang LH, Zhang XL, Li RX, Wang ZL and others (2005) Impact of scallop culture in dinoflagellate abundance in the Sanggou Bay. *Adv Mar Sci* 23:342–346 (in Chinese with English abstract)
- Zhao J, Zhou SL, Sun Y, Fang JG (1996) Research on Sanggou bay aquaculture hydro-environment. *Mar Fish Res* 17:68–79
- Zhou Y, Mao YZ, Yang HS, He YZ, Zhang FS (2002a) Clearance rate, ingestion rate and absorption efficiency of the scallop *Chlamys farreri* measured by in situ biodeposition method. *Acta Ecol Sin* 22:1455–1462 (in Chinese with English abstract)
- Zhou Y, Yang HS, Liu SL, He YZ, Zhang FS (2002b) Chemical composition and net organic production of cultivated and fouling organisms in Sishili Bay and their ecological effects. *J Fish China* 26:21–27 (in Chinese with English abstract)

Editorial responsibility: Sebastien Lefebvre, (Guest Editor)
Wimereux, France

Submitted: June 1, 2015; Accepted: March 7, 2016
Proofs received from author(s): March 24, 2016